Accessing Arene-Fused Eight-Membered Carbo- and Heterocycles via Bidentate Lewis Acid Catalysis

---

Inauguraldissertation zur Erlangung des Doktorgrades (Dr. rer. nat.)
der Naturwissenschaftlichen Fachbereiche im Fachgebiet Chemie
der Justus-Liebig-Universität Gießen

vorgelegt von

Michel Große

aus Greiz

Betreuer: Prof. Dr. Hermann A. Wegner

Gießen 2025

Versicherung nach §17 der Promotionsordnung

Ich erkläre: Ich habe die vorgelegte Dissertation selbstständig und ohne unerlaubte fremde Hilfe und nur mit den Hilfen angefertigt, die ich in der Dissertation angegeben habe. Alle Textstellen, die wörtlich oder sinngemäß aus veröffentlichten Schriften entnommen sind, und alle Angaben, die auf mündlichen Auskünften beruhen, sind als solche kenntlich gemacht. Ich stimme einer evtl. Überprüfung meiner Dissertation durch eine Antiplagiat-Software zu. Bei den von mir durchgeführten und in der Dissertation erwähnten Untersuchungen habe ich die Grundsätze guter wissenschaftlicher Praxis, wie sie in der „Satzung der Justus-Liebig-Universität Gießen zur Sicherung guter wissenschaftlicher Praxis“ niedergelegt sind, eingehalten.

Angaben zu auf künstlicher Intelligenz (KI) basierender Hilfen wie ChatGPT oder SchulKI von OpenAI oder Gemini von Google zur Erstellung meiner Dissertation (Zutreffendes angekreuzt):

☐ Ich habe bei der Erstellung dieses Textes kein KI-Tool verwendet.

☒ Ich habe ein KI-Tool in den folgenden Bereichen eingesetzt (Mehrfachnennungen möglich):

- ☐ Ideen finden, meine Kreativität anregen
- ☐ Verstehen von Konzepten, Recherche von Fakten und Definitionen
- ☒ Optimierung eines von mir verfassten Textes
- ☐ Erstellen ganzer Textpassagen nach meinen Vorgaben

Folgende KI-Tools habe ich verwendet, damit aufgeführte Teile meines Textes von dem Tool wie folgt profitiert haben:
Ich habe die KI-Tools ChatGPT (OpenAI) und DeepL genutzt, um von mir vorformulierte Sätze auf sprachliche Fehler zu überprüfen sowie Synonyme und alternative Formulieren zu finden.

_____ _____

Michel Große Ort, Datum

Dekan: Prof. Dr. Holger Zorn
Erstgutachter: Prof. Dr. Hermann A. Wegner
Zweitgutachter: Prof. Dr. Richard Göttlich

As no better man advances to take this matter in hand, I hereupon offer my own poor endeavors. I promise nothing complete; because any human thing supposed to be complete, must for that very reason infallibly be faulty.

— Hermann Melville, *Moby-Dick*, Chapter 32

Table of Content

Abstract

Eight-membered carbo- and heterocycles constitute unique structural elements not only found in a plethora of biologically active natural products and medicinally relevant synthetic compounds, but also in various functional molecules and materials. Especially arene-annulated cyclooctanoids have attracted increasing attention as they combine the properties of rigid aromatic structures and flexible cyclooctene-derived ring systems. However, entropic and enthalpic difficulties generally encountered in the synthesis of medium-sized rings have largely hampered the development of general synthetic methods to access these structures.

In this thesis, new strategies for the synthesis of arene-annulated eight-membered carbo- and *N*-heterocycles were developed by employing a boron-based bidentate Lewis acid (BDLA) catalyst previously established in our group for facilitating inverse electron-demand Diels–Alder (IEDDA) reactions of phthalazines. The utilization of different cyclooctyne derivatives as highly reactive dienophiles gave rise to a series of cyclooctenes and cycloocta-1,5-dienes fused to substituted polycyclic aromatic hydrocarbons. X-ray crystallographic analysis and variable temperature NMR studies of selected derivatives provided valuable insights into the conformational behaviour of these polycyclic structures.

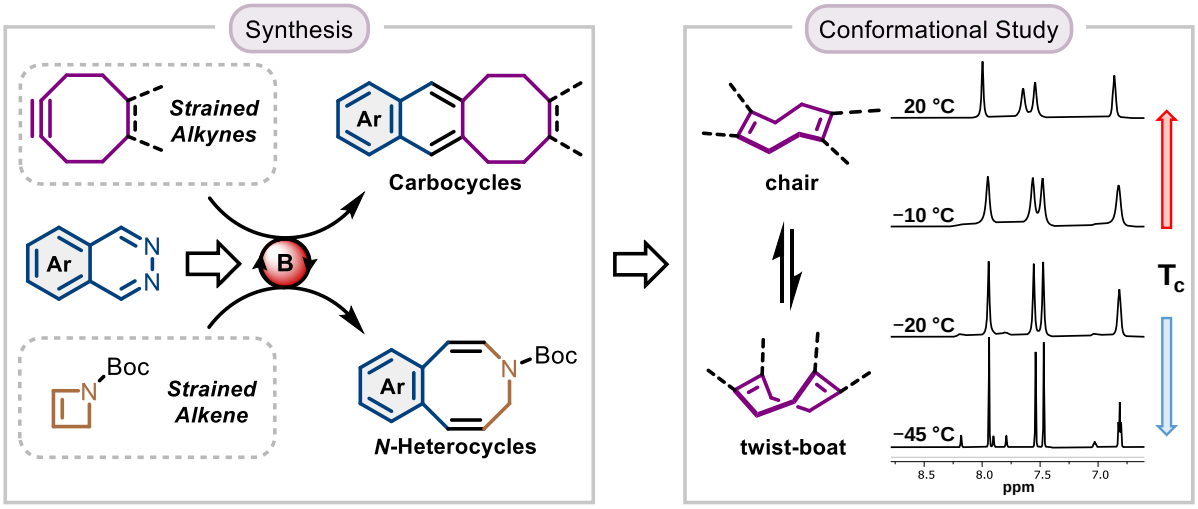

Additionally, the same catalytic principle was employed to develop a one-step synthesis of arene-annulated eight-membered nitrogen heterocycles from phthalazines and Boc-protected 2-azetine as a strained alkene dienophile. Key to this transformation was the formation of a highly reactive *o*-quinodimethane intermediate that thermally rearranged in a 10π electrocyclic ring opening to yield the desired azocine structures. These mechanistic considerations were supported by the isolation and characterization of the main by-product, and final proof for the eight-membered ring structure was obtained via X-ray crystallographic analysis of a degradation product.

Zusammenfassung

Achtgliedrige Carbo- und Heterocyclen sind einzigartige Strukturelemente, die nicht nur in einer Vielzahl biologisch aktiver Verbindungen, sondern auch in verschiedensten funktionalen Molekülen und Materialen vorkommen. Hierbei haben insbesondere anellierte Ringsysteme, in denen starre aromatische Strukturen mit flexiblen Cyclooctanoiden verbunden sind, zunehmend an Bedeutung gewonnen. Da die Synthese mittelgroßer Ringsysteme jedoch generell entropisch und enthalpisch erschwert ist, stellt die Herstellung solcher Strukturen noch immer eine große Herausforderung dar.

Die vorliegende Arbeit befasst sich mit der Entwicklung neuer Strategien zur Synthese anellierter Ringsysteme, welche achtgliedrige Carbo- und Heterocyclen mit aromatischen Strukturen kombinieren. Diese Synthesestrategien basieren auf dem Einsatz eines Bor-basierten, bidentaten Lewis-Säure-Katalysators, dessen Verwendung in Diels–Alder-Reaktionen mit inversem Elektronenbedarf zuvor in unserer Arbeitsgruppe etabliert wurde. Unter Einsatz Cyclooctin-basierter Dienophile konnten hierbei aus einfachen Phthalazinen verschiedenste polycyclische aromatische Kohlenwasserstoffe synthetisiert werden, welche mit Cyclooctenen kondensiert sind. Durch Röntgenkristallstrukturanalyse und temperaturabhängige NMR-Spektroskopie ausgewählter Verbindungen konnten wertvolle Einblicke in die Konformationseigenschaften dieser Verbindungen erhalten werden.

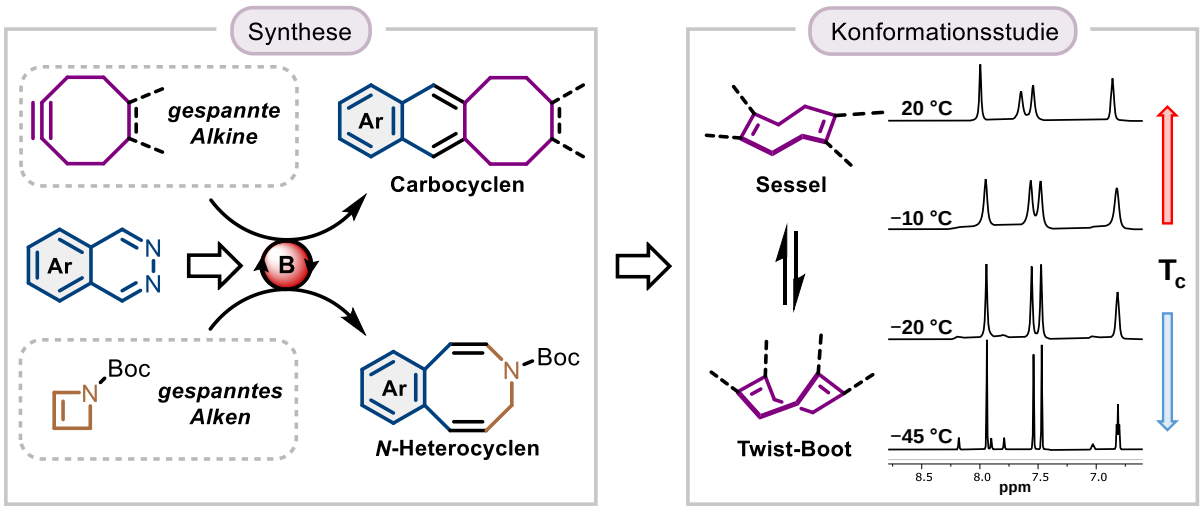

Darüber hinaus ermöglichte die Anwendung desselben katalytischen Prinzips die Synthese benzanellierter achtgliedriger Stickstoff-Heterocyclen aus Phthalazinen und Boc-geschütztem 2-Azetin. Der Schlüssel für diese Transformation war die Bildung eines reaktiven *o*-Chinodimethan-Intermediats, welches sich thermisch über eine elektrocyclische Ringöffnung zur gewünschten Azocin-Struktur umlagerte. Der vorgeschlagene Mechanismus konnte durch die Isolation und Charakterisierung des Hauptnebenprodukts unterstützt werden und der endgültige Beweis für die achtgliedrige Struktur wurde mittels Röntgenkristallstrukturanalyse erbracht.

1 Eight-Membered Rings in Materials and Life Sciences

In the realm of cyclic molecular architectures, medium sized rings (MSRs) (8-11 membered) stand out compared to normal sized (5-7 membered) and macrocyclic (12+ membered) structures due to their distinctive conformational features and three-dimensional shape.[1,2] Among these MSRs, especially eight-membered carbo- and heterocycles display several well-defined conformational geometries that can, depending on the degree of (un)saturation and the substitution pattern, coexist or interconvert. This balance between flexibility and rigidity, especially in arene-fused eight-membered ring systems, holds vast potential of these structures in functional materials, catalysis and bioactive small molecules. In the following chapters, applications and synthetic strategies of arene-annulated eight-membered carbo- and heterocycles are discussed. Parts of these sections have been published as an overview article by our group beforehand.[3]

1.1 Arene-Fused Eight-Membered Carbocycles in Materials Sciences

Combining eight-membered rings with rigid aromatic moieties in annulated polycyclic structures has become a promising strategy to construct functional molecules with applications in supramolecular chemistry, organic photonics and electronics.[4–8] Additionally, arene-annulated eight-membered carbocycles are of growing importance in the rapidly emerging field of organic on-surface synthesis,[9,10] where non-hexagonal rings recently attracted more and more attention.[11] As the key structures in these systems, typically cycloocta-1,5-dienes (CODs) or cyclooctatetraenes (COT) are integrated. On the one hand, the geometric constraints of these eight-membered rings can be utilized to integrate curvature into larger molecular frameworks.[12] On the other hand, their conformational flexibility serves as the basis of switchable materials and molecular probes.[5,13] Dibenzo[*a*,*e*]-COT (**1**) typically exists in a tub conformation in solution as well as in the solid state. A tub-to-tub interconversion usually proceeds at room temperature with a calculated barrier of 52 kJ/mol and is thought to go through a planar, antiaromatic transition state (Scheme 1).[14–16]

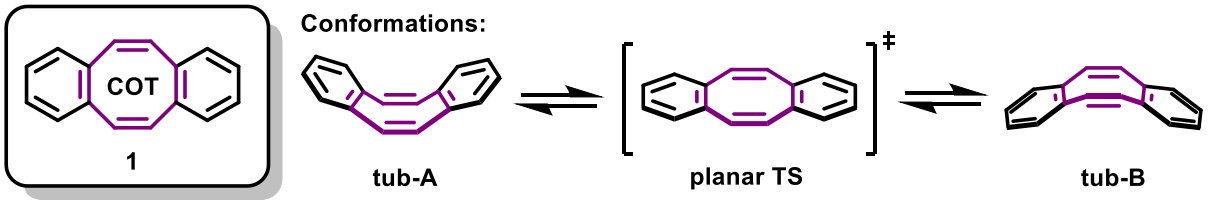

Scheme 1. Structure and tub-to-tub inversion of Dibenzo[*a*,*e*]-COT (**1**).

This has been extensively employed by Saito and co-workers in their design of fluorescent molecules such as anthraceneimide dimer **2** bearing a COT core with two fluorescent side arms (Figure 1). In the excited state, a conformational change results in a blue or green emission, depending on the molecular environment.[5,17–22]

With two additional annulated benzene rings at the COT core, tetraphenylene exhibits a drastically increased barrier for the tub inversion of 330 kJ/mol, as calculated by Bachrach.[23] This high barrier leads to a stable, saddle-shaped geometry which was employed by Sygula and co-workers in their design of COT **3** bearing two bowl-shaped corannulene side arms. Due to the tub conformation of the central eight-membered ring, **3** acts as a molecular tweezer that forms a 1:1 inclusion complex with C_{60} fullerene through concave−convex π-π interactions, as shown by X-ray crystallographic analysis as well as NMR titration experiments.[4] When the benzene rings in tetraphenylene-derived structures are further annulated to form [8]circulenes such as compound **4**, negatively curved nanographenes are obtained. In comparison to tetraphenylene, persubstituted [8]circulene **4** exhibits lower barriers of around 88 kJ/mol for the tub-to-tub inversion, as established via variable temperature (VT) NMR analysis.[24]

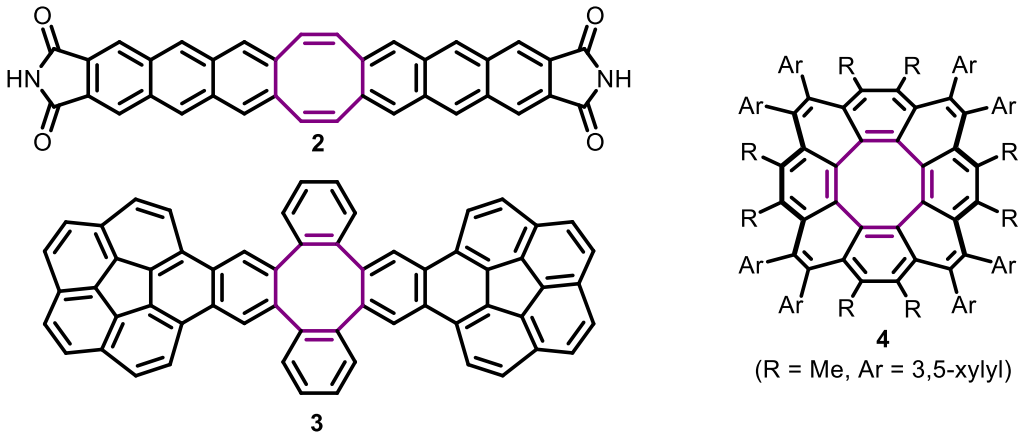

Figure 1. Representative literature examples of compounds featuring a COT core motif.[4,5,24]

In contrast to arene-fused COTs, the corresponding CODs show a higher conformational freedom. In the solid state, unsubstituted dibenzo-COD (DBCOD) (**5**) preferentially exists in the chair conformation due to energetically favorable π-π interactions, as confirmed via X-ray crystallographic analysis.[25] However, solutions of DBCODs were reported to contain mixtures of different conformers, as established via dynamic NMR (DNMR) spectroscopy in combination with *ab initio* calculations.[26–30] Of the three low-energy conformations chair (C), twist-boat (TB) and twist (T) (Scheme 2), only C- and TB-DBCOD were found to be present in solution in substantial amounts. Similar energies were calculated for the C and TB forms, but the results were contradictory regarding which form is more stable. Experimental results, however, identified the TB as the lowest energy conformer, with barriers of 42 kJ/mol for the TB-C interconversion and 33 kJ/mol for the TB-TB'-interconversion, respectively. T-DBCOD, albeit higher in energy, represents a pivotal intermediate for these conformational changes. Furthermore, the TB conformers can be seen as two, rapidly interconverting enantiomeric forms (+)-TB and (−)-TB that are connected via an achiral boat (B) transition state.[27,28,30]

Lu and co-workers were the first to employ the conformational switching of DBCOD derivatives in the construction of responsive polymeric materials.[13,31] Their DBCOD-containing polymers exhibited an unusual and completely reversible thermal

contraction triggered by low-energy near-infrared (NIR) or thermal stimulation. They showed that this mechanical response arises from the thermally induced conformational change of polymer-bound DBCOD from the ground state TB conformer to the metastable C conformer (Scheme 3, A).[13]

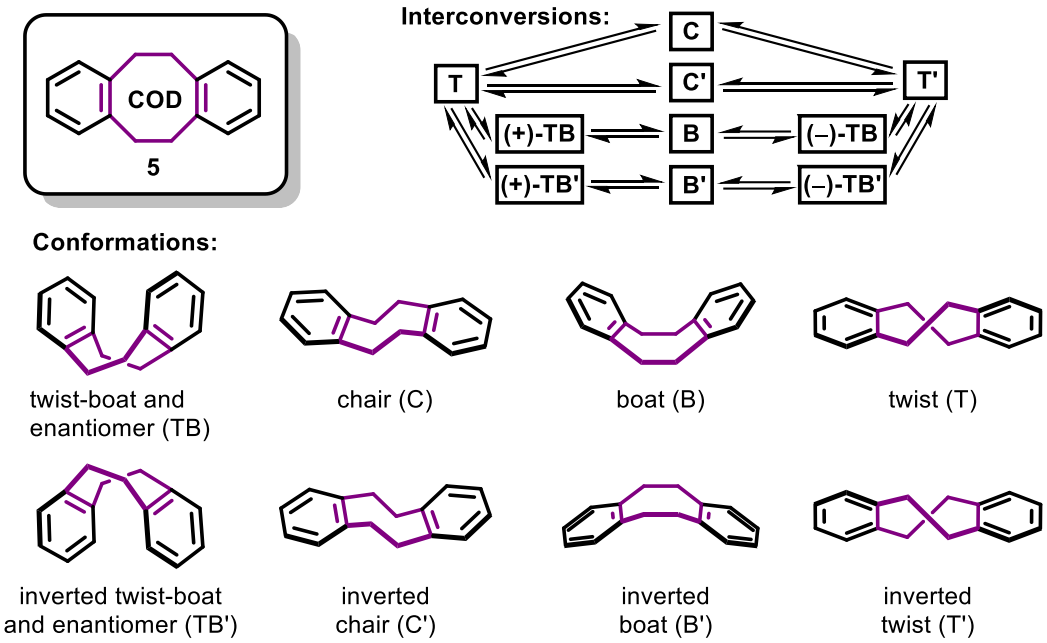

Scheme 2. Structure and main conformational interconversions of DBCOD (**5**).

Since this pioneering work, extensive research has been dedicated not only to the design of new DBCOD-containing materials, but also to deeper understanding and fine-tuning of this new type of molecular switch.[32–45] In a follow-up study, Lu and co-workers showed that the TB conformation can be stabilized by substituents capable of forming intramolecular hydrogen bonds as confirmed by DNMR analysis and X-ray crystallography (Scheme 3, B). In contrast, repulsive substituent interactions lead to a destabilization of the TB conformer.[44]

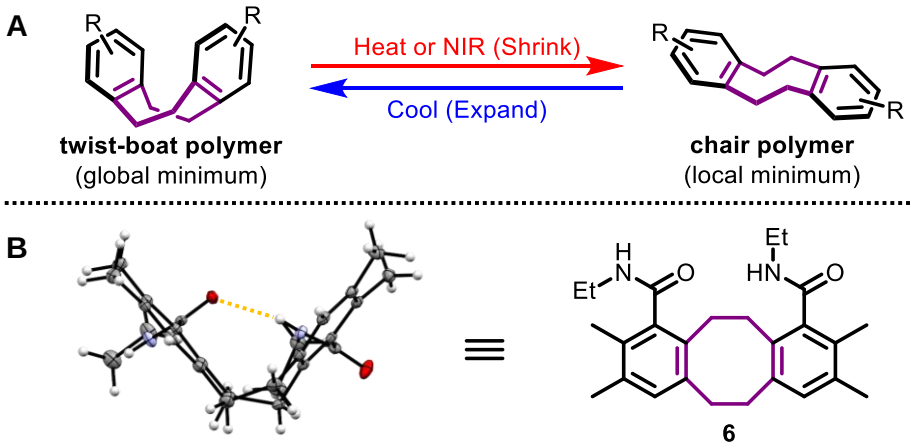

Scheme 3. A) Schematic representation of the reversible conformational switching of DBCOD-containing polymers.[13] B) Crystal structure of substituted DBCOD **6** (from CCDC: 2033976) showing the stabilization of the TB conformer via intramolecular hydrogen bonding. Thermal ellipsoids are shown at 50% probability.[44]

While this study provides a comprehensive overview of the effects of various substituents on the conformational behaviour of benzannulated COD derivatives, π-extended analogues have rarely been prepared or investigated.[46,47] One of the few examples was presented by Sygula and co-workers, who synthesized π-extended DBCOD analogue **7** bearing two bowl-shaped corannulene side arms and studied its conformational behaviour (Figure 2).[47] Density functional theory (DFT) calculations revealed a strong preference for the TB conformation in the gas phase due to strongly stabilizing intramolecular π-π interactions between the corannulene subunits. However, X-ray crystallography revealed its C conformation in the solid state with encapsulation of one nitrobenzene molecule between two corannulene units of neighboring molecules (Figure 2, B). Unfortunately, the poor solubility of COD **7** prevented further investigation of its conformational preferences via VT NMR spectroscopy. Further systematic conformational studies of π-extended DBCOD analogues remain elusive, most probably due to synthetic and solubility limitations.

A

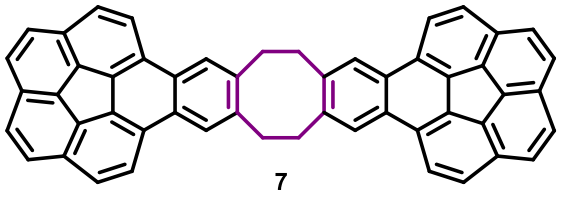

7

Conformer	Relative Energy [kJ/mol]
TB-7	0
C-7	33.1
T-7	47.8

B

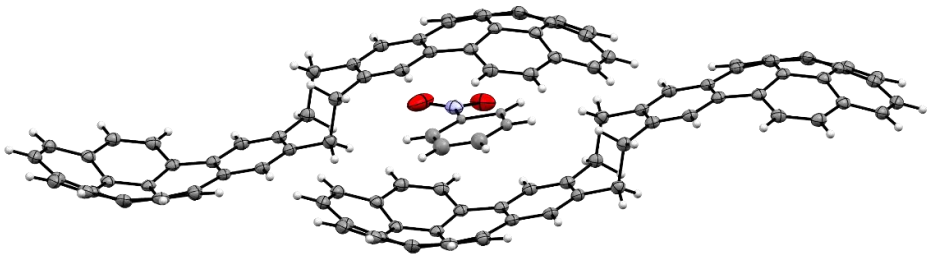

Figure 2. A) Structure and relative energies of the respective conformers of π-extended DBCOD analogue **7** [calculated at B97-D/TZVP level of theory]. B) Crystal structure of **7** (from CCDC: 746258). A second molecule of **7** is added to show the solvent encapsulation. Only one orientation of the disordered solvent molecule is shown. Thermal ellipsoids are shown at 50% probability.[47]

1.2 Biologically Active Compounds Bearing Eight-Membered Rings

1.2.1 Natural Products Containing Eight-Membered Rings

Besides their integration into functional molecules and materials, eight-membered rings play a pivotal role in biologically active natural products as well as medicinally important synthetic compounds. Cyclooctanoid natural products have been isolated from various biological sources including terrestrial plants, insects, fungi, and marine organisms.[48–50] Paclitaxel (**8**), as one of the most remarkable examples, has been extracted from the bark of the western yew and is used to treat various types of cancer.[51,52] Other medicinally relevant compounds include the fungus-derived

antibiotic pleuromutilin (**9**)[53,54] and the algal pigment caulerpin (**10**), which has been reported to exhibit anti-inflammatory, antimicrobial, and anticancer activities, among others.[55–57]

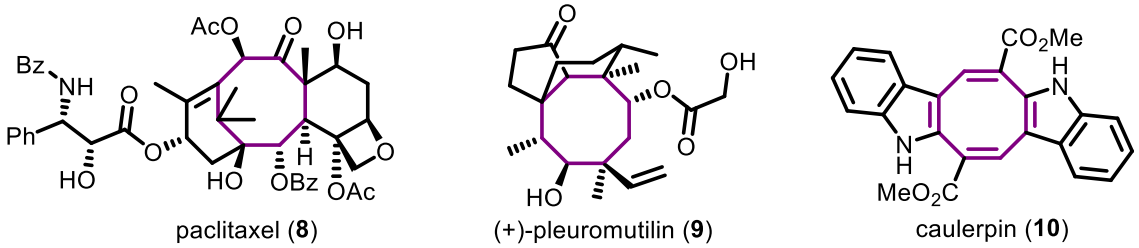

Figure 3. Representative examples of biologically active cyclooctanoid natural products.[51,53,55]

Besides these carbocyclic cyclooctanoids, a large number of bioactive molecules containing eight-membered nitrogen heterocycles have been isolated from biological sources.[58,59] In particular, partially saturated and arene-annulated azocines represent a central structural motif in various natural products showing promising biological activities (Figure 4).[60–62] Examples include the eight-membered lactams balasubramide (**11**) and ζ-clausenamide (**12**), isolated from different *Clausena* species,[63,64] which exhibit anti-neuroinflammatory and hepatoprotective activities, respectively.[65,66]

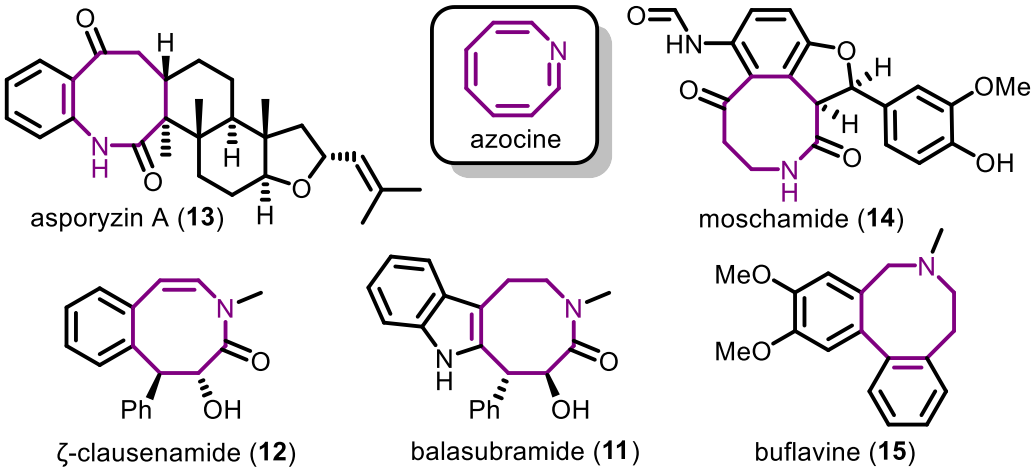

Figure 4. Representative examples azocines-containing alkaloids.[60–64]

1.2.2 Eight-Membered Rings in Medicinal Chemistry

Owing to their rich biological activities, eight-membered nitrogen-containing heterocycles are commonly regarded as privileged structures for drug discovery.[58,67] On the one hand, this can be attributed to the crucial role of nitrogen in binding to biological targets.[68] On the other hand, medium-sized rings themselves are often reported to increase crucial drug parameters such as binding affinity, oral bioavailability and cell permeability compared to acyclic analogues as a result of tunable molecular flexibility.[69–71] While bridged eight-membered ring systems, such as those found in benzomorphane-type structures, exhibit highly rigid three-dimensional geometries,[72] unbridged cycloctanoids offer an adjustable balance between conformational flexibility and rigidity, modulated by the degree of unsaturation, annulation and substitution.

Romines and co-workers employed the flexible nature of medium-sized alkyl rings to enhance the binding affinity of human immunodeficiency virus (HIV) protease inhibitors based on the coumarin lead compound **16** (Figure 5).[70] When they replaced the planar benzene ring of coumarin **16** with different alkyl rings, a significant increase in enzyme inhibitory activity was observed for certain medium-sized cycles, as can be seen from the enzyme inhibition constants K_i of derivatives **17**-**23**. The cyclooctyl derivative **21** was identified as the most active inhibitor in the series, showing a more than 50-fold increase in enzyme inhibition compared to the original lead structure **16**. The improved binding affinity was explained by the efficient folding of the flexible eight-membered ring into the enzymatic pocket of the protease, as revealed by X-ray crystallographic analysis of the enzyme-inhibitor complexes.[70]

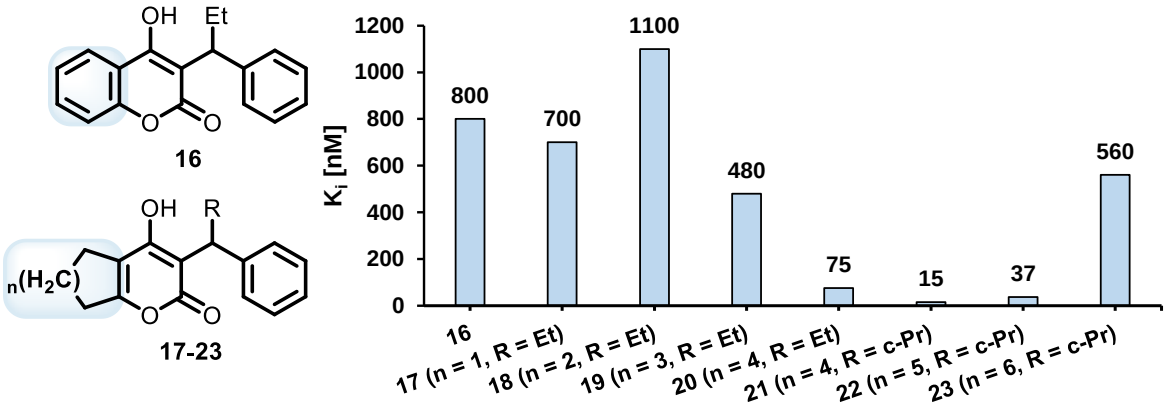

Figure 5. HIV protease inhibitory activities of coumarin lead compound **16** and its analogues **17**-**23**.[70]

Eight-membered rings have also been used in medicinal chemistry to rigidify active conformations, especially when it comes to axial chirality.[73] In their search for new neurokinin 1 (NK_1) receptor antagonist with clinical potential in the treatment of pain, inflammation, rheumatoid arthritis and asthma, Natsugari and co-workers developed amide **24** (Scheme 4).[74] This compound acts as a potent, orally available NK_1 antagonist but exists as a mixture of four separable stereoisomers due to restricted rotation around two stereogenic bonds.[75] Since all four isomers showed different biological activity, more rigid conformational mimics of **24** were synthesized by constraining its geometry through the integration of different normal- to medium-sized rings. This led to the discovery of atropisomerically pure diazocine **25** as an effective NK_1 antagonist that showed the highest *in vitro* and *in vivo* activity compared to six-, seven- and nine-membered analogues.[75] Ohnmacht, Albert and co-workers at AstraZeneca later adapted the same strategy in the development of NK_1 receptor antagonists as potential treatment for depression.[76,77] They faced a similar problem of equilibrating atropisomers in their lead compound, which prompted them to design rigid conformational mimics bearing an eight-membered ring.

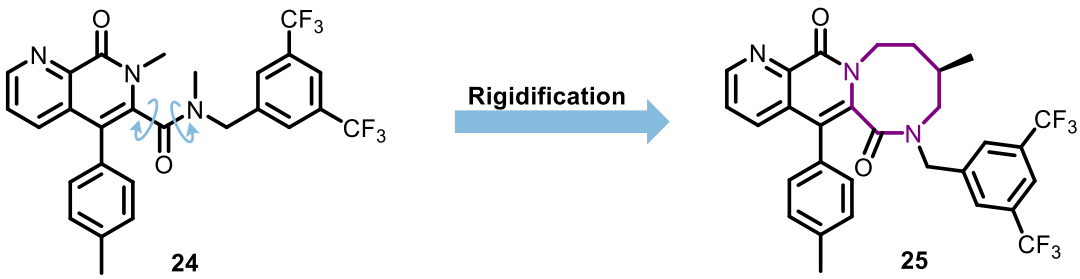

Scheme 4. Structures of NK_1 receptor antagonist **24** and its more rigid conformational mimic **25**.[75]

Natsugari and co-workers further investigated the influence of the ring size of different dibenzolactams **26**-**28** on the thermal stability of the respective atropisomers (Scheme 5).[78] The eight-membered lactam **27** was found to have a higher barrier for the rotation around the aryl-aryl bond compared to the corresponding seven- and nine-membered analogues. The ability to stabilize axial chirality in that way further highlights the importance of benzannulated eight-membered ring systems, not only in medicinal chemistry but also in chiral catalysis and functional materials.[79]

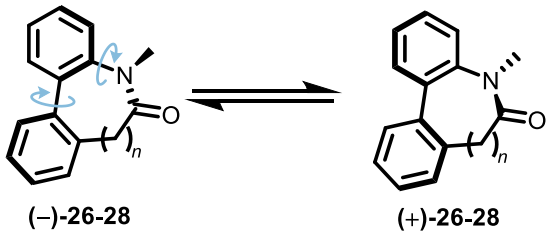

Compound	$\Delta G^{\ddagger}_{rac}$[kJ/mol]
26 (n = 1)	98
27 (n = 2)	112
28 (n = 3)	102

Scheme 5. Enantiomeric equilibrium and activation barriers of the racemization of atropisomeric dibenzolactams **26**-**28**. $\Delta G^{\ddagger}_{rac}$ values were determined from the time-depended conversion rate estimated by chiral HPLC analysis.[78]

2 Synthetic Strategies for the Construction of Arene-Annulated Eight-Membered Ring Systems

2.1 Challenges of Synthesizing Medium-Sized Rings

Due to the importance of eight-membered ring structures in materials and life sciences, their synthesis represents a major goal in organic chemistry.[48,80,81] However, this still poses a challenging subject due to unfavorable enthalpic and entropic factors generally associated with the construction of MSRs.[82,83] Firstly, compared to normal-sized and macrocyclic rings, MSRs exhibit a relatively high ring strain as a result of severe torsional strain (Pitzer strain) and transannular strain (Prelog strain) (Figure 6), which is reflected in high activation energies required for the cyclization of linear precursors.[84,85] Additionally, the conversion of flexible open-chain precursors to MSRs via cyclic transition states comes with a drastic reduction of conformational freedom and therefore more negative entropies of activation.[86] This represents a major challenge in the synthesis of eight-membered rings, since the cyclization from linear precursors is intrinsically difficult, even under highly diluted conditions.[84]

Nevertheless, typical cyclization reactions such as ring closing metathesis were successfully applied to the construction of eight-membered rings systems. However, the success of the reaction highly depends on the reactivity and especially the geometry of the acyclic precursors.[87] Consequently, extensive efforts have been made to develop general alternative strategies for the construction of functionalized eight-membered rings systems.

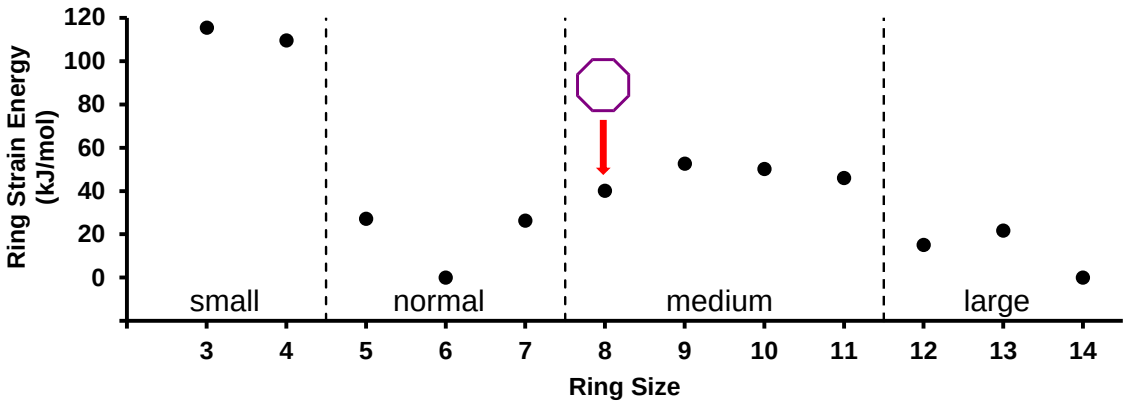

Figure 6. Ring strain energies of cycloalkanes as a function of ring size.[88]

2.2 Functionalization of Eight-Membered Rings via Diels–Alder Reactions

Commercially available or readily synthesizable cyclooctanoids represent a rich source of buildings blocks that can be further derivatized to obtain highly complex natural products or functional molecules and materials.[89–92] Especially arene-annulated CODs and COTs are commonly obtained through Diels−Alder (DA) reactions of cyclooctyne derivatives with various types of dienes (Scheme 6).[3] The typical reaction sequence starts with the initial [4+2] cycloaddition that furnishes, in most cases, a bridged intermediate. Depending on the nature of the respective diene, this intermediate can be either transient or isolable.[93] In the former case, spontaneous cycloreversion directly furnishes the arene-fused structure, whereas in the latter, additional synthetic steps are required for re-aromatization. These reactions represent a powerful tool to directly annulate eight-membered rings to the aromatic systems of interest with exceptional selectivity and functional group tolerance. The highly reactive, strained triple bond of the cyclooctyne derivative represents the key component in these transformations.

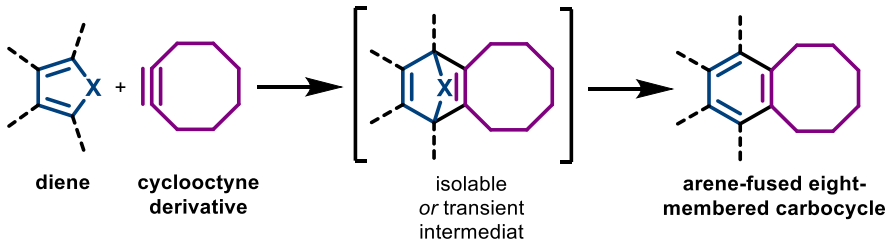

Scheme 6. General reaction sequence of the DA reaction of cyclooctynes and various dienes. For the definition of X, see section 2.2.2.

2.2.1 Cyclooctyne Derivatives

With angles of around 160°, the carbon-carbon triple bond in cyclooctyne shows a significant deviation from the ideal linear geometry at the sp-hybridized atoms.[94–96] This results in high ring strain and consequently increased reactivity of this bond compared to linear alkynes.[97] With an estimated ring strain energy of 75 kJ/mol, cyclooctyne occupies a unique position among all cyclic alkynes, being the smallest and thus most reactive member that is still stable enough to be isolated and stored (Figure 7). Smaller homologues have to be generated *in situ* in the presence of a trapping agent.[98]

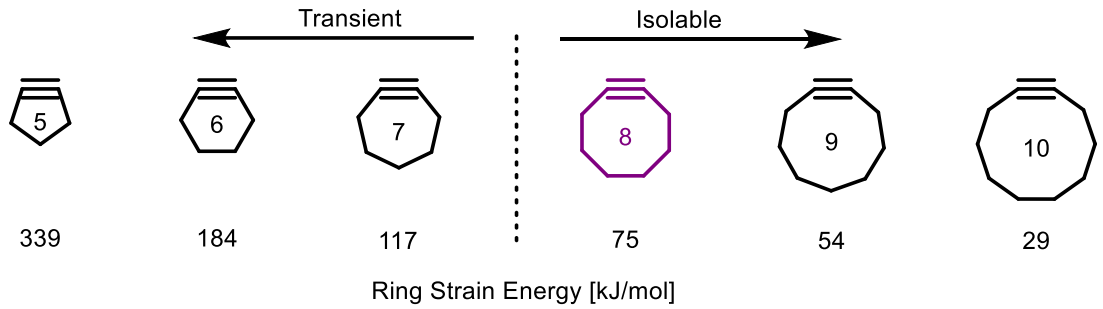

Figure 7. Calculated ring strain energies of different cycloalkynes [calculated at M06-2X/6-311G+(d,p) level of theory].[98]

This balance between stability and reactivity facilitated the use of cyclooctynes in strain-promoted cycloaddition reactions, especially in the context of bioorthogonal chemistry. Numerous strategies for fine-tuning the reactivity and stability of these strained alkynes have been developed and extensively reviewed.[98–100] While cyclooctynes in bioorthogonal chemistry mainly function as reactive linkers, materials-oriented molecular design typically places the eight-membered ring at the geometric center of the target molecule, which necessitates the use of symmetric 1,5-cyclooctadienes rather than simple monoalkynes (Figure 8).

Kloster-Jensen and Wirz were the first to synthesize and describe 1,2-cyclooctadiyne (**29**) in 1973.[101,102] It was obtained as a crystalline solid in 2% yield by dimerization of butatriene and found to be stable at 0 °C under exclusion of air. X-ray crystallographic analysis revealed its essentially planar geometry with bond angles of 159° around the triple bonds.[101] In 1974, Sondheimer and co-workers synthesized planar dibenzocyclooctadiyne **30**, which is now commonly referred to as Sondheimer−Wong diyne (SWD).[103] It was obtained from the corresponding, readily available alkene via a bromination-dehydrobromination sequence and found to be relatively stable, showing only partial decomposition after two days of storage at room temperature without protection from air or light. In contrast, diyne **31**, which was described by Sondheimer and Wong two years later, proved to be extremely unstable and quickly decomposed after a few minutes at 0 °C.[104] As a more reactive surrogate of diyne **29**, Meier and co-workers synthesized enyne **32**, which contains a highly reactive, strained alkyne together with a vinyl bromide moiety that serves as a latent alkyne precursor.[105] Isolated as a colourless liquid, enyne **32** solidifies at temperatures below −55 °C and remains stable for several days only in its solid form. In 2007, Hopf and co-workers synthesized and described strained alkyne **33** as another highly reactive, benzo-fused diyne.[106,107]

In contrast to the SWD (**30**), crystalline samples of diyne **33** were reported to quickly decompose upon storage at room temperature, even under exclusion of air.[106] Of the five cyclooctyne derivatives **29**-**33**, especially the SWD (**30**) and enyne **32** have since been widely employed in DA reactions with a broad range of dienes to synthesize arene-fused COTs and CODs.

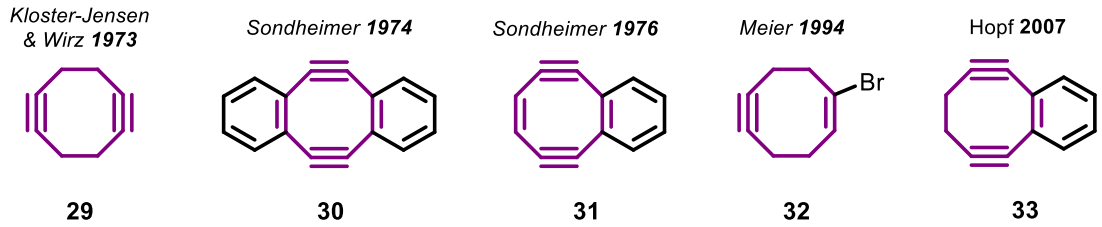

Figure 8. Structures of cycloocta-1,5-diynes (**29**-**31**,**33**) and a synthetic equivalent (**32**).[101–107]

2.2.2 Diels−Alder Reactions of Cyclooctynes

DA reactions involving strained alkyne dienophiles usually proceed with significantly increased reaction rates compared to linear alkynes. As shown by Sauer and co-workers for reactions with 1,2,4,5-tetrazine (**34**), going from acyclic alkynes like simple acetylene (**35**), phenylacetylene (**36**) or ynamine **37** to strained cyclooctyne (**38**) leads to a drastic increase in reaction rate (Scheme 7).[97] This can, on the one hand, be attributed to the bending of the alkyne moiety in cyclooctyne leading to a pre-distortion toward the required transition state geometry. According to a computational analysis by Houk and co-workers, going from linear 2-butyne to strained cyclooctyne reduces the distortion energy required to reach the DA transition state with tetrazine (**34**) by 49 kJ/mol, leading to an equivalent reduction in activation energy.[108] On the other hand, the rate of DA reactions highly depends on the electronic nature of the reactants.[109] According to the frontier molecular orbital (FMO) theory, DA reactions with normal electron demand (NEDDA) proceed through an overlap of the highest occupied molecular orbital (HOMO) of the diene with the lowest unoccupied molecular orbital (LUMO) of the dienophile. In contrast, inverse electron-demand Diels−Alder (IEDDA) reactions require an overlap between the HOMO of the dienophile and the LUMO of the diene. Accordingly, the electronic demand of a DA reaction can be altered by adjusting the energy levels of the FMOs of diene and dienophile, e.g. by attaching electron-withdrawing (EWG) or electron-donating groups (EDG).[109]

Cyclooctynes typically react as electron-rich dienophiles in IEDDA reactions with electron-poor dienes.[89] This is favored by the fact that bending of an alkyne leads to a destabilizing overlap of the π bonds with adjacent σ bonds, which increases the energy level of the HOMO of strained cycloalkynes compared to linear ones.[110] This enables precise adjustment of the HOMO energy levels and consequently the reaction rates of cyclooctyne derivatives in DA reactions (Figure 9).[111] One approach to further increase the strain of cyclooctynes is through cylopropane fusion.[112] Van Delft and co-workers applied this strategy in their synthesis of bicyclo[6.1.0]nonyn **40** as a highly reactive strained alkyne for bioorthogonal cycloaddition reactions.[113]

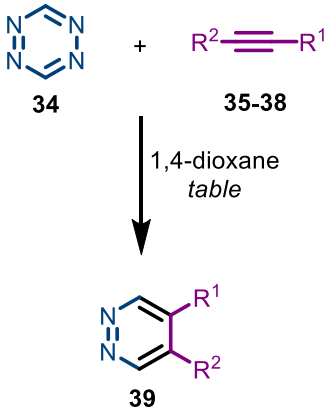

Dienophile		k·10^5 at 20 °C [l mol^{-1} s^{-1}]
	**38**	2710000
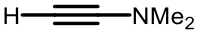	**37**	50200
	**36**	0.168
	**35**	2.91

Scheme 7. IEDDA reaction of alkynes **35**-**38** and tetrazine (**34**) and the corresponding rate constants at 20 °C in 1,4-dioxane.[97]

The increased strain is reflected in the increase of the HOMO energy level by 6.3 kJ/mol and the higher reaction rates compared to parent cyclooctyne. In contrast, electron-withdrawing substituents next to the strained alkyne cause a significant decrease of the HOMO energy level as can be seen in the cyclooctyne derivatives **41** and **42**.[111] Furthermore, this attachment of EWGs can even lead to a switch from inverse to normal electron demand in the DA reaction, especially when dienes featuring EDGs are employed.[114] However, as previously described, most DA reactions of cyclooctyne derivatives follow the inverse electron-demand pathway.

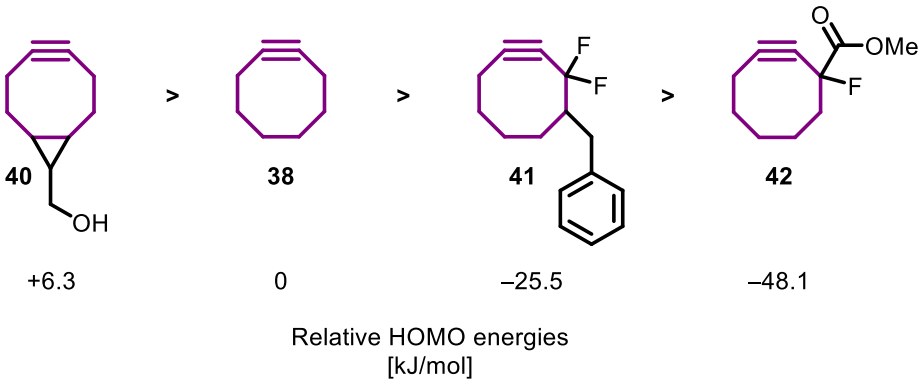

Figure 9. Relative HOMO energies of cyclooctynes **38**,**40**-**42** [calculated at B3LYP/ 6-31G** level of theory].[111]

When 1,5-cyclooctadiynes are employed as dienophiles, the question of selectivity arises. All diynes **29**-**31** and **33** depicted in Figure 8 have previously been used as dienophiles in DA reactions with different types of dienes, yielding always double DA adducts **43** (Scheme 8).[102,104,107,115] In no case, a selective addition to only one of the triple bonds was achieved, even with excess of dienophile, indicating that the intermediate cyclooct-1-ene-5-ynes **44** are more reactive than the parent diynes.[102,105] Sondheimer and co-workers also synthesized the monoalkyne analog of the SWD (**30**) bearing a double bond instead of one of the triple bonds. Indeed, this monoalkyne proofed to be much more reactive and unstable than the corresponding diyne.[103] The same reactivity trend was later reported in strain-promoted click reactions of the SWD (**30**) with azides, highlighting the difficulties in achieving selective mono-addition.[116]

One possibility to overcome this limitation was reported by Meier and co-workers by using enyne **32**, as it allows for the generation of the second alkyne after the first DA reaction via a base-mediated elimination. In that way, previously unattainable mono-adducts **45** become accessible and two sequential DA reactions can be performed in a controlled manner.[105]

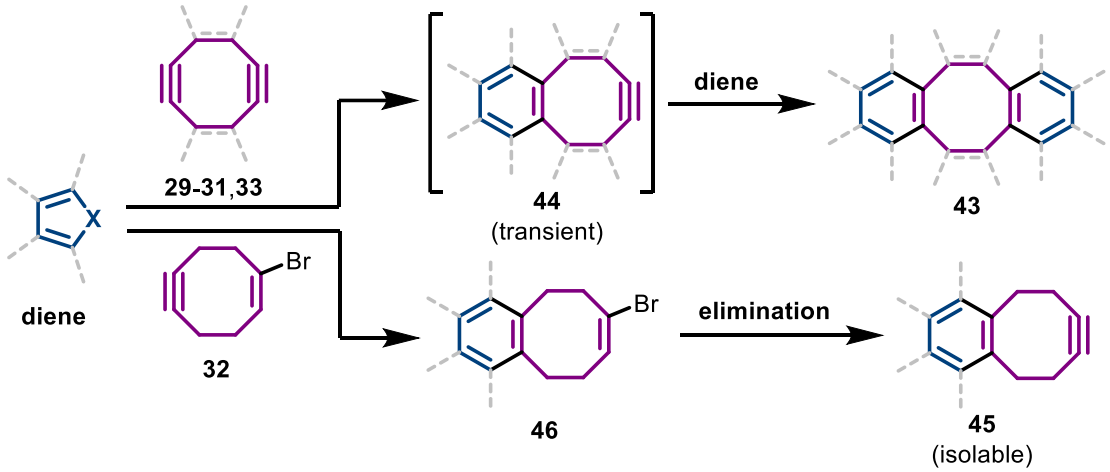

Scheme 8. Schematic representation of DA reactions using diynes **29**-**31** and **33** and enyne **32**.

To obtain arene-fused cyclooctenes from cyclooctyne derivatives via a DA reaction, a variety of possible methods has been described. Furans are among the most commonly used dienes in this regard and have been reported to react with enyne **32**, the SWD (**30**) as well as π-extended derivatives. The initial cycloaddition furnishes stable, oxygen bridged intermediates, as seen from the reaction of diyne **30** with unsubstituted furane (**47**) (Scheme 9, first step).[115] A one-step protocol for deoxygenation of cycloadduct **48** using *in situ* generated low valent titanium was developed by Xing and Huang in 1982 (Scheme 9, second step)[117] and later applied to the synthesis of π-extended tetraphenylenes as well as the molecular tweezers **3** and **7**.[4,47,118] In 2019, Miao and co-workers applied a different deoxygenation protocol using iodotrimethylsilane and sodium iodide in their synthesis of octabenzo[8]circulene derivatives.[119]

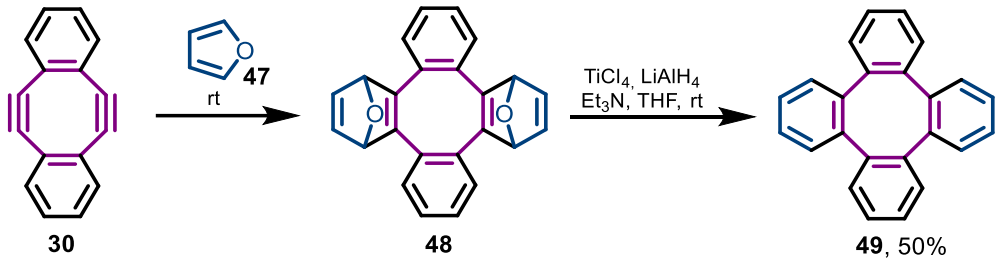

Scheme 9. DA reaction of furan (**47**) and the SWD (**30**) followed by titanium-mediated deoxygenation.[115,117]

Although less commonly applied than furans, thiophene *S*-oxides and *S*,*S*-dioxides have proven to be valuable dienes for the construction of arene-annulated eight-membered carbocycles. The initially formed bridged intermediates spontaneously extrude sulfur monoxide or dioxide to yield the desired aromatic ring without the need for an additional aromatization step.

In their synthesis of tetrabenzo[8]circulene, Whalley and co-workers employed a DA reaction of the SWD (**30**) and thiophene *S*-oxide **50** as a key step to furnish substituted tetraphenylene **51** (Scheme 10, A).[120] Despite their lower reactivity,[121] thiophene *S*,*S*-dioxides have also been utilized in DA reactions with strained alkynes. Especially derivative **52** carrying electron-withdrawing chlorine substituents allows for cycloadditions with alkynes **40** and **53** to proceed under mild conditions as shown by Hosoya and co-workers, demonstrating the inverse electron-demand of the reaction.[122]

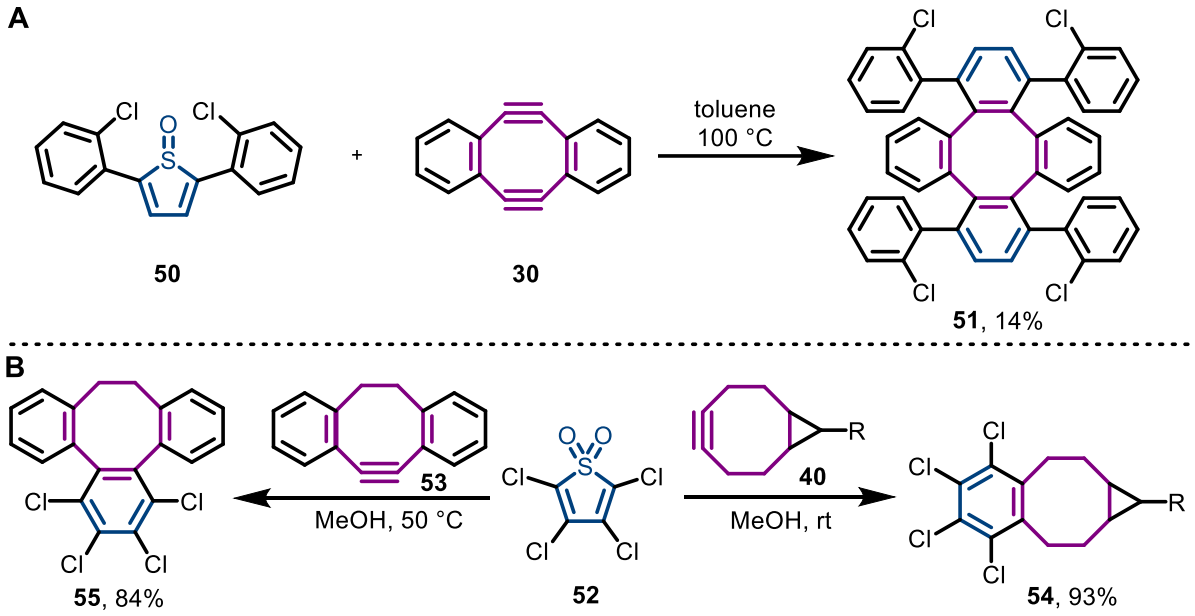

Scheme 10. A) Synthesis of tetraphenylene **51** via double DA addition of thiophene *S*-oxide **50** by Whalley and co-workers.[120] B) DA reaction of thiophene *S*,*S*-dioxide **52** and cyclooctyne derivatives by Hosoya and co-workers.[122]

Substituted cyclopentadienones represent another group of electron-poor dienes commonly employed in IEDDA reactions with cyclooctynes. Analogous to thiophene oxides, spontaneous extrusion of carbon monoxide after the initial cycloaddition directly furnishes the desired aromatic structure. Müllen and co-workers used this reactivity to synthesize octaphenyltetraphenylene **56** from tetracyclone (**57**) and the SWD **30** via double DA addition (Scheme 11).[123] Despite the reported thermal instability of diyne **30**, the reaction could be performed at 150 °C over 12 h and furnished the desired arene-annulated COT **56** in 95% yield. In contrast, sterically less hindered enyne **32** reacts smoothly with tetracyclone (**57**) under ambient conditions to furnish benzo-fused COD **58**, as shown by Meier and co-workers.[105] Subsequent elimination yielded the corresponding alkyne, which was again reacted with diene **57** at room temperature to obtain octaphenydibenzo-COD **59** in quantitative yield.

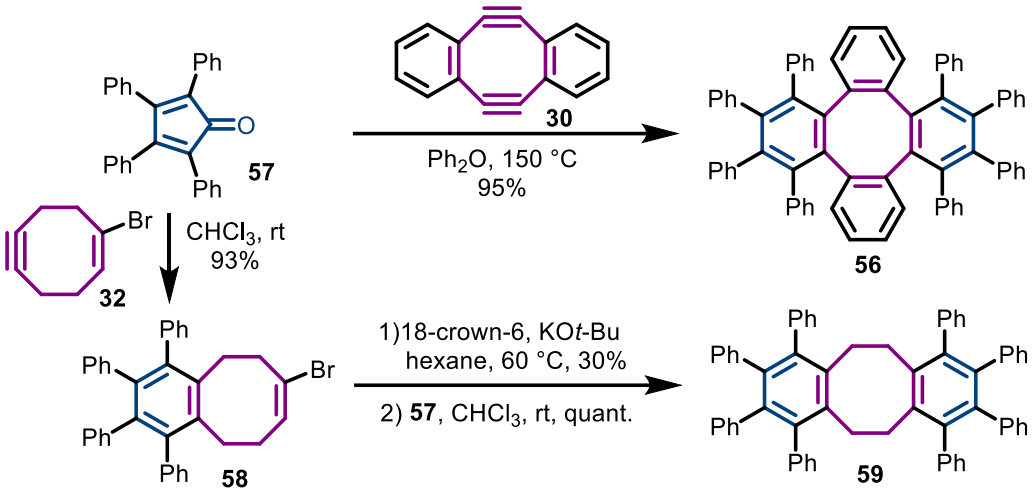

Scheme 11. DA reactions of tetracyclone (**57**) with diyne **30** (Müllen and co-workers)[123] and enyne **32** (Meier and co-workers).[105]

α-Pyrones are common dienes employed in NEDDA and IEDDA reactions depending on the substitution pattern and the nature of the dienophile.[124] With cyclooctynes, the initial cycloaddition typically proceeds via an inverse-electron demand pathway and is consequently facilitated by electron-withdrawing substituents of the pyrone ring.[125] In the subsequent *retro*-DA reaction, the benzo-fused eight-membered ring is obtained after extrusion of carbon dioxide. Kele and co-workers employed coumalic acid ester **60** as an electron-poor α-pyrone in an IEDDA reaction with enyne **32** (Scheme 12).[126] The reaction proceeded smoothly at room temperature and furnished the desired benzo-COD in 36% yield. Subsequent elimination yielded the corresponding strained alkyne **61**, which was used for bioorthogonal fluorescence labelling. In addition to α-pyrone, the reactivity of its thio-analogues in IEDDA reactions with cyclooctynes has been the subject of computational and experimental investigations. These studies identified the aromaticity of the respective heterocycle as well as the distortion energy in the cycloaddition as the crucial parameters for differences in the diene reactivity.[127,128]

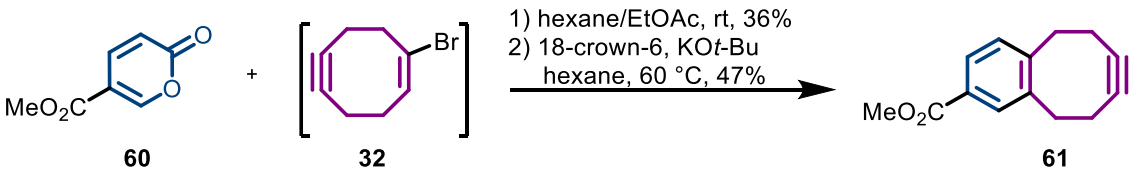

Scheme 12. DA reaction of α-pyrone **60** and enyne **32** followed by base-mediated elimination by Kele and co-workers.[126]

As another group of six-membered heterocycles, azines are highly versatile dienes for IEDDA reactions and have found extensive application in natural product total synthesis, chemical biology and materials science.[129–131] The reactivity of azines and the nature of their cycloaddition products vary significantly depending on the number of nitrogen atoms in the aromatic ring (Scheme 13). With an increasing number of nitrogen atoms, the aromaticity of the azine decreases and more favorable distortion and interaction energies reduce the overall activation energy in the cycloaddition.[132]

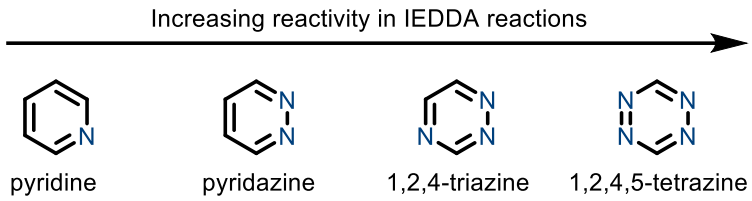

Scheme 13. Reactivity ranking of selected azines in IEDDA reactions.[132]

Due to the fast kinetics, as shown in Scheme 7, the reaction of tetrazine (**34**) and cycooctyne (**38**) has become an important tool in bioorthogonal chemistry. However, for the synthesis of (polycyclic) aromatic hydrocarbons fused to eight-membered carbocycles, new strategies are required that go beyond classical tetrazine ligation. To this end, Hosoya and co-workers established a modular synthetic approach based on two sequential DA reactions starting from oxadiazinone **62** (Scheme 14).[133] The initial cycloaddition with strained alkyne **63** proceeded smoothly at room temperature to afford substituted pyrone **64** after extrusion of nitrogen. Subsequent treatment with *in situ* generated benzyne yielded the desired naphtho-fused cyclooctene **65** via another DA/*retro*-DA sequence.

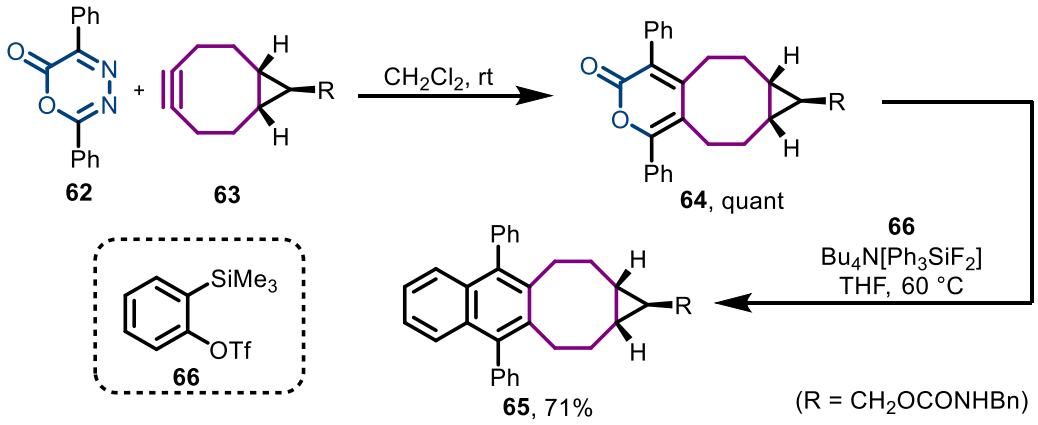

Scheme 14. Sequential DA reactions in the synthesis of naphtha-fused cyclooctene **65** by Hosoya and co-workers.[133]

In contrast to tetrazines or oxadiazinones, 1,2-diazines (pyridazines) usually require much higher temperatures for IEDDA reactions to take place and are often limited to very electron-poor dienes and electron-rich dienophiles.[134–138] Due to the known temperature sensitivity of cyclooctyne and its derivatives (see section 2.2.1), strategies are required to overcome the intrinsic lack of reactivity of pyridazines.

A common way to accelerate DA reactions is by utilizing Lewis acid (LA) catalysts such as aluminum trichloride.[139] These LA catalysts act by coordinating to Lewis basic centers of the dienophile (NEDDA) or the diene (IEDDA), thereby lowering the energy of the LUMO and leading to a stronger polarization. This results in improved selectivity as well as increased reaction rates due to a reduction of the HOMO-LUMO gap.[140–143] More recent computational analysis attributed the effect of LA catalysis to reduced Pauli repulsion between the π-systems of the diene and the dienophile.[144]

Although LA catalysis represents a common strategy to facilitate DA reaction, only a few examples of catalyzed IEDDA reactions of 1,2-diazines are reported. Rawal and co-workers developed a formal IEDDA reaction of phthalazines **67** and siloxy alkynes **68** mediated by the action of silver, copper or nickel catalysts (Scheme 15).[145,146] The proposed reaction mechanism involves the coordination of the metal to both the diazine as well as the alkyne, presumably leading to a stepwise addition process via intermediate **69**. A metal free addition of phthalazines **67** and ynamides **70** using triflic anhydride as catalyst was later reported by Wang and Chang.[147]

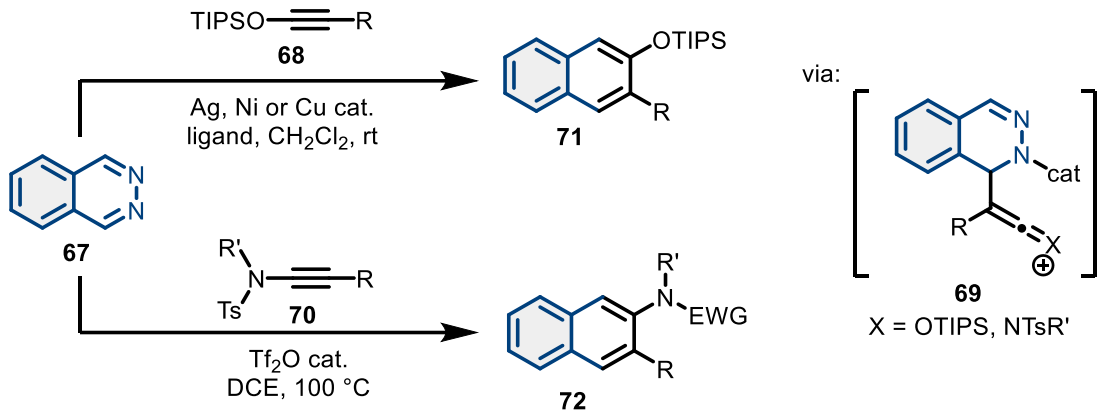

Scheme 15. Catalyzed IEDDA reactions of phthalazines by Rawal and co-workers (top)[145,146] and Wang and Chang (bottom).[147]

An alternative catalytic principle to activate 1,2-diazines was introduced by Wegner and co-workers in 2010, relying on the bidentate coordination of diboraanthracene **73** to phthalazines **67** (Scheme 16).[148] According to DFT calculations, the resulting complex **74** exhibits a large decrease in LUMO energy compared to the uncomplexed phthalazine (Scheme 16, A), enabling IEDDA reactions with various, electron-rich dienophiles under comparatively mild conditions.

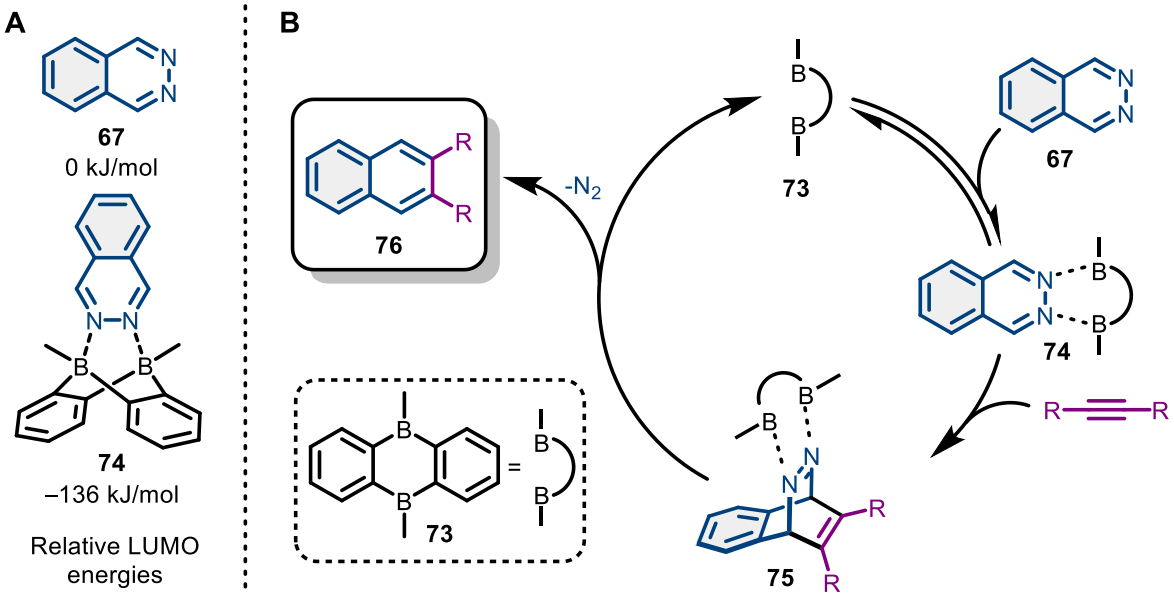

Scheme 16. A) Relative LUMO energies of phthalazine (**67**) and the complex **74** [calculated at B3LYP/6-31G*//HF/6-31G* level of theory]. B) Catalytic cycle of the BDLA-catalyzed IEDDA reaction of phthalazine and alkynes.[148]

When alkyne dienophiles are used, extrusion of nitrogen from the initially formed bridged intermediate **75** directly furnishes the desired naphthalene **76** and the bidentate Lewis Acid (BDLA) **73** re-enters the catalytic cycle (Scheme 16, B). In this thesis, I utilized this catalytic principle to facilitate IEDDA reactions of various phthalazines with cyclooctyne (**38**) and its derivative **40** in the synthesis of (substituted) polycyclic aromatic structures fused to eight-membered carbocycles.[149] Additionally, this methodology was expanded to the use of enyne **32** as dienophile, enabling the modular synthesis of naphto-fused CODs, the conformational behaviour of which was studied via X-ray crystallography, VT NMR analysis and computational methods.[150]

With only one nitrogen in the aromatic ring, pyridines exhibit the lowest reactivity in DA reactions among all azines. To overcome this lack of reactivity, Studer and co-workers established a one-pot reaction sequence of de-aromatization, cycloaddition and re-aromatizing *retro*-cycloaddition (Scheme 17, A).[151] This is achieved by treatment of substituted pyridines like **77** with dimethyl acetylenedicarboxylate (DMAD) and methyl pyruvate (MP) to generate oxazino pyridine **78** as the actual electron-rich diene *in situ*. This intermediate was shown to react with a variety of cyclic and acyclic alkyne dienophiles, including cyclooctyne (**38**) as well as its derivative **40** to furnish the aromatic system after *retro*-cycloaddition.[151] Another skeletal editing approach based on a de-aromatization/cycloaddition/*retro*-cycloaddition sequence was developed by Bouffard and co-workers for the functionalization of non-activated arenes.[152] The key component in their reaction was the *in situ* generated 1,3-diaza-2-azoniaallene cation **79** that undergoes a de-aromative 1,3-dipolar cycloaddition with substituted benzenes like *o*-xylene (**80**) to afford the stable and isolable triazolinium cycloadduct **81** (Scheme 17, B). This adduct acts as diene in follow-up DA reactions with various reactive alkynes, including cyclooctyne (**38**) and its derivative **40**.[152]

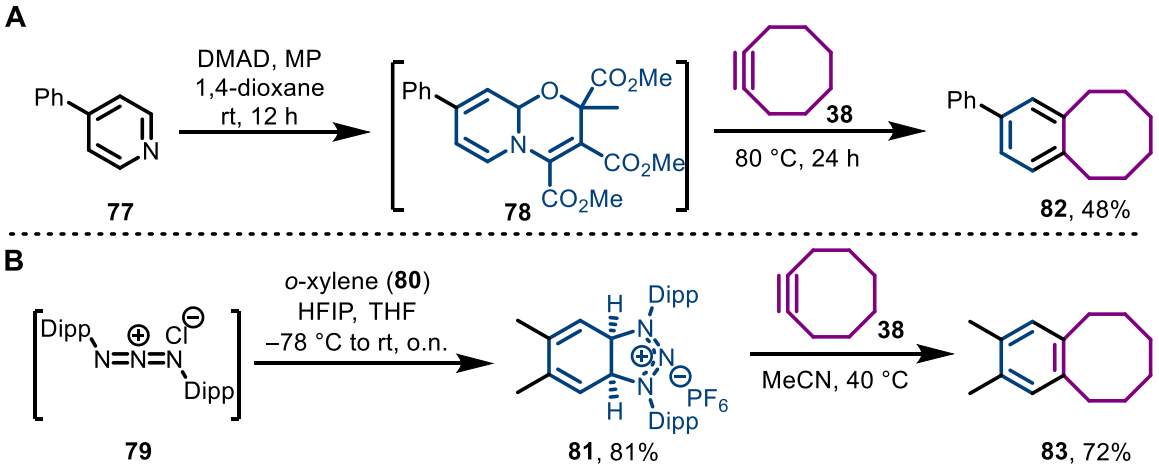

Scheme 17. A) Skeletal editing of pyridines by Studer and co-workers.[151] B) Skeletal editing of arenes by Bouffard and co-workers.[152]

As another highly reactive diene species, *o*-quinodimethanes (*o*-QDMs) found broad application in organic synthesis.[153,154] Siegel and co-workers used a DA reaction of cyclooctyne (**38**) and *in situ* generated *o*-QDM **84** to synthesize the cyclooctene-fused PAH **85** (Scheme 18). The reactive diene was obtained from 1,2-bis(bromomethyl)-arene **86** via an anion-induced 1,4-elimination and directly trapped with the strained alkyne. The subsequent oxidation to the final aromatic structure was achieved in one-pot by either stirring the reaction mixture open to air for prolonged time or treating it with 2,3-dichloro-5,6-dicyano-1,4-benzoquinone (DDQ).[155]

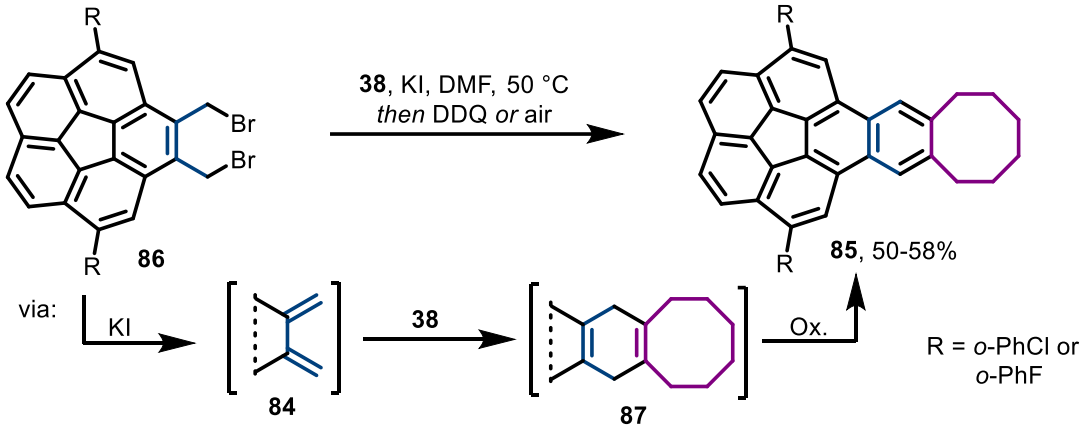

Scheme 18. DA reaction of cyclooctyne (**38**) and *o*-QDM **84** by Siegel and co-workers.[155]

2.3 Ring expansion reactions

2.3.1 General Principle in the Construction of Medium-Sized Rings

Besides the functionalization of readily accessible eight-membered ring systems, an alternative approach to build up arene-annulated cyclooctanoids involves ring expansion reactions. The key principle of this strategy is to synthesize ring systems that are generally considered less challenging to make, mostly 5- to 7-membered rings, and subsequently expand these either by breaking the shared bond of annulated bicycles or by inserting side chains.[156] In that way, high entropic and enthalpic barriers associated with the formation of MSRs from linear precursors, as described in section 2.1, can be avoided. However, an appropriate driving force is required to compensate for the fact that the formation of MSRs from normal-sized ones is generally thermodynamically unfavorable. According to Clarke and Unsworth, the main driving forces in this regard are neutralization or stabilization of charged intermediates, aromatization, relief of ring strain, radical stabilization, and favorable changes in overall bonding energies.[71]

2.3.2 Electrocyclic Ring Expansion Reactions

Pericyclic reactions, including sigmatropic rearrangements and electrocyclic reactions, represent one of the most common strategies for synthesizing MSRs via ring expansion, alongside fragmentation-type and radical-mediated ring openings.[156] In 2021, Wegner and co-workers establishes an efficient method to synthesize benzo-fused MSRs in one step from readily accessible phthalazines and cyclic enamines via

an IEDDA/photo-induced ring-opening (PIRO) domino sequence (Scheme 19).[157] The reaction follows the same catalytic principle as previously shown in Scheme 16, using the BDLA **73** to activate the diazine. In contrast to the reactions described above, the utilization of alkene dienophiles rather than alkynes furnishes a highly reactive *o*-QDM intermediate **88** after the extrusion of nitrogen.[158] This intermediate can be used to initiate different domino processes depending on the reaction conditions and the nature of the dienophile.[159–165] When cyclic enamines like **89** are used, a photo-induced electrocyclic ring opening transforms the *o*-QDM intermediate **88** into medium-sized cycles while regaining the aromaticity of the fused six-membered ring.[157] While this method proved to be valuable in the synthesis of nine- and eleven-membered ring structures, it doesn't provide access to eight-membered carbo- or heterocycles.

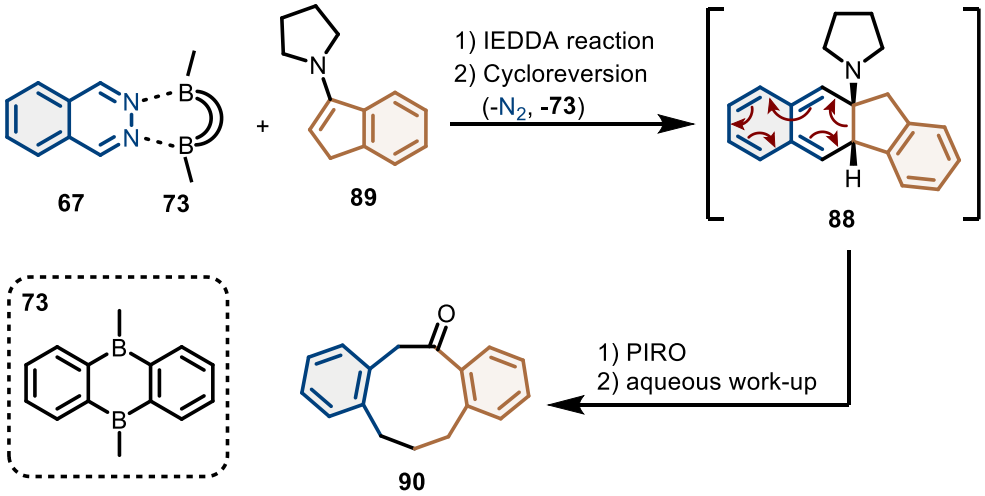

Scheme 19. BDLA-catalyzed IEDDA/PIRO domino reaction for the synthesis of arene-fused MSRs by Wegner and co-workers.[157]

A corresponding electrocyclic reaction involving the formation of an eight-membered ring was firstly described by Cope and co-workers, who investigated the valence tautomeric equilibrium of bicyclo[4.2.0]octa-2,4-diene (BCOD) (**91**) and cycloocta-1,3,5-triene (COTR) (**92**) (Scheme 20).[166] According to the Woodward–Hoffmann rules, this 6π electrocyclic reaction proceeds in a disrotatory fashion under thermal conditions. The isomerization represents a dynamic equilibrium where the monocyclic COTR **92** is energetically favored by 6.3 kJ/mol at 100 °C.[167,168] Due to the small energetic difference, the introduction of substituents or additional annulated rings can completely shift the equilibrium to one or the other side through steric or electronic effects.[167–171] Huisgen and co-workers demonstrated that by increasing the number of substituents at the 7- and 8-position of the COTR, the equilibrium is shifted toward the bicyclic structure **91**. The exact ratio of BCOD to COTR depends on the nature of the substituents and their relative configuration (Scheme 20).[168] In contrast, substituents at the 1- and 6-position were reported to shift the equilibrium toward the monocyclic form.[169]

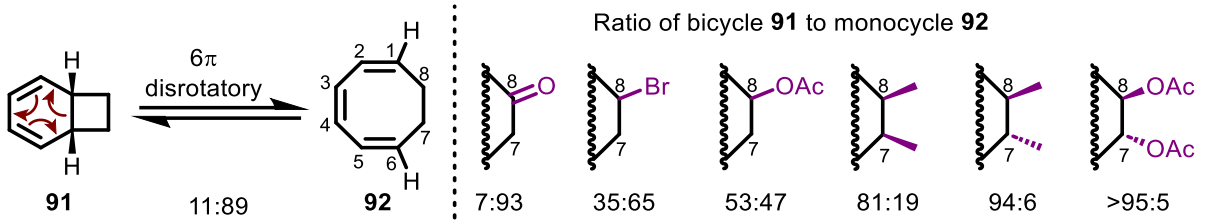

Scheme 20. Influence of different substituents at the 7- and 8-position on the dynamic equilibrium between BCOD (**91**) and COTR (**92**). Depicted ratios were determined at 60 °C.[168]

Paquette and co-workers investigated different aza-analogues of the system and found that the bicyclic form is heavily favored in all cases (Scheme 21, A).[172] Especially sulfonamides **93c** and **93d** were found to purely exist in the aza-BCOD form **93** rather than the aza-COTR form **94**, which was attributed to the greater steric interference between the sulfonamide group and the methylene protons in the monocyclic structure. This reactivity was also observed by Davies and co-workers in the rhodium-catalyzed intramolecular domino reaction of vinyldiazomethanes **95** leading to aza-BCODs **96** (Scheme 21, B).[173,174] The suggested reaction mechanism involves the formation Boc-protected azocine **97** via an 8π electrocyclic ring closure followed by a 6π electrocyclic ring contraction.

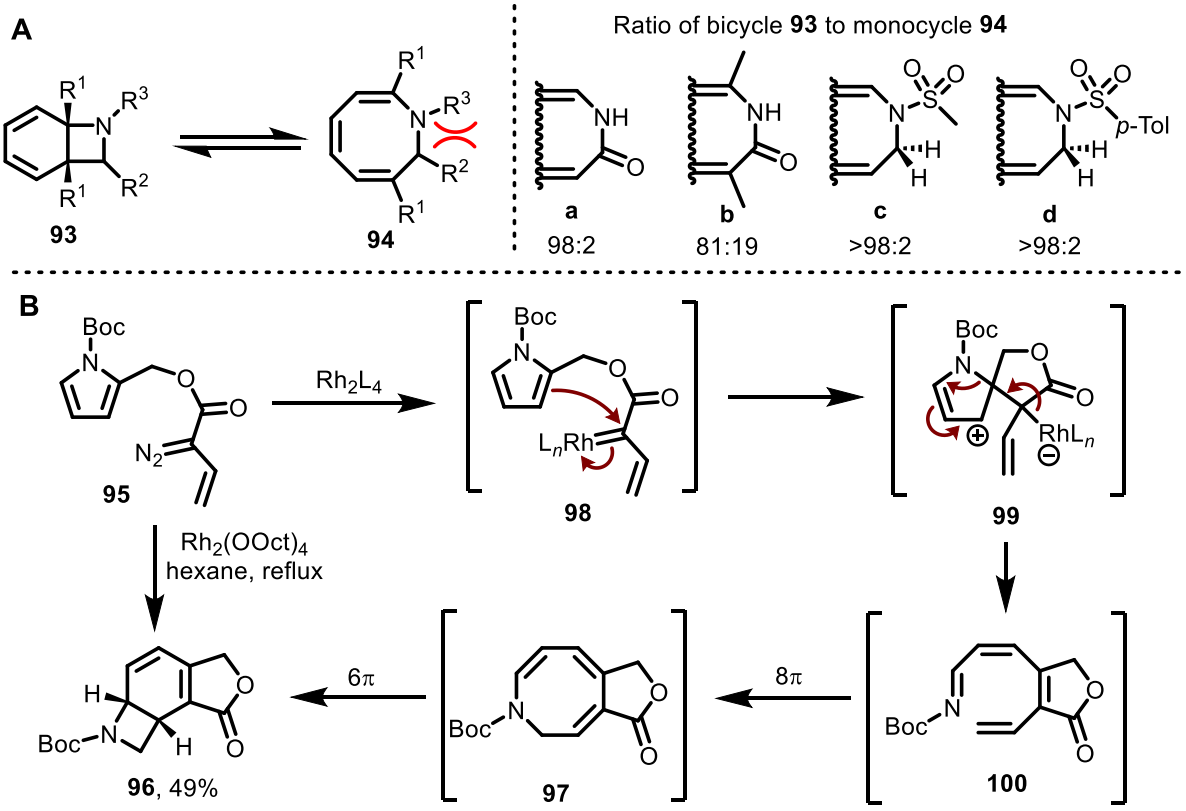

Scheme 21. A) Influence of substituents on the equilibrium between aza-BCOD **93** and aza-COTR **94**.[172] B) Suggested reaction mechanism for the formation of aza-BCOD **96** from vinyldiazomethane **95** by Davies and co-workers.[173,174]

A contrasting way to obtain COTR structures from the corresponding bicyclic isomers was shown by Greenfield and Mackenzie who reported the reaction of substituted cyclopentadienones **101** with the cycobutene dienophile **102** (Scheme 22). The initial DA cycloaddition furnishes a bridged intermediate that yields BCODs **103** after extrusion of carbon monoxide. Depending on the substitution pattern of the employed dienes **101**, the formation of BCODs **103** or COTR **104** can be favored.[170]

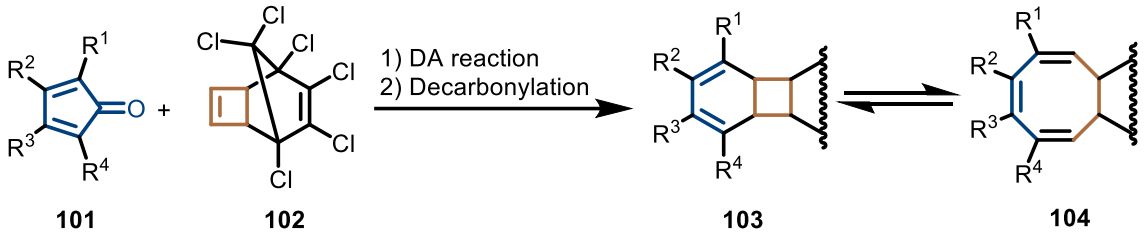

Scheme 22. DA/*retro*-DA/ring expansion sequence by Greenfield and Mackenzie (R^1 - R^4 = H, Ph or Me).[170]

The high reactivity of cyclobutene dienophiles forms the basis of this DA/*retro*-DA/ring expansion sequence. Sauer and co-workers demonstrated in 1990 that replacing cyclopentene with cyclobutene in the IEDDA reaction with substituted tetrazine results in a 14-fold increase in reaction rate.[175] Based on computational analysis, Houk and co-workers attributed this increase in IEDDA reactivity observed with decreasing ring size to more favorable secondary orbital interactions in smaller ring alkenes rather than to simple strain release.[176]

In this thesis, a strategy similar to that of Greenfield and Mackenzie was employed for the synthesis of arene-annulated eight-membered nitrogen heterocycles based on the electrocyclic ring opening of an aza-BCOD intermediate (Scheme 23). Building on the previous work by our group shown in Scheme 19, phthalazine (**67**) is activated using the BDLA catalyst **73** and treated with Boc-protected 2-azetine **105** as dienophile. Extrusion of nitrogen after the initial cycloaddition furnishes the aza-BCOD intermediate **106** that is subsequently converted into the desired azocine **107**. It was reasoned that the formation of an annulated aromatic ring provides the driving force to shift the equilibrium toward the MSR structure and prevented its back reaction.[177]

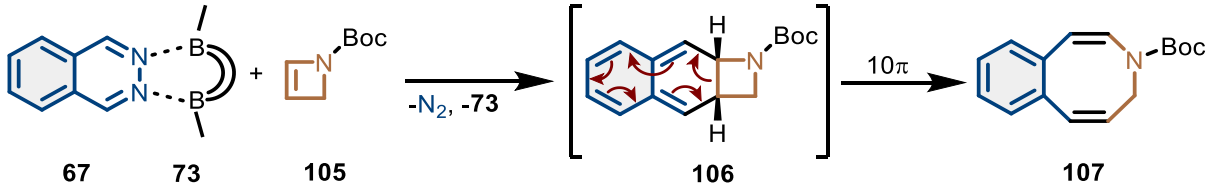

Scheme 23. BDLA-catalyzed IEDDA/thermal ring expansion sequence for the synthesis of arene-fused azocines.[177]

3 Contributions to the Literature

3.1 Bidentate Lewis Acid-Catalyzed Inverse Electron-Demand Diels–Alder Reaction of Phthalazines and Cyclooctynes

Reference: M. Große, H. A. Wegner, *Synlett* **2024**, *35*, 1019.

DOI: 10.1055/a-2204-9522

“Herein we report a method for facilitating the inverse-electron-demand Diels–Alder reaction of 1,2-diazines and cyclooctynes by utilizing a boron-based bidentate Lewis acid catalyst. Readily available electron-deficient and electron-rich phthalazines proved to be suitable substrates in this transformation. The described method enables the facile construction of diversely substituted polycyclic aromatic hydrocarbons fused to eight-membered carbocycles.”

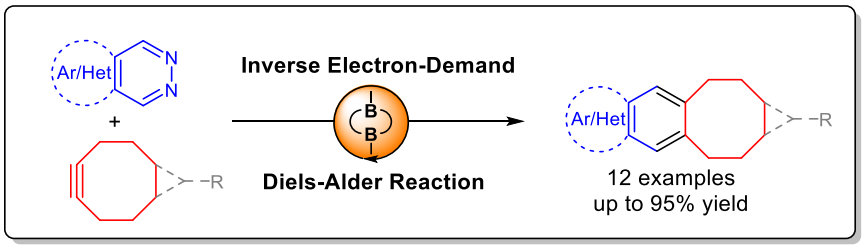

Synlett M. Große, H. A. Wegner Cluster

Bidentate Lewis Acid-Catalyzed Inverse Electron-Demand Diels–Alder Reaction of Phthalazines and Cyclooctynes

Michel Große[a,b]
Hermann A. Wegner*[a,b]

[a] Institute of Organic Chemistry, Justus Liebig University, Heinrich-Buff-Ring 17, 35392 Giessen, Germany
Hermann.A.Wegner@org.chemie.uni-giessen.de
[b] Center of Material Research (LaMa/ZfM), Justus Liebig University, Heinrich-Buff-Ring 16, 35392 Giessen, Germany

Published as part of the Cluster
Chemical Synthesis and Catalysis in Germany

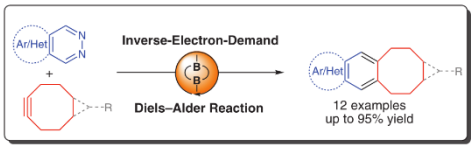

Received: 15.10.2023
Accepted after revision: 06.11.2023
Published online: 06.11.2023 (Accepted Manuscript), 13.12.2023 (Version of Record)
DOI: 10.1055/a-2204-9522; Art ID: ST-2023-10-0462-L
Crowd-Reviewed

Abstract Herein we report a method for facilitating the inverse-electron-demand Diels–Alder reaction of 1,2-diazines and cyclooctynes by utilizing a boron-based bidentate Lewis acid catalyst. Readily available electron-deficient and electron-rich phthalazines proved to be suitable substrates in this transformation. The described method enables the facile construction of diversely substituted polycyclic aromatic hydrocarbons fused to eight-membered carbocycles.

Key words cycloaddition, diazines, cyclooctyne, bidentate catalysis, polycyclic aromatic hydrocarbons, Diels–Alder reactions

The inverse-electron-demand Diels–Alder (IEDDA) reaction has emerged as a powerful and versatile synthetic tool for the construction of various complex molecular architectures.[1] This cycloaddition reaction has been utilized extensively in natural product total synthesis,[2] chemical biology,[3] and materials science.[1] In contrast to the requirements for normal-electron-demand Diels–Alder reactions, electron-poor dienes and electron-rich dienophiles are needed for IEDDA reactions to take place. As a commonly used diene, 1,2,4,5-tetrazine has found broad application in bioorthogonal chemistry and the construction of functional materials.[4] Due to the low-energy LUMO of this compound, cycloaddition reactions with tetrazine usually proceed rapidly and at low temperatures without the need for an additional catalyst.[5] By contrast, azines containing fewer nitrogen atoms require much harsher conditions or additional modes of activation to enable IEDDA reactions.[6]

In the past decade, we established the bidentate Lewis acid **BDLA** as an effective catalyst for the activation of phthalazines **1** for IEDDA reactions (Scheme 1).[7] The boron-based catalyst acts by lowering the LUMO energy of the diazine through complexation, facilitating the cycloaddition with various dienophiles like enamines or enol ethers.[8] Through subsequent cycloreversion, N_2 is released and, depending on the reaction conditions and the dienophile, different domino processes are initiated.[9] Another way to accelerate IEDDA reactions is by raising the HOMO energy level of the dienophile, which can be achieved not only by attaching electron-donating groups but also by implementing ring strain into cyclic dienophiles.[3b]

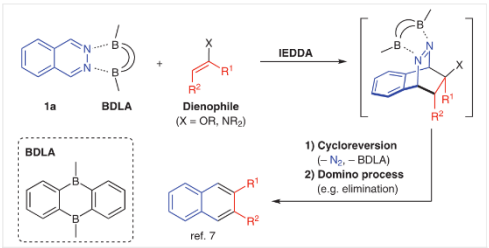

Scheme 1 Basic principle of the BDLA-catalyzed IEDDA reaction

As demonstrated by Sauer et al., a change from open-chain alkynes to strained cyclooctyne (**2**) significantly increases the reaction rate of the cycloaddition with 1,2,4,5-tetrazine.[5,10] Further fine-tuning of the HOMO–LUMO energy gap can be realized by installing different substituents at the cyclooctyne core.[11] Therefore, cyclooctyne derivatives have found broad application as highly reactive alkynes in bioorthogonal chemistry and materials science,[12] mostly with 1,2,4,5-tetrazines or 1,2,4-triazines as reaction partners. However, the IEDDA reaction of cyclooctynes with much less reactive 1,2-diazines has not been reported so far, to the best of our knowledge. Therefore, we envisaged to facilitate this reaction by making use of the bidentate Lewis acid catalyst **BDLA**.

Georg Thieme Verlag KG, Rüdigerstraße 14, 70469 Stuttgart, Germany

To begin our investigation with a comparatively reactive 1,2-diazine, we subjected the electron-deficient nitrophthalazine **1b** to the IEDDA reaction with cyclooctyne (**2**) (Table 1, entries 1–3) and analyzed the reactions by ^{1}H NMR spectroscopy. In all cases, no formation of side products was observed and the NMR spectra of the crude reaction mixtures only showed signals of the desired product **3b** and unreacted phthalazine **1b** in varying ratios. In the presence of 5 mol% **BDLA** catalyst at 40 °C, 71% of the phthalazine was converted into the substituted naphthalene **3b**. By contrast, only 43% conversion was observed without the catalyst, a result indicating that the **BDLA** indeed catalyzes the IEDDA reaction efficiently. Upon raising of the temperature to 80 °C, full conversion was observed and naphthalene **3b** was isolated in 95% yield. A change of the 1,2-diazine to the electron-neutral phthalazine **1a** resulted in only 50% conversion in the presence of the catalyst, even at a higher temperature of 100 °C (Table 1, entry 5). An increase in the amount of cyclooctyne (**2**) from 1.3 to 2.0 equivalents resulted in nearly full conversion and led to the isolation of naphthalene **3a** in 86% yield (Table 1, entry 6).

Table 1 Optimization of the Reaction Conditions[a]

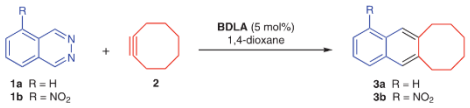

Entry	R	Temp (°C)	Time (h)	**3**:**1**[b] (yield)
1[c]	NO_2	40	72	43:57
2	NO_2	40	72	71:29
3	NO_2	80	24	>99:1 (95%)
4[c]	H	100	48	33:77
5	H	100	48	50:50
6[d]	H	100	48	94:6 (86%)

[a] Reaction conditions: 1,2-Diazine **1a** or **b** (0.10 mmol, 1.0 equiv), cyclooctyne (**2**; 0.13 mmol, 1.3 equiv), **BDLA** (5.0 µmol, 5.0 mol%), and 1,4-dioxane (1 mL).
[b] Ratio was determined by ^{1}H NMR spectroscopy of the crude product. Yields of isolated products are given in brackets.
[c] Reaction performed without catalyst.
[d] Reaction performed with 2.0 equivalents of cyclooctyne.

To explore the scope of dienes in this transformation, we screened differently substituted 1,2-diazines (**1c–l**; Scheme 2), most of which were readily available from the corresponding aldehydes by a one-pot procedure previously developed in our laboratory.[13] As expected, phthalazines carrying electron-withdrawing groups (**1c**, **d**, and **e**) gave the corresponding naphthalenes **3c**, **d**, and **e** in very good to excellent yields after the IEDDA reaction at 80 °C.

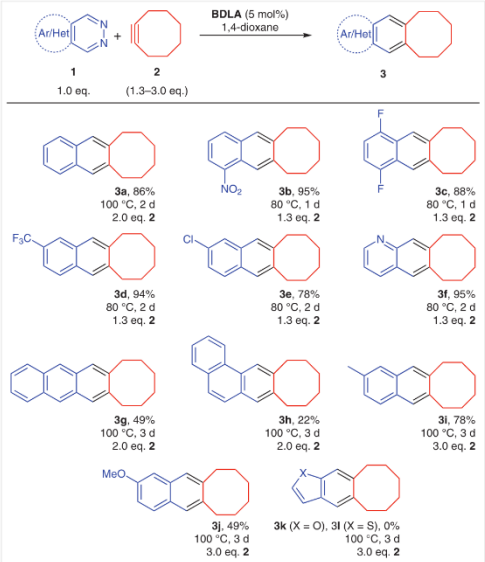

Scheme 2 Scope of 1,2-diazines in the IEDDA reaction with cyclooctyne (**2**)

Similarly, the substituted quinoline **3f** was obtained from pyridopyridazine **1f** in nearly quantitative yield under the same conditions. Benzo[*g*]phthalazine (**1g**) also smoothly underwent the IEDDA reaction to form the anthracene derivative **3g**. However, the yield was diminished by the formation of a side product through Diels–Alder reaction of the excess cyclooctyne with the central ring of the newly formed anthracene. In the case of benzo[*f*]phthalazine (**1h**), low conversion was observed by ^{1}H NMR spectroscopic analysis of the crude product mixture and the desired phenanthrene **3h** was only isolated in 22% yield. This might be attributable to the greater resonance stabilization and aromatic character of phenanthrene in comparison with anthracene,[14] which results in lower reactivity of benzo[*f*]phthalazine (**1h**) relative to benzo[*g*]phthalazine (**1g**). Even the more electron-rich methyl- and methoxy-substituted phthalazines **1i** and **1j** underwent the IEDDA reaction to give the substituted naphthalenes **3i** and **3j**, respectively. However, 3.0 equivalents of cyclooctyne (**2**) were necessary to obtain satisfactory yields. Only in the cases of furopyridazine **1k** and thienopyridazine **1l** no product was formed, and the unreacted diazines were recovered. We rationalized this outcome by the lower aromatic character of furan and thiophene relative to that of benzene.[15] As a consequence, the initial cycloaddition step with either furopyridazine **1k**

or thienopyridazine **1l** would lead to a greater net loss in aromaticity relative to the cycloaddition with phthalazine (**1a**).

As a readily available and versatile cyclooctyne derivative, bicyclo[6.1.0]non-4-yn-9-ylmethanol (**BCN**) has found broad application in bioorthogonal chemistry.[16] Therefore, we synthesized ***exo*-BCN** and subjected it to the IEDDA reaction with two different phthalazines (**1a** and **1c**) (Table 2). In accordance with the reported reactivity enhancement of cyclooctyne by cyclopropane annulation,[11,17] ***exo*-BCN** proved to be much more reactive in the IEDDA reaction with phthalazines than **2**. Hence, the reaction temperature could be lowered to 40 °C.

Table 2 IEDDA Reaction of Phthalazines (**1**) with ***exo*-BCN**[a]

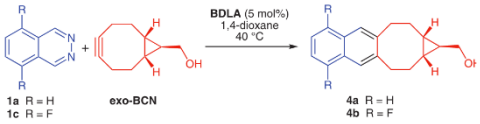

Entry	R	Time (h)	**4**:1[b] (Yield)
1[c]	F	48	93:7 (80%)
2	F	48	>99:1 (90%)
3[c]	H	72	38:62 (28%)
4	H	72	66:44 (52%)

[a] Reaction conditions: phthalazine **1a** or **c** (0.10 mmol, 1.0 equiv), ***exo*-BCN** (0.11 mmol, 1.1 equiv), **BDLA** (5.0 µmol, 5.0 mol%), and 1,4-dioxane (1 mL).
[b] Ratio was determined by ^{1}H NMR spectroscopy of the crude product. Yields of isolated products are given in brackets.
[c] Reaction performed without catalyst.

With the electron-deficient difluorophthalazine **1c**, over 90% conversion was achieved in the presence or absence of **BDLA** catalyst (Table 2, entries 1 and 2). However, with the much less reactive unsubstituted phthalazine (**1a**), the conversion was almost doubled by the use of the catalyst compared to that in the uncatalyzed reaction (Table 2, entries 3 and 4). Notably, **BDLA** was active even in the presence of the unprotected alcohol.

In summary, we have developed a convenient method for facilitating the IEDDA reaction of phthalazines **1** and cyclooctynes **2** or ***exo*-BCN** by employing the bidentate Lewis acid catalyst **BDLA**. Moderate to excellent yields can be achieved with various substituted phthalazines, including *N*-heterocyclic (**1f**) and benzophthalazines (**1g**,**h**). The presented method provides rapid access to (substituted) polycyclic aromatic hydrocarbons fused to eight-membered carbocycles, a class of compounds that has recently received considerable attention in materials science and chemical sensing.[18–20]

Conflict of Interest

The authors declare no conflict of interest.

Funding Information

The authors acknowledge the LOEWE Program of Excellence of the Federal State of Hesse (LOEWE Focus Group PriOSS 'Principles of On-Surface Synthesis') for financial support.

Acknowledgment

The authors thank the Organic Chemistry Analytics Department (Institute of Organic Chemistry, Justus Liebig University, Heinrich-Buff-Ring 17, Giessen) for NMR spectroscopy and HRMS measurements.

Supporting Information

Supporting information for this article is available online at https://doi.org/10.1055/a-2204-9522.

References and Notes

(1) Png, Z. M.; Zeng, H.; Ye, Q.; Xu, J. *Chem. Asian J.* **2017**, *12*, 2142.
(2) (a) Zhang, J.; Shukla, V.; Boger, D. L. *J. Org. Chem.* **2019**, *84*, 9397. (b) Huang, G.; Kouklovsky, C.; de La Torre, A. *Chem. Eur. J.* **2021**, *27*, 4760.
(3) (a) Mayer, S.; Lang, K. *Synthesis* **2017**, *49*, 830. (b) Oliveira, B. L.; Guo, Z.; Bernardes, G. J. L. *Chem. Soc. Rev.* **2017**, *46*, 4895. (c) Pagel, M. *J. Pept. Sci.* **2019**, *25*, e3141. (d) Haiber, L. M.; Kufleitner, M.; Wittmann, V. *Front. Chem.* **2021**, *9*, 654932.
(4) (a) Blackman, M. L.; Royzen, M.; Fox, J. M. *J. Am. Chem. Soc.* **2008**, *130*, 13518. (b) Devaraj, N. K.; Weissleder, R.; Hilderbrand, S. A. *Bioconjugate Chem.* **2008**, *19*, 2297. (c) Pipkorn, R.; Waldeck, W.; Didinger, B.; Koch, M.; Mueller, G.; Wiessler, M.; Braun, K. *J. Pept. Sci.* **2009**, *15*, 235. (d) Wiessler, M.; Waldeck, W.; Kliem, C.; Pipkorn, R.; Braun, K. *Int. J. Med. Sci.* **2009**, *7*, 19. (e) Knall, A.-C.; Kovačič, S.; Hollauf, M.; Reishofer, D.; Saf, R.; Slugovc, C. *Chem. Commun.* **2013**, *49*, 7325. (f) Ye, Q.; Neo, W. T.; Lin, T.; Song, J.; Yan, H.; Zhou, H.; Shah, K. W.; Chua, S. J.; Xu, J. *Polym. Chem.* **2015**, *6*, 1487. (g) Knall, A.-C.; Jones, A. O. F.; Kunert, B.; Resel, R.; Reishofer, D.; Zach, P. W.; Kirkus, M.; McCulloch, I.; Rath, T. *Monatsh. Chem.* **2017**, *148*, 855. (h) Edem, P. E.; Sinnes, J.-P.; Pektor, S.; Bausbacher, N.; Rossin, R.; Yazdani, A.; Miederer, M.; Kjær, A.; Valliant, J. F.; Robillard, M. S.; Rösch, F.; Herth, M. M. *EJNMMI Res.* **2019**, *9*, 49. (i) Ravasco, J. M. J. M.; Coelho, J. A. S. *J. Am. Chem. Soc.* **2020**, *142*, 4235.
(5) Sauer, J.; Heldmann, D. K.; Hetzenegger, J.; Krauthan, J.; Sichert, H.; Schuster, J. *Eur. J. Org. Chem.* **1998**, 2885.
(6) (a) Boger, D. L.; Coleman, R. S. *J. Org. Chem.* **1984**, *49*, 2240. (b) Anderson, E. D.; Boger, D. L. *J. Am. Chem. Soc.* **2011**, *133*, 12285. (c) Türkmen, Y. E.; Montavon, T. J.; Kozmin, S. A.; Rawal, V. H. *J. Am. Chem. Soc.* **2012**, *134*, 9062. (d) Sumaria, C. S.; Türkmen, Y. E.; Rawal, V. H. *Org. Lett.* **2014**, *16*, 3236. (e) Glinkerman, C. M.; Boger, D. L. *Org. Lett.* **2015**, *17*, 4002. (f) Glinkerman, C. M.; Boger, D. L. *J. Am. Chem. Soc.* **2016**, *138*, 12408. (g) Le Fouler, V.; Chen, Y.; Gandon, V.; Bizet, V.; Salomé, C.; Fessard, T.; Liu, F.; Houk, K. N.; Blanchard, N. *J. Am. Chem. Soc.* **2019**, *141*, 15901.

(7) Kessler, S. N.; Neuburger, M.; Wegner, H. A. *Eur. J. Org. Chem.* **2011**, 3238.
(8) Wegner, H.; Kessler, S. *Synlett* **2012**, *23*, 699.
(9) (a) Kessler, S. N.; Neuburger, M.; Wegner, H. A. *J. Am. Chem. Soc.* **2012**, *134*, 17885. (b) Schweighauser, L.; Bodoky, I.; Kessler, S.; Häussinger, D.; Wegner, H. *Synthesis* **2012**, *44*, 2195. (c) Schweighauser, L.; Bodoky, I.; Kessler, S. N.; Häussinger, D.; Donsbach, C.; Wegner, H. A. *Org. Lett.* **2016**, *18*, 1330. (d) Ahles, S.; Götz, S.; Schweighauser, L.; Brodsky, M.; Kessler, S. N.; Heindl, A. H.; Wegner, H. A. *Org. Lett.* **2018**, *20*, 7034. (e) Ahles, S.; Ruhl, J.; Strauss, M. A.; Wegner, H. A. *Org. Lett.* **2019**, *21*, 3927. (f) Ruhl, J.; Ahles, S.; Strauss, M. A.; Leonhardt, C. M.; Wegner, H. A. *Org. Lett.* **2021**, *23*, 2089. (g) Beeck, S.; Ahles, S.; Wegner, H. A. *Chem. Eur. J.* **2022**, *28*, e202104085.
(10) Thalhammer, F.; Wallfahrer, U.; Sauer, J. *Tetrahedron Lett.* **1990**, *31*, 6851.
(11) Chen, W.; Wang, D.; Dai, C.; Hamelberg, D.; Wang, B. *Chem. Commun.* **2012**, *48*, 1736.
(12) (a) Borrmann, A.; Milles, S.; Plass, T.; Dommerholt, J.; Verkade, J. M. M.; Wiessler, M.; Schultz, C.; van Hest, J. C. M.; van Delft, F. L.; Lemke, E. A. *ChemBioChem* **2012**, *13*, 2094. (b) Chupakhin, E. G.; Krasavin, M. Y. *Chem. Heterocycl. Comp.* **2018**, *54*, 483. (c) Glaser, T.; Meinecke, J.; Freund, L.; Länger, C.; Luy, J.-N.; Tonner, R.; Koert, U.; Dürr, M. *Chem. Eur. J.* **2021**, *27*, 8082. (d) Glaser, T.; Meinecke, J.; Länger, C.; Heep, J.; Koert, U.; Dürr, M. *J. Phys. Chem. C* **2021**, *125*, 4021. (e) Šlachtová, V.; Bellová, S.; La-Venia, A.; Galeta, J.; Dračínský, M.; Chalupský, K.; Dvořáková, A.; Mertlíková-Kaiserová, H.; Rukovanský, P.; Dzijak, R.; Vrabel, M. *Angew. Chem. Int. Ed.* **2023**, *62*, e202306828.
(13) Kessler, S. N.; Wegner, H. A. *Org. Lett.* **2012**, *14*, 3268.
(14) Poater, J.; Duran, M.; Solà, M. *Front. Chem.* **2018**, *6*, 561.
(15) Dey, S.; Manogaran, D.; Manogaran, S.; Schaefer, H. F. *J. Phys. Chem. A* **2018**, *122*, 6953.
(16) (a) Dommerholt, J.; Schmidt, S.; Temming, R.; Hendriks, L. J. A.; Rutjes, F. P. J. T.; van Hest, J. C. M.; Lefeber, D. J.; Friedl, P.; van Delft, F. L. *Angew. Chem. Int. Ed.* **2010**, *49*, 9422. (b) Lang, K.; Davis, L.; Wallace, S.; Mahesh, M.; Cox, D. J.; Blackman, M. L.; Fox, J. M.; Chin, J. W. *J. Am. Chem. Soc.* **2012**, *134*, 10317. (c) Li, F.; Dong, J.; Hu, X.; Gong, W.; Li, J.; Shen, J.; Tian, H.; Wang, J. *Angew. Chem. Int. Ed.* **2015**, *127*, 4680.
(17) Meier, H.; Schuh-Popitz, C.; Peiersen, H. *Angew. Chem. Int. Ed.* **1981**, *20*, 270.
(18) (a) Kobryn, L.; Henry, W. P.; Fronczek, F. R.; Sygula, R.; Sygula, A. *Tetrahedron Lett.* **2009**, *50*, 7124. (b) Yuan, C.; Saito, S.; Camacho, C.; Irle, S.; Hisaki, I.; Yamaguchi, S. *J. Am. Chem. Soc.* **2013**, *135*, 8842. (c) Kotani, R.; Sotome, H.; Okajima, H.; Yokoyama, S.; Nakaike, Y.; Kashiwagi, A.; Mori, C.; Nakada, Y.; Yamaguchi, S.; Osuka, A.; Sakamoto, A.; Miyasaka, H.; Saito, S. *J. Mater. Chem. C* **2017**, *5*, 5248. (d) Yamakado, T.; Takahashi, S.; Watanabe, K.; Matsumoto, Y.; Osuka, A.; Saito, S. *Angew. Chem. Int. Ed.* **2018**, *57*, 5438.
(19) **General procedure for the BDLA-catalyzed IEDDA reaction**: In a nitrogen-filled glove box, (substituted) phthalazine **1** (0.10 mmol, 1.0 equiv) and **BDLA** catalyst (5.0 µmol, 5.0 mol%) were suspended in anhydrous and degassed 1,4-dioxane (1.0 mL) in a 4 mL screw-cap vial with a stirrer bar. Cyclooctyne (**2**) or ***exo*-BCN** (1.1–3.0 equiv) was added to the mixture, and the vial was sealed and taken out of the glove box. The mixture was stirred at the given temperature for the given time. Afterwards, the reaction mixture was concentrated in vacuo. The ratio of product to unreacted phthalazine was determined by ^{1}H NMR spectroscopic analysis of the crude mixture. The crude mixture was purified by column chromatography (3 g of silica gel) to afford product **3** or **4**
(20) **((1*r*,1a*R*,11a*S*)-1a,2,3,10,11,11a-hexahydro-1*H*-cyclopropa[5,6]cycloocta[1,2-*b*]naphthalen-1-yl)methanol (4a)**: Yield: 13 mg (52%); colorless oil. ^{1}H NMR (400 MHz, $CDCl_3$): δ = 7.76–7.71 (m, 2 H), 7.56 (s, 2 H), 7.41–7.36 (m, 2 H), 3.38 (d, *J* = 6.5 Hz, 2 H), 3.10 (ddd, *J* = 14.1, 8.3, 5.7 Hz, 2 H), 2.92 (dt, *J* = 14.1, 5.8 Hz, 2 H), 2.59–2.45 (m, 2 H), 1.42–1.25 (m, 3 H), 0.77–0.66 (m, 3 H) ppm. ^{13}C NMR (101 MHz, $CDCl_3$): δ = 141.21 (2 C), 132.49 (2 C), 128.04 (2 C), 127.08 (2 C), 125.24 (2 C), 66.78, 33.63 (2 C), 30.16 (2 C), 29.76 (2 C), 22.03. HRMS (ESI): *m*/*z* calcd for $C_{18}H_{20}ONa$: 275.1406 [M + Na]$^+$; found: 275.1406.

3.2 Lewis Acid-Catalyzed Domino Inverse Electron-Demand Diels–Alder/Thermal Ring Expansion Reaction for the Synthesis of Arene-Annulated Eight-Membered Nitrogen Heterocycles

Reference: M. Große, C. M. Leonhardt, P. A. R. Campbell, H. A. Wegner, *Org. Lett.* **2025**, *27*, 4893.

DOI: 10.1021/acs.orglett.5c01150

“A domino inverse electron-demand Diels–Alder reaction/thermal ring expansion sequence was developed to enable the one-step synthesis of arene-annulated eight-membered nitrogen heterocycles from readily available aromatic 1,2-diazines. A boron-based, bidentate Lewis acid catalyst facilitates the initial cycloaddition of Boc-protected 2-azetine with various electron-poor and electron-rich phthalazines. The subsequent electrocyclic ring expansion furnishes azocines fused to differently substituted aromatics, a structural motif that holds vast potential for further derivatization.”

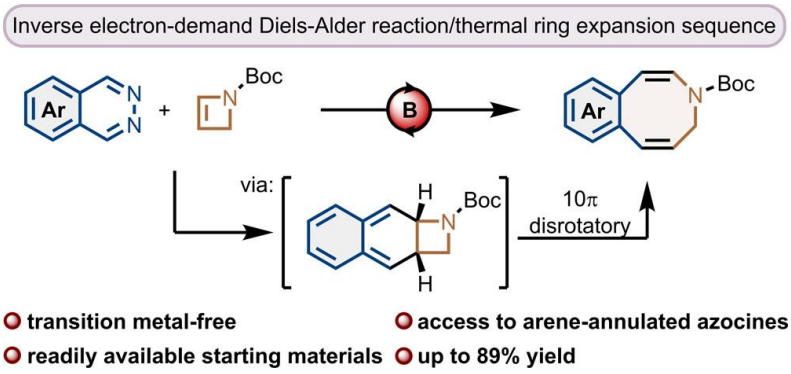

OL Organic Letters

pubs.acs.org/OrgLett

Letter

Lewis Acid-Catalyzed Domino Inverse Electron-Demand Diels–Alder/Thermal Ring Expansion Reaction for the Synthesis of Arene-Annulated Eight-Membered Nitrogen Heterocycles

Michel Große, Christopher M. Leonhardt, Patrick A. R. Campbell, and Hermann A. Wegner*

Cite This: *Org. Lett.* 2025, 27, 4893–4897

Read Online

ACCESS | Metrics & More | Article Recommendations | Supporting Information

ABSTRACT: A domino inverse electron-demand Diels–Alder reaction/thermal ring expansion sequence was developed to enable the one-step synthesis of arene-annulated eight-membered nitrogen heterocycles from readily available aromatic 1,2-diazines. A boron-based, bidentate Lewis acid catalyst facilitates the initial cycloaddition of Boc-protected 2-azetine with various electron-poor and electron-rich phthalazines. The subsequent electrocyclic ring expansion furnishes azocines fused to differently substituted aromatics, a structural motif that holds vast potential for further derivatization.

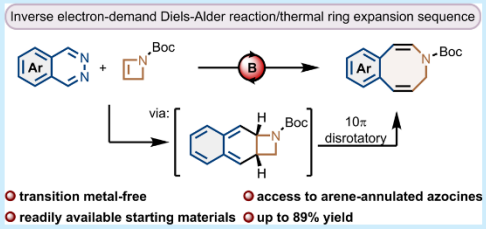

Eight-membered nitrogen-containing heterocycles are widely found in biologically active natural products[1] as well as medicinally relevant synthetic compounds.[2−5] They are commonly regarded as privileged scaffolds for drug discovery owing to their distinctive structural features.[6] In comparison to smaller rings, eight-membered carbo- and heterocycles offer a balance between conformational flexibility and rigidity which can lead to improved binding properties to biological targets by either allowing effective folding into enzymatic pockets[7] or by rigidifying active conformations.[8] In particular, benzannulated azocines are the core structural motif of a variety of synthetic compounds and natural products showing promising biological activity (Figure 1).[9−13]

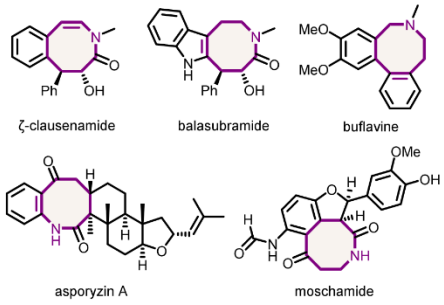

Figure 1. Representative examples of arene-annulated azocine alkaloids.

Consequently, extensive efforts have been made to synthetically access these benzo-fused scaffolds as well as structurally related eight-membered ring systems,[6,14−16] primarily via ring expansion strategies[17−19] or transition metal-promoted cyclizations.[20−23] However, medium-sized heterocycles are still strongly underrepresented in screening libraries and drug approvals,[24] most probably due to the persisting synthetic challenges caused by unfavorable entropic and enthalpic factors.[25,26] Therefore, new general strategies, especially for the synthesis of benzannulated azocines, are highly desirable. In the light of sustainability and the shortage of resources, these strategies should be based on simple, readily available starting materials and work in the absence of transition metals.

In the past, we established the bidentate Lewis acid **BDLA** as an effective catalyst to promote inverse electron-demand Diels–Alder (IEDDA) reactions of phthalazines (**1**) and various dienophiles (Scheme 1a).[27−35] These reactions usually proceed via a reactive *o*-quinodimethane (*o*-QDM) intermediate **2** which is formed after the initial IEDDA-cycloreversion sequence.[36] This reactive intermediate can be utilized to initiate different domino processes, depending on the reaction conditions and the nature of the dienophile. Recently, we have shown that benzannulated, medium-sized carbocycles can be accessed through a photoinduced ring opening of the *o*-

Received: March 21, 2025
Revised: April 23, 2025
Accepted: April 28, 2025
Published: May 1, 2025

https://doi.org/10.1021/acs.orglett.5c01150
Org. Lett. 2025, 27, 4893–4897

Scheme 1. BDLA-Catalyzed IEDDA Reactions for the Construction of Medium-Sized Rings

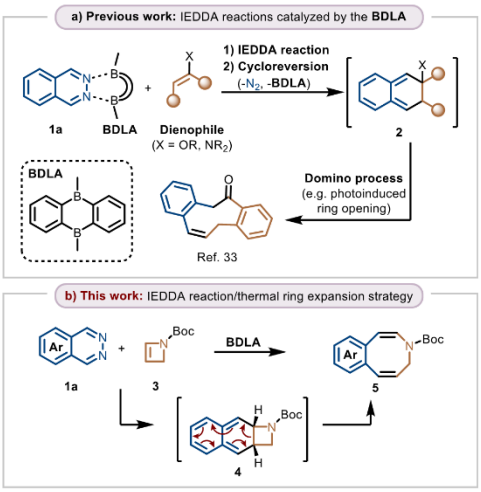

QDM intermediate.[33] We wanted to further expand this methodology to the synthesis arene-annulated, eight-membered nitrogen heterocycles. We envisaged that the use of highly strained 2-azetine **3** as dienophile would afford *o*-QDM intermediate **4**, which would then react under thermal conditions to the desired benzannulated azocine **5** through a 10π disrotatory electrocylic ring expansion (Scheme 1b). Prior reports indicate that analogous 6π azacycles thermodynamically favor the formation of the bridged four-membered structure.[37] However, we hypothesized that in azocine **5**, the formation of an annulated aromatic ring would significantly shift the equilibrium toward the ring-expanded product.

We decided to utilize Boc-protected azetine **3** as it can be easily prepared from commercial *tert*-butyl 3-hydroxyazetidine-1-carboxylate over two steps and should allow easy functionalization of the final azocine at the nitrogen atom. We commenced our study by treating very reactive, electron-poor difluorophthalazine **1b** with azetine **3** (1.2 equiv) in the presence and absence of the **BDLA** (5 mol %) at 70 °C (Table 1, Entries 1 and 2). Without the catalyst, no visible consumption of phthalazine **1b** was observed by ^{1}H NMR spectroscopic analysis and no traces of the desired product were detected. To our delight, in the presence of the **BDLA** catalyst, all of the staring material was consumed and the desired azocine **5b** could be isolated in 25% yield.

A substantial amount of different, chromatographically inseparable byproducts was obtained as well. Judging by high resolution mass spectrometry, we hypothesized that these byproducts were a mixture of regio- and stereoisomers formed by a follow-up Diels–Alder reaction of *o*-QDM intermediate **4** with another equivalent of azetine **3**. To prove this hypothesis, we treated phthalazine **1b** with an excess of azetine **3**, which suppressed the formation of azocine **5b** and resulted almost exclusively in a mixture of double Diels–Alder adducts, the structure of which was further proven by X-ray crystallography of *meso* compound **6** after partial purification via preparative HPLC (Scheme 2 and the Supporting Information (SI)).

Table 1. Optimization of the Reaction Conditions[a]

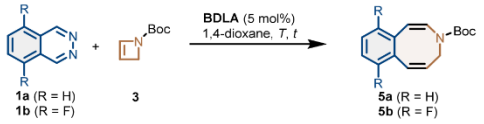

Entry	R	T (°C)	t (h)	Addition of **3**	Yield (%)
1[b]	F	70	20	at once	0
2	F	70	20	at once	25
3	F	70	16	over 10 h	75
4	F	80	22	over 20 h	87
5	H	70	16	over 10 h	12
6	H	90	22	over 20 h	55
7[c]	H	110	22	over 20 h	73

[a]Reaction conditions unless noted otherwise: phthalazine **1a** or **1b** (0.25 mmol, 1.0 equiv) and **BDLA** (13 μmol, 5.0 mol %) in 1,4-dioxane (4 mL), azetine **3** (0.31 mmol, 1.2 equiv) in 1,4-dioxane (1 mL). [b]Reaction was performed without the **BDLA** catalyst. [c]Reaction was performed on a 1.0 mmol scale: phthalazine **1a** (1.0 mmol, 1.0 equiv) and **BDLA** (30 μmol, 3.0 mol %) in diglyme (16 mL), and azetine **3** (1.2 mmol, 1.2 equiv) in diglyme (4 mL) yielded azocine **5a** (188 mg, 73%).

Scheme 2. Synthesis and Crystal Structure of Double Diels–Alder Adducts

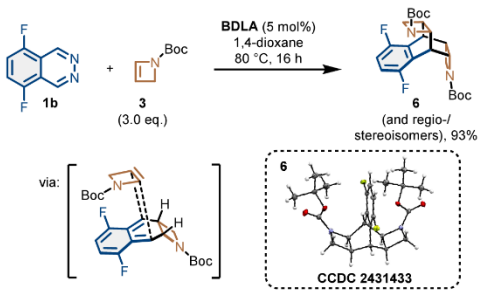

With an explanation for the byproduct formation in hand, we further optimized the conditions for the IEDDA reaction/thermal ring expansion sequence by adding azetine **3** slowly via syringe pump to a mixture of phthalazine **1b** and **BDLA** catalyst to prevent an excess of the dienophile (Table 1, Entries 3 and 4). With a longer addition time of 20 h, the isolated yield of azocine **5b** could be improved to 87%. Changing the diene to electron-neutral, unsubstituted phthalazine (**1a**) led to a significant decrease in product formation, and the temperature had to be increased to 110 °C to furnish azocine **1a** in a good yield of 73% (Table 1, Entries 5 to 7).

With optimized reaction conditions in hand, we set out to explore the scope of this transformation by testing different phthalazines and pyridazino-aromatics (**1c–m**), most of which can be readily synthesized from commercially available aldehydes by a convenient one-pot procedure previously developed in our laboratory (Scheme 3).[38] As expected, all tested diazines carrying electron-withdrawing groups (**1b–j**) underwent the IEDDA reaction smoothly and afforded the desired azocines after ring expansion in good to very good yields up to 89% (Scheme 3). In that way, synthetically valuable functional groups such as esters (**5j**), nitro groups

https://doi.org/10.1021/acs.orglett.5c01150
Org. Lett. 2025, 27, 4893–4897

Scheme 3. Scope of 1,2-Diazines in the IEDDA/Thermal Ring Expansion Reaction[a]

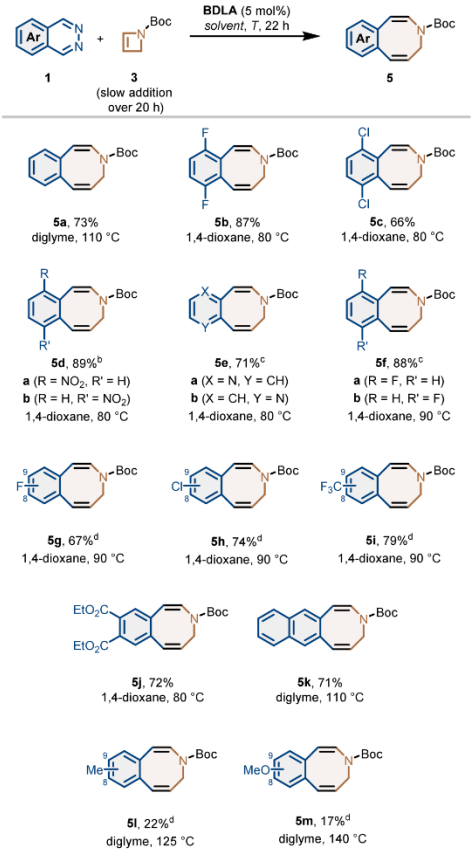

[a]Reaction conditions: phthalazine **1a**−**m** (0.25 mmol, 1.0 equiv) and **BDLA** (13 μmol, 5.0 mol %) in 1,4-dioxane or diglyme (4 mL), azetine **3** (0.31 mmol, 1.2 equiv) in 1,4-dioxane or diglyme (1 mL). [b]Constitutional isomers were separated (**a**, 42%; **b**, 47%). [c]Isolated yield as a mixture of C7/C10-constitutional isomers. [d]Isolated yield as a mixture of C8/C9-constitutional isomers.

(**5d**) or different halogens (**5c,f**−**h**) were introduced at the fused aromatic ring. Furthermore, pyridine-annulated azocine **5e** was obtained in a good yield of 71% from pyridopyridazine **1e**. In the case of monohalogenated phthalazines **1f**−**h** and trifluoromethylated phthalazine **1i**, a slight increase in temperature to 90 °C was required to achieve good yields over 70%. Similarly, benzophthalazine **1k** furnished naphthoazocine **5k** in 71% yield at an elevated reaction temperature of 110 °C. Even electron-rich methyl- (**1l**) and methoxyphthalazine (**1m**) were reactive in this transformation. However, higher temperatures of 125 and 140 °C, respectively, were required for the IEDDA reaction to take place. This led to an increased formation of side products and the desired azocines **5l,m** were isolated in a yield of around 20%.

For all asymmetrically substituted phthalazines, mixtures of regioisomers were obtained in this transformation. In the case of nitrobenzazocine **5d**, both isomers could be separated via column chromatography and were obtained in a ratio of 47:53. Most of the other nonsymmetrically substituted phthalazines yielded a similar ratio of isomers. Only in the case of pyridopyridazine **1e**, the strong polarization of the substrate led to the formation of the major isomer in a 4-fold excess (see the SI). As a final structural proof, we attempted to analyze the ring expansion products via X-ray crystallography. However, all azocines **5a-m** were obtained as oils or amorphous solids, and every attempt to produce single crystals failed. Unexpectedly, we observed the formation of a crystalline dimerization product of azocine **5a** during NMR measurements in nonstabilized $CDCl_3$. After separation of the formed stereoisomers via preparative chiral HPLC, single crystals suitable for X-ray diffraction were obtained. The product was found to be hemiaminal ether **7** formed in the presence of water and catalytic amounts of acid (Figure 2). In that way, we were finally able to confirm the formation of the azocine ring in our IEDDA reaction/thermal ring expansion sequence.

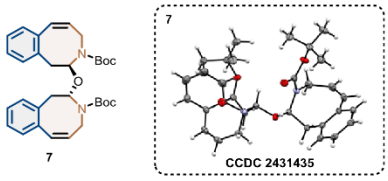

Figure 2. Structure of the hemiaminal ether **7** formed from azocine **5a** in acidic $CDCl_3$ in the presence of water.

In summary, we have developed a novel Lewis acid-catalyzed domino IEDDA/thermal ring expansion reaction that provides rapid access to arene-annulated, eight-membered nitrogen heterocycles. The key to successfully optimizing the reaction was the very slow addition of the azetine dienophile, which suppressed the undesired follow-up Diels−Alder reaction of the highly reactive *o*-QDM intermediate and ensured its conversion via a 10π disrotatory electrocylic ring expansion. Various, readily available phthalazines and pyridazino-aromatics can be used as dienes in this transformation, giving rise to the azocine core structure fused to diversely functionalized aromatics. The electronic nature of the phthalazine was found to be a crucial parameter for this transformation, with electron-poor substrates providing the medium-sized nitrogen heterocycles in high yields up to 89%, whereas electron-neutral and -rich phthalazines required higher temperatures and showed diminished yields. The final proof of the eight-membered ring structure was provided by X-ray crystallography of a hemiaminal ether degradation product. The presented methodology holds great potential to synthetically address different, biologically active azocine natural products as well as their derivatives in order to tap into the full potential of eight-membered nitrogen heterocycles in medicinal chemistry and drug discovery.

■ ASSOCIATED CONTENT

Data Availability Statement

The data underlying this study are available in the published article and its Supporting Information.

https://doi.org/10.1021/acs.orglett.5c01150
Org. Lett. 2025, 27, 4893−4897

Supporting Information

The Supporting Information is available free of charge at https://pubs.acs.org/doi/10.1021/acs.orglett.5c01150.

Experimental details, analytical data, NMR spectra, and crystallographic details (PDF)

Accession Codes

Deposition Numbers 2431433 and 2431435 contain the supplementary crystallographic data for this paper. These data can be obtained free of charge via the joint Cambridge Crystallographic Data Centre (CCDC) and Fachinformationszentrum Karlsruhe Access Structures service.

AUTHOR INFORMATION

Corresponding Author

Hermann A. Wegner − *Institute of Organic Chemistry and Center for Materials Research (LaMa), Justus Liebig University Giessen, 35392 Giessen, Germany;* orcid.org/0000-0001-7260-6018; Email: hermann.a.wegner@org.chemie.uni-giessen.de

Authors

Michel Große − *Institute of Organic Chemistry and Center for Materials Research (LaMa), Justus Liebig University Giessen, 35392 Giessen, Germany*

Christopher M. Leonhardt − *Institute of Organic Chemistry and Center for Materials Research (LaMa), Justus Liebig University Giessen, 35392 Giessen, Germany*

Patrick A. R. Campbell − *Institute of Organic Chemistry and Center for Materials Research (LaMa), Justus Liebig University Giessen, 35392 Giessen, Germany*

Complete contact information is available at: https://pubs.acs.org/10.1021/acs.orglett.5c01150

Notes

The authors declare no competing financial interest.

ACKNOWLEDGMENTS

The financial support by the LOEWE Program of Excellence of the Federal State of Hesse (LOEWE Focus Group PriOSS "Principles of On-Surface Synthesis") is gratefully acknowledged. We thank the Organic Chemistry Analytics Department (Institute of Organic Chemistry, Justus Liebig University, Giessen) for NMR, HRMS and HPLC measurements as well as preparative HPLC purifications.

REFERENCES

(1) Lee, S.; Sperry, J. Isolation and biological activity of azocine and azocane alkaloids. *Bioorg. Med. Chem.* **2022**, *54*, No. 116560.

(2) Sun, H.; Nikolovska-Coleska, Z.; Lu, J.; Meagher, J. L.; Yang, C.-Y.; Qiu, S.; Tomita, Y.; Ueda, Y.; Jiang, S.; Krajewski, K.; Roller, P. P.; Stuckey, J. A.; Wang, S. Design, synthesis, and characterization of a potent, nonpeptide, cell-permeable, bivalent Smac mimetic that concurrently targets both the BIR2 and BIR3 domains in XIAP. *J. Am. Chem. Soc.* **2007**, *129* (49), 15279−15294.

(3) Putey, A.; Popowycz, F.; Do, Q.-T.; Bernard, P.; Talapatra, S. K.; Kozielski, F.; Galmarini, C. M.; Joseph, B. Indolobenzazepin-7-ones and 6-, 8-, and 9-membered ring derivatives as tubulin polymerization inhibitors: synthesis and structure−activity relationship studies. *J. Med. Chem.* **2009**, *52* (19), 5916−5925.

(4) George, K. M.; Frantz, M.-C.; Bravo-Altamirano, K.; Lavalle, C. R.; Tandon, M.; Leimgruber, S.; Sharlow, E. R.; Lazo, J. S.; Wang, Q. J.; Wipf, P. Design, Synthesis, and Biological Evaluation of PKD Inhibitors. *Pharmaceutics* **2011**, *3* (2), 186−228.

(5) Sumi, K.; Inoue, Y.; Nishio, M.; Naito, Y.; Hosoya, T.; Suzuki, M.; Hidaka, H. IOP-lowering effect of isoquinoline-5-sulfonamide compounds in ocular normotensive monkeys. *Bioorg. Med. Chem. Lett.* **2014**, *24* (3), 831−834.

(6) Li, J.; Dong, Z.; Zhao, C. Recent progress in the construction of eight-membered nitrogen-heterocycles. *New J. Chem.* **2024**, *48* (11), 4645−4669.

(7) Romines, K. R.; Watenpaugh, K. D.; Tomich, P. K.; Howe, W. J.; Morris, J. K.; Lovasz, K. D.; Mulichak, A. M.; Finzel, B. C.; Lynn, J. C.; Horng, M. M. Use of medium-sized cycloalkyl rings to enhance secondary binding: discovery of a new class of human immunodeficiency virus (HIV) protease inhibitors. *J. Med. Chem.* **1995**, *38* (11), 1884−1891.

(8) Clayden, J.; Moran, W. J.; Edwards, P. J.; LaPlante, S. R. The challenge of atropisomerism in drug discovery. *Angew. Chem., Int. Ed.* **2009**, *48* (35), 6398−6401.

(9) Yang, L.; Wang, D.-X.; Zheng, Q.-Y.; Pan, J.; Huang, Z.-T.; Wang, M.-X. Highly efficient and concise synthesis of both antipodes of SB204900, Clausenamide, neoclausenamide, homoclausenamide and zeta-Clausenamide. Implication of biosynthetic pathways of Clausena alkaloids. *Org. Biomol. Chem.* **2009**, *7* (12), 2628−2634.

(10) Riemer, B.; Hofer, O.; Greger, H. Tryptamine derived amides from Clausena indica. *Phytochemistry* **1997**, *45* (2), 337−341.

(11) Viladomat, F.; Bastida, J.; Codina, C.; Campbell, W. E.; Mathee, S. Alkaloids from Boophane flava. *Phytochemistry* **1995**, *40* (1), 307−311.

(12) Qiao, M.-F.; Ji, N.-Y.; Liu, X.-H.; Li, K.; Zhu, Q.-M.; Xue, Q.-Z. Indoloditerpenes from an algicolous isolate of Aspergillus oryzae. *Bioorg. Med. Chem. Lett.* **2010**, *20* (19), 5677−5680.

(13) Sarker, S. D.; Dinan, L.; Šik, V.; Underwood, E.; Waterman, P. G. Moschamide: An unusual alkaloid from the seeds of Centaurea moschata. *Tetrahedron Lett.* **1998**, *39* (11), 1421−1424.

(14) Chattopadhyay, P.; Pada Majhi, T.; Achari, B. Advances in the Synthesis and Biological Perspectives of Benzannulated Medium Ring Heterocycles. *Heterocycles* **2007**, *71* (5), 1011.

(15) Hussain, A.; Yousuf, S. K.; Mukherjee, D. Importance and synthesis of benzannulated medium-sized and macrocyclic rings (BMRs). *RSC Adv.* **2014**, *4* (81), 43241−43257.

(16) Clarke, A. K.; Unsworth, W. P. A happy medium: the synthesis of medicinally important medium-sized rings via ring expansion. *Chem. Sci.* **2020**, *11* (11), 2876−2881.

(17) Guney, T.; Wenderski, T. A.; Boudreau, M. W.; Tan, D. S. Synthesis of Benzannulated Medium-ring Lactams via a Tandem Oxidative Dearomatization-Ring Expansion Reaction. *Chem. Eur. J.* **2018**, *24* (50), 13150−13157.

(18) Hall, J. E.; Matlock, J. V.; Ward, J. W.; Gray, K. V.; Clayden, J. Medium-Ring Nitrogen Heterocycles through Migratory Ring Expansion of Metalated Ureas. *Angew. Chem., Int. Ed.* **2016**, *55* (37), 11153−11157.

(19) Zhou, Y.; Wei, Y.-L.; Rodriguez, J.; Coquerel, Y. Enantioselective Organocatalytic Four-Atom Ring Expansion of Cyclobutanones: Synthesis of Benzazocinones. *Angew. Chem., Int. Ed.* **2019**, *58* (2), 456−460.

(20) Ji, M.-M.; Liu, P.-R.; Yan, J.-D.; He, Y.-Y.; Li, H.; Ma, A.-J.; Peng, J.-B. Ruthenium-Catalyzed Carbonylation of α-Aminoaryl-Tethered Alkylidenecyclopropanes: Synthesis of Eight-Membered Benzolactams. *Org. Lett.* **2024**, *26* (1), 231−235.

(21) Hasegawa, D.; Tsuji, A.; Greiner, L. C.; Arichi, N.; Inuki, S.; Ohno, H. Synthesis of Azocine-Fused Indoles via Gold(I)-Catalyzed Cyclization of Azido-alkynes. *J. Org. Chem.* **2025**, *90* (1), 925−930.

(22) Cheng, Z.; Chen, J.; Zhang, Y.; Shao, Y.; Sun, J.; Tang, S. Decarboxylative Cyclization of Ethynyl Benzoxazinanones with Imidazolidines to Access 2,3-Indole-Fused 1,4-Diazocines. *Org. Lett.* **2024**, *26* (23), 4863−4867.

(23) Zhang, Z.; Fang, X.; Aili, A.; Wang, S.; Tang, J.; Lin, W.; Xie, L.; Chen, J.; Sun, K. Cascade Radical Trifluoromethylthiolation/

Cyclization of Dienes To Access SCF3-Containing Medium-Sized Heterocycles. *Org. Lett.* **2023**, *25* (24), 4598−4602.
(24) McGrath, N. A.; Brichacek, M.; Njardarson, J. T. A Graphical Journey of Innovative Organic Architectures That Have Improved Our Lives. *J. Chem. Educ.* **2010**, *87* (12), 1348−1349.
(25) Galli, C.; Mandolini, L. The Role of Ring Strain on the Ease of Ring Closure of Bifunctional Chain Molecules. *Eur. J. Org. Chem.* **2000**, *2000* (18), 3117−3125.
(26) Illuminati, G.; Mandolini, L. Ring closure reactions of bifunctional chain molecules. *Acc. Chem. Res.* **1981**, *14* (4), 95−102.
(27) Kessler, S. N.; Neuburger, M.; Wegner, H. A. Bidentate Lewis Acids for the Activation of 1,2-Diazines − A New Mode of Catalysis. *Eur. J. Org. Chem.* **2011**, *2011* (17), 3238−3245.
(28) Kessler, S. N.; Neuburger, M.; Wegner, H. A. Domino inverse electron-demand Diels-Alder/cyclopropanation reaction of diazines catalyzed by a bidentate Lewis acid. *J. Am. Chem. Soc.* **2012**, *134* (43), 17885−17888.
(29) Schweighauser, L.; Bodoky, I.; Kessler, S.; Häussinger, D.; Wegner, H. Bidentate Lewis Acid Catalyzed Inverse-Electron-Demand Diels-Alder Reaction for the Selective Functionalization of Aldehydes. *Synthesis* **2012**, *44* (14), 2195−2199.
(30) Schweighauser, L.; Bodoky, I.; Kessler, S. N.; Häussinger, D.; Donsbach, C.; Wegner, H. A. Bidentate Lewis Acid Catalyzed Domino Diels-Alder Reaction of Phthalazine for the Synthesis of Bridged Oligocyclic Tetrahydronaphthalenes. *Org. Lett.* **2016**, *18* (6), 1330−1333.
(31) Ahles, S.; Götz, S.; Schweighauser, L.; Brodsky, M.; Kessler, S. N.; Heindl, A. H.; Wegner, H. A. An Amine Group Transfer Reaction Driven by Aromaticity. *Org. Lett.* **2018**, *20* (22), 7034−7038.
(32) Ahles, S.; Ruhl, J.; Strauss, M. A.; Wegner, H. A. Combining Bidentate Lewis Acid Catalysis and Photochemistry: Formal Insertion of o-Xylene into an Enamine Double Bond. *Org. Lett.* **2019**, *21* (11), 3927−3930.
(33) Ruhl, J.; Ahles, S.; Strauss, M. A.; Leonhardt, C. M.; Wegner, H. A. Synthesis of Medium-Sized Carbocycles via a Bidentate Lewis Acid-Catalyzed Inverse Electron-Demand Diels-Alder Reaction Followed by Photoinduced Ring-Opening. *Org. Lett.* **2021**, *23* (6), 2089−2093.
(34) Beeck, S.; Ahles, S.; Wegner, H. A. Orthogonal Catalysis for an Enantioselective Domino Inverse-Electron Demand Diels-Alder/Substitution Reaction. *Chem. Eur. J.* **2022**, *28* (5), No. e202104085.
(35) Große, M.; Wegner, H. A. Bidentate Lewis Acid-Catalyzed Inverse Electron-Demand Diels−Alder Reaction of Phthalazines and Cyclooctynes. *Synlett* **2024**, *35* (09), 1019−1022.
(36) Strauss, M. A.; Kohrs, D.; Ruhl, J.; Wegner, H. A. Mechanistic Study of Domino Processes Involving the Bidentate Lewis Acid Catalyzed Inverse Electron-Demand Diels−Alder Reaction. *Eur. J. Org. Chem.* **2021**, *2021* (28), 3866−3873.
(37) Paquette, L. A.; Kakihana, T.; Kelly, J. F. Unsaturated heterocyclic systems. LXXVII. 1-Aza-2,4,6-cyclooctatriene-7-azabicyclo[4,2,] octadiene valence tautomeric equilibrium. Substituent effects and an attempted synthesis of azetes (azacyclobutadienes). *J. Org. Chem.* **1971**, *36* (3), 435−442.
(38) Kessler, S. N.; Wegner, H. A. One-pot synthesis of phthalazines and pyridazino-aromatics: a novel strategy for substituted naphthalenes. *Org. Lett.* **2012**, *14* (13), 3268−3271.

https://doi.org/10.1021/acs.orglett.5c01150
Org. Lett. 2025, 27, 4893−4897

3.3 Cyclooctynes as Building Blocks for the Synthesis of Arene-Annulated Eight-Membered Ring Systems

Reference: M. Große, H. A. Wegner, *Synlett*.

DOI: 10.1055/a-2661-3958

“Arene-annulated eight-membered carbocycles constitute a unique class of molecular architectures, combining the rigidity of aromatic ring systems with the distinctive conformational features of cyclooctene-derived frameworks. Among the various synthetic routes developed to prepare these structures, Diels–Alder reactions employing cyclooctyne derivatives as dienophiles stand out for their high degree of modularity as well as functional group tolerance. Herein, we provide an overview of these Diels–Alder-based strategies by comparing commonly employed strained alkyne dienophiles and classifying different types of diene systems. This systematic compilation of synthetic methods may help guide future developments in the synthesis of polycyclic structures containing eight-membered rings and foster their usage in functional materials and biological applications.”

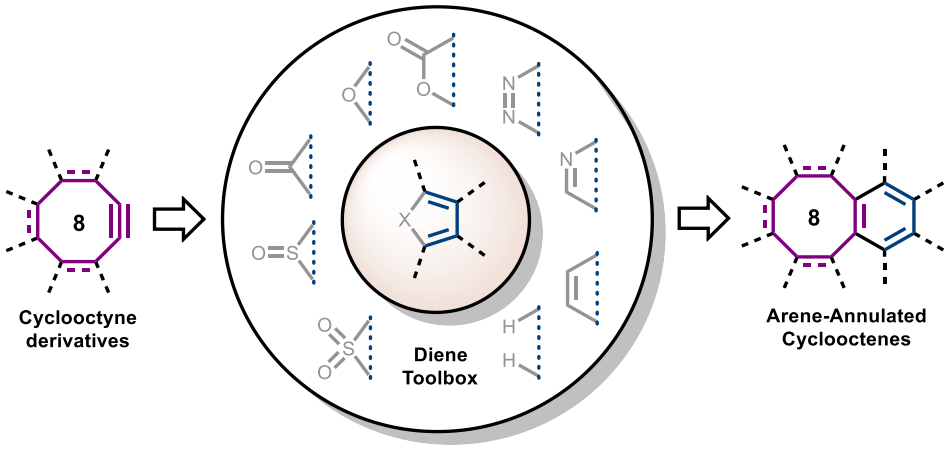

Thieme Synlett

Account

Cyclooctynes as Building Blocks for the Synthesis of Arene-Annulated Eight-Membered Ring Systems

Michel Große[1,2], Hermann A. Wegner[1,2]
Affiliation addresses are listed at the end of the article.

GRAPHICAL ABSTRACT

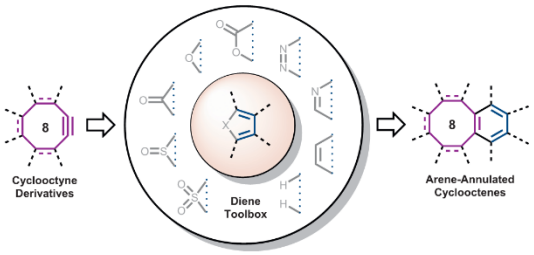

ABSTRACT

Arene-annulated eight-membered carbocycles constitute a unique class of molecular architectures, combining the rigidity of aromatic ring systems with the distinctive conformational features of cyclooctene-derived frameworks. Among the various synthetic routes developed to prepare these structures, Diels–Alder reactions employing cyclooctyne derivatives as dienophiles stand out for their high degree of modularity as well as functional group tolerance. Herein, we provide an overview of these Diels–Alder-based strategies by comparing commonly employed strained alkyne dienophiles and classifying different types of diene systems. This systematic compilation of synthetic methods may help guide future developments in the synthesis of polycyclic structures containing eight-membered rings and foster their usage in functional materials and biological applications.

Keywords Cycloaddition, Strained alkynes, Cyclooctyne, Diels–Alder reaction, Skeletal editing, Polycyclic aromatic hydrocarbons

received June 26, 2025 | **accepted after revision** July 20, 2025 | **article published online** 2025

Bibliography Synlett **DOI** 10.1055/a-2661-3958 **Art ID** ST-2025-06-0267-A

Correspondence Prof. Hermann A. Wegner, Institute of Organic Chemistry, Justus Liebig University, Heinrich-Buff-Ring 17, 35392 Giessen, Germany, Email: Hermann.A.Wegner@org.Chemie.uni-giessen.de

*Alkynes in Organic Synthesis

1 Introduction

Eight-membered carbocycles annulated to (polycyclic) aromatic ring systems have attracted increasing attention in recent years, particularly in the context of supramolecular chemistry,[1] organic photonics and electronics,[2] as well as molecular sensors.[3] Additionally, these structures are of growing importance in the rapidly emerging field of on-surface synthesis,[4] where nonhexagonal rings have recently gained more and more attention.[5] Arene-fused cycloocta-1,5-dienes (CODs) and cyclooctatetraenes (COTs) (**Fig. 1**) are particularly valuable building blocks for the construction of functional materials. On the one hand, the geometric constraints of these eight-membered rings can be utilized to integrate curvature into the larger molecular framework.[6] On the other hand, their conformational flexibility serves as the basis of switchable materials and molecular probes.[1b,2a]

Among the various synthetic strategies to access arene-annulated CODs and COTs, Diels–Alder (DA) reactions employing strained alkynes, mostly cyclooctyne derivatives, have emerged as a powerful tool to directly fuse eight-membered rings to the aromatic systems of interest with high selectivity and functional group tolerance. The aim of this article is to provide a systematic

Fig. 1 General structure of arene-annulated cycloocta-1,5-dienes (CODs) and cyclooctatetraenes (COTs).

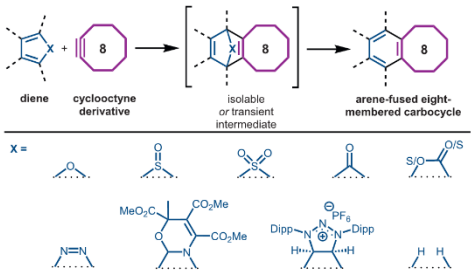

Scheme 1 General reaction sequence of the Diels–Alder reaction of cyclooctynes and various dienes.

overview of these DA-based annulation strategies by discussing commonly used dienophiles as well as categorizing and comparing different types of dienes, ranging from classical heterocycles to the more recently introduced scaffolds relevant to skeletal editing. **Scheme 1** illustrates the typical reaction sequence starting with the initial [4+2] cycloaddition to give, in most cases, a bridged intermediate. Depending on the nature of the diene, this intermediate can be either transient or isolable. In the former case, spontaneous cycloreversion directly furnishes the arene-annulated structure, whereas in the latter, additional synthetic steps for re-aromatization are required.

2 Cyclooctyne Derivatives

The growing importance of bioorthogonal chemistry has led to significant interest in cyclooctyne derivatives as reactive linkers for strain-promoted click reactions. Numerous strategies for fine-tuning the reactivity and stability of these strained alkynes have been developed and extensively reviewed.[7] While cyclooctynes in bioorthogonal chemistry mainly function as reactive handles, material-oriented molecular design typically places the eight-membered ring at the geometric center of the target molecule, which necessitates the use of symmetric 1,5-cyclooctadiynes rather than simple monoalkynes (**Fig. 2**).

Kloster-Jensen and Wirz were the first to synthesize and describe 1,5-cyclooctadiyne (**1**) in 1973.[8] It was obtained as a crystalline solid in 2% yield by the dimerization of butatriene and found to be stable at 0 °C under exclusion of air. It was reported to smoothly undergo DA reactions with 1,3-butadienes at both triple bonds.[8b] However, no mono-DA adducts were detected, even when diyne **1** was used in excess, indicating that cyclooct-1-ene-5-yne is more reactive than the parent diyne. In 1974,

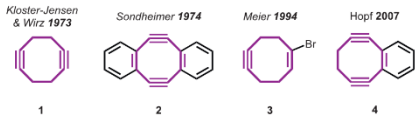

Fig. 2 Cycloocta-1,5-diynes (**1**,**2**,**4**) and a synthetic equivalent (**3**) used in Diels–Alder reactions.

Sondheimer and coworkers synthesized planar dibenzocycloocta-diyne **2**, which is now commonly referred to as Sondheimer–Wong diyne (SWD).[9] It was obtained from the corresponding alkene via a bromination–dehydrobromination sequence and found to be relatively stable, showing only partial decomposition after two days of storage at room temperature without protection from air or light. Similarly to the observations of Kloster-Jensen and Wirz, the monoalkyne analogue of **2** was reported to be more reactive than the corresponding diyne. The same reactivity trend was later reported in strain-promoted click reactions of the SWD with azides,[10] highlighting the difficulties in achieving selective mono-addition. To overcome this limitation, Meier and coworkers developed enyne **3**, which contains a highly reactive, strained alkyne together with a vinyl bromide moiety that serves as a latent alkyne precursor.[11] This gives access to previously unattainable mono-adducts and allows for two sequential DA reactions to be performed in a controlled manner. In 2007, Hopf and coworkers synthesized and described diyne **4** as another highly reactive, benzo-fused bis-dienophile.[12] The corresponding double-DA adduct with tetracyclone was obtained in excellent yield.[12b] However, no monoaddition has been described for this bis-dienophile either. In contrast to the SWD (**2**), crystalline samples of diyne **4** were reported to quickly decompose upon storage at room temperature, even under exclusion of air.[12a]

Of the four cyclooctyne derivatives **1**-**4**, especially the SWD (**2**) and enyne **3** have since been widely employed in DA reactions with a broad range of dienes, as discussed in the next section.

3 Types of Dienes

3.1 Furans

Furans are among the most commonly used dienes for the construction of arene-annulated eight-membered carbocycles. The initial cycloaddition using the SWD (**2**) furnishes the stable, oxygen-bridged intermediate **5**, as demonstrated by Sondheimer and Wong (**Scheme 2**).[13] A convenient one-step protocol for the deoxygenation of **5** to tetraphenylene (**6**) was later developed by Xing and Huang.[14] They made use of low-valent titanium, which is generated in situ by reduction of $TiCl_4$ with $LiAlH_4$ in the presence of triethylamine.[15] This DA/deoxygenation sequence was later expanded to the synthesis of π-extended analogues of tetraphenylene using benzo-fused versions of the SWD and isobenzofuran.[16]

Sygula and coworkers employed the same strategy to synthesize COT **7** bearing two bowl-shaped corannulene side arms (**Scheme 3**).[1a] Due to the tub conformation of the central eight-membered ring, **7** acts as a molecular tweezer that forms a 1:1 inclusion complex with C_{60} fullerene through concave–convex

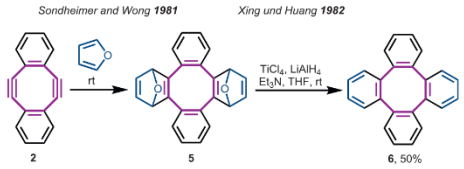

Scheme 2 DA reaction of the SWD (**2**) and furan followed by titanium-mediated deoxygenation.

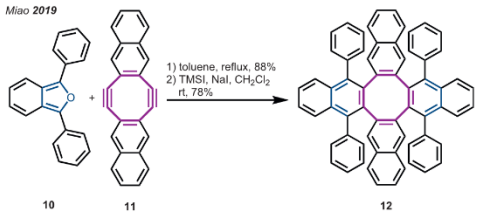

Scheme 4 Synthesis of tetranaphtho-COT **12** from isobenzofuran **10** and π-extended SWD **11**.

π–π interactions, as shown by X-ray crystallographic analysis as well as NMR titration experiments. A more conformationally flexible analogue **8** of this molecular tweezer was obtained via two sequential DA reactions using isocorannulenofuran **9** in combination with enyne **3**.[17] The first DA reaction was followed by a titanium-mediated deoxygenation and a subsequent dehydrobromination to afford another strained alkyne intermediate that was again reacted with furan **9** to furnish COD **8**. Enyne **3** appeared to be more reactive in these transformations compared to the SWD (**2**), as evident by the lower reaction temperatures. This is in good agreement with earlier reports demonstrating the higher reactivity of enyne **3** toward common dienes compared to the corresponding diyne **1**.[11] Additionally, lower reactivity of the SWD (**2**) has been attributed to increased steric hindrance caused by the annulated benzene rings.[18]

Miao and coworkers employed the same DA chemistry in their synthesis of octabenzo[8]circulene derivatives, targeting negatively curved nanographenes.[19] As a key step in their synthetic strategy, they used a DA reaction of isobenzofuran **10** and π-extended SWD **11** (**Scheme 4**). Subsequent cleavage of the oxygen bridge and aromatization mediated by trimethylsilyl iodide and sodium iodide furnished tetranaphtho-COT **12**, which was further oxidized to obtain the desired circulene derivative.

3.2 Thiophene Oxides

Although less frequently employed than furans, thiophene *S*-oxides and *S*,*S*-dioxides have proven to be valuable dienes for the construction of arene-annulated eight-membered carbocycles. The initially formed bridged intermediates can spontaneously extrude sulfur monoxide or sulfur dioxide to yield the desired aromatic ring without the need for an additional aromatization step. Additionally, in some cases, thiophene oxides display a higher reactivity compared to the corresponding furans.[20] In their synthesis of tetrabenzo[8]circulene, Whalley and coworkers employed a DA reaction of the SWD (**2**) and thiophene *S*-oxide **13** as a key step to furnish substituted tetraphenylene **14** (**Scheme 5**).[20] Attempts to use 2,5-diaryl furan or thiophene *S*,*S*-dioxide as alternative dienes in this transformation were unsuccessful, which was ascribed to the higher temperature (180 °C) required to facilitate the cycloaddition coupled with the temperature sensitivity of diyne **2**. In contrast, sulfoxide **13** was found to be a more active diene and a reaction temperature of 100 °C was sufficient for the DA reaction to take place, avoiding the decomposition of the dienophile. Yamaguchi and coworkers also made use of the high reactivity of sulfoxides for the synthesis of hexaarylbenzenes by reacting tetraarylthiophene *S*-oxides with various alkyne dienophiles, including dibenzo[a,e]cyclooctyne (**15**).[21]

Despite their lower reactivity, thiophene *S*,*S*-dioxides have also been employed in DA reactions with strained alkynes. Nakayama and coworkers showed that the reaction of cyclooctyne and 3,4-di-*tert*-butylthiophene *S*,*S*-dioxide affords the corresponding benzocyclooctene in 92% yield, albeit under harsh conditions requiring reflux in *o*-dichlorobenzene (180 °C).[22] As a more reactive diene, tetrachlorothiophene *S*,*S*-dioxide **16** was later introduced and shown to

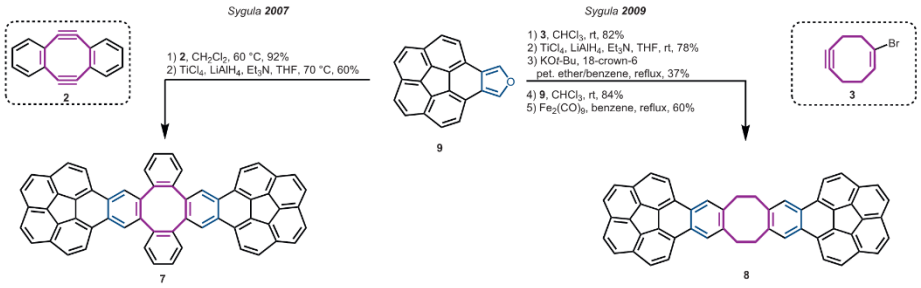

Scheme 3 Synthesis of molecular tweezers with corannulene side arms and COT (**7**) or COD (**8**) core via DA reaction of furan **9**.

Große Michel et al. doi: 10.1055/a-2661-3958

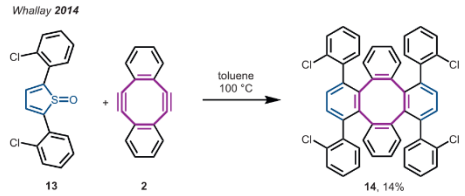

Scheme 5 Synthesis of substituted tetraphenylene **14** via double DA addition of thiophene *S*-oxide **13**.

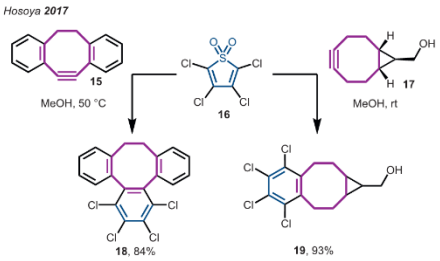

Scheme 6 DA reactions of tetrachlorothiophene *S*,*S*-dioxide **16** and cyclooctyne derivatives.

undergo DA reactions with cyclooctynes **15** and **17** at 50 °C and room temperature, respectively (**Scheme 6**).[23] The electron-withdrawing chlorine substituents reduce the energy level of the lowest unoccupied molecular orbital (LUMO), which allows for the DA reactions to proceed at drastically reduced temperatures, demonstrating the inverse electron demand of the reaction.

3.3 Cyclopentadienones

Substituted cyclopentadienones represent another group of electron-poor dienes commonly employed in inverse electron-demand Diels–Alder (IEDDA) reactions. Analogous to thiophene oxides, spontaneous extrusion of carbon monoxide after the initial cycloaddition directly furnishes the desired aromatic structure. Müllen and coworkers used this reactivity to synthesize octaphenyltetraphenylene **20** from tetraphenyl-cyclopentadienone **21** and diyne **2** via double DA addition (**Scheme 7**).[24] Despite the reported thermal instability of the SWD (**2**), the reaction could be performed at 150 °C over 12 h and furnished the desired arene-annulated COT **20** in 95% yield. This crowded oligophenylene was subsequently transformed into large polycyclic aromatic hydrocarbons (PAHs) via oxidative cyclodehydrogenation and skeletal rearrangement.

Miao and coworkers employed the same DA strategy in their synthesis of an aromatic saddle-shaped molecule featuring a COT core.[25] However, they used the π-extended Sondheimer–Wong diyne **11** in the DA reaction, which proved crucial for the subsequent Scholl reaction, as the incorporated naphthalene

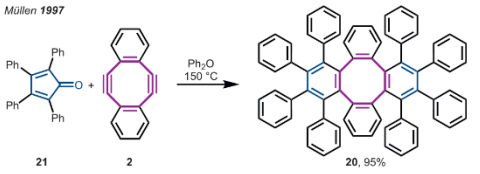

Scheme 7 Synthesis of octaphenyltetraphenylene **20** from the SWD (**2**) and cyclopentadienone **21**.

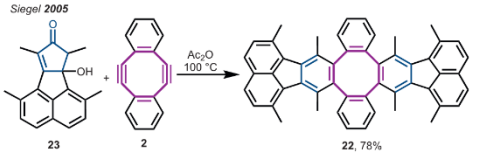

Scheme 8 Cyclopentadienone precursor **23** in the DA reaction with the SWD (**2**).

units favored the oxidative cyclodehydrogenation over the skeletal rearrangement previously reported by Müllen.[24] Miao and coworkers further employed several DA reactions of cyclooctyne derivatives and cyclopentadienones as well as furans in their synthetic strategy toward a negatively curved carbon nanobelt.[26] Although their synthesis did not yield the desired nanobelt, they were able to obtain an oligomeric structure containing five eight-membered carbocycles.

For their synthesis of fluoranthene-annulated COT **22**, Siegel and coworkers utilized cyclopentadienone precursor **23**, from which the desired reactive diene is generated in situ and directly trapped by a DA reaction with diyne **2** at 100 °C (**Scheme 8**).[27] In that way, the rapid dimerization of the reactive cyclopentadienone is prevented.[28]

In contrast to the elevated temperatures required for DA reactions of the SWD (**2**) with cyclopentadienones, sterically less hindered strained alkynes typically react smoothly under ambient conditions. Meier and coworkers showed this by treating enyne **3** with tetraphenyl-substituted cyclopentadienone **21** at room temperature, which furnished benzo-fused COD **24** in 93% yield (**Scheme 9**).[11] Subsequent elimination yielded alkyne **25**, which was again reacted with diene **21** to obtain octaphenyldibenzo-COD **26** in quantitative yield.

The possibility to perform these reactions under ambient conditions enabled further investigations on bioorthogonal reactions of cyclopentadienones and cyclooctynes designed for fluorescence labeling and controlled carbon monoxide release under physiological conditions.[29]

3.4 α-Pyrones and Thio-Analogues

α-Pyrones are common dienes employed in normal and inverse electron-demand DA reactions depending on their substitution

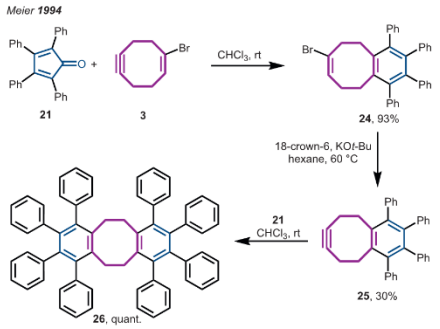

Scheme 9 Enyne **3** in sequential DA reactions with cyclopentadienone **21**.

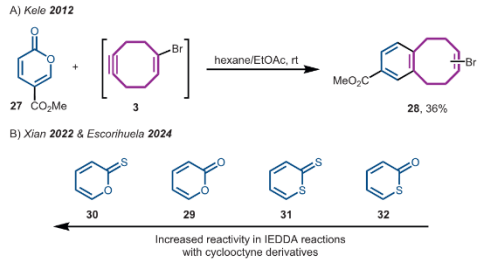

Scheme 10 DA reaction of substituted α-pyrone **27** and enyne **3** (A) and reactivity trend of α-pyrone (**29**) and its thio-analogues **30–32** (B).

pattern and the nature of the dienophile.[30] With cyclooctyne derivatives, the initial cycloaddition typically proceeds via an inverse electron-demand pathway and is consequently facilitated by electron-withdrawing substituents on the pyrone ring.[31] In the subsequent *retro*-DA reaction, the benzo-fused eight-membered ring is obtained after extrusion of carbon dioxide. Kele and coworkers employed coumalic acid ester **27** as an electron-poor α-pyrone in an IEDDA reaction with enyne **3** (**Scheme 10**, **A**).[32] The reaction proceeded smoothly at room temperature and furnished benzo-COD **28** in 36% yield. Subsequent elimination yielded the corresponding strained alkyne, which was used for bioorthogonal fluorescence labeling.

The reactivity of α-pyrone (**29**) and its thio-analogues **30–32** in IEDDA reactions with cyclooctyne derivatives has also been the subject of computational and experimental investigations.[33] Xian and coworkers identified pyranthione **30** as the most reactive diene in the series followed by α-pyrone (**29**) (**Scheme 10**, **B**).[33a] Dienes **31** and **32** with the sulfur atom in the six-membered ring were found to be the least reactive substrates. This order of reactivity was associated with the aromaticity of the respective dienes, showing that lower aromaticity results in a reduced activation barrier for the cycloaddition step. The computational studies of Escorihuela and coworkers confirmed this reactivity trend.[33b] However, they attributed the increased reactivity to lower distortion energy in the cycloaddition.

3.5 Azines

Six-membered aromatic nitrogen heterocycles (azines) are highly versatile dienes for IEDDA reactions extensively employed in natural product total synthesis, chemical biology, and materials science.[34] The reactivity of azines and the nature of their cycloaddition products vary significantly depending on the number and position of the nitrogen atoms. Especially the reaction of 1,2,4,5-tetrazine and cyclooctyne derivatives has become an important tool in bioorthogonal chemistry.[35] However, for the synthesis of (polycyclic) aromatic hydrocarbons fused to eight-membered carbocycles, new strategies are required that go beyond classical tetrazine ligation. To this end, Hosoya and coworkers established a modular synthetic approach based on two sequential DA reactions starting from oxadiazinone **33** (**Scheme 11**).[36]

The initial cycloaddition with strained alkyne **34** proceeded smoothly at room temperature to afford substituted pyrone **35** after extrusion of nitrogen. As the newly formed diene **35** exhibits a lower reactivity toward IEDDA reactions compared to the parent oxadiazinone **33**, no double addition products were observed under these conditions. Subsequent treatment with benzyne, obtained in situ from *o*-silylphenyl triflate **36**, yielded the desired naphtha-fused cyclooctene **37** via another DA/*retro*-DA reaction sequence.

In contrast to tetrazines and oxadiazinones, azines containing fewer heteroatoms in the ring require much harsher conditions or additional modes of activation to enable IEDDA reactions. In the past decade, our group established the bidentate Lewis acid (BDLA) **38** as an effective catalyst to facilitate IEDDA reactions of phthalazines (**39**) and various dienophiles.[37] The boron-based catalyst acts by lowering the LUMO energy of the diazine through complexation, which increases its reactivity toward various electron-rich dienophiles.[38] We recently showed that the BDLA **38** facilitates IEDDA reactions of various phthalazines (**39**) and cyclooctyne derivatives to directly furnish (substituted) polycyclic aromatic structures fused to eight-membered carbocycles in one step (**Scheme 12**).[37i] Efforts to expand this approach to other cyclooctyne derivatives are currently on-going in our laboratory.

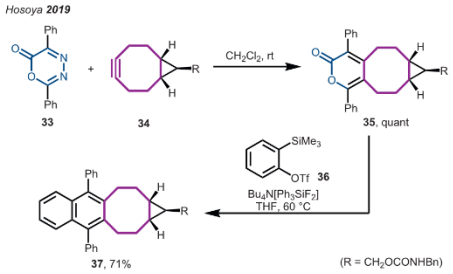

Scheme 11 Two sequential DA reactions using oxadiazinone **33** as electron-poor diene.

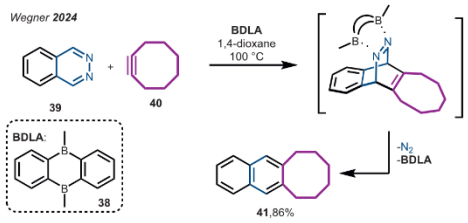

Scheme 12 IEDDA reaction of phthalazine (**39**) and cyclooctyne (**40**) catalyzed by the BDLA **38**.

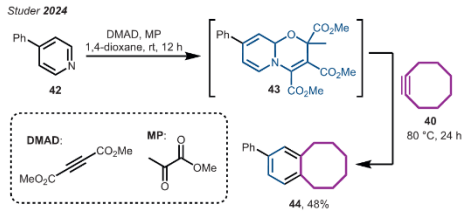

Scheme 13 One-pot sequence of de-aromatization, cycloaddition, and re-aromatizing *retro*-cycloaddition for the skeletal editing of pyridines.

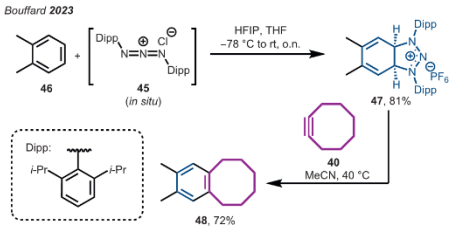

Scheme 14 Skeletal editing of arenes via de-aromative 1,3-dipolar cycloaddition and subsequent DA reaction.

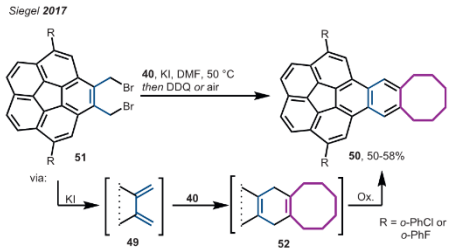

Scheme 15 DA reaction of cyclooctyne (**40**) and in situ generated *o*-QDM intermediate **49**.

With only one nitrogen in the aromatic ring, pyridines exhibit the lowest reactivity in DA reactions among all azines.[39] To overcome this intrinsic lack of reactivity and harness pyridines as versatile dienes, Studer and coworkers established a convenient one-pot reaction sequence of de-aromatization, cycloaddition, and re-aromatizing *retro*-cycloaddition to transform pyridines into diversely substituted benzenes and naphthalenes (**Scheme 13**).[40] The initial dearomatization is achieved by treating substituted pyridine **42** with dimethyl acetylenedicarboxylate (DMAD) and methyl pyruvate (MP) to generate oxazino pyridine **43** as the actual electron-rich diene in situ. This intermediate was shown to react with a variety of cyclic and acyclic alkyne dienophiles, including cyclooctyne (**40**) as well as its derivative **17** to furnish the aromatic system after *retro*-cycloaddition. While developed as a general approach for skeletal editing of pyridines, this strategy offers a unique route to benzannulated eight-membered ring structures.

3.6 Other Dienes

Another skeletal editing approach based on a de-aromatization/cycloaddition/*retro*-cycloaddition sequence was developed by Bouffard and coworkers for the functionalization of nonactivated arenes.[41] The key component in their reaction was the in situ generated 1,3-diaza-2-azoniaallene cation **45** that undergoes a de-aromative 1,3-dipolar cycloaddition with substituted benzenes like *o*-xylene (**46**) to afford the stable and isolable triazolinium cycloadduct **47** (**Scheme 14**). This adduct acts as diene in follow-up DA reactions with various reactive alkynes, including cyclooctyne (**40**) and its derivative **17**. Diene **47** was found to decompose at reaction temperatures above 50°C, thereby limiting this method to potent dienophiles. However, the employed cyclooctynes reacted smoothly below this degradation temperature to yield substituted aromatics like the benzo-fused cyclooctene **48**.

As another highly reactive diene species, *o*-quinodimethanes (*o*-QDMs) found broad application in organic synthesis.[42] Siegel and coworkers used a DA reaction of cyclooctyne (**40**) and in situ generated *o*-QDM **49** to synthesize the cyclooctene-fused PAH **50** (**Scheme 15**).[43] The reactive diene was obtained from 1,2-bis(bromomethyl)-arene **51** via an anion-induced 1,4-elimination and directly trapped with the strained alkyne. The subsequent oxidation to the final aromatic structure was achieved in one-pot by either stirring the reaction mixture open to air for prolonged time or treating it with DDQ.

4 Summary

Employing cyclooctyne derivatives in DA reactions has emerged as a powerful tool to construct fused ring systems that combine the properties of rigid, aromatic structures with the distinctive conformational features of eight-membered carbocycles. This article gives a systematic summary of the existing DA-based approaches to synthesize such arene-annulated cyclooctene derivatives.

To this end, a concise overview of important dienophiles, namely cycloocta-1,5-diynes, was provided, discussing their reactivity and, in some cases, surprisingly high stability. Furthermore, different classes of dienes were systematically reviewed, highlighting differences in reactivity and illustrating key examples. This compilation spans classical heterocyclic dienes as well as new catalytic systems and unique skeletal editing approaches. Although not all of these methods were developed with the primary goal to synthesize arene-annulated eight-membered carbocycles, they offer a valuable toolbox of synthetic strategies that may inspire the development of new routes toward this intriguing class of molecules and facilitate their integration into functional materials and biological applications.

Author affiliations

1 Institute of Organic Chemistry, Justus Liebig University, Giessen, Germany.
2 Center of Material Research (LaMa/ZfM), Justus Liebig University, Giessen, Germany.

Statements and additional information

Conflict of Interest The authors declare that they have no conflict of interest.

Funding Information The authors acknowledge the LOEWE Program of Excellence of the Federal State of Hesse (LOEWE Focus Group PriOSS 'Principles of On-Surface Synthesis') for financial support.

References

1 (a) Sygula A, Fronczek FR, Sygula R, Rabideau PW, Olmstead MM. J Am Chem Soc 2007; 129: 3842 (b) Shen X, Viney C, Johnson ER, Wang C, Lu JQ. Nat Chem 2013; 5: 1035 (c) Wang Z, Huang Y, Guo J et al. Macromolecules 2018; 51: 1377 (d) Kim H, Son JB, Jeong M et al. J Am Chem Soc 2025; 147: 16429
2 (a) Yuan C, Saito S, Camacho C, Irle S, Hisaki I, Yamaguchi S. J Am Chem Soc 2013; 135: 8842 (b) Yuan C, Saito S, Camacho C, Kowalczyk T, Irle S, Yamaguchi S. Chem Eur J 2014; 20: 2193 (c) Yamakado T, Takahashi S, Watanabe K, Matsumoto Y, Osuka A, Saito S. Angew Chem Int Ed 2018; 57: 5438 (d) Xiong Y, Gong Q, Miao Q. Chem Asian J 2023; 18: e202300623
3 Kotani R, Sotome H, Okajima H et al. Mater Chem C 2017; 5: 5248
4 (a) Nakamura K, Li Q-Q, Krejčí O et al. J Am Chem Soc 2020; 142: 11363 (b) Villalobos F, Mendieta-Moreno JI, Lobo-Checa J et al. J Am Chem Soc 2025; 147: 7245
5 Qu H, Zhao M, Xu W. Chem Eur J 2025: e202501399
6 González Miera G, Matsubara S, Kono H, Murakami K, Itami K. Chem Sci 1848; 2022: 13
7 (a) Chupakhin EG, Krasavin MY. Chem Heterocycl Compd 2018; 54: 483 (b) Harris T, Alabugin IV. Mendeleev Commun 2019; 29: 237 (c) Fang Y, Hillman AS, Fox JM. Top Curr Chem 2024; 382: 15
8 (a) Kloster-Jensen E, Wirz J. Angew Chem 1973; 85: 723 (b) Kloster-Jensen E, Wirz J. Helv Chim Acta 1975; 58: 162
9 Wong HNC, Garratt PJ, Sondheimer F. J Am Chem Soc 1974; 96: 5604
10 Kii I, Shiraishi A, Hiramatsu T et al. Org Biomol Chem 2010; 8: 4051
11 Detert H, Rose B, Mayer W, Meier H. Chem Ber 1994; 127: 1529
12 (a) Werner C, Hopf H, Dix I, Bubenitschek P, Jones PG. Chem Eur J 2007; 13: 9462 (b) Werner C, Hopf H, Grunenberg J, Jones PG. Eur J Org Chem 2010; 2010: 4027
13 Wong HN, Sondheimer F. Tetrahedron 1981; 37: 99
14 Xing Y, de Huang NZ. J Org Chem 1982; 47: 140
15 Wong HNC. Acc Chem Res 1989; 22: 145
16 Man YM, Mak TCW, Wong HNC. J Org Chem 1990; 55: 3214
17 Kobryn L, Henry WP, Fronczek FR, Sygula R, Sygula A. Tetrahedron Lett 2009; 50: 7124
18 Kumar RA, Pattanayak MR, Yen-Pon E et al. Angew Chem Int Ed 2019; 58: 14544
19 (a) Pun SH, Wang Y, Chu M et al. J Am Chem Soc 2019; 141: 9680 (b) Zhang Y, Zhu Y, Lan D et al. J Am Chem Soc 2021; 143: 5231
20 Miller RW, Duncan AK, Schneebeli ST, Gray DL, Whalley AC. Chem Eur J 2014; 20: 3705
21 Suzuki S, Segawa Y, Itami K, Yamaguchi J. Nat Chem 2015; 7: 227
22 Nakayama J, Yamaoka S, Nakanishi T, Hoshino M. J Am Chem Soc 1988; 110: 6598
23 (a) Meguro T, Yoshida S, Hosoya T. Chem Lett 2017; 46: 1137 (b) Wang W, Ji X, Du Z, Wang B. Chem Commun 2017; 53: 1370
24 Müller M, Iyer VS, Kübel C, Enkelmann V, Müllen K. Angew Chem Int Ed 1997; 36: 1607
25 Pun SH, Chan CK, Liu Z, Miao Q. Org Mater 2020; 2: 248
26 Chen H, Miao Q. ChemPlusChem 2019; 84: 627
27 Elliott EL, Orita A, Hasegawa D, Gantzel P, Otera J, Siegel JS. Org Biomol Chem 2005; 3: 581
28 Duda B, Lentz D. Org Biomol Chem 2015; 13: 5625
29 (a) Wang D, Viennois E, Ji K et al. Chem Commun 2014; 50: 15890 (b) Ji X, Ji K, Chittavong V, Aghoghovbia RE, Zhu M, Wang B. J Org Chem 2017; 82: 1471
30 Huang G, Kouklovsky C, La Torre A d. Chem Eur J 2021; 27: 4760
31 Huang W, Gunawardhana N, Zhang Y, Escorihuela J, Laughlin ST. Chem Eur J 2024; 30: e202303465
32 Varga BR, Kállay M, Hegyi K, Béni S, Kele P. Chem Eur J 2012; 18: 822
33 (a) Cui Q, Pan TW, Shieh M et al. Org Lett 2022; 24: 7334 (b) Huang W, Wen K, Laughlin ST, Escorihuela J. Org Biomol Chem 2024; 22: 8285
34 (a) Png ZM, Zeng H, Ye Q, Xu J. Chem Asian J 2017; 12: 2142 (b) Zhang J, Shukla V, Boger DL. J Org Chem 2019; 84: 9397 (c) Zhang F-G, Chen Z, Tang X, Ma J-A. Chem Rev 2021; 121: 14555
35 (a) Sun H, Xue Q, Zhang C, Wu H, Feng P. Org Chem Front 2022; 9: 481 (b) Venrooij KR, Bondt L, de Bonger KM. Top Curr Chem 2024; 382: 24 (c) Yu A, He X, Shen T et al. Chem Soc Rev 2025; 54: 2984
36 Meguro T, Chen S, Kanemoto K, Yoshida S, Hosoya T. Chem Lett 2019; 48: 582
37 (a) Kessler SN, Neuburger M, Wegner HA. Eur J Org Chem 2011; 2011: 3238 (b) Kessler SN, Neuburger M, Wegner HA. J Am Chem Soc 2012; 134: 17885 (c) Schweighauser L, Bodoky I, Kessler S, Häussinger D, Wegner H. Synthesis 2012; 44: 2195 (d) Schweighauser L, Bodoky I, Kessler SN, Häussinger D, Donsbach C, Wegner HA. Org Lett 2016; 18: 1330 (e) Ahles S, Götz S, Schweighauser L et al. Org Lett 2018; 20: 7034 (f) Ahles S, Ruhl J, Strauss MA, Wegner HA. Org Lett 2019; 21: 3927 (g) Ruhl J, Ahles S, Strauss MA, Leonhardt CM, Wegner HA. Org Lett 2021; 23: 2089 (h) Beeck S, Ahles S, Wegner HA. Chem Eur J 2022; 28: e202104085 (i) Große M, Wegner HA. Synlett 2024; 35: 1019 (j) Große M, Leonhardt CM, Campbell PAR, Wegner HA. Org Lett 2025; 27: 4893
38 Wegner H, Kessler S. Synlett 2012; 23: 699
39 Yang Y-F, Liang Y, Liu F, Houk KN. J Am Chem Soc 2016; 138: 1660
40 Cheng Q, Bhattacharya D, Haring M, Cao H, Mück-Lichtenfeld C, Studer A. Nat Chem 2024; 16: 741
41 Pradhan S, Mohammadi F, Bouffard J. J Am Chem Soc 2023; 145: 12214
42 (a) Segura JL, Martín N. Chem Rev 1999; 99: 3199 (b) Yang B, Gao S. Chem Soc Rev 2018; 47: 7926
43 Tian X, Roch LM, Baldridge KK, Siegel JS. Eur J Org Chem 2017; 2017: 2801

About the authors

Michel Große

Michel Große received his BSc in Biotechnical Chemistry from Ilmenau University of Technology, Germany, and his MSc in Chemical Biology from Friedrich Schiller University Jena, Germany. Since 2022, he has been pursuing his PhD in Organic Chemistry at Justus Liebig University Giessen, Germany, under the supervision of Prof. Dr. Hermann A. Wegner. His research focuses on inverse electron-demand Diels–Alder reactions involving strained alkenes and alkynes.

Thieme

Synlett

Hermann A. Wegner

Hermann A. Wegner received his education in Chemistry in Göttingen, Germany, and Boston College, USA. After finishing his PhD under the guidance of Prof. Dr. Armin de Meijere, including a stay in the group of Prof. Dr. Paul Wender at Stanford University, USA, he completed his Postdoc at Oxford University, UK, in the group of Sir Prof. Dr. Jack Baldwin. He started his independent career at Basel University, Switzerland, before he moved to his current position at the Justus Liebig University, Giessen, Germany. His research focuses on physical organic chemistry and synthetic method development, including flow chemistry in view of molecular materials applications.

Große Michel et al. doi: 10.1055/a-2661-3958

3.4 Modular Assembly of Conformationally Dynamic Dinaphthocycloocta-1,5-dienes

Reference: M. Große, C. M. Leonhardt, H. A. Wegner, *ChemRxiv*, 10.26434/chemrxiv-2025-6dlz2.

DOI: 10.26434/chemrxiv-2025-6dlz2

“The integration of cyclooctene-derived motifs into larger molecular frameworks has emerged as a promising strategy to construct switchable molecules and materials that rely on conformational changes of the central eight-membered ring. In this work, we developed a facile synthetic route to access dinaphthocycloocta-1,5-dienes (DNCODs) relying on Lewis acid catalyzed inverse electron-demand Diels−Alder (IEDDA) reactions of phthalazines and cyclooct-1-en-5-yne derivatives. By employing two sequential IEDDA reactions, the modular annulation of different naphthalene units to the cyclooctadiene core was achieved. While the resulting DNCODs were found to adopt a chair conformation in the crystalline state, variable temperature (VT) NMR spectroscopy revealed a dynamic equilibrium in solution, with the twist-boat conformer being favoured. These findings offer new opportunities for engineering switchable cyclooctene-based structures and integrating them into functional materials.”

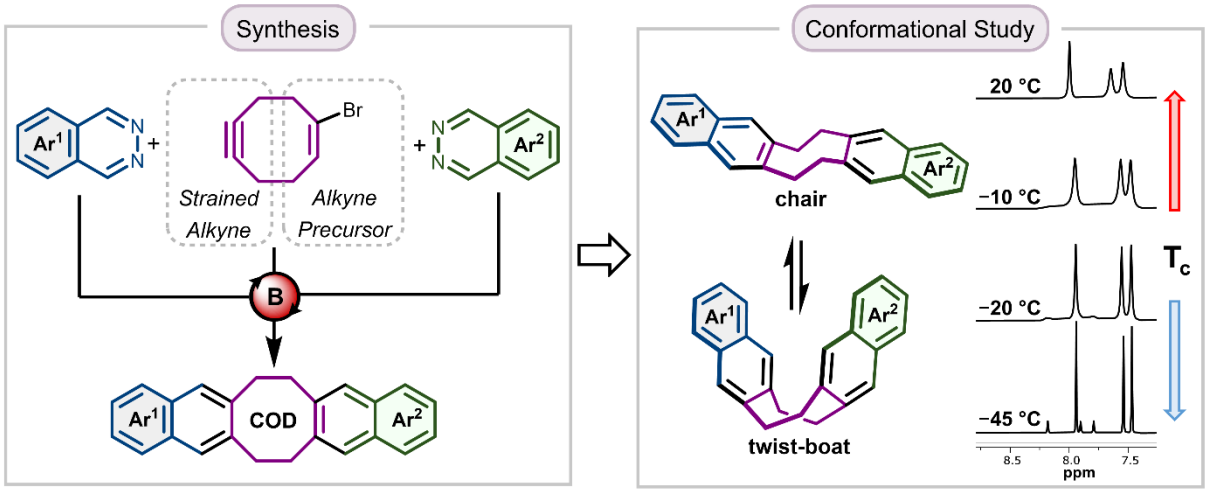

Modular Assembly of Conformationally Dynamic Dinaphthocyclo-octa-1,5-dienes

Michel Große,[a, b] Christopher M. Leonhardt,[a, b] and Hermann A. Wegner*[a, b]

[a] Institute of Organic Chemistry
Justus Liebig University Giessen
Heinrich-Buff-Ring 17, 35392 Giessen (Germany)
E-mail: hermann.a.wegner@org.chemie.uni-giessen.de
[b] Center for Materials Research (ZfM/LaMa)
Justus Liebig University Giessen
Heinrich-Buff-Ring 16, 35392 Giessen (Germany)

Abstract: The integration of cyclooctene-derived motifs into larger molecular frameworks has emerged as a promising strategy to construct switchable molecules and materials that rely on conformational changes of the central eight-membered ring. In this work, we developed a facile synthetic route to access dinaphthocycloocta-1,5-dienes (DNCODs) relying on Lewis acid catalyzed inverse electron-demand Diels–Alder (IEDDA) reactions of phthalazines and cyclooct-1-en-5-yne derivatives. By employing two sequential IEDDA reactions, the modular annulation of different naphthalene units to the cyclooctadiene core was achieved. While the resulting DNCODs were found to adopt a chair conformation in the crystalline state, variable temperature (VT) NMR spectroscopy revealed a dynamic equilibrium in solution, with the twist-boat conformer being favoured. These findings offer new opportunities for engineering switchable cyclooctene-based structures and integrating them into functional materials.

Introduction

Eight-membered carbo- and heterocycles fused to aromatic ring systems have emerged as versatile scaffolds in the construction of functional molecules and materials. The ability of eight-membered rings, especially cycloocta-1,5-dienes (CODs) and cyclooctatetraenes (COTs), to bring flexibility into larger, otherwise rigid polycyclic ring structures has led to their application in organic photonics and electronics,[1–4] molecular sensors,[5] and supramolecular assemblies.[6,7] In this regard, a new class of materials has been developed over the last decade based on conformational changes of dibenzocycloocta-1,5-diene (DBCOD), which consists of a flexible eight-membered ring fused to two rigid aromatic rings on opposite sites. Lu and coworkers were the first to describe a DBCOD-containing polymer that exhibited an unusual and completely reversible thermal contraction triggered by NIR stimulation.[8] They further showed that this mechanical response arises from the thermally induced conformational change of DBCOD from the twist-boat (global minimum) to the chair (local minimum) conformer (Scheme 1a).[9] This intriguing conformational effect led to extensive research not only on DBCOD in material applications,[10–22] but also aiming at better understanding and fine-tuning this new type of molecular switch as well as its heterocyclic analogs.[23–26] In a comprehensive study, Lu and coworkers showed that the twist-boat conformer can be stabilized by substituents capable of forming intramolecular hydrogen bonds while the chair conformer is stabilized by repulsive substituent interactions.[26] The DBCOD derivatives used in this study were synthesized by dimerizing substituted *α,α'*-dibromo-*o*-xylene in the presence of lithium metal as previously described by Boudjouk and co-workers.[27]

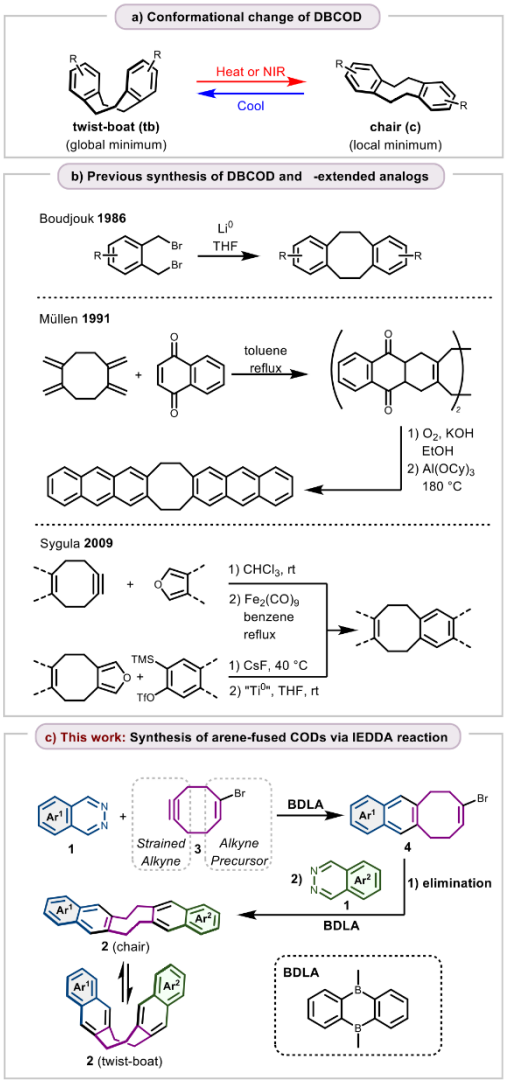

Scheme 1. Conformational behaviour and synthesis of arene-annulated CODs.

https://doi.org/10.26434/chemrxiv-2025-6dlz2 **ORCID:** https://orcid.org/0000-0001-7260-6018

However, while this method yields symmetric dimerization products, DBCOD derivatives having differently substituted aromatic rings on opposite sides have rarely been prepared or investigated. Similarly, only a few methods for the synthesis of π-extended DBCOD analogues have been reported,[6,28] most of which require multiple-step preparation and do not offer a broad substrate scope (Scheme 1b). Furthermore, reported solubility issues prevented the investigation of the conformational behaviour of these compounds in solution.[6]

In light of these limitations, we reasoned that a modular synthetic approach to arene-fused CODs would be highly desirable to further enable systematic investigations and application of this class of molecular materials. We recently reported a method for the synthesis of arene-annulated cyclooctenes via inverse electron-demand Diels–Alder (IEDDA) reaction of phthalazines (**1**) and cyclooctynes catalyzed by a bidentate Lewis acid (**BDLA**).[29] The boron-based catalyst functions by lowering the LUMO energy of the diazine through complexation and thus facilitates the cycloaddition step.[30]

Herein, we report the expansion of this strategy to the synthesis of naphthalene-fused CODs **2** by employing previously described (*E*)-1-bromocyclooct-1-en-5-yne (**3**) (Scheme 1c).[31] This dienophile contains a strained alkyne on one side and a vinyl bromide as a latent alkyne precursor on the opposite site,[6,32] which enabled the modular synthesis of dinaphtho-CODs (DNCODs) **2** by two sequential IEDDA reactions. Variable temperature (VT) NMR studies gave valuable insights into the conformational behaviour of these compounds.

Results and Discussion

Synthesis

To realize the envisaged synthetic strategy, we commenced our investigation with the IEDDA reaction of different phthalazines **1a-d** and alkyne **3** (Table 1), which can be easily prepared from cycloocta-1,5-diene over three steps. As the strained alkyne **3** is reported to be highly reactive and unstable,[31] we decided to use it in excess as a crude extract that has to be deoxygenated prior to the addition of the oxygen-sensitive **BDLA** catalyst. By treating this extract with a mixture of reactive, electron-poor difluorophthalazine **1b** and the catalyst, we were able to isolate the desired substituted naphthalene **4b** in 40% yield (Table 1, Entry 1). With a larger excess of alkyne, the yield was improved to 60%. To make the reaction suitable for higher temperatures, the solvent was exchanged for 1,4-dioxane which resulted in a further increase in yield to 72%. Similarly, phthalazine **1c** carrying two ester groups underwent the IEDDA smoothly under the same conditions and furnished the substituted naphthalene **4c** in 78% yield. For less reactive unsubstituted phthalazine (**1a**) and methoxyphthalazine **1d**, yields in the same range were achieved by using a larger excess of alkyne und higher temperatures (Table 1, Entries 4 and 5).

With optimized conditions for the first IEDDA reaction of electron-poor, -neutral and -rich phthalazines in hand, we proceeded by subjecting the obtained vinyl bromides **4a-d** to the elimination reaction with KO*t*-Bu and catalytic amounts of 18-crown-6 ether. Contrary to literature reports,[32] performing the reaction at elevated temperature (60 °C) did not yield the desired strained alkynes **6** in our case but rather resulted in the exclusive formation of dienes **7**.

Table 1. Reaction conditions of the IEDDA reaction of (*E*)-1-bromocyclooct-1-en-5-yne (**3**) with different phthalazines.

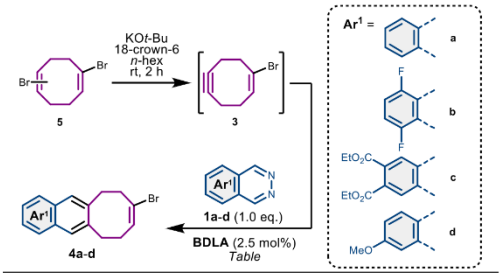

Entry	Ar¹	**5** (eq.)	Solvent	T (°C)	t (h)	Yield (%)
1[a]	b	1.5	EA/*n*-hex	reflux	24	40
2[a]	b	2.5	EA/*n*-hex	reflux	24	60
3[b]	b	2.5	1,4-dioxane	80	24	72
4[b]	c	2.5	1,4-dioxane	80	24	78
5[b]	a	4.0	1,4-dioxane	100	48	72
6[b]	d	6.0	1,4-dioxane	100	72	68[c]

[a]Crude extracts containing alkyne **3** were deoxygenated by bubbling nitrogen through the solution for 1 h. [b]Crude extracts containing alykne **3** were concentrated *in vacuo*, re-dissolved in 1,4-dioxane and degassed by three freeze-pump-thaw cycles. [c]A 1:1 mixture of regioisomers was obtained (EA = ethyl acetate, *n*-hex = *n*-hexane).

Temperatures below 0 °C led to an incomplete conversion with the diene formation still not completely suppressed. Optimal conditions with less than 10% diene formation and complete conversion were found by performing the addition at 0 °C and subsequent warming to room temperature. In that way, the strained alkynes **6a** and **6d** were obtained in 89% yield after filtration over silica. Alkyne **6b** bearing an electron-deficient aromatic part had to be purified via column chromatography, which resulted in a diminished yield of 63% together with 9% of diene **7b**. In the case of diethyl naphthalenedicarboxylate **3c**, treatment with KO*t*-Bu furnished a mixture of different transesterification products rather than the desired alkyne **6c**.

With three strained alkynes **6a**,**b** and **d** in hand, we set out to explore the scope of the second IEDDA reaction. Differently substituted phthalazines and pyridazino-aromatics were reacted with alkyne **6b** in the presence of the **BDLA** catalyst adapting the previously described conditions for analogues reactions with cyclooctyne (Scheme 2).[29]

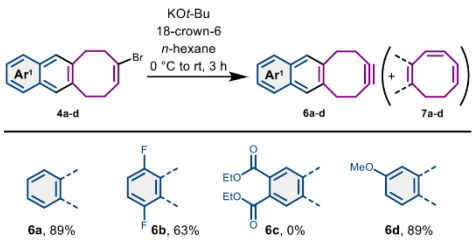

Scheme 2. Synthesis of naphthalene-fused cyclooct-1-en-5-ynes **6** via elimination. Reaction conditions: vinyl bromide **4a-d** (0.6-0.7 mmol, 1 equiv.), KO*t*-Bu (1.6-1.7 mmol, 2.5 equiv.) and 18-crown-6 (0.16-0.17 mol, 0.25 equiv.) in anhydrous *n*-hexane (50 mL).

https://doi.org/10.26434/chemrxiv-2025-6dlz2 **ORCID:** https://orcid.org/0000-0001-7260-6018

Good to excellent yields were achieved for the second IEDDA reaction with electron-deficient mono- and dihalogenated (**1b**,**e**,**f**) as well as CF_3- (**1g**), nitro- (**1h**) and ester-substituted (**1c**) phthtalazines. Similarly, pyridopyridazine **1i** furnished the desired quinoline **2bi** in a very good yield of 82%.

Unfortunately, electron-neutral, unsubstituted phthalazine (**1a**) gave the desired DNCOD **2ba** only in 15% yield. Nevertheless, we were able to synthesize dinaphthalene **2ba** (= **2ab**) in a very good yield by reacting alkyne **6a** with difluorophthalazine **1b**. In that way, the yield for the synthesis of the desired DNCOD was improved from 10% (**2ba**) to 29% (**2ab**) over three steps simply by switching the order of phthalazines in the reaction sequence. Accordingly, only traces of product **2bd** could be isolated from the reaction of alkyne **6b** and electron-rich methoxyphthalazine **1d**. Methoxy-substituted dinaphthalene **2dc** was obtained in a very good yield by utilizing alkyne **6d**, though. Although this method is not suitable for the synthesis of DNCODs with two electron-rich aromatic parts, it enables many other possible combinations, provided that at least one aromatic unit is electron-deficient.

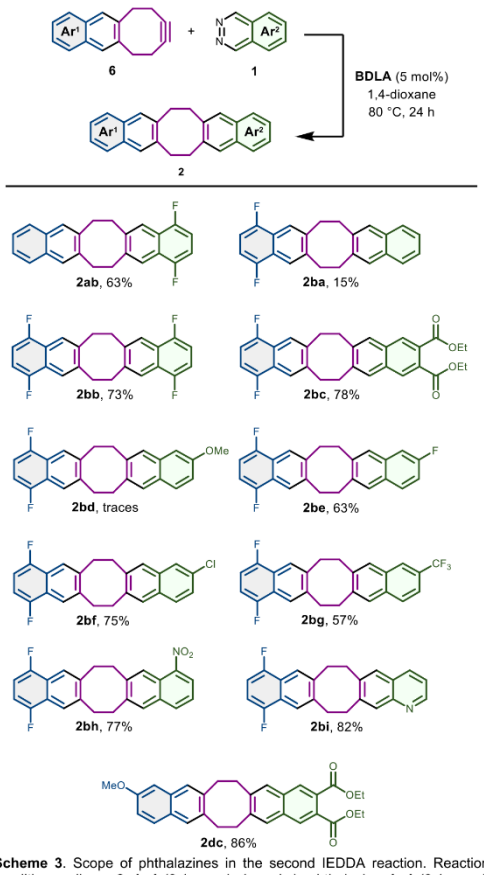

Scheme 3. Scope of phthalazines in the second IEDDA reaction. Reaction conditions: alkyne **6a**,**b**,**d** (0.1 mmol, 1 equiv.), phthalazine **1a-i** (0.1 mmol, 1 equiv.) and BDLA (5 µmol, 5 mol%) in 1,4-dioxane (2 mL).

In addition to the electronic nature of the employed phthalazine, the solubility of the resulting dinaphthalenes had a significant influence on the yields. With the exception of **2bc**, **2bi** and **2dc**, all other DNCODs showed only very limited solubility in common organic solvents. Thus, recrystallization was sometimes preferred over chromatography for purification, which in turn led to reduced yields.

Conformational Study

With a modular route for the synthesis of diversely substituted DNCODs established, we focused on a detailed examination of the conformational preferences of the target compounds. DBCODs lacking intramolecular hydrogen bonding have been reported to preferentially crystallize in the chair conformation.[26,33] In line with these findings, we observed that our DNCODs adopt the same conformation in the solid state due to energetically favourable π-π interactions, as confirmed by X-ray crystallographic analysis of tetrafluoro derivative **2bb** (Figure 1). However, solutions of (substituted) DBCODs have been reported to contain mixtures of chair and twist-boat conformers in varying ratios, depending on the temperature and substitution pattern.[26] Additionally, earlier reports identified a twist form as a third local minimum conformation. This twist conformer, although reported to be too high in energy to be present in solution in significant amounts, is thought to represent a pivotal intermediate in several interconversion pathways.[34]

Given these findings, we aimed to investigate the in-solution behaviour of our DNCODs by VT NMR spectroscopic analysis. As model substrates, we chose naphtho-CODs **2bc** and **2dc**, as they both feature two electron-withdrawing ester substituents on one naphthalene unit and differ significantly in the electronic nature of the second aromatic ring system. Additionally, both compounds exhibited good solubility in common organic solvents, even at low temperatures. At 20 °C, the ^{1}H NMR spectra of both compounds displayed only merged signals from the twist-boat and the chair conformers (Figure 2). Upon cooling, all signals further broadened until the coalescence temperature T_c was reach between 0 °C and −10 °C. Below −10 °C, the interconversion rate of both conformers slowed down sufficiently, allowing the individual signals of the twist-boat and chair conformers to be detected. While the methylene protons of the eight-membered ring in the chair conformer showed two distinct signals belonging to the axial and equatorial protons, only one, broadened peak was observed for the twist-boat due to rapid boat inversion even at −45 °C.[35] Further cooling to −60 °C slowed down this inversion, causing the broad singlet to split up into two separate signals (see Figure S5). In the aromatic region, proton resonances of the chair conformer appeared at higher frequencies compared to the twist-boat, due to reduced shielding in the former.[36]

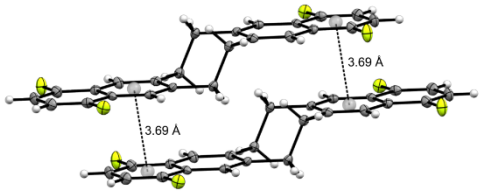

Figure 1. Solid-state structure of DNCOD **2bb** (CCDC: 2433662). Thermal ellipsoids are shown at 50% probability.

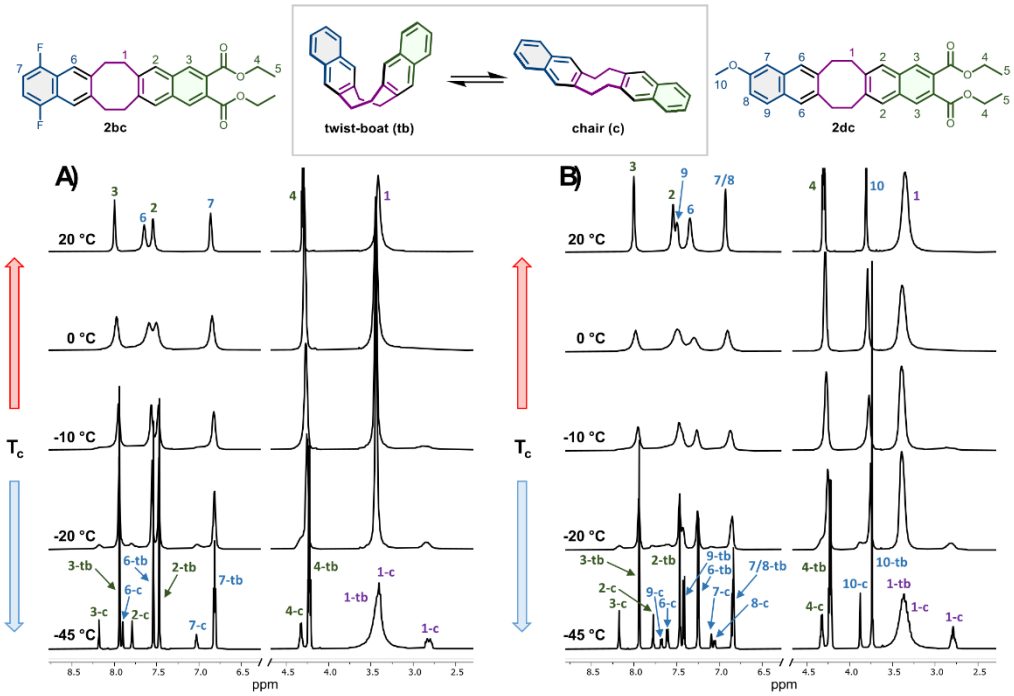

Figure 2. Variable temperature ^{1}H NMR (600 MHz) spectra with peak assignment of DNCODs **2bc** (A) and **2dc** (B) in CD_2Cl_2 (c = chair, tb = twist-boat).

Across the entire temperature range, the twist-boat conformer was found to be the dominant form. This experimental observation is supported by our computational analysis (see section 3 of the SI), which also identified the twist-boat as the most stable conformer, followed by the chair. The twist form, however, was found to be too high in energy to be present in detectable amounts.

The VT NMR data enabled the determination of the thermodynamic and kinetic parameters of the twist-boat/chair equilibrium. The spectra acquired below T_c were used to calculate the Gibbs free energy difference ΔG^0 between the twist-boat and chair forms of DNCODs **2bc** and **2dc** based on the relative populations of both conformers obtained by integration (see Section 2.2.1 of the SI). For both derivatives, the twist-boat conformer was found to be thermodynamically favoured by 2.8 kJ/mol at 25 °C, corresponding well to the observed twist-boat-to-chair ratio of approximately 3:1 at this temperature. The equilibrium only shows a minor temperature dependence, with a temperature increase from −80 °C to 25 °C resulting in just a 10% increase in the chair population (See SI). These values indicate that DNCODs generally exhibit a stronger preference for the twist-boat conformation across a wider temperature range compared to related DBCOD derivatives. As both naphthalene units in one DNCOD are too far apart to show any non-covalent intramolecular interactions, even in the twist-boat form (see Figures S12 and S13), no effect of the electronic nature of the aromatic rings was observed.

For the determination of the kinetic parameters of the equilibrium, rate constants of the interconversion were obtained via dynamic NMR lineshape analysis (see section 2.2.2 of the SI). For DNCODs **2bc** and **2dc**, similar activation energies of 53.5 kJ/mol and 55.5 kJ/mol, respectively, were obtained, with both derivatives showing negative entropies of activation for the conformational change. This barrier is about 10 kJ/mol higher than that reported for unsubstituted DBCOD and more comparable to values previously obtained for derivatives, where intramolecular hydrogen bonding stabilizes the twist-boat conformer.[26,34] However, as mentioned above, no such interactions, nor comparable ones, were identified for the DNCODs **2bc** and **2dc** through our computational analysis. This further underlines that naphthalene units fused to a COD core generally provide a greater stabilization of the twist-boat conformer in comparison to benzannulated analogues.

Conclusion

In summary, we developed a concise route for the synthesis of substituted DNCODs from readily available phthalazines, employing two sequential **BDLA**-catalyzed IEDDA reactions. The first IEDDA reaction furnished bromocyclooctanaphthalenes **4a-d** in good yields with electron-poor and electron-rich phthalazines under optimized conditions. Subsequent base-mediated elimination afforded comparatively stable cyclooctenynes **6a**, **6b** and **6d**, which were further converted into the desired DNCODs via a second IEDDA reaction. This sequence enabled the direct

annulation of differently substituted naphthalenes to the COD core in a modular fashion. X-ray crystallographic analysis of dinaphthalene **2bb** revealed that these DNCODs adopt a chair conformation in the solid state. In solution, however, the twist-boat form was found to predominate independent of the electronic nature of the naphthalene units. Furthermore, the activation energy of the twist-boat/chair interconversion was found to be slightly higher compared to related DBCOD derivatives, as determined by DNMR spectroscopy. These results provide a basis to guide future developments in the design of switchable molecules relying on conformational interconversions of cyclooctene-derived scaffolds and foster their integration into functional materials.

Author Contributions

M. G. and H. A. W. conceptualized the project. M. G. performed the organic synthesis and collected experimental data. C. M. L. performed the DFT calculations. All authors were involved in discussing the data and preparing the manuscript.

Conflicts of Interest

There are no conflicts to declare.

Data Availability

The data supporting this article have been included as part of the Supplementary Information. Crystallographic data for compound 2bb has been deposited at the Cambridge Crystallographic Data Centre (CCDC) under deposition number 2433662.

Acknowledgements

The financial support by the LOEWE Program of Excellence of the Federal State of Hesse (LOEWE Focus Group PriOSS “Principles of On-Surface Synthesis”) is gratefully acknowledged. The authors thank the Organic Chemistry Analytics Department (Institute of Organic Chemistry, Justus Liebig University, Giessen) for NMR spectroscopy and HRMS measurements, especially Dr. Heike Hausmann for performing the VT NMR measurements and for helpful discussions regarding their evaluation.

References

1 Y. Xiong, Q. Gong and Q. Miao, *Chem. Asian J.*, 2023, **18**, e202300623.
2 T. Yamakado, S. Takahashi, K. Watanabe, Y. Matsumoto, A. Osuka and S. Saito, *Angew. Chem. Int. Ed.*, 2018, **57**, 5438–5443.
3 C. Yuan, S. Saito, C. Camacho, T. Kowalczyk, S. Irle and S. Yamaguchi, *Chem. Eur. J.*, 2014, **20**, 2193–2200.
4 C. Yuan, S. Saito, C. Camacho, S. Irle, I. Hisaki and S. Yamaguchi, *J. Am. Chem. Soc.*, 2013, **135**, 8842–8845.
5 R. Kotani, H. Sotome, H. Okajima, S. Yokoyama, Y. Nakaike, A. Kashiwagi, C. Mori, Y. Nakada, S. Yamaguchi, A. Osuka, A. Sakamoto, H. Miyasaka and S. Saito, *J. Mater. Chem. C*, 2017, **5**, 5248–5256.
6 L. Kobryn, W. P. Henry, F. R. Fronczek, R. Sygula and A. Sygula, *Tetrahedron Lett.*, 2009, **50**, 7124–7127.
7 A. Sygula, F. R. Fronczek, R. Sygula, P. W. Rabideau and M. M. Olmstead, *J. Am. Chem. Soc.*, 2007, **129**, 3842–3843.
8 G. Uğur, J. Chang, S. Xiang, L. Lin and J. Lu, *Adv. Mater.*, 2012, **24**, 2685–2690.
9 X. Shen, C. Viney, E. R. Johnson, C. Wang and J. Q. Lu, *Nat. Chem.*, 2013, **5**, 1035–1041.
10 Y. Feng, Q. Sun, J. Guo and C. Wang, *Macromolecules*, 2024, **57**, 1808–1818.
11 Q. Sun, Y. Feng, J. Guo and C. Wang, *Eur. Polym. J.*, 2023, **189**, 111986.
12 C. Guo, Q. Peng, H. Wei, J. Liu, X. Hu, J. Peng, J. Ma, X. Ye and J. Yang, *ACS omega*, 2023, **8**, 9464–9474.
13 Q. Sun, Y. Feng, J. Guo and C. Wang, *Chem. Eng. J.*, 2022, **450**, 138295.
14 Y. Feng, K. Jin, J. Guo and C. Wang, *Polym. Chem.*, 2021, **12**, 4812–4821.
15 J. C. Foster, C. L. Staiger, J. W. Dugger and E. M. Redline, *ACS Macro Lett.*, 2021, **10**, 940–944.
16 K. Jin, Q. Sun, Y. Feng, J. Guo, J. Xu and C. Wang, *ACS Appl. Polym. Mater.*, 2021, **3**, 2120–2130.
17 K. Zhang, G. Ji, N. Zhang, N. Wang, X. Yin, Q. Li and P. Chen, *J. Mater. Chem. C*, 2021, **9**, 13851–13859.
18 M. Leveille, X. Shen, W. Fu, K. Jin, M. Acerce, C. Wang, J. Bustamante, A. M. Casas, Y. Feng, N.-H. Ge, L. S. Hirst, S. Ghosh and J. Q. Lu, *Adv. Sci.*, 2021, **8**, e2102077.
19 Z. Wang, Y. Huang, J. Guo, Z. Li, J. Xu, J. Q. Lu and C. Wang, *Macromolecules*, 2018, **51**, 1377–1385.
20 Y. Huang, X. Shen, Z. Wang, K. Jin, J. Q. Lu and C. Wang, *Macromolecules*, 2018, **51**, 8477–8485.
21 X. Shen, T. Connolly, Y. Huang, M. Colvin, C. Wang and J. Lu, *Macromol. Rapid Commun.*, 2016, **37**, 1904–1911.
22 X. Shen, C. Viney, C. Wang and J. Q. Lu, *Adv. Funct. Mater.*, 2014, **24**, 77–85.
23 R. Weiss, Y. Cornaton, H. Khartabil, L. Groslambert, E. Hénon, P. Pale, J.-P. Djukic and V. Mamane, *ChemPlusChem*, 2022, **87**, e202100518.
24 F. Ishiwari, S. Miyake, K. Inoue, K. Hirose, T. Fukushima and A. Saeki, *Asian J. Org. Chem.*, 2021, **10**, 1377–1381.
25 Q. Sun, K. Jin, Y. Huang, J. Guo, T. Rungrotmongkol, P. Maitarad and C. Wang, *Chin. Chem. Lett.*, 2021, **32**, 1515–1518.
26 W. Fu, T. M. Alam, J. Li, J. Bustamante, T. Lien, R. W. Adams, S. J. Teat, B. J. Stokes, W. Yang, Y. Liu and J. Q. Lu, *J. Am. Chem. Soc.*, 2020, **142**, 16651–16660.
27 P. Boudjouk, R. Sooriyakumaran and B. H. Han, *J. Org. Chem.*, 1986, **51**, 2818–2819.
28 B. Becker, A. Bohnen, M. Ehrenfreund, W. Wohlfarth, Y. Sakata, W. Huber and K. Muellen, *J. Am. Chem. Soc.*, 1991, **113**, 1121–1127.
29 M. Große and H. A. Wegner, *Synlett*, 2024, **35**, 1019–1022.
30 H. Wegner and S. Kessler, *Synlett*, 2012, **23**, 699–705.
31 H. Detert, B. Rose, W. Mayer and H. Meier, *Chem. Ber.*, 1994, **127**, 1529–1532.
32 B. R. Varga, M. Kállay, K. Hegyi, S. Béni and P. Kele, *Chem. Eur. J.*, 2012, **18**, 822–828.
33 P. Domiano, P. Cozzini, R. M. Claramunt, J. L. Lavandera, D. Sanz and J. Elguero, *J. Chem. Soc., Perkin Trans. 2*, 1992, 1609–1620.
34 M. L. Jimeno, I. Alkorta, J. Elguero, J. E. Anderson, R. M. Claramunt and J. L. Lavandera, *New J. Chem.*, 1998, **22**, 1079–1083.
35 F. Sauriol-Lord and M. St-Jacques, *Can. J. Chem.*, 1975, **53**, 3768–3776.
36 D. Montecalvo, M. St. Jacques and R. Wasylishen, *J. Am. Chem. Soc.*, 1973, **95**, 2023–2024.

4 Conclusion

Combining aromatic ring systems with cyclooctene-derived motifs has become a promising strategy to access molecules with unique conformational behaviour and potential applications in functional materials and medicinal chemistry. In this thesis, two different strategies were developed for the synthesis of arene-fused eight-membered carbo- and heterocycles, respectively. The first approach was based on BDLA-catalyzed IEDDA reactions of phthalazines and strained alkynes. While the feasibility of this concept was demonstrated using simple cyclooctyne dienophiles, it was further extended to the synthesis of dinaphtho-fused CODs by employing a bifunctional cycloocta-1,5-diyne surrogate in two sequential IEDDA reactions. In contrast to existing protocols for the synthesis of arene-annulated CODs, this approach enabled the modular introduction of different aromatic moieties with diverse substitution pattern on both sides of the COD core. X-ray crystallographic analysis in combination with VT NMR spectroscopy provided insights into the geometric preferences of the central eight-membered ring, which might help to guide future developments in the design of functional materials with potential applications in polymer science and supramolecular chemistry.

The second approach was dedicated to the synthesis of benzo-fused eight-membered nitrogen heterocycles, a structural motif commonly found in biologically active natural products and synthetic compounds. To this end, the same catalytic principle was employed to activate phthalazines using the BDLA catalyst. In contrast to the first approach, utilization of a 2-azetine dienophile generated a highly reactive *o*-QDM intermediate after the extrusion of nitrogen. This intermediate subsequently underwent an electrocyclic ring expansion to furnish the desired azocine scaffold. The simultaneous formation of a fused aromatic ring provided a suitable driving force for the rearrangement to the eight-membered ring structure. In comparison to existing strategies for the synthesis of benzannulated azocine frameworks, this approach relies on simple, readily available starting materials and works in the absence of transition metals. The resulting heterocyclic ring structures offer great potential for further derivatization to explore the full potential of eight-membered rings in medicinal chemistry.

5 Abbreviations

Ac	acyl
Ar	aryl
B	boat
BCOD	bicyclo[4.2.0]octa-2,4-diene
BDLA	bidentate Lewis acid
Boc	*tert*-butyloxycarbonyl
Bz	benzoyl
C	chair
CCDC	Cambridge Crystallographic Data Centre
COD	cycloocta-1,5-diene
COT	cyclooctatetraene
COTR	cycloocta-1,3,5-triene
c-Pr	cyclopropyl
DA	Diels–Alder
DBCOD	dibenzocycloocta-1,5-diene
DCE	1,2-dichloroethane
DDQ	2,3-dichloro-5,6-dicyano-1,4-benzoquinone
DFT	density functional theory
Dipp	diisopropylphenyl
DMAD	dimethyl acetylenedicarboxylate
DMF	dimethylformamide
DNMR	dynamic nuclear magnetic resonance
EDG	electron-donating group
Et	ethyl
EWG	electron-withdrawing group
FMO	frontier molecular orbital
HFIP	1,1,1,3,3,3-hexafluoropropan-2-ol
HIV	human immunodeficiency virus
HOMO	highest occupied molecular orbital
HPLC	high-performance liquid chromatography
IEDDA	inverse electron-demand Diels–Alder
L	ligand
LA	Lewis acid
LUMO	lowest unoccupied molecular orbital
Me	methyl

MP	methyl pyruvate
MSR	medium-sized ring
NEDDA	normal electron-demand Diels–Alder
NIR	near-infrared
NK_1	neurokinin 1
NMR	nuclear magnetic resonance
o	*ortho*
Oct	octyl
o.n.	overnight
o-QDM	*ortho*-quinodimethane
Ox.	oxidation
Ph	phenyl
PIRO	photo-induced ring-opening
p-Tol	*para*-tolyl
rt	room temperature
SWD	Sondheimer–Wong diyne
T	twist
TB	twist-boat
Tf	triflyl
THF	tetrahydrofuran
TIPS	triisopropylsilyl
Ts	tosyl
VT	variable temperature

6 Acknowledgement

An erster Stelle möchte ich mich herzlich bei meinem Doktorvater Prof. Dr. Hermann A. Wegner für die Möglichkeit bedanken, meine Doktorarbeit in seiner Arbeitsgruppe anzufertigen. Vor allem sein Vertrauen in meine Arbeit sowie seine Unterstützung werden mir in sehr guter Erinnerung bleiben.

Weiterhin möchte ich mich bei Prof. Dr. Richard Göttlich für die Anfertigung des Zweitgutachtens bedanken.

Besonders dankbar bin ich meiner Freundin Julia für ihre kompromisslose Unterstützung und ihr Verständnis in allen Lebenslagen. Sie stand mir während der gesamten Zeit immer zur Seite und hat maßgeblichen Anteil am Erfolg dieser Arbeit. Ebenfalls danke ich meiner gesamten Familie, allen voran meinen Eltern sowie meinen Schwestern, die immer eine riesige Unterstützung für mich waren. Auch allen meinen Freunden bin ich sehr dankbar für die vielen schönen Stunden, die ein wichtiger Ausgleich zum Laboralltag waren.

Natürlich möchte ich mich auch bei der gesamten Arbeitsgruppe Wegner für die schöne Zeit bedanken. Sei es im Labor, beim Feierabendbier, beim Skat- oder Pen-and-Paper-Spielen oder auf den schönen Gruppenausflügen, ich habe mich von Anfang an sehr willkommen und gut aufgehoben gefühlt. Besonderer Dank gilt Christopher Leonhardt und Dr. Dominic Schatz für ihre fachliche Unterstützung sowie die vielen wissenschaftlichen Diskussionen, aber natürlich auch allen anderen aktuellen und früheren Mitgliedern der Arbeitsgruppe: Silke Müsse, Conrad Averdunk, Kai Hanke, Marten Pfaff, Pia Mader, Rouven Fritzius, Dr. Nathaniel Ukah, Dr. Julia Ruhl, Dr. Daniel Kohrs, Dr. Felix Bernt, Dr. Jannis Volkmann, Dr. Jan Griwatz, Dr. Anne Kunz, Finn Schneider, Mari Janse van Rensburg sowie allen Bachelor- und Master-Student:innen.

Daneben danke ich den Arbeitsgruppen Schreiner, Göttlich und Gellrich für die entspannte und kollegiale Arbeitsatmosphäre im Institut.

Ebenfalls möchte ich mich bei allen Mitarbeiter:innen des Fachbereichs 08 bedanken, die mich immer freundlich und zuvorkommend bei allen wissenschaftlichen, technischen sowie administrativen Fragen unterstützt haben: Dr. Heike Hausmann, Anja Platt, Inna Klein, Anika Bernhardt, Dr. Raffael Wende, Steffen Wagner, Stefan Bernhardt, Dr. Jörg Neudert, Eike Santowski, Mario Dauber, Anja Beneckenstein, Jana Küchenmeister, Edgar Reitz, Brigitte Weinl-Boulakhrouf, Anika Jäger, Michaela Richter und Maurice Monnard.

7 References

[1] V. Prelog, *Pure Appl. Chem.* **1963**, *6*, 545.
[2] H. C. Brown, R. S. Fletcher, R. B. Johannesen, *J. Am. Chem. Soc.* **1951**, *73*, 212.
[3] M. Große, H. A. Wegner, *Synlett,* DOI 10.1055/a-2661-3958.
[4] A. Sygula, F. R. Fronczek, R. Sygula, P. W. Rabideau, M. M. Olmstead, *J. Am. Chem. Soc.* **2007**, *129*, 3842.
[5] C. Yuan, S. Saito, C. Camacho, S. Irle, I. Hisaki, S. Yamaguchi, *J. Am. Chem. Soc.* **2013**, *135*, 8842.
[6] C. Yuan, S. Saito, C. Camacho, T. Kowalczyk, S. Irle, S. Yamaguchi, *Chem. Eur. J.* **2014**, *20*, 2193.
[7] T. Yamakado, S. Takahashi, K. Watanabe, Y. Matsumoto, A. Osuka, S. Saito, *Angew. Chem. Int. Ed.* **2018**, *57*, 5438.
[8] Y. Xiong, Q. Gong, Q. Miao, *Chem. Asian J.* **2023**, *18*, e202300623.
[9] K. Nakamura, Q.-Q. Li, O. Krejčí, A. S. Foster, K. Sun, S. Kawai, S. Ito, *J. Am. Chem. Soc.* **2020**, *142*, 11363.
[10] F. Villalobos, J. I. Mendieta-Moreno, J. Lobo-Checa, S. P. Morcillo, J. I. Martínez, J. M. Gómez-Fernández, P. L. de Andres, J. A. Martin-Gago, J. M. Cuerva, A. G. Campaña et al., *J. Am. Chem. Soc.* **2025**, *147*, 7245.
[11] H. Qu, M. Zhao, W. Xu, *Chem. Eur. J.* **2025**, *31*, e202501399.
[12] G. González Miera, S. Matsubara, H. Kono, K. Murakami, K. Itami, *Chem. Sci.* **2022**, *13*, 1848.
[13] X. Shen, C. Viney, E. R. Johnson, C. Wang, J. Q. Lu, *Nat. Chem.* **2013**, *5*, 1035.
[14] A. A. Kroeger, A. Karton, *J. Comput. Chem.* **2022**, *43*, 96.
[15] P. B. Karadakov, *J. Phys. Chem. A* **2008**, *112*, 12707.
[16] P. v. R. Schleyer, C. Maerker, A. Dransfeld, H. Jiao, N. J. R. van Eikema Hommes, *J. Am. Chem. Soc.* **1996**, *118*, 6317.
[17] R. Kotani, H. Sotome, H. Okajima, S. Yokoyama, Y. Nakaike, A. Kashiwagi, C. Mori, Y. Nakada, S. Yamaguchi, A. Osuka et al., *J. Mater. Chem. C* **2017**, *5*, 5248.
[18] W. Nakanishi, S. Saito, N. Sakamoto, A. Kashiwagi, S. Yamaguchi, H. Sakai, K. Ariga, *Chem. Asian J.* **2019**, *14*, 2869.
[19] T. Yamakado, S. Saito, *J. Am. Chem. Soc.* **2022**, *144*, 2804.
[20] R. Kimura, H. Kitakado, A. Osuka, S. Saito, *Bull. Chem. Soc. Jpn.* **2020**, *93*, 1102.
[21] R. Kimura, H. Kitakado, T. Yamakado, H. Yoshida, S. Saito, *Chem. Commun.* **2022**, *58*, 2128.
[22] R. Kotani, S. Yokoyama, S. Nobusue, S. Yamaguchi, A. Osuka, H. Yabu, S. Saito, *Nat. Commun.* **2022**, *13*, 303.
[23] S. M. Bachrach, *J. Org. Chem.* **2009**, *74*, 3609.
[24] C.-N. Feng, W.-C. Hsu, J.-Y. Li, M.-Y. Kuo, Y.-T. Wu, *Chem. Eur. J.* **2016**, *22*, 9198.
[25] P. Domiano, P. Cozzini, R. M. Claramunt, J. L. Lavandera, D. Sanz, J. Elguero, *J. Chem. Soc., Perkin Trans. 2* **1992**, 1609.
[26] F. Sauriol-Lord, M. St-Jacques, *Can. J. Chem.* **1975**, *53*, 3768.

[27] D. Montecalvo, M. St. Jacques, R. Wasylishen, *J. Am. Chem. Soc.* **1973**, *95*, 2023.
[28] M. L. Jimeno, I. Alkorta, J. Elguero, J. E. Anderson, R. M. Claramunt, J. L. Lavandera, *New J. Chem.* **1998**, *22*, 1079.
[29] R. Crossley, A. P. Downing, M. Nógrádi, A. B. de Oliveira, W. D. Ollis, I. O. Sutherland, *J. Chem. Soc., Perkin Trans. 1* **1973**, 205.
[30] N. L. Allinger, J. T. Sprague, *Tetrahedron* **1975**, *31*, 21.
[31] G. Uğur, J. Chang, S. Xiang, L. Lin, J. Lu, *Adv. Mater.* **2012**, *24*, 2685.
[32] X. Shen, T. Connolly, Y. Huang, M. Colvin, C. Wang, J. Lu, *Macromol. Rapid Commun.* **2016**, *37*, 1904.
[33] Y. Huang, X. Shen, Z. Wang, K. Jin, J. Q. Lu, C. Wang, *Macromolecules* **2018**, *51*, 8477.
[34] Z. Wang, Y. Huang, J. Guo, Z. Li, J. Xu, J. Q. Lu, C. Wang, *Macromolecules* **2018**, *51*, 1377.
[35] M. Leveille, X. Shen, W. Fu, K. Jin, M. Acerce, C. Wang, J. Bustamante, A. M. Casas, Y. Feng, N.-H. Ge et al., *Adv. Sci.* **2021**, *8*, e2102077.
[36] K. Zhang, G. Ji, N. Zhang, N. Wang, X. Yin, Q. Li, P. Chen, *J. Mater. Chem. C* **2021**, *9*, 13851.
[37] K. Jin, Q. Sun, Y. Feng, J. Guo, J. Xu, C. Wang, *ACS Appl. Polym. Mater.* **2021**, *3*, 2120.
[38] J. C. Foster, C. L. Staiger, J. W. Dugger, E. M. Redline, *ACS Macro Lett.* **2021**, *10*, 940.
[39] Y. Feng, K. Jin, J. Guo, C. Wang, *Polym. Chem.* **2021**, *12*, 4812.
[40] Q. Sun, Y. Feng, J. Guo, C. Wang, *Chem. Eng. J.* **2022**, *450*, 138295.
[41] C. Guo, Q. Peng, H. Wei, J. Liu, X. Hu, J. Peng, J. Ma, X. Ye, J. Yang, *ACS omega* **2023**, *8*, 9464.
[42] Q. Sun, Y. Feng, J. Guo, C. Wang, *Eur. Polym. J.* **2023**, *189*, 111986.
[43] Y. Feng, Q. Sun, J. Guo, C. Wang, *Macromolecules* **2024**, *57*, 1808.
[44] W. Fu, T. M. Alam, J. Li, J. Bustamante, T. Lien, R. W. Adams, S. J. Teat, B. J. Stokes, W. Yang, Y. Liu et al., *J. Am. Chem. Soc.* **2020**, *142*, 16651.
[45] Q. Sun, K. Jin, Y. Huang, J. Guo, T. Rungrotmongkol, P. Maitarad, C. Wang, *Chin. Chem. Lett.* **2021**, *32*, 1515.
[46] B. Becker, A. Bohnen, M. Ehrenfreund, W. Wohlfarth, Y. Sakata, W. Huber, K. Muellen, *J. Am. Chem. Soc.* **1991**, *113*, 1121.
[47] L. Kobryn, W. P. Henry, F. R. Fronczek, R. Sygula, A. Sygula, *Tetrahedron Lett.* **2009**, *50*, 7124.
[48] Y.-J. Hu, L.-X. Li, J.-C. Han, L. Min, C.-C. Li, *Chem. Rev.* **2020**, *120*, 5910.
[49] G. Mehta, V. Singh, *Chem. Rev.* **1999**, *99*, 881.
[50] N. A. Petasis, M. A. Patane, *Tetrahedron* **1992**, *48*, 5757.
[51] M. C. Wani, H. L. Taylor, M. E. Wall, P. Coggon, A. T. McPhail, *J. Am. Chem. Soc.* **1971**, *93*, 2325.
[52] J. Gallego-Jara, G. Lozano-Terol, R. A. Sola-Martínez, M. Cánovas-Díaz, T. de Diego Puente, *Molecules* **2020**, *25*.
[53] F. Kavanagh, A. Hervey, W. J. Robbins, *Proc. Natl. Acad. Sci. U.S.A.* **1951**, *37*, 570.
[54] S. Paukner, R. Riedl, *Cold Spring Harb. Perspect. Med.* **2017**, *7*.
[55] G. Aguilar-Santos, *J. Chem. Soc. C* **1970**, *6*, 842.

[56] B. C. Maiti, R. H. Thomson in *Marine Natural Products Chemistry* (Eds.: D. J. Faulkner, W. H. Fenical), Springer US, Boston, MA, **1977**, pp. 159–163.
[57] K. Krautforst, J. Kulbacka, M. Fornasier, R. Mocci, A. Porcheddu, A. Pusceddu, D. Moccia, S. Murgia, U. Bazylińska, *Mol. Pharmaceutics* **2025**, *22*, 4747.
[58] J. Li, Z. Dong, C. Zhao, *New J. Chem.* **2024**, *48*, 4645.
[59] S. Lee, J. Sperry, *Bioorg. Med. Chem.* **2022**, *54*, 116560.
[60] M.-F. Qiao, N.-Y. Ji, X.-H. Liu, K. Li, Q.-M. Zhu, Q.-Z. Xue, *Bioorg. Med. Chem. Lett.* **2010**, *20*, 5677.
[61] S. D. Sarker, L. Dinan, V. Šik, E. Underwood, P. G. Waterman, *Tetrahedron Lett.* **1998**, *39*, 1421.
[62] F. Viladomat, J. Bastida, C. Codina, W. E. Campbell, S. Mathee, *Phytochemistry* **1995**, *40*, 307.
[63] B. Riemer, O. Hofer, H. Greger, *Phytochemistry* **1997**, *45*, 337.
[64] M.-H. Yang, Y.-Y. Chen, L. Huang, *Chin. Chem. Lett.* **1991**, *2*, 291.
[65] J. Li, J. Li, Y. Xu, Y. Wang, L. Zhang, L. Ding, Y. Xuan, T. Pang, H. Lin, *Nat. Prod. Res.* **2016**, *30*, 800.
[66] N. Ma, K. Wu, L. Huang, *Eur. J. Med. Chem.* **2008**, *43*, 893.
[67] P. Chattopadhyay, T. Pada Majhi, B. Achari, *Heterocycles* **2007**, *71*, 1011.
[68] M. M. Heravi, V. Zadsirjan, *RSC Adv.* **2020**, *10*, 44247.
[69] D. F. Veber, S. R. Johnson, H.-Y. Cheng, B. R. Smith, K. W. Ward, K. D. Kopple, *J. Med. Chem.* **2002**, *45*, 2615.
[70] K. R. Romines, K. D. Watenpaugh, P. K. Tomich, W. J. Howe, J. K. Morris, K. D. Lovasz, A. M. Mulichak, B. C. Finzel, J. C. Lynn, M. M. Horng, *J. Med. Chem.* **1995**, *38*, 1884.
[71] A. K. Clarke, W. P. Unsworth, *Chem. Sci.* **2020**, *11*, 2876.
[72] R. Turnaturi, A. Marrazzo, C. Parenti, L. Pasquinucci, *Eur. J. Med. Chem.* **2018**, *148*, 410.
[73] K. Ramig, *Tetrahedron* **2013**, *69*, 10783.
[74] H. Natsugari, Y. Ikeura, Y. Kiyota, Y. Ishichi, T. Ishimaru, O. Saga, H. Shirafuji, T. Tanaka, I. Kamo, T. Doi, *J. Med. Chem.* **1995**, *38*, 3106.
[75] H. Natsugari, Y. Ikeura, I. Kamo, T. Ishimaru, Y. Ishichi, A. Fujishima, T. Tanaka, F. Kasahara, M. Kawada, T. Doi, *J. Med. Chem.* **1999**, *42*, 3982.
[76] C. J. Ohnmacht, J. S. Albert, P. R. Bernstein, W. L. Rumsey, B. B. Masek, B. T. Dembofsky, G. M. Koether, D. W. Andisik, D. Aharony, *Bioorg. Med. Chem.* **2004**, *12*, 2653.
[77] J. S. Albert, C. Ohnmacht, P. R. Bernstein, W. L. Rumsey, D. Aharony, B. B. Masek, B. T. Dembofsky, G. M. Koether, W. Potts, J. L. Evenden, *Tetrahedron* **2004**, *60*, 4337.
[78] H. Tabata, H. Suzuki, K. Akiba, H. Takahashi, H. Natsugari, *J. Org. Chem.* **2010**, *75*, 5984.
[79] S. Jia, Y. Hao, Y. Li, Y. Lan, *Nat. Rev. Chem.* **2025**.
[80] L. Cai, J. Chen, Y. Zhu, G. Yang, S. Gu, *Adv. Synth. Catal.* **2025**, *367*.
[81] X.-C. Yu, C.-C. Zhang, L.-T. Wang, J.-Z. Li, T. Li, W.-T. Wei, *Org. Chem. Front.* **2022**, *9*, 4757.
[82] C. Galli, L. Mandolini, *Eur. J. Org. Chem.* **2000**, *2000*, 3117.
[83] M. A. Casadei, C. Galli, L. Mandolini, *J. Am. Chem. Soc.* **1984**, *106*, 1051.
[84] G. Illuminati, L. Mandolini, *Acc. Chem. Res.* **1981**, *14*, 95.

[85] N. L. Allinger, M. T. Tribble, M. A. Miller, D. H. Wertz, *J. Am. Chem. Soc.* **1971**, *93*, 1637.
[86] G. Illuminati, L. Mandolini, B. Masci, *J. Am. Chem. Soc.* **1975**, *97*, 4960.
[87] A. Michaut, J. Rodriguez, *Angew. Chem. Int. Ed.* **2006**, *45*, 5740.
[88] J. F. Liebman, A. Greenberg, *Chem. Rev.* **1976**, *76*, 311.
[89] D. Heber, P. Rösner, W. Tochtermann, *Eur. J. Org. Chem.* **2005**, *2005*, 4231.
[90] J. A. König, S. Frey, B. Morgenstern, J. Jauch, *Org. Lett.* **2025**, *27*, 2157.
[91] J. A. König, B. Morgenstern, J. Jauch, *Org. Lett.* **2024**, *26*, 7083.
[92] D. Scharf, M. Dürr, U. Koert, *Synlett,* DOI 10.1055/a-2608-1808.
[93] T. Molz, P. König, R. Goes, G. Gauglitz, H. Meier, *Chem. Ber.* **1984**, *117*, 833.
[94] J. Haase, A. Krebs, *Z. Naturforsch. A* **1971**, *26*, 1190.
[95] M. Trætteberg, W. Lüttke, R. Machinek, A. Krebs, H. J. Hohlt, *J. Mol. Struct.* **1985**, *128*, 217.
[96] H. Meier, H. Petersen, H. Kolshorn, *Chem. Ber.* **1980**, *113*, 2398.
[97] J. Sauer, D. K. Heldmann, J. Hetzenegger, J. Krauthan, H. Sichert, J. Schuster, *Eur. J. Org. Chem.* **1998**, *1998*, 2885.
[98] T. Harris, I. V. Alabugin, *Mendeleev Commun.* **2019**, *29*, 237.
[99] E. G. Chupakhin, M. Y. Krasavin, *Chem. Heterocycl. Compd.* **2018**, *54*, 483.
[100] Y. Fang, A. S. Hillman, J. M. Fox, *Top. Curr. Chem.* **2024**, *382*, 15.
[101] E. Kloster-Jensen, J. Wirz, *Angewandte Chemie* **1973**, *85*, 723.
[102] E. Kloster-Jensen, J. Wirz, *Helv. Chim. Acta* **1975**, *58*, 162.
[103] H. N. C. Wong, P. J. Garratt, F. Sondheimer, *J. Am. Chem. Soc.* **1974**, *96*, 5604.
[104] H. N. C. Wong, F. Sondheimer, *Angewandte Chemie* **1976**, *88*, 126.
[105] H. Detert, B. Rose, W. Mayer, H. Meier, *Chem. Ber.* **1994**, *127*, 1529.
[106] C. Werner, H. Hopf, I. Dix, P. Bubenitschek, P. G. Jones, *Chem. Eur. J.* **2007**, *13*, 9462.
[107] C. Werner, H. Hopf, J. Grunenberg, P. G. Jones, *Eur. J. Org. Chem.* **2010**, *2010*, 4027.
[108] F. Liu, Y. Liang, K. N. Houk, *J. Am. Chem. Soc.* **2014**, *136*, 11483.
[109] J. Sauer, R. Sustmann, *Angew. Chem. Int. Ed.* **1980**, *19*, 779.
[110] T. A. Hamlin, B. J. Levandowski, A. K. Narsaria, K. N. Houk, F. M. Bickelhaupt, *Chem. Eur. J.* **2019**, *25*, 6342.
[111] W. Chen, D. Wang, C. Dai, D. Hamelberg, B. Wang, *Chem. Commun.* **2012**, *48*, 1736.
[112] H. Meier, C. Schuh-Popitz, H. Peiersen, *Angew. Chem. Int. Ed.* **1981**, *20*, 270.
[113] J. Dommerholt, S. Schmidt, R. Temming, L. J. A. Hendriks, F. P. J. T. Rutjes, J. C. M. van Hest, D. J. Lefeber, P. Friedl, F. L. van Delft, *Angew. Chem. Int. Ed.* **2010**, *49*, 9422.
[114] J. A. Wagner, D. Mercadante, I. Nikić, E. A. Lemke, F. Gräter, *Chem. Eur. J.* **2015**, *21*, 12431.
[115] H. N. Wong, F. Sondheimer, *Tetrahedron* **1981**, *37*, 99.
[116] I. Kii, A. Shiraishi, T. Hiramatsu, T. Matsushita, H. Uekusa, S. Yoshida, M. Yamamoto, A. Kudo, M. Hagiwara, T. Hosoya, *Org. Biomol. Chem.* **2010**, *8*, 4051.
[117] Y. de Xing, N. Z. Huang, *J. Org. Chem.* **1982**, *47*, 140.
[118] Y. M. Man, T. C. W. Mak, H. N. C. Wong, *J. Org. Chem.* **1990**, *55*, 3214.

[119] S. H. Pun, Y. Wang, M. Chu, C. K. Chan, Y. Li, Z. Liu, Q. Miao, *J. Am. Chem. Soc.* **2019**, *141*, 9680.
[120] R. W. Miller, A. K. Duncan, S. T. Schneebeli, D. L. Gray, A. C. Whalley, *Chem. Eur. J.* **2014**, *20*, 3705.
[121] B. J. Levandowski, D. Herath, N. M. Gallup, K. N. Houk, *J. Org. Chem.* **2018**, *83*, 2611.
[122] T. Meguro, S. Yoshida, T. Hosoya, *Chem. Lett.* **2017**, *46*, 1137.
[123] M. Müller, V. S. Iyer, C. Kübel, V. Enkelmann, K. Müllen, *Angew. Chem. Int. Ed.* **1997**, *36*, 1607.
[124] G. Huang, C. Kouklovsky, A. de La Torre, *Chem. Eur. J.* **2021**, *27*, 4760.
[125] W. Huang, N. Gunawardhana, Y. Zhang, J. Escorihuela, S. T. Laughlin, *Chem. Eur. J.* **2024**, *30*, e202303465.
[126] B. R. Varga, M. Kállay, K. Hegyi, S. Béni, P. Kele, *Chem. Eur. J.* **2012**, *18*, 822.
[127] Q. Cui, T. W. Pan, M. Shieh, S. S. Kelly, S. Xu, W.-J. Qian, M. Xian, *Org. Lett.* **2022**, *24*, 7334.
[128] W. Huang, K. Wen, S. T. Laughlin, J. Escorihuela, *Org. Biomol. Chem.* **2024**, *22*, 8285.
[129] Z. M. Png, H. Zeng, Q. Ye, J. Xu, *Chem. Asian J.* **2017**, *12*, 2142.
[130] J. Zhang, V. Shukla, D. L. Boger, *J. Org. Chem.* **2019**, *84*, 9397.
[131] F.-G. Zhang, Z. Chen, X. Tang, J.-A. Ma, *Chem. Rev.* **2021**, *121*, 14555.
[132] Y.-F. Yang, Y. Liang, F. Liu, K. N. Houk, *J. Am. Chem. Soc.* **2016**, *138*, 1660.
[133] T. Meguro, S. Chen, K. Kanemoto, S. Yoshida, T. Hosoya, *Chem. Lett.* **2019**, *48*, 582.
[134] Y. Murata, N. Kato, K. Komatsu, *J. Org. Chem.* **2001**, *66*, 7235.
[135] U. Gruseck, M. Heuschmann, *Tetrahedron Lett.* **1987**, *28*, 6027.
[136] S. Turchi, R. Nesi, D. Giomi, *Tetrahedron* **1998**, *54*, 1809.
[137] H. Neunhoeffer, G. Werner, *Liebigs Ann. Chem.* **1985**, *1985*, 853.
[138] H. Neunhoeffer, G. Werner, *Liebigs Ann. Chem.* **1973**, *1973*, 437.
[139] P. Yates, P. Eaton, *J. Am. Chem. Soc.* **1960**, *82*, 4436.
[140] K. N. Houk, R. W. Strozier, *J. Am. Chem. Soc.* **1973**, *95*, 4094.
[141] D. M. Birney, K. N. Houk, *J. Am. Chem. Soc.* **1990**, *112*, 4127.
[142] K. L. Williamson, Y.-F. L. Hsu, *J. Am. Chem. Soc.* **1970**, *92*, 7385.
[143] T. Inukai, T. Kojima, *J. Org. Chem.* **1966**, *31*, 2032.
[144] P. Vermeeren, T. A. Hamlin, I. Fernández, F. M. Bickelhaupt, *Angew. Chem. Int. Ed.* **2020**, *59*, 6201.
[145] C. S. Sumaria, Y. E. Türkmen, V. H. Rawal, *Org. Lett.* **2014**, *16*, 3236.
[146] Y. E. Türkmen, T. J. Montavon, S. A. Kozmin, V. H. Rawal, *J. Am. Chem. Soc.* **2012**, *134*, 9062.
[147] J. Xue, E. Gao, X.-N. Wang, J. Chang, *Org. Lett.* **2018**, *20*, 6055.
[148] S. N. Kessler, H. A. Wegner, *Org. Lett.* **2010**, *12*, 4062.
[149] M. Große, H. A. Wegner, *Synlett* **2024**, *35*, 1019.
[150] M. Große, C. M. Leonhardt, H. A. Wegner, *ChemRxiv,* DOI 10.26434/chemrxiv-2025-6dlz2.
[151] Q. Cheng, D. Bhattacharya, M. Haring, H. Cao, C. Mück-Lichtenfeld, A. Studer, *Nat. Chem.* **2024**, *16*, 741.
[152] S. Pradhan, F. Mohammadi, J. Bouffard, *J. Am. Chem. Soc.* **2023**, *145*, 12214.
[153] B. Yang, S. Gao, *Chem. Soc. Rev.* **2018**, *47*, 7926.
[154] J. L. Segura, N. Martín, *Chem. Rev.* **1999**, *99*, 3199.

[155] X. Tian, L. M. Roch, K. K. Baldridge, J. S. Siegel, *Eur. J. Org. Chem.* **2017**, *2017*, 2801.
[156] J. R. Donald, W. P. Unsworth, *Chem. Eur. J.* **2017**, *23*, 8780.
[157] J. Ruhl, S. Ahles, M. A. Strauss, C. M. Leonhardt, H. A. Wegner, *Org. Lett.* **2021**, *23*, 2089.
[158] M. A. Strauss, D. Kohrs, J. Ruhl, H. A. Wegner, *Eur. J. Org. Chem.* **2021**, *2021*, 3866.
[159] S. N. Kessler, M. Neuburger, H. A. Wegner, *Eur. J. Org. Chem.* **2011**, *2011*, 3238.
[160] S. N. Kessler, M. Neuburger, H. A. Wegner, *J. Am. Chem. Soc.* **2012**, *134*, 17885.
[161] L. Schweighauser, I. Bodoky, S. Kessler, D. Häussinger, H. Wegner, *Synthesis* **2012**, *44*, 2195.
[162] L. Schweighauser, I. Bodoky, S. N. Kessler, D. Häussinger, C. Donsbach, H. A. Wegner, *Org. Lett.* **2016**, *18*, 1330.
[163] S. Ahles, S. Götz, L. Schweighauser, M. Brodsky, S. N. Kessler, A. H. Heindl, H. A. Wegner, *Org. Lett.* **2018**, *20*, 7034.
[164] S. Ahles, J. Ruhl, M. A. Strauss, H. A. Wegner, *Org. Lett.* **2019**, *21*, 3927.
[165] S. Beeck, S. Ahles, H. A. Wegner, *Chem. Eur. J.* **2022**, *28*, e202104085.
[166] A. C. Cope, A. C. Haven, F. L. Ramp, E. R. Trumbull, *J. Am. Chem. Soc.* **1952**, *74*, 4867.
[167] E. Vogel, O. Roos, K.-H. Disch, *Liebigs Ann. Chem.* **1962**, *653*, 55.
[168] R. Huisgen, G. Boche, A. Dahmen, W. Hechtl, *Tetrahedron Lett.* **1968**, *9*, 5215.
[169] E. R. Lippincott, R. C. Lord, *J. Am. Chem. Soc.* **1957**, *79*, 567.
[170] S. Greenfield, K. Mackenzie, *J. Chem. Soc., Perkin Trans. 2* **1986**, 1651.
[171] M. M. Rahman, B. A. Secor, K. M. Morgan, P. R. Shafer, D. M. Lemal, *J. Am. Chem. Soc.* **1990**, *112*, 5986.
[172] L. A. Paquette, T. Kakihana, J. F. Kelly, *J. Org. Chem.* **1971**, *36*, 435.
[173] H. M. Davies, J. J. Matasi, *Tetrahedron Lett.* **1994**, *35*, 5209.
[174] H. M. L. Davies, J. J. Matasi, G. Ahmed, *J. Org. Chem.* **1996**, *61*, 2305.
[175] F. Thalhammer, U. Wallfahrer, J. Sauer, *Tetrahedron Lett.* **1990**, *31*, 6851.
[176] B. J. Levandowski, T. A. Hamlin, F. M. Bickelhaupt, K. N. Houk, *J. Org. Chem.* **2017**, *82*, 8668.
[177] M. Große, C. M. Leonhardt, P. A. R. Campbell, H. A. Wegner, *Org. Lett.* **2025**, *27*, 4893.

8 Appendix

8.1 Reprint of Parts of the Supporting Information: Bidentate Lewis Acid-Catalyzed Inverse Electron-Demand Diels–Alder Reaction of Phthalazines and Cyclooctynes

Synlett
Accounts and Rapid Communications in Chemical Synthesis

Supporting Information
for DOI: 10.1055/a-2204-9522

Georg Thieme Verlag KG, Rüdigerstraße 14, 70469 Stuttgart, Germany

Thieme

Table of Contents

List of Figures

1 Experimental procedures and characterization data

1.1 General experimental

Reagents and solvents:

Chemicals were purchased from Sigma-Aldrich, Acros Organics, Alfa Aesar, chemPUR, abcr GmbH, TCI Europe or BLDpharm. Deuterated solvents were purchased from Deutero GmbH. Technical grade solvents used during work-up and purification were distilled prior to use. Bidentate Lewis acid **BDLA** was synthesized according to the literature, stored and handled in a nitrogen-filled glove box.[1]

Air and moisture sensitive reactions:

Sensitive reactions were performed in dry glassware under nitrogen atmosphere using Schlenk techniques or in a nitrogen-filled MBRAUN UNIlab glove box.

NMR spectroscopy:

NMR spectra were measured on a Bruker Avance II 200 MHz, Avance II 400 MHz or Avance III 400 MHz HD spectrometer at 25 °C if not stated otherwise. Chemical shifts (δ) are reported in parts per million (ppm) relative to residual solvent signals. Coupling constants (*J*) are reported in Hertz (Hz). Multiplicities are abbreviated as s (singlet), d (dublet), t (triplet) and m (multiplet).

Chromatography:

Flash column chromatography was carried out with Silica 60 (0.04 – 0.063 mm) from Marcherey-Nagel GmbH & Co. KG. Thin layer chromatography was performed on Polygram®SIL G/UV254 from Macherey Nagel GmbH & Co. KG. Spots were visualized under UV-light and with basic $KMnO_4$ stain.

High-resolution mass spectrometry:

ESI- and APCI-MS spectra were recorded on a Bruker Impact II. Samples were dissolved in methanol.

Melting points:

Melting points were measured on a M5000 melting point meter from A. KRÜSS Optronic GmbH, Germany.

1.2 Synthesis of cyclooctynes

1.2.1 Synthesis of cyclooctyne (2)

The synthesis of cyclooctyne (**2**) was adapted from literature with slight modifications:[2]

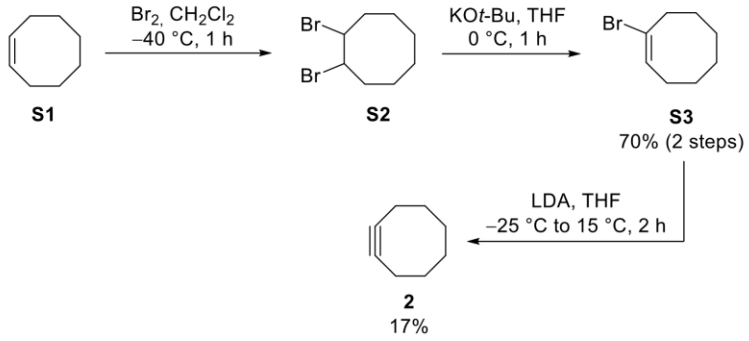

Figure S1. Synthesis scheme of cyclooctyne (**2**).

Synthesis of (1*E*)-1-bromocyclooct-1-ene (S3)

A solution of cyclooctene (**S1**) (11 mL, 80 mmol, 1.0 eq.) in dry CH_2Cl_2 (40 mL) was cooled to −40 °C and a solution of bromine (5.0 mL, 97 mmol, 1.2 eq.) in dry CH_2Cl_2 (5.5 mL) was added dropwise under nitrogen atmosphere over 30 min. The solution turned yellow at the end of the addition. An aqueous solution of $Na_2S_2O_3$ (10% w/v, 20 mL) was added, the cooling bath was removed and the mixture was stirred for 1 h. Afterwards, the organic layer was separated and the aqueous layer was extracted with CH_2Cl_2 (2 x 40 mL). The combined organic layers were dried with Na_2SO_4, filtered and concentrated *in vacuo* to give the crude dibromide **S2** (22.9 g), which was used in the next step without further purification.

Crude dibromide **S2** (22.9 g) in dry THF (10 mL) was added dropwise over 30 min to a solution of KO*t*-Bu (13.7 g, 120 mmol, 1.50 eq.) in dry THF (45 mL) at 0 °C under nitrogen atmosphere. The resulting light brown suspension was stirred at 0 °C for 50 min before being quenched by the addition of saturated, aqueous NH_4Cl solution (40 mL). THF was removed *in vacuo* and the aqueous layer was extracted with CH_2Cl_2 (3 x 40 mL). The combined organic layers were dried with $MgSO_4$, filtered and concentrated *in vacuo* (50 °C, minimal pressure: 50 mbar). Purification via distillation (b.p. 75 – 80 °C, 10 mbar) yielded the vinylbromide **S3** as a colourless oil (10.6 g, 55.9 mmol, 70% over two steps).

^{1}H NMR (200 MHz, $CDCl_3$): δ = 6.03 (t, *J* = 8.5 Hz, 1H), 2.68 – 2.54 (m, 2H), 2.21 – 2.00 (m, 2H), 1.71 – 1.44 (m, 8H) ppm.

Analytical data corresponds to literature.[2]

Synthesis of cyclooctyne (2)

A solution of *i*-Pr_2NH (5.93 mL, 42.3 mmol, 1.00 eq.) in dry THF (20 mL) was cooled to −25 °C and *n*-BuLi (1.6 M in hexane, 26.4 mL, 42.3 mmol, 1.00 eq.) was added dropwise under nitrogen atmosphere. Afterwards, vinylbromide **S3** (8.00 g, 42.3 mmol, 1.00 eq.) was added over 2 min and an orange solution was formed. The temperature of the reaction mixture was allowed to rise to 15 °C over 50 min and maintained at that temperature for 1.5 h. Afterwards, the mixture was poured into aqueous HCl (3 M, 14 mL) under cooling in an ice bath. It was extracted with pentane (6 x 12 mL) and the combined organic extracts were washed with water (3 x 12 mL), dried with Na_2SO_4, filtered and the solvent was removed *in vacuo* at 0 °C (100 to 60 mbar). Purification via distillation (b.p. 50 – 55 °C, 27 mbar) yielded cyclooctyne (**2**) as a colourless oil (0.78 g, 7.2 mmol, 17%).

^{1}H NMR (200 MHz, CD_2Cl_2): δ = δ 2.20 – 2.06 (m, 4H), 1.92 – 1.77 (m, 4H), 1.69 – 1.55 (m, 4H) ppm.

Analytical data corresponds to literature.[2]

1.2.2 Synthesis of [(1*R*,8*S*,9*r*)-bicyclo[6.1.0]non-4-yn-9-yl]methanol (*exo*-BCN)

The synthesis of [(1*R*,8*S*,9*r*)-bicyclo[6.1.0]non-4-yn-9-yl]methanol (***exo*-BCN**) was adapted from literature with slight modifications:[3]

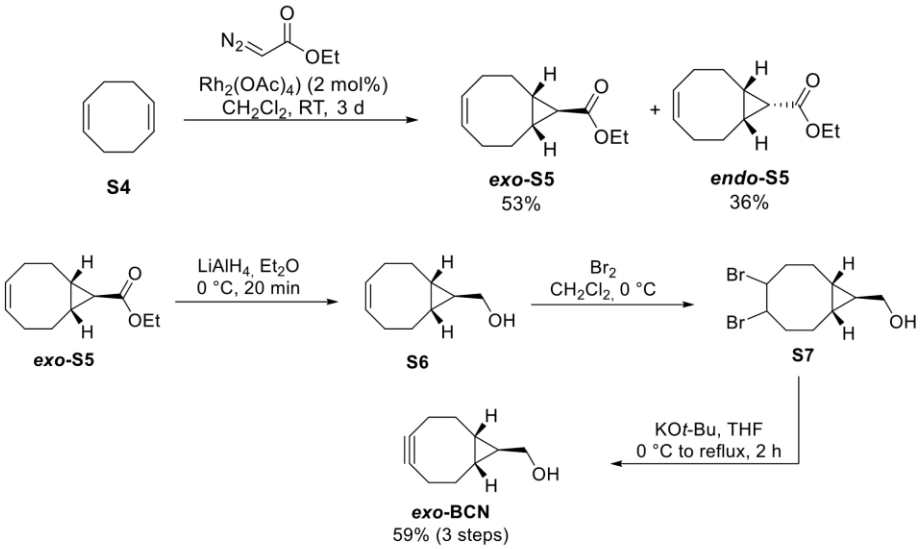

Figure S2. Synthesis scheme of [(1*R*,8*S*,9*r*)-bicyclo[6.1.0]non-4-yn-9-yl]methanol (***exo*-BCN**).

Synthesis of ethyl (1*R*,4*Z*,8*S*,9*r*)-bicyclo[6.1.0]non-4-ene-9-carboxylate (*exo*-S5)
Cyclooctadiene (**S4**) (7.0 mL, 56 mmol, 8.0 eq.) was added to a suspension of $Rh_2(OAc)_4$ (62 mg, 0.14 mmol, 0.020 eq.) in dry CH_2Cl_2 (3.5 mL) under nitrogen atmosphere. A solution of ethyl diazoacetate (0.92 mL, 80% purity, 7.0 mmol, 1.0 eq.) in dry CH_2Cl_2 (3.5 mL) was added dropwise over 2 h. The green solution was stirred for 3 d at room temperature. Afterwards, the solvent was removed *in vacuo* and the crude product was purified via flash chromatography (pure hexane to elute the excess cyclooctadiene, hexane/Et_2O, 9:0.5 to separate the isomers). Fractions containing both isomers were combined, concentrated *in vacuo*, purified again via flash chromatography (hexane to hexane/Et_2O, 97:3) and combined with the pure fractions of the first column to obtain ***endo*-S5** (0.49 g, 2.5 mmol, 36%) and ***exo*-S5** (0.72 g, 3.7 mmol, 53%) as colourless, slightly cloudy oils. R_F (***endo*-S5**) = 0.5, R_F (***exo*-S5**) = 0.3 (hexane/Et_2O, 9:0.5).

***endo*-S5**: **^{1}H NMR (400 MHz, $CDCl_3$)**: δ = 5.66 – 5.54 (m, 2H), 4.11 (q, *J* = 7.1 Hz, 2H), 2.57 – 2.44 (m, 2H), 2.27 – 2.13 (m, 2H), 2.13 – 1.98 (m, 2H), 1.89 – 1.76 (m, 2H), 1.70 (t, *J* = 8.8 Hz, 1H), 1.46 – 1.32 (m, 2H), 1.26 (t, *J* = 7.1 Hz, 3H) ppm.

***exo*-S5**: **^{1}H NMR (400 MHz, $CDCl_3$)**: δ = 5.69 – 5.57 (m, 2H), 4.10 (q, *J* = 7.1 Hz, 2H), 2.35 – 2.25 (m, 2H), 2.24 – 2.14 (m, 2H), 2.14 – 2.02 (m, 2H), 1.62 – 1.53 (m, 2H), 1.52 – 1.41 (m, 2H), 1.25 (t, *J* = 7.1 Hz, 3H), 1.18 (t, *J* = 4.5 Hz, 1H) ppm.

Analytical data corresponds to literature.[3]

Synthesis of [(1*R*,8*S*,9*r*)-bicyclo[6.1.0]non-4-yn-9-yl]methanol (*exo*-BCN)

A solution of ***exo*-S5** (0.73 g, 3.7 mmol, 1.0 eq.) in dry Et_2O (10 mL) was added dropwise to a suspension of $LiAlH_4$ (0.13 g, 3.3 mmol, 0.90 eq.) in dry Et_2O (14 mL) at 0 °C under nitrogen atmosphere. The mixture was stirred for 10 min at 0 °C and 10 min at room temperature. Afterwards, it was cooled to 0 °C again and quenched carefully with water until the grey solid turned white. Na_2SO_4 (2.7 g) was added and the mixture was filtered through celite and washed thoroughly with Et_2O (140 mL). The filtrate was concentrated *in vacuo* to obtain the crude alcohol **S6** as a pale yellow oil (0.56 mg, 3.7 mmol, quant.), which was used in the next step without further purification.

A solution of bromine (0.24 mL, 4.8 mmol, 1.3 eq.) in dry CH_2Cl_2 (3 mL) was added dropwise to a solution of alcohol **S6** (556 mg, 3.65 mmol, 1.00 eq.) in dry CH_2Cl_2 (25 mL) at 0 °C under nitrogen atmosphere. When the yellow colour in the reaction mixture persisted, an aqueous solution of $Na_2S_2O_3$ (10% w/v, 5 mL) was added. The organic layer was separated and the aqueous layer was extracted with CH_2Cl_2 (2 x 30 mL). The combined organic layers were dried with Na_2SO_4, filtered and concentrated *in vacuo* to obtain the dibromide **S7** as a viscous, colourless oil (1.16 g, 3.56 mmol assuming 98% purity and quant. yield), which was used in the next step without further purification.

A turbid solution of KO*t*-Bu (1.39 g, 12.0 mmol, 3.30 eq.) in dry THF (12 mL) was added dropwise to a solution of dibromide **S7** (1.16 g, 3.56 mmol assuming 98% purity, 1.00 eq.) in dry THF (40 mL) at 0 °C under nitrogen atmosphere. The resulting yellow suspension was refluxed for 2 h (78 °C oil bath). Afterwards, the mixture was cooled to room temperature and a saturated, aqueous solution of NH_4Cl (30 mL) was added. THF was removed *in vacuo* and the remaining aqueous layer was extracted with CH_2Cl_2 (3 x 30 mL). The combined organic layers were dried with Na_2SO_4, filtered and concentrated *in vacuo*. The crude product was purified via flash chromatography (pentane:EtOAc, 3:1) to obtain the strained alkyne ***exo*-BCN** as a pale yellow solid (319 mg, 2.12 mmol, 59%).

^{1}H NMR (400 MHz, $CDCl_3$): δ = 3.55 (d, *J* = 6.3 Hz, 2H), 2.46 – 2.35 (m, 2H), 2.34 – 2.22 (m, 2H), 2.22 – 2.10 (m, 2H), 1.49 (bs, 1H), 1.44 – 1.30 (m, 2H), 0.77 – 0.59 (m, 3H) ppm.

Analytical data corresponds to literature.[3]

1.3 Synthesis of phthalazines

Phthalazines **1b-f** and **1h-l** were synthesized according to literature.[4] The synthesis of benzo[*g*]phthalazine (**1g**) was adapted from literature with slight modifications.[5,6]

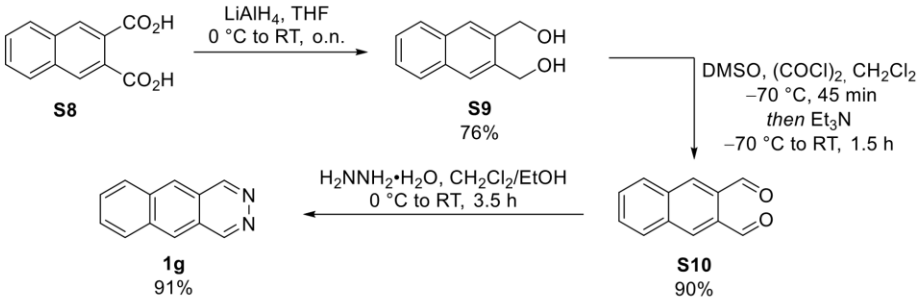

Figure S3. Synthesis scheme of benzo[g]phthalazine (**1g**).

Synthesis of 2,3-bis-(hydroxymethyl)naphthalene (S9)

2,3-Naphthalenedicarboxylic acid (**S8**) (1.5 g, 6.8 mmol, 1.0 eq.) was suspended in dry THF (20 mL) and added dropwise to a stirred and ice-cooled suspension of $LiAlH_4$ (1.4 g, 34 mmol, 5.0 eq.) in dry THF (45 mL) under nitrogen atmosphere. After addition, the reaction mixture was stirred for 1 h at 0 °C and at room temperature overnight. The reaction mixture was cooled to 0 °C, quenched carefully with saturated NH_4Cl solution (45 mL), diluted with EtOAc (60 mL) and decanted. The residual grey precipitate was diluted with EtOAc (60 mL) and saturated NH_4Cl (60 mL) and filtered through a pad of celite (rinsed with EtOAc, 3 x 60 mL). All organic layers were combined and the aqueous layer was extracted with EtOAc (60 mL). The combined organic layers were washed with brine, dried with Na_2SO_4, filtered and concentrated in vacuo. Flash chromatography [EtOAc:Cy, 9:1 to 100 % EtOAc; dry loading (acetone)] yielded the pure 2,3-bis-(hydroxymethyl)naphthalene (**S9**) as a colourless, crystalline solid (0.98 g, 5.20 mmol, 76%).

^{1}H NMR (200 MHz, Acetone-d6): δ = 7.93 – 7.82 (m, 4H), 7.51 – 7.42 (m, 2H), 4.87 (d, *J* = 5.6 Hz, 4H), 4.45 (t, *J* = 5.8 Hz, 2H) ppm.

Analytical data corresponds to literature.[7]

Synthesis of 2,3-naphthalenedicarboxaldehyde (S10)

A solution of dry DMSO (1.66 mL, 23.4 mmol, 4.40 eq.) in dry CH_2Cl_2 (6 mL) was added dropwise to a stirred solution of oxalyl chloride (1.14 mL, 11.7 mmol, 2.20 eq.) in dry CH_2Cl_2 (27 mL) at 70 °C under nitrogen atmosphere. After stirring for 10 min at the same temperature, a solution of 2,3-bis-(hydroxymethyl)naphthalene (**S9**) (1.0 g, 5.3 mmol, 1.0 eq.) in dry THF (7.2 mL) and dry DMSO (0.6 mL) was added dropwise. The mixture was stirred for

45 min at 70 °C before Et_3N (9.30 mL, 63.6 mmol, 12.0 eq.) was added. The resulting white suspension was slowly allowed to warm to room temperature over 1.5 h. The reaction mixture was quenched with cold water (30 mL). The aqueous layer was separated and extracted with CH_2Cl_2 (2 x 30 mL). The combined organic layers were washed with brine, dried with $MgSO_4$, filtered and concentrated *in vacuo*. Flash chromatography [Cy:EtOAc, 9:1 to 7:3; dry loading (CH_2Cl_2)] yielded the 2,3-naphthalenedicarboxaldehyde (**S10**) as a colourless solid (0.88 g, 4.77 mmol, 90%).

^{1}H NMR (200 MHz, $CDCl_3$): δ = 10.64 (s, 2H), 8.46 (s, 2H), 8.11 – 8.01 (m, 2H), 7.79 – 7.70 (m, 2H) ppm.

Analytical data corresponds to literature.[7]

Synthesis of benzo[*g*]phthalazine (1g)

A solution of 2,3-naphthalenedicarboxaldehyde (**S10**) (0.88 g, 4.75 mmol, 1.00 eq.) in CH_2Cl_2 (9 mL) and EtOH (4.5 mL) was added dropwise to a solution of hydrazine monohydrate (0.71 mL, 14.3 mmol, 3.00 eq.) in EtOH (7.5 mL) at 0 °C over 1.5 h. The reaction was allowed to warm to room temperature and stirred for 2 h. Afterwards, the reaction mixture was concentrated *in vacuo*. Toluene (22 mL) was added to the crude material, the resulting mixture was stirred for 10 min at room temperature and the solvent was again removed *in vacuo*. This process was repeated with CH_2Cl_2 (22 mL). Flash chromatography [EtOAc to EtOAc:*i*-PrOH (9:1); dry loading (warm EtOH)] yielded benzo[*g*]phthalazine (**1g**) as a yellow solid (0.78 g, 4.32 mmol, 91%).

^{1}H NMR (200 MHz, CD_3OD): δ = 9.66 (s, 2H), 8.77 (s, 2H), 8.32 – 8.21 (m, 2H), 7.82 – 7.74 (m, 2H) ppm.

Melting point: 205 – 206 °C

Analytical data corresponds to literature.[6]

1.4 General procedure for IEDDA reaction (GP1)

In a nitrogen filled glove box, (substituted) phthalazine (**1**) (1.0 eq.) and **BDLA** catalyst (5 mol%) were suspended in anhydrous and degassed 1,4-dioxane (1.0 mL) in a 4 mL-screw cap vial with a stir bar. Cyclooctyne (**2**) or ***exo*-BCN** (1.1 – 3 eq.) was added to the mixture, the vial was sealed and taken out of the glove box. The mixture was stirred at the given temperature for the given time. Afterwards, the reaction mixture was concentrated *in vacuo*. The ratio of product to unreacted phthalazine was determined via ^{1}H NMR of the crude mixture. The product was purified by column chromatography (3 g silica gel) with the given eluent. If additional purification was required, it is noted below.

1.4.1 Synthesis of 6,7,8,9,10,11-hexahydrocycloocta[*b*]naphthalene (3a)

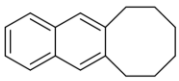

According to **GP1**, phthalazine (**1a**) (13 mg, 0.099 mmol, 1.0 eq.), **BDLA** catalyst (1.0 mg, 5.0 µmol, 5.0 mol%) and cyclooctyne (**2**) (22 mg, 0.20 mmol, 2.0 eq.) in 1,4-dioxane (1.0 mL) were stirred at 100 °C for 2 d. The mixture was concentrated *in vacuo* and purified via column chromatography (toluene). Substituted naphthalene **3a** was obtained as a colourless oil (18 mg, 0.086 mmol, 86%).

^{1}H NMR (200 MHz, $CDCl_3$): δ = 7.80 – 7.70 (m, 2H), 7.59 (s, 2H), 7.43 – 7.33 (m 2H), 3.00 – 2.88 (m, 4H), 1.84 – 1.69 (m, 4H), 1.44 – 1.33 (m, 4H) ppm.

^{13}C NMR (101 MHz, $CDCl_3$): δ = 140.8 (2C), 132.3 (2C), 127.2 (2C), 127.1 (2C), 125.1 (2C), 33.1 (2C), 32.5 (2C), 26.1 (2C) ppm.

HRMS (APCI): *m/z* calculated for $C_{16}H_{18}$+H: 211.1481 $[M+H]^+$, found: 211.1483.

1.4.2 Synthesis of 1-nitro-6,7,8,9,10,11-hexahydrocycloocta[*b*]-naphthalene (3b)

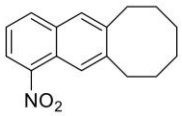

According to **GP1**, phthalazine **1b** (19 mg, 0.11 mmol, 1.0 eq.), **BDLA** catalyst (1.0 mg, 5.0 µmol, 5.0 mol%) and cyclooctyne (**2**) (14 mg, 0.13 mmol, 1.3 eq.) in 1,4-dioxane (1.0 mL) were stirred at 80 °C for 1 d. The mixture was concentrated *in vacuo* and purified via column chromatography (toluene). Substituted naphthalene **3b** was obtained as a as a yellow solid (26 mg, 0.10 mmol, 95%).

^{1}H NMR (200 MHz, $CDCl_3$): δ = 8.34 (s, 1H), 8.15 (dd, *J* = 7.6, 1.2 Hz, 1H), 8.01 (d, *J* = 8.2 Hz, 1H), 7.68 (s, 1H), 7.43 (t, *J* = 7.9 Hz, 1H), 3.04 –2.90 (m, 4H), 1.87 – 1.69 (m, 4H), 1.46 – 1.29 (m, 4H) ppm.

^{13}C NMR (50 MHz, $CDCl_3$): δ = 146.1, 145.2, 142.6, 134.0, 133.9, 127.9, 124.4, 123.4, 123.2, 122.5, 33.0, 32.8 (2C), 32.4, 26.0, 25.9 ppm.

HRMS (APCI): *m/z* calculated for $C_{16}H_{17}NO_2$+H: 256.1332 $[M+H]^+$, found: 256.1330.

Melting point: 81 – 82 °C

1.4.3 Synthesis of 1,4-difluoro-6,7,8,9,10,11-hexahydrocycloocta[*b*]-naphthalene (3c)

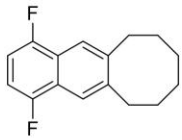

According to **GP1**, phthalazine **1c** (16 mg, 0.097 mmol, 1.0 eq.), **BDLA** catalyst (1.0 mg, 5.0 µmol, 5.0 mol%) and cyclooctyne (**2**) (14 mg, 0.13 mmol, 1.3 eq.) in 1,4-dioxane (1.0 mL) were stirred at 80 °C for 1 d. The mixture was concentrated *in vacuo* and purified via column chromatography (toluene). Substituted naphthalene **3c** was obtained as a as a pale yellow solid (21 mg, 0.085 mmol, 88%).

^{1}H NMR (200 MHz, $CDCl_3$): δ = 7.81 (s, 2H), 6.93 (dd, *J* = 7.5, 6.5 Hz, 2H), 3.02 – 2.90 (m, 4H), 1.85 – 1.69 (m, 4H), 1.44 – 1.33 (m, 4H) ppm.

^{13}C NMR (101 MHz, $CDCl_3$): δ = 154.6 (dd, *J* = 249.5, 5.1 Hz, 2C), 142.5 (2C), 123.7 (dd, *J* = 13.5, 10.5 Hz, 2C), 120.0 (t, *J* = 3.0 Hz, 2C), 107.6 (dd, *J* = 18.2, 13.3 Hz, 2C), 32.9 (2C), 32.7 (2C), 26.0 (2C) ppm.

HRMS (APCI): *m/z* calculated for $C_{16}H_{16}F_2$+H: 247.1293 $[M+H]^+$, found: 247.1291.

Melting point: 52 – 53 °C

1.4.4 Synthesis of 2-(trifluoromethyl)-6,7,8,9,10,11-hexahydrocycloocta[*b*]naphthalene (3d)

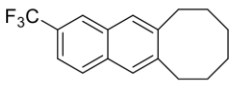

According to **GP1**, phthalazine **1d** (20 mg, 0.10 mmol, 1.0 eq.), **BDLA** catalyst (1.0 mg, 5.0 µmol, 5.0 mol%) and cyclooctyne (**2**) (14 mg, 0.13 mmol, 1.3 eq.) in 1,4-dioxane (1.0 mL) were stirred at 80 °C for 2 d. The mixture was concentrated *in vacuo* and purified via column chromatography (toluene). Substituted naphthalene **3d** was obtained as a as a pale yellow oil (26 mg, 0.093 mmol, 94%).

^{1}H NMR (400 MHz, $CDCl_3$): δ = 8.05 (s, 1H), 7.84 (d, *J* = 8.6 Hz, 1H), 7.67 (s, 1H), 7.64 (s, 1H), 7.54 (dd, *J* = 8.6, 1.8 Hz, 1H), 2.99 – 2.91 (m, 4H), 1.83 – 1.72 (m, 4H), 1.42 – 1.33 (m, 4H) ppm.

^{13}C NMR (101 MHz, $CDCl_3$): δ = 143.4, 142.4, 133.9, 131.5, 128.13, 128.09, 127.2, 126.9 (q, *J* = 32.3 Hz), 125.0 (q, *J* = 4.6 Hz), 124.8 (q, *J* = 272.7 Hz), 120.6 (q, *J* = 3.1 Hz), 32.97, 32.94, 32.6, 32.5, 26.0 (2C) ppm.

^{19}F NMR (377 MHz, $CDCl_3$): δ = -62.11 ppm.

HRMS (APCI): *m/z* calculated for $C_{17}H_{17}F_3$-F^{-}: 259.1292 $[M\text{-}F^{-}]^{+}$, found: 259.1294.

1.4.5 Synthesis of 2-chloro-6,7,8,9,10,11-hexahydrocycloocta[*b*]-naphthalene (3e)

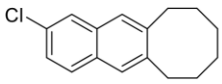

According to **GP1**, phthalazine **1e** (17 mg, 0.10 mmol, 1.0 eq.), **BDLA** catalyst (1.0 mg, 5.0 µmol, 5.0 mol%) and cyclooctyne (**2**) (14 mg, 0.13 mmol, 1.3 eq.) in 1,4-dioxane (1.0 mL) were stirred at 80 °C for 2 d. The mixture was concentrated *in vacuo* and purified via column chromatography (toluene). Substituted naphthalene **3e** was obtained as a as a pale yellow solid (19 mg, 0.078 mmol, 78%).

^{1}H NMR (400 MHz, $CDCl_3$): δ = 7.72 (d, *J* = 2.1 Hz, 1H), 7.67 (d, *J* = 8.7 Hz, 1H), 7.55 (s, 1H), 7.49 (s, 1H), 7.31 (dd, *J* = 8.7, 2.1 Hz, 1H), 2.96 – 2.87 (m, 4H), 1.80 – 1.69 (m, 4H), 1.43 – 1.31 (m, 4H) ppm.

^{13}C NMR (101 MHz, $CDCl_3$): δ = 142.0, 141.2, 133.3, 131.0, 130.7, 128.4, 127.1, 126.4, 125.9, 125.8, 33.0 (2C), 32.5 (2C), 26.0, 26.0 ppm.

HRMS (APCI): *m/z* calculated for $C_{16}H_{17}Cl$+H: 245.1092 $[M+H]^{+}$, found: 245.1092.

Melting point: 55 °C

1.4.6 Synthesis of 6,7,8,9,10,11-hexahydrocycloocta[*g*]quinoline (3f)

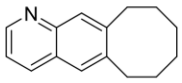

According to **GP1**, phthalazine **1f** (13 mg, 0.10 mmol, 1.0 eq.), **BDLA** catalyst (1.0 mg, 5.0 µmol, 5.0 mol%) and cyclooctyne (**2**) (14 mg, 0.13 mmol, 1.3 eq.) in 1,4-dioxane (1.0 mL) were stirred at 80 °C for 2 d. The mixture was concentrated *in vacuo* and purified via column chromatography (toluene/EtOAc, 100:0 to 95:5 to 90:10). Substituted naphthalene **3f** was obtained as a as a yellow oil (20 mg, 0.095 mmol, 95%).

^{1}H NMR (200 MHz, CD_2Cl_2): δ = 8.77 (dd, *J* = 4.2, 1.8 Hz, 1H), 8.14 – 7.99 (m, 1H), 7.81 (s, 1H), 7.57 (s, 1H), 7.30 (dd, *J* = 8.3, 4.2 Hz, 1H), 3.05 – 2.87 (m, 4H), 1.90 – 1.65 (m, 4H), 1.49 – 1.22 (m, 4H) ppm.

^{13}C NMR (101 MHz, CD_2Cl_2): δ = 149.9, 148.1, 145.1, 142.0, 135.2, 128.7, 127.6, 127.1, 120.7, 33.3, 33.2, 32.8, 32.5, 26.3, 26.3 ppm.

HRMS (ESI): *m/z* calculated for $C_{15}H_{17}N$+Na: 234.1253 $[M+Na]^+$, found: 234.1251.

1.4.7 Synthesis of 6,7,8,9,10,11-hexahydrocycloocta[*b*]anthracene (3g)

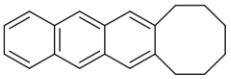

According to **GP1**, phthalazine **1g** (18 mg, 0.10 mmol, 1.0 eq.), **BDLA** catalyst (1.0 mg, 5.0 µmol, 5.0 mol%) and cyclooctyne (**2**) (21 mg, 0.20 mmol, 2.0 eq.) in 1,4-dioxane (1.0 mL) were stirred at 100 °C for 3 d. The mixture was concentrated *in vacuo* and purified via column chromatography (toluene). The obtained pale yellow solid was further purified via column chromatography [cyclohexane/toluene, 97:3, dry loading (CH_2Cl_2)]. The resulting white solid was crystallized from hexane/CH_2Cl_2 to obtain the substituted naphthalene **3g** as a white solid (8.0 mg, 0.031 mmol, 31%). The filtrate of the crystallization was concentrated *in vacuo* and the residual white solid was triturated with *n*-hexane to obtain an additional fraction of the product as a white solid (4.6 mg, 0.018 mmol, 18%).

^{1}H NMR (400 MHz, $CDCl_3$): δ = 8.31 (s, 2H), 7.99 – 7.93 (m, 2H), 7.75 (s, 2H), 7.43 – 7.38 (m, 2H), 3.02 – 2.94 (m, 4H), 1.86 – 1.75 (m, 4H), 1.45 – 1.37 (m, 4H) ppm.

^{13}C NMR (101 MHz, $CDCl_3$): δ = 140.94 (2C), 131.53 (2C), 131.49 (2C), 128.21 (2C), 126.85 (2C), 125.04 (2C), 124.91 (2C), 33.23 (2C), 32.66 (2C), 26.11 (2C) ppm.

HRMS (APCI): *m/z* calculated for $C_{20}H_{20}$+H: 261.1638 $[M+H]^+$, found: 261.1640.

Melting point: 167 – 168 °C

1.4.8 Synthesis of 6,7,8,9,10,11-hexahydrocycloocta[*b*]phenanthrene (3h)

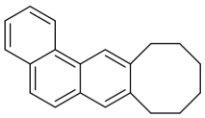

According to **GP1**, phthalazine **1h** (18 mg, 0.10 mmol, 1.0 eq.), **BDLA** catalyst (1.0 mg, 5.0 µmol, 5.0 mol%) and cyclooctyne (**2**) (21 mg, 0.20 mmol, 2.0 eq.) in 1,4-dioxane (1.0 mL) were stirred at 100 °C for 3 d. The mixture was concentrated *in vacuo* and purified via column chromatography [cyclohexane/toluene, 97:3, dry loading (CH_2Cl_2)]. The obtained colourless oil was further purified via column chromatography (cyclohexane) to obtain the substituted naphthalene **3h** as a white solid (5.7 mg, 0.022 mmol, 22%).

^{1}H NMR (400 MHz, $CDCl_3$): δ = 8.67 (dd, *J* = 8.4, 1.1 Hz, 1H), 8.42 (s, 1H), 7.86 (dd, *J* = 7.7, 1.5 Hz, 1H), 7.73 – 7.59 (m, 4H), 7.55 (ddd, *J* = 8.1, 7.0, 1.3 Hz, 1H), 3.09 – 3.01 (m, 2H), 3.00 – 2.92 (m, 2H), 1.87 – 1.73 (m, 4H), 1.44 – 1.35 (m, 4H) ppm.

^{13}C NMR (101 MHz, $CDCl_3$): δ = 141.05, 140.98, 131.96, 131.05, 130.26, 129.09, 128.64, 128.36, 126.66, 126.39, 126.14, 126.07, 122.67, 122.62, 33.06, 32.99, 32.90, 32.48, 26.12, 26.06 ppm.

HRMS (APCI): *m/z* calculated for $C_{20}H_{20}$+H: 261.1638 $[M+H]^+$, found: 261.1646.

1.4.9 Synthesis of 2-methyl-6,7,8,9,10,11-hexahydrocycloocta[*b*]-naphthalene (3i)

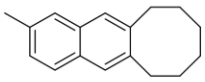

According to **GP1**, phthalazine **1i** (13 mg, 0.090 mmol, 1.0 eq.), **BDLA** catalyst (0.92 mg, 4.5 µmol, 5.0 mol%) and cyclooctyne (**2**) (29 mg, 0.27 mmol, 3.0 eq.) in 1,4-dioxane (1.0 mL) were stirred at 100 °C for 3 d. The mixture was concentrated *in vacuo* and purified via column chromatography [cyclohexane, dry loading (CH_2Cl_2)] to obtain the substituted naphthalene **3i** as a white solid (16 mg, 0.070 mmol, 78%).

^{1}H NMR (400 MHz, $CDCl_3$): δ = 7.65 (d, *J* = 8.3 Hz, 1H), 7.55 – 7.48 (m, 3H), 7.22 (dd, *J* = 8.3, 1.8 Hz, 1H), 2.95 – 2.89 (m, 4H), 2.49 (s, 3H), 1.79 – 1.70 (m, 4H), 1.41 – 1.33 (m, 4H) ppm.

^{13}C NMR (101 MHz, $CDCl_3$): δ = 140.74, 139.76, 134.53, 132.98, 131.02, 127.34, 126.96, 126.92, 126.54, 126.06, 33.08 (2C), 32.53, 32.49, 26.08, 26.06, 21.82 ppm.

HRMS (APCI): *m/z* calculated for $C_{17}H_{20}$+H: 225.1638 $[M+H]^+$, found: 225.1637.

Melting point: 62 – 64 °C

1.4.10 Synthesis of 2-methoxy-6,7,8,9,10,11-hexahydro-cycloocta[*b*]naphthalene (3j)

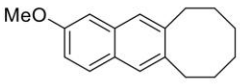

According to **GP1**, phthalazine **1j** (15 mg, 0.092 mmol, 1.0 eq.), BDLA catalyst (0.94 mg, 4.6 µmol, 5.0 mol%) and cyclooctyne (**2**) (31 mg, 0.29 mmol, 3.1 eq.) in 1,4-dioxane (1.0 mL) were stirred at 100 °C for 3 d. The mixture was concentrated *in vacuo* and purified via column chromatography (toluene). The resulting yellow solid was further purified via column chromatography (cyclohexane/toluene, 95:5) to obtain the substituted naphthalene **3j** as a white solid (11 mg, 0.045 mmol, 49%).

^{1}H NMR (200 MHz, $CDCl_3$): δ = 7.65 (d, *J* = 9.7 Hz, 1H), 7.50 (s, 1H), 7.49 (s, 1H), 7.13 – 6.98 (m, 2H), 3.91 (s, 3H), 2.98 – 2.82 (m, 4H), 1.80 – 1.63 (m, 4H), 1.45 – 1.28 (m, 4H) ppm.

^{13}C NMR (101 MHz, $CDCl_3$): δ = 157.21, 141.25, 138.30, 133.71, 128.67, 128.30, 127.03, 126.19, 117.90, 105.12, 55.40, 33.09, 33.04, 32.55, 32.40, 26.11, 26.06 ppm.

HRMS (ESI): *m/z* calculated for $C_{17}H_{20}O$+Na: 263.1406 $[M+Na]^+$, found: 263.1407.

Melting point: 70 – 71 °C

1.4.11 Synthesis of ((1*r*,1a*R*,11a*S*)-1a,2,3,10,11,11a-hexahydro-1*H*-cyclopropa[5,6]cycloocta[1,2-*b*]naphthalen-1-yl)methanol (4a)

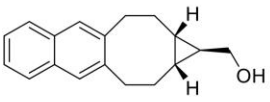

According to **GP1**, phthalazine **1a** (13 mg, 0.10 mmol, 1.0 eq.), **BDLA** catalyst (1.0 mg, 5.0 µmol, 5.0 mol%) and ***exo*-BCN** (17 mg, 0.11 mmol, 1.1 eq.) in 1,4-dioxane (1.0 mL) were stirred at 40 °C for 4 d. The mixture was concentrated *in vacuo* and purified via column chromatography (cyclohexane/EtOAc, 8:2 to 75:25) to obtain substituted naphthalene **4a** as a colourless oil (13 mg, 0.052 mmol, 52%).

^{1}H NMR (400 MHz, $CDCl_3$): δ = 7.76 – 7.71 (m, 2H), 7.56 (s, 2H), 7.41 – 7.36 (m, 2H), 3.38 (d, *J* = 6.5 Hz, 2H), 3.10 (ddd, *J* = 14.1, 8.3, 5.7 Hz, 2H), 2.92 (dt, *J* = 14.1, 5.8 Hz, 2H), 2.59 – 2.45 (m, 2H), 1.42 – 1.25 (m, 3H), 0.77 – 0.66 (m, 3H) ppm.

^{13}C NMR (101 MHz, $CDCl_3$): δ = 141.21 (2C), 132.49 (2C), 128.04 (2C), 127.08 (2C), 125.24 (2C), 66.78, 33.63 (2C), 30.16 (2C), 29.76 (2C), 22.03 ppm.

HRMS (ESI): *m/z* calculated for $C_{18}H_{20}O$+Na: 275.1406 $[M+Na]^+$, found: 275.1406.

1.4.12 Synthesis of ((1*r*,1a*R*,11a*S*)-5,8-difluoro-1a,2,3,10,11,11a-hexahydro-1*H*-cyclopropa[5,6]cycloocta[1,2-*b*]naphthalen-1-yl)methanol (4b)

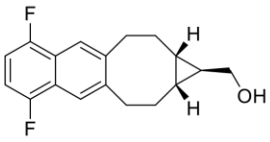

According to **GP1**, phthalazine **1c** (17 mg, 0.10 mmol, 1.0 eq.), **BDLA** catalyst (1.0 mg, 5.0 µmol, 5.0 mol%) and ***exo*-BCN** (17 mg, 0.11 mmol, 1.1 eq.) in 1,4-dioxane (1.0 mL) were stirred at 40 °C for 2 d. The mixture was concentrated *in vacuo* and purified via column chromatography [cyclohexane/EtOAc, 75:25, dry loading (CH2Cl2)] to obtain substituted naphthalene **4b** as a white solid (26 mg, 0.090 mmol, 90%).

^{1}H NMR (400 MHz, $CDCl_3$): δ = 7.78 (s, 2H), 6.94 (dd, *J* = 7.5, 6.4 Hz, 2H), 3.38 (d, *J* = 6.6 Hz, 2H), 3.14 (ddd, *J* = 14.1, 8.1, 5.9 Hz, 2H), 2.95 (dt, *J* = 14.1, 5.9 Hz, 2H), 2.60 – 2.47 (m, 2H), 1.41 – 1.29 (m, 3H), 0.77 – 0.66 (m, 3H) ppm.

^{13}C NMR (101 MHz, $CDCl_3$): δ = 154.52 (dd, *J* = 248.5, 5.1 Hz, 2C), 142.91 (2C), 123.40 (dd, *J* = 13.2, 10.5 Hz, 2C)), 120.79 (t, *J* = 2.9 Hz, 2C), 107.90 (dd, *J* = 18.3, 13.3 Hz, 2C), 66.64, 33.75 (2C), 30.21 (2C), 29.54 (2C), 21.79 ppm.

^{19}F NMR (377 MHz, $CDCl_3$): δ = -128.74 ppm.

HRMS (ESI): *m/z* calculated for $C_{18}H_{18}F_2O$+Na: 311.1218 $[M+Na]^+$, found: 311.1218.

Melting point: 125 – 127 °C

3 References

(1) Kessler, S. N.; Neuburger, M.; Wegner, H. A. *Eur. J. Org. Chem.* **2011**, *2011*, 3238.

(2) Facchini, S. V.; Cettolin, M.; Bai, X.; Casamassima, G.; Pignataro, L.; Gennari, C.; Piarulli, U. *Adv. Synth. Catal.* **2018**, *360*, 1054.

(3) Dommerholt, J.; Schmidt, S.; Temming, R.; Hendriks, L. J. A.; Rutjes, F. P. J. T.; van Hest, J. C. M.; Lefeber, D. J.; Friedl, P.; van Delft, F. L. *Angew. Chem. Int. Ed.* **2010**, *49*, 9422.

(4) Kessler, S. N.; Wegner, H. A. *Org. Lett.* **2012**, *14*, 3268.

(5) Carlson, R. G.; Srinivasachar, K.; Givens, R. S.; Matuszewski, B. K. *J. Org. Chem.* **1986**, *51*, 3978.

(6) Türkmen, Y. E.; Montavon, T. J.; Kozmin, S. A.; Rawal, V. H. *J. Am. Chem. Soc.* **2012**, *134*, 9062.

(7) Lin, C.-H.; Lin, K.-H.; Pal, B.; Tsou, L.-D. *Chem. Commun.* **2009**, 803.

8.2 Reprint of Parts of the Supporting Information: Lewis Acid-Catalyzed Domino Inverse Electron-Demand Diels–Alder/Thermal Ring Expansion Reaction for the Synthesis of Arene-Annulated Eight-Membered Nitrogen Heterocycles

Supporting Information

Lewis Acid-Catalyzed Domino Inverse Electron-Demand Diels-Alder/Thermal Ring Expansion Reaction for the Synthesis of Arene-Annulated Eight-Membered Nitrogen Heterocycles

Michel Große[†,‡], Christopher M. Leonhardt[†,‡], Patrick A. R. Campbell[†,‡] and Hermann A. Wegner[†,‡,*]

[†]Institute of Organic Chemistry, Justus Liebig University Giessen, Heinrich-Buff-Ring 17, 35392 Giessen, Germany

[‡]Center for Materials Research (LaMa), Justus Liebig University Giessen, Heinrich-Buff-Ring 16, 35392 Giessen, Germany

*hermann.a.wegner@org.chemie.uni-giessen.de

Table of Contents

1 Experimental procedures and characterization data

1.1 General experimental

Chemicals were purchased from Sigma-Aldrich, Acros Organics, Alfa Aesar, chemPUR, abcr GmbH, TCI Europe or BLDpharm. Deuterated solvents were purchased from Deutero GmbH or Sigma-Aldrich. Technical grade solvents used during work-up and purification were distilled prior to use. The Bidentate Lewis acid **BDLA** was synthesized according to the literature,[1] stored and handled in a nitrogen-filled glove box. Sensitive reactions were performed in dry glassware under nitrogen atmosphere using Schlenk techniques or in a nitrogen-filled MBRAUN UNIlab glove box. An oil bath was used for all reactions requiring heating.

NMR spectra were measured on a Bruker Avance II 200 MHz, Avance II 400 MHz or Avance III 400 MHz HD spectrometer at 25 °C if not stated otherwise. Chemical shifts (δ) are reported in parts per million (ppm) relative to residual solvent signals. Coupling constants (*J*) are reported in Hertz (Hz). Multiplicities are abbreviated as s (singlet), d (doublet), t (triplet), q (quartet) and m (multiplet). Structural assignments were made with additional information from gCOSY, gHSQC, and gHMBC experiments. Regioisomeric ratios were determined from appropriate integrals in the respective ^{1}H NMR spectra.

Flash chromatography was carried out with Silica 60 (0.04 – 0.063 mm) from Marcherey-Nagel GmbH & Co. KG. Automated flash chromatography was performed on an Advion Interchim puriFlash XS 520 Plus system using PF-30SIHP or PF-15SIHP columns. Thin layer chromatography was performed on Polygram®SIL G/UV254 from Macherey Nagel GmbH & Co. KG. Spots were visualized under UV-light and with basic $KMnO_4$ stain.

High-resolution mass spectra were recorded on a Bruker Impact II spectrometer featuring a quadrupole time-of-flight (Q-TOF) mass analyzer. Samples were dissolved in methanol.

Melting points were measured on a M5000 melting point meter from A. KRÜSS Optronic GmbH, Germany.

Analytical reverse phase HPLC measurements were performed on a Dionex Ultimate 3000 system equipped with an LPG-3400A pump, a VWD-3100 detector and a Shodex RI-101 refractive index detector. Preparative reverse phase HPLC separations were carried out with a Knauer Azura system equipped with a P2.1L pump, a UVD 2.1L detector and an ASM 2.1L module. Analytical chiral HPLC measurements were performed on a Dionex system equipped with a P680 pump and a UVD 170U detector. Preparative chiral HPLC separations were carried out with a Knauer Azura system equipped with a P6.1L pump, a DAD 2.1L detector and an ASM 2.2L module.

1.2 Synthesis of phthalazines

Phthalazines **1b-i**,**k-m** were synthesized according to literature.[2–5] Phthalazine **1j** was synthesized using the following route.

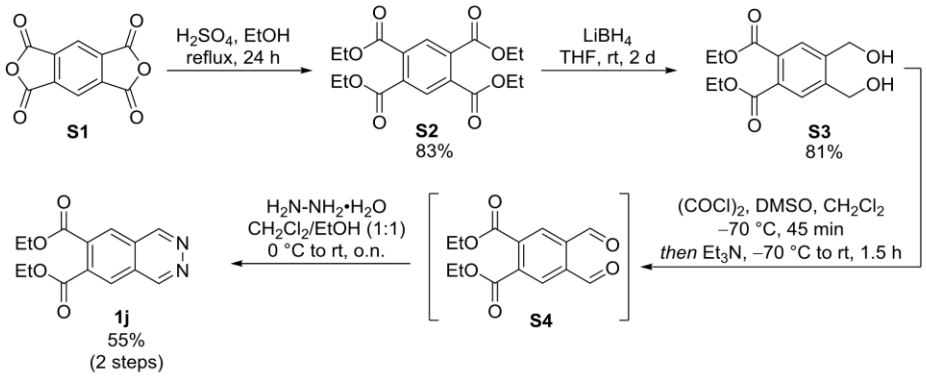

Scheme S1. Synthesis scheme of diethyl phthalazine-6,7-dicarboxylate (**1j**).

Synthesis of tetraethyl benzene-1,2,4,5-tetracarboxylate (S2**)**

The synthesis of tetraethyl benzene-1,2,4,5-tetracarboxylate (**S2**) was adapted from literature with slight modifications.[6]

Pyromellitic dianhydride (**S1**) (5.02 g, 22.3 mmol, 1.00 eq.) was suspended in absolute ethanol (50 mL) and refluxed until it was completely dissolved. H_2SO_4 (3.0 mL, 54 mmol, 2.4 eq.) was added dropwise and the mixture was refluxed for 20 h. Afterwards, more H_2SO_4 (2.0 mL, 36 mmol, 1.6 eq.) was added and it was reflux for further 4 h. Subsequently, 25 mL of ethanol were distilled off under atmospheric pressure and the remaining solution was cooled to rt and poured into ice-cold aq. NaOH solution (2 N, 40 mL). The aqueous layer was extracted with diethyl ether (40 mL). Afterwards, the aqueous layer was basified with aq. NaOH solution (2 N) and extracted with diethyl ether (2 x 30 mL). The combined organic extracts were washed with aq. NaOH solution (1 N, 20 mL) and brine, dried (Na_2SO_4) filtered and concentrated *in vacuo* to give the desired ester **S2** as a colorless oil (6.75 g, 18.4 mmol, 83%) which solidified upon storage at rt over two weeks. It was used in the next step without further purification.

^{1}H NMR (200 MHz, $CDCl_3$): δ = 8.04 (s, 2H), 4.39 (q, *J* = 7.1 Hz, 8H), 1.38 (t, *J* = 7.1 Hz, 12H) ppm.

Analytical data corresponds to literature.[6]

Synthesis of diethyl 4,5-bis(hydroxymethyl)benzene-1,2-dicarboxylate (S3**)**

The synthesis of diethyl 4,5-bis(hydroxymethyl)benzene-1,2-dicarboxylate (**S3**) was adapted from literature with slight modifications.[7]

$LiBH_4$ (207 mg, 9.01 mmol, 2.20 eq.) was added to a solution of ester **S2** (1.5 g, 4.1 mmol, 1.0 eq.) in anhydrous THF (17 mL) under nitrogen atmosphere and the mixture was stirred at rt for 2 d. Afterwards, aq. HCl (1 N, 2.7 mL) was added carefully. The resulting precipitate was removed by filtration and washed with CH_2Cl_2. The filtrate was diluted with water (15 mL) and extracted with CH_2Cl_2 (3 x 15 mL). The combined organic extracts were washed with brine, dried ($MgSO_4$), filtered and concentrated *in vacuo*. Purification via flash chromatography [30 g silica, Cy/EA (3:7)] yielded the desired diol **S3** as a colorless oil (933 mg, 3.31 mmol, 81%).

^{1}H NMR (200 MHz, DMSO-d_6): δ = 7.72 (s, 2H), 5.50 (t, *J* = 5.5 Hz, 2H), 4.55 (d, *J* = 5.5 Hz, 4H), 4.25 (q, *J* = 7.1 Hz, 4H), 1.26 (t, *J* = 7.1 Hz, 6H) ppm.

Analytical data corresponds to literature.[7]

Synthesis of diethyl phthalazine-6,7-dicarboxylate (1j**)**

A solution of anhydrous DMSO (1.0 mL, 14 mmol, 4.4 eq.) in anhydrous CH_2Cl_2 (4 mL) was added dropwise to a solution of oxalyl chloride (0.63 mL, 7.2 mmol, 2.2 eq.) in anhydrous CH_2Cl_2 (15 mL) at −70 °C under nitrogen atmosphere. After stirring for 15 min at the same temperature, a solution of diol **S3** (0.92 g, 3.3 mmol, 1.0 eq.) in anhydrous THF (4 mL) was added dropwise. The mixture was stirred for further 45 min at −70 °C before anhydrous Et_3N (5.7 mL, 39 mmol, 12 eq.) was added. The resulting suspension was slowly warmed to rt over 1.5 h. Afterwards, water (20 mL) was added and the organic layer was separated. The aqueous layer was extracted with CH_2Cl_2 (2 x 25 mL). The combined organic layers were washed with brine, dried ($MgSO_4$), filtered and concentrated *in vacuo* to give the crude dialdehyde **S4** as yellow oil that was directly used in the next step without further purification.

Dialdehyde **S4** was dissolved in ethanol (10 mL) and CH_2Cl_2 (17 mL) and a solution of hydrazine monohydrate (0.170 mL, 3.42 mmol, 1.05 eq.) in ethanol (7 mL) was added dropwise at 0 °C. The mixture was slowly warmed to rt overnight. Afterwards, the solvent was removed *in vacuo* and the crude product was purified via flash chromatography [50 g silica, Cy/EA (2:8 to 1:9), dry loading (acetone/CH_2Cl_2)]. Phthalazine **1j** was obtained as a yellow solid (489 mg, 1.78 mmol, 55%).

^{1}H NMR (400 MHz, $CDCl_3$): δ = 9.69 (s, 2H), 8.38 (s, 2H), 4.46 (q, *J* = 7.1 Hz, 4H), 1.43 (t, *J* = 7.1 Hz, 6H) ppm.

$^{13}C\{^{1}H\}$ NMR (101 MHz, $CDCl_3$): δ = 166.0 (2C), 151.0 (2C), 136.1 (2C), 128.1 (2C), 126.7 (2C), 62.7 (2C), 14.2 (2C) ppm.

HRMS (ESI): *m/z* calculated for $C_{14}H_{14}N_2O_4$+Na: 297.0846 $[M+Na]^+$, found: 297.0850.

R_f: 0.34 (EtOAc).

Melting Point: 87-88 °C.

1.3 Synthesis of *tert*-butyl azete-1(2*H*)-carboxylate (3)

The synthesis of *tert*-butyl azete-1(2*H*)-carboxylate (**3**) was adopted from the literature with slight modifications:[8,9]

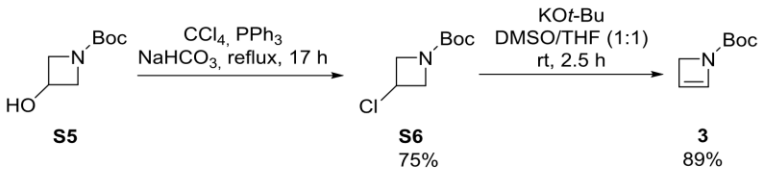

S5 **S6** 75% **3** 89%

Scheme S2. Synthesis route of *tert*-butyl azete-1(2*H*)-carboxylate (**3**).

Synthesis of *tert*-butyl 3-chloroazetidine-1-carboxylate (S6)

To a solution of alcohol **S5** (4.07 g, 23.0 mmol, 1.00 eq.) in CCl_4 (25 mL) were added PPh_3 (6.70 g, 25.3 mmol, 1.10 eq.) and $NaHCO_3$ (15 mg, 0.18 mmol, 0.78 mol%) and the mixture was stirred under reflux for 17 h. Afterwards, the mixture was cooled to rt and concentrated *in vacuo*. The residue was suspended in pentane (25 mL) and filtered. The filtered cake was washed with pentane (25 mL) and the combined filtrates were concentrated *in vacuo*. The crude product was purified via flash chromatography [150 g silica gel, pentane/Et_2O (100:0 to 80:20)] to obtain the desired chloroazetidine **S6** as a colorless oil (3.30 g, 17.2 mmol, 75%).

^{1}H NMR (200 MHz, $CDCl_3$): δ = 4.61 – 4.44 (m, 1H), 4.44 – 4.31 (m, 2H), 4.10 – 3.97 (m, 2H), 1.44 (s, 9H) ppm.

Analytical data corresponds to literature.[8]

Synthesis of *tert*-butyl azete-1(2*H*)-carboxylate (3)

A solution of KO*t*-Bu (578 mg, 5.00 mmol, 1.47 eq.) in anhydrous DMSO (25 mL) was added dropwise to a solution of chlorazetidine **S6** (652 mg, 3.40 mmol, 1.00 eq.) in anhydrous THF (25 mL) at rt under nitrogen atmosphere. After stirring for 2.5 h at rt, water (20 mL) was added and the mixture was extracted with Et_2O (3 x 30 mL). The combined organic layers were washed with water (3 x 40 mL) and brine (40 mL), dried (Na_2SO_4), filtered and concentrated *in vacuo* to obtain the azetine **3** as a colorless to pale yellow oil (472 mg, 3.04 mmol, 89%) that was used in the next step without further purification.
The azetine **3** was stored at −25 °C in a nitrogen filled glove box.

^{1}H NMR (200 MHz, CD_2Cl_2): δ = 6.57 (dt, *J* = 1.7, 0.8 Hz, 1H), 5.54 (dt, *J* = 1.7, 0.8 Hz, 1H), 4.36 (t, *J* = 0.8 Hz, 2H), 1.44 (s, 9H) ppm.

Analytical data corresponds to literature.[9]

1.4 General procedure for the IEDDA reaction/thermal ring expansion sequence (GP1)

In a nitrogen filled glove box, (substituted) phthalazine (**1**) (0.25 mmol, 1.0 eq.) and **BDLA** catalyst (2.6 mg, 13 µmol, 5.0 mol%) were suspended in anhydrous and degassed 1,4-dioxane or diglyme (4 mL) in a round bottom flask. In a separate flask, azetine **3** (48 mg, 0.31 mmol, 1.2 eq.) was dissolved in anhydrous and degassed 1,4-dioxane or diglyme (1 mL). Both flasks were sealed with a septum and taken out of the glove box. The following reaction steps were performed in the fume hood under Schlenk conditions. The azetine solution was transferred to a 1 mL syringe and added to the phthalazine/**BDLA** mixture with a syringe pump over 20 h at the indicated temperature. After the complete addition, the mixture was stirred for further 2 h at the same temperature. Afterwards, the mixture was concentrated *in vacuo*. If the reaction was performed in diglyme, the residue was diluted with cyclohexane (10 mL), washed with water (4 x 1 mL) and brine (2 mL), dried (Na_2SO_4), filtered and concentrated *in vacuo*. The crude products were purified via automated flash chromatography using the conditions given below.

1.4.1 Synthesis of *tert*-butyl (1*Z*,5*Z*)-benzo[*d*]azocine-3(4*H*)-carboxylate (5a)

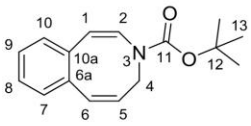

According to **GP1**, azetine **3** (186 mg, 1.20 mmol, 1.20 eq.) in diglyme (4 mL) was added to a mixture of phthalazine (**1a**) (133 mg, 1.00 mmol, 1.0 eq.) and **BDLA** catalyst (6.1 mg, 30 µmol, 3.0 mol%) in diglyme (16 mL) at 110 °C. Purification via automated flash chromatography [12 g silica gel, cyclohexane/EtOAc (100:0 to 99:1)] yielded azocine **5a** as a colorless oil (188 mg, 0.731 mmol, 73%).

^{1}H NMR (400 MHz, CD_3CN): δ = 7.25 (td, *J* = 7.5, 1.5 Hz, 1H, H-9), 7.18 (td, *J* = 7.5, 1.5 Hz, 1H, H-8), 7.15 – 7.10 (m, 1H, H-10), 7.08 – 7.00 (m, 1H, H-7), 6.94 (d, *J* = 10.4 Hz, 1H, H-6), 6.87 (d, *J* = 11.4 Hz, 1H, H-2), 6.10 (dt, *J* = 10.4, 8.4 Hz, 1H, H-5), 5.38 (s, br, 1H, H-1), 4.31 (d, *J* = 8.4 Hz, 2H, H-4), 1.48 (s, 9H, H-13) ppm.

^{13}C{^{1}H} NMR (101 MHz, CD_3CN): δ = 153.7 (br, C-11), 137.7 (br, C-6), 136.6 (C-10a), 135.2 (C-6a), 132.2 (C-10), 130.2 (C-7), 129.2 (C-9), 128.6 (br, C-5), 127.4 (C-8), 127.3 (C-2), 107.7 (br, C-1), 82.3 (C-12), 42.7 and 41.6 (br, C-4), 28.3 (3C, C-13) ppm. Due to conformational changes, C-4 shows two broad signals with low intensity (compare Figure S9 and Figure S10).

HRMS (ESI): *m/z* calculated for $C_{16}H_{19}NO_2$+Na: 280.1308 $[M+Na]^+$, found: 280.1308.

R_f: 0.39 (Cy/EtOAc, 95:5).

1.4.2 Synthesis of *tert*-butyl (1*Z*,5*Z*)-7,10-difluorobenzo[*d*]azocine-3(4*H*)-carboxylate (5b)

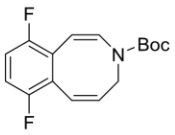

According to **GP1**, azetine **3** (48 mg, 0.31 mmol, 1.2 eq.) was added to a mixture of phthalazine **1b** (42 mg, 0.25 mmol, 1.0 eq.) and **BDLA** catalyst (2.6 mg, 13 µmol, 5.0 mol%) in 1,4-dioxane at 80 °C. Purification via automated flash chromatography [12 g silica gel, cyclohexane/EtOAc (100:0 to 90:10), dry loading on celite with CH_2Cl_2] yielded azocine **5b** as a colorless to pale yellow oil (63 mg, 0.22 mmol, 87%).

^{1}H NMR (400 MHz, CD_3CN): δ = 7.13 – 7.02 (m, 2H), 6.96 (td, *J* = 9.0, 4.4 Hz, 1H), 6.88 (dd, *J* = 10.4, 3.0 Hz, 1H), 6.25 (dt, *J* = 10.4, 8.4 Hz, 1H), 5.24 (d, *J* = 11.5 Hz, 1H), 4.41 (d, *J* = 8.4 Hz, 2H), 1.48 (s, 9H) ppm.

^{13}C{^{1}H} NMR (101 MHz, CD_3CN): δ = 158.7 (dd, *J* = 79.0, 2.3 Hz), 156.3 (dd, br, *J* = 78.2, 2.4 Hz), 153.5, 131.4, 130.4 (d, *J* = 2.1 Hz), 130.1 (br), 126.6 (dd, *J* = 14.9, 3.4 Hz), 125.1 (dd, *J* = 18.2, 2.1 Hz), 116.7 (dd, *J* = 26.5, 9.5 Hz), 115.0 (dd, *J* = 25.2, 9.5 Hz), 98.7, 82.8, 41.8 (br), 28.3 (3C) ppm.

^{19}F{^{1}H} NMR (377 MHz, CD_3CN): δ = -118.27 (br), -120.64 (d, *J* = 16.4 Hz) ppm.

HRMS (ESI): *m/z* calculated for $C_{16}H_{17}F_2NO_2$+Na: 316.1120 $[M+Na]^+$, found: 316.1121.

R_f: 0.22 (Cy/EtOAc, 97:3).

1.4.3 Synthesis of *tert*-butyl (1*Z*,5*Z*)-7,10-dichlorobenzo[*d*]azocine-3(4*H*)-carboxylate (5c)

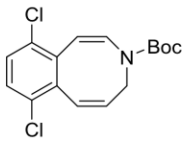

According to **GP1**, azetine **3** (48 mg, 0.31 mmol, 1.2 eq.) was added to a mixture of phthalazine **1c** (50 mg, 0.25 mmol, 1.0 eq.) and **BDLA** catalyst (2.6 mg, 13 µmol, 5.0 mol%) in 1,4-dioxane at 80 °C. Purification via automated flash chromatography [12 g silica gel, cyclohexane/EtOAc (100:0 to 99:1), dry loading on celite with CH_2Cl_2] yielded azocine **5c** as a colorless to pale yellow oil (54 mg, 0.17 mmol, 66%).

^{1}H NMR (400 MHz, CD_3CN): δ = 7.40 (d, *J* = 8.6 Hz, 1H), 7.28 (d, *J* = 8.6 Hz, 1H), 7.09 – 6.88 (m, 2H), 6.15 (td, *J* = 10.3, 7.7 Hz, 1H), 5.29 (d, *J* = 11.4 Hz, 1H), 4.55 (s, br, 1H), 4.06 (s, br, 1H), 1.48 (s, 9H) ppm.

^{13}C{^{1}H} NMR (101 MHz, CD_3CN): δ = 137.1, 135.9, 134.8 (br), 134.1, 132.8, 131.1, 129.4, 129.3 (br), 129.2, 105.3 (br), 82.8, 28.3 (3C) ppm. Due to peak broadening caused by conformational changes, two signals cannot be detected (compare Figure S9 and Figure S10).

HRMS (ESI): *m/z* calculated for $C_{16}H_{17}Cl_2NO_2$+Na: 348.0529 $[M+Na]^+$, found: 348.0529.

R_f: 0.44 (Cy/EtOAc, 95:5).

1.4.4 Synthesis of *tert*-butyl (1*Z*,5*Z*)-10-nitrobenzo[*d*]azocine-3(4*H*)-carboxylate (5da) and *tert*-butyl (1*Z*,5*Z*)-7-nitrobenzo[*d*]azocine-3(4*H*)-carboxylate (5db)

According to **GP1**, azetine **3** (48 mg, 0.31 mmol, 1.2 eq.) was added to a mixture of phthalazine **1d** (44 mg, 0.25 mmol, 1.0 eq.) and **BDLA** catalyst (2.6 mg, 13 µmol, 5.0 mol%) in 1,4-dioxane at 80 °C. Purification via automated flash chromatography [12 g silica gel, cyclohexane/EtOAc (99:1 to 89:11), dry loading on celite with CH_2Cl_2] yielded azocine **5db** as a yellow oil (36 mg, 0.12 mmol, 47%) and azocine **5da** as a yellow oil (32 mg, 0.11 mmol, 42%).

Tert-butyl (1*Z*,5*Z*)-10-nitrobenzo[*d*]azocine-3(4*H*)-carboxylate (**5da**)

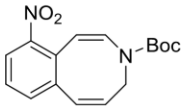

^{1}H NMR (400 MHz, CD_2Cl_2): δ = 7.66 (dd, *J* = 7.9, 1.4 Hz, 1H), 7.31 (t, *J* = 7.9 Hz, 1H), 7.25 (d, *J* = 7.9 Hz, 1H), 7.13 – 6.88 (m, 2H), 6.17 (dt, *J* = 10.3, 8.4 Hz, 1H), 5.26 (d, *J* = 11.2 Hz, 1H), 4.37 (s, br, 2H), 1.49 (s, 9H) ppm.

^{13}C{^{1}H} NMR (101 MHz, CD_2Cl_2): δ = 152.9 (br), 151.6, 138.3, 135.2, 132.9, 129.8 (br), 129.7 (br), 129.4, 127.2, 123.7, 100.8 (br), 82.4, 40.9 (br), 28.3 (3C) ppm.

HRMS (ESI): *m/z* calculated for $C_{16}H_{18}N_2O_4$+Na: 325.1159 $[M+Na]^+$, found: 325.1156.

R_f: 0.26 (Cy/EtOAc, 9:1).

The position of the nitro group was assigned via NOESY (see Figure S15).

Tert-butyl (1*Z*,5*Z*)-7-nitrobenzo[*d*]azocine-3(4*H*)-carboxylate (**5db**)

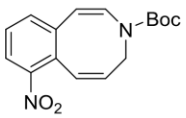

^{1}H NMR (400 MHz, CD_2Cl_2): δ = 7.78 (dd, *J* = 7.4, 2.0 Hz, 1H), 7.45 – 7.34 (m, 2H), 7.11 (d, *J* = 10.6 Hz, 1H), 6.92 (s, br, 1H), 6.17 (dt, *J* = 10.6, 8.4 Hz, 1H), 5.39 (s, br, 1H), 4.36 (s, br, 2H), 1.49 (s, 9H) ppm.

^{13}C NMR{^{1}H} (101 MHz, CD_2Cl_2): δ = 152.9 (br), 149.6, 140.1, 136.0, 132.4 (br), 129.7, 129.1, 128.7, 128.6, 122.8, 105.5 (br), 82.3, 42.5 and 41.4 (br, 1C), 28.3 (3C) ppm.

HRMS (ESI): *m/z* calculated for $C_{16}H_{18}N_2O_4$+Na: 325.1159 $[M+Na]^+$, found: 325.1155.

R_f: 0.33 (Cy/EtOAc, 9:1).

1.4.5 Synthesis of *tert*-butyl (5*Z*,9*Z*)-pyrido[2,3-*d*]azocine-8(7*H*)-carboxylate (5ea) and *tert*-butyl (5*Z*,9*Z*)-pyrido[3,2-*d*]azocine-7(8*H*)-carboxylate (5eb)

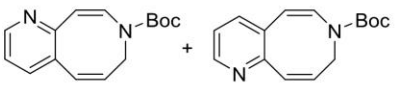

According to **GP1**, azetine **3** (48 mg, 0.31 mmol, 1.2 eq.) was added to a mixture of pyridazine **1e** (33 mg, 0.25 mmol, 1.0 eq.) and **BDLA** catalyst (2.6 mg, 13 µmol, 5.0 mol%) in 1,4-dioxane at 80 °C. Purification via automated flash chromatography [12 g silica gel, cyclohexane/EtOAc (88:12 to 25:75), dry loading on celite with CH_2Cl_2] yielded a mixture of azocines **5ea** and **5eb** as a yellow oil (46 mg, 0.18 mmol, 71%, regioisomeric ratio: 81:19).

^{1}H NMR (400 MHz, CD_3CN): δ = 8.45 (dd, *J* = 4.7, 1.8 Hz, 1H, minor isomer), 8.38 (dd, *J* = 4.7, 1.7 Hz, 1H, major isomer), 7.46 (dd, *J* = 7.9, 1.7 Hz, 1H, major isomer), 7.39 (dd, *J* = 7.8, 1.7 Hz, 1H, minor isomer), 7.20 (dd, *J* = 7.9, 4.6 Hz, 1H, major isomer), 7.13 (dd, *J* = 7.7, 4.7 Hz, 1H, minor isomer), 7.05 – 6.76 (m, 4H, major and minor isomer), 6.28 – 6.11 (m, 2H, major and minor isomer), 5.45 (s, br, 1H, minor isomer), 5.29 (s, br, 1H, major isomer), 4.38 – 4.30 (m, 4H, major and minor isomer), 1.49 and 1.48 (two overlapping s, 18H, major and minor isomer) ppm.

^{13}C{^{1}H} NMR (101 MHz, CD_3CN): δ = 154.4, 153.5, 150.1, 148.1, 139.6, 138.2 (br), 137.8, 135.4 (br), 132.6, 130.9, 129.5 (br), 128.5, 128.2, 123.7, 121.9, 105.1 (br), 82.6 (br), 41.7 (br), 28.3 ppm.

NMR spectra could not be assigned unambiguously.

HRMS (ESI): *m/z* calculated for $C_{15}H_{18}N_2O_2$+Na: 281.1260 $[M+Na]^+$, found: 281.1262.

R_f: 0.35 (Cy/EtOAc, 1:1).

1.4.6 Synthesis of *tert*-butyl (1*Z*,5*Z*)-10-fluorobenzo[*d*]azocine-3(4*H*)-carboxylate (5fa) and *tert*-butyl (1*Z*,5*Z*)-7-fluorobenzo[*d*]azocine-3(4*H*)-carboxylate (5fb)

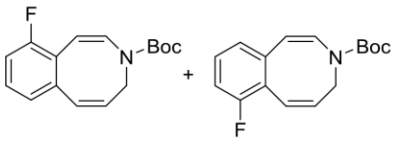

According to **GP1**, azetine **3** (48 mg, 0.31 mmol, 1.2 eq.) was added to a mixture of phthalazine **1f** (37 mg, 0.25 mmol, 1.00 eq.) and **BDLA** catalyst (2.6 mg, 13 µmol, 5.0 mol%) in 1,4-dioxane at 90 °C. Purification via automated flash chromatography [12 g silica gel, cyclohexane/EtOAc (99:1 to 88:12), dry loading on celite with CH_2Cl_2] yielded a mixture of azocines **5fa** and **5fb** as a colorless oil (60 mg, 0.22 mmol, 88%, regioisomeric ratio: 51:49).

^{1}H NMR (400 MHz, CD_3CN): δ = 7.32 – 7.16 (m, 2H), 7.08 – 6.98 (m, 2H), 6.99 – 6.70 (m, 6H), 6.21 (dt, *J* = 10.4, 8.3 Hz, 1H), 6.13 (dt, *J* = 10.4, 8.4 Hz, 1H), 5.38 (s, br, 1H), 5.29 (s, br, 1H), 4.36 and 4.35 (two overlapping d, *J* = 8.4 Hz, 4H), 1.482 and 1.480 (two overlapping s, 18H) ppm.

^{13}C{^{1}H} NMR (101 MHz, CD_3CN): δ = 163.3, 162.6, 160.8, 160.2, 153.6 (br), 139.6, 139.5, 138.1, 138.1, 136.6 (br), 130.9, 130.8, 130.8, 130.5 (br), 129.6, 129.4 (br), 128.9, 128.8, 128.2, 127.9, 127.9, 125.9, 125.8, 124.7, 124.6, 123.3, 123.1, 115.5, 115.3, 113.9, 113.7, 106.5 (br), 99.5 (br), 82.5, 41.7 (br), 28.3 ppm.

^{19}F{^{1}H} NMR (377 MHz, CD_3CN): δ = -113.47, -115.85 ppm.

NMR spectra could not be assigned unambiguously.

HRMS (ESI): *m/z* calculated for $C_{16}H_{18}FNO_2$+Na: 298.1214 $[M+Na]^+$, found: 298.1215.

R_f: 0.44 (Cy/EtOAc, 9:1).

1.4.7 Synthesis of *tert*-butyl (1*Z*,5*Z*)-9-fluorobenzo[*d*]azocine-3(4*H*)-carboxylate and *tert*-butyl (1*Z*,5*Z*)-8-fluorobenzo[*d*]azocine-3(4*H*)-carboxylate (5g)

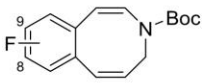

According to **GP1**, azetine **3** (48 mg, 0.31 mmol, 1.2 eq.) was added to a mixture of phthalazine **1g** (37 mg, 0.25 mmol, 1.00 eq.) and **BDLA** catalyst (2.6 mg, 13 µmol, 5.0 mol%) in 1,4-dioxane at 90 °C. Purification via automated flash chromatography [12 g silica gel, cyclohexane/EtOAc (100:0 to 95:5), dry loading on celite with CH_2Cl_2] yielded a mixture of azocines **5g** as a colorless oil (42 mg, 0.17 mmol, 67%, regioisomeric ratio: 52:48).

^{1}H NMR (400 MHz, CD_3CN): δ = 7.18 – 7.09 (m, 1H), 7.07 – 6.97 (m, 2H), 6.97 – 6.76 (m, 7H), 6.23 – 6.00 (m, 2H), 5.32 (s, br, 2H), 4.31 (d, *J* = 8.4 Hz, 4H), 1.48 and 1.47 (two overlapping s, 18H) ppm.

^{13}C{^{1}H} NMR (101 MHz, CD_3CN): δ = 164.9, 163.6, 162.5, 161.2, 153.6 (br), 139.2, 139.2, 137.6, 137.5, 136.7 (br), 134.1, 134.0, 133.0, 132.9, 132.1, 132.0, 131.6, 131.6, 129.7 (br), 128.8 (br), 128.3, 127.3, 118.0, 116.4, 116.2, 116.1, 115.9, 114.3, 114.1, 106.6 (br), 82.5 (br), 82.4 (br), 42.6 (br), 41.6 (br), 28.3, 28.3 ppm.

^{19}F{^{1}H} NMR (377 MHz, CD_3CN): δ = -117.17, -118.83 ppm.

NMR spectra could not be assigned unambiguously.

HRMS (ESI): *m/z* calculated for $C_{16}H_{18}FNO_2$+Na: 298.1214 $[M+Na]^+$, found: 298.1216.

R_f: 0.37 (Cy/EtOAc, 95:5).

1.4.8 Synthesis of *tert*-butyl (1*Z*,5*Z*)-8-chlorobenzo[*d*]azocine-3(4*H*)-carboxylate and *tert*-butyl (1*Z*,5*Z*)-9-chlorobenzo[*d*]azocine-3(4*H*)-carboxylate (5h)

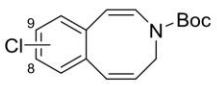

According to **GP1**, azetine **3** (48 mg, 0.31 mmol, 1.2 eq.) was added to a mixture of phthalazine **1h** (41 mg, 0.25 mmol, 1.0 eq.) and **BDLA** catalyst (2.6 mg, 13 µmol, 5.0 mol%) in 1,4-dioxane at 90 °C. Purification via automated flash chromatography [12 g silica gel, cyclohexane/EtOAc (99:1 to 93:7), dry loading on celite with CH_2Cl_2] yielded a mixture of azocines **5h** as a colorless to pale yellow oil (54 mg, 0.18 mmol, 74%, regioisomeric ratio: 53:47).

^{1}H NMR (400 MHz, CD_3CN): δ = 7.24 (dd, *J* = 8.4, 2.4 Hz, 1H), 7.21 – 7.13 (m, 2H), 7.09 (d, *J* = 8.4 Hz, 1H), 7.07 (d, *J* = 2.3 Hz, 1H), 7.01 (d, *J* = 8.3 Hz, 1H), 6.95 – 6.84 (m, 4H), 6.20 – 6.06 (m, 2H), 5.31 (s, 2H), 4.31 (d, *J* = 8.4 Hz, 4H), 1.48 and 1.47 (two overlapping s, 18H) ppm.

^{13}C{^{1}H} NMR (101 MHz, CD_3CN): δ = 153.6 (br), 138.8, 137.3, 136.6 (br), 136.5 (br), 135.6, 134.4, 134.1, 133.8, 132.6, 131.7, 131.6, 129.8 (br), 129.7, 129.3 (br), 129.0, 128.5, 128.0, 127.2, 106.4 (br), 82.5, 42.6 (br), 41.5 (br), 28.3 ppm.

NMR spectra could not be assigned unambiguously.

HRMS (ESI): *m/z* calculated for $C_{16}H_{18}ClNO_2$+Na: 314.0918 $[M+Na]^+$, found: 314.0918.

R_f: 0.34 (Cy/EtOAc, 95:5).

1.4.9 Synthesis of *tert*-butyl (1*Z*,5*Z*)-8-(trifluoromethyl)benzo[*d*]azocine-3(4*H*)-carboxylate and *tert*-butyl (1*Z*,5*Z*)-9-(trifluoromethyl)-benzo[*d*]azocine-3(4*H*)-carboxylate (5i)

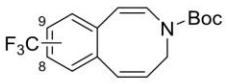

According to **GP1**, azetine **3** (48 mg, 0.31 mmol, 1.2 eq.) was added to a mixture of phthalazine **1i** (50 mg, 0.25 mmol, 1.0 eq.) and **BDLA** catalyst (2.6 mg, 13 µmol, 5.0 mol%) in 1,4-dioxane at 90 °C. Purification via automated flash chromatography [12 g silica gel, cyclohexane/EtOAc (98:2 to 96:4), dry loading on celite with CH_2Cl_2] yielded a mixture of azocines **5i** as a colorless oil (65 mg, 0.20 mmol, 79%, regioisomeric ratio: 54:46) that solidified upon storage at 2 °C.

^{1}H NMR (400 MHz, CD_3CN): δ = 7.53 (dd, *J* = 8.3, 2.1 Hz, 1H), 7.46 (dd, *J* = 8.3, 2.0 Hz, 1H), 7.43 (s, 1H), 7.35 (s, 1H), 7.29 (d, *J* = 8.2 Hz, 1H), 7.21 (d, *J* = 8.2 Hz, 1H), 7.05 – 6.87 (m, 4H), 6.29 – 6.28 (m, 2H), 5.39 (d, *J* = 11.6 Hz, 2H), 4.33 (d, *J* = 8.4 Hz, 4H), 1.48 (s, 18H) ppm.

^{13}C{^{1}H} NMR (101 MHz, CD_3CN): δ = 153.6 (br), 141.0, 139.4, 137.8, 136.5 (br), 136.2, 132.9, 131.0, 130.7, 130.4, 130.1 (br), 130.0 (br), 129.0, 128.8 (br), 128.7, 128.5, 127.0 (br), 126.8, 126.7, 125.6 (br), 124.1, 124.0, 123.8 (br), 106.3 (br), 82.7, 41.6 (br), 28.3 ppm.

^{19}F{^{1}H} NMR (377 MHz, CD_3CN): δ = -63.11, -63.27 ppm.

NMR spectra could not be assigned unambiguously.

HRMS (ESI): *m/z* calculated for $C_{17}H_{18}F_3NO_2$+Na: 348.1182 $[M+Na]^+$, found: 348.1181.

R_f: 0.44 (Cy/EtOAc, 9:1).

Melting Point: 77-78 °C.

1.4.10 Synthesis of 3-(*tert*-butyl) 8,9-diethyl (1*Z*,5*Z*)-benzo[*d*]azo-cine-3,8,9(4*H*)-tricarboxylate (5j)

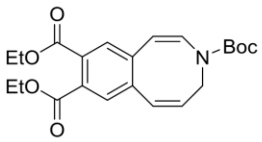

According to **GP1**, azetine **3** (33 mg, 0.21 mmol, 1.2 eq.) was added to a mixture of phthalazine **1j** (48 mg, 0.18 mmol, 1.0 eq.) and **BDLA** catalyst (1.8 mg, 9.0 µmol, 5.0 mol%) in 1,4-dioxane at 80 °C. Purification via automated flash chromatography [12 g silica gel, cyclohexane/EtOAc (96:4 to 74:26), dry loading on celite with CH_2Cl_2] yielded azocine **5j** as a colorless to pale yellow oil (50 mg, 0.13 mmol, 72%).

^{1}H NMR (400 MHz, CD_3CN): δ = 7.41 (s, 1H), 7.39 (s, 1H), 7.08 – 6.88 (m, 2H), 6.22 (dt, *J* = 10.4, 8.4 Hz, 1H), 5.36 (d, *J* = 11.4 Hz, 1H), 4.34 (d, *J* = 8.4 Hz, 2H), 4.32 – 4.24 (m, 4H), 1.48 (s, 9H), 1.37 – 1.22 (m, 6H) ppm.

^{13}C{^{1}H} NMR (101 MHz, CD_3CN): δ = 168.2, 167.8, 153.5 (br), 140.2, 138.1, 136.2 (br), 133.2, 132.4, 130.8, 130.6 (br), 130.5, 129.4, 105.9 (br), 82.8, 62.5, 62.4, 41.5 (br), 28.3 (3C), 14.4 (2C) ppm.

HRMS (ESI): *m/z* calculated for $C_{22}H_{27}NO_6$+Na: 424.1730 $[M+Na]^+$, found: 424.1730.

R_f: 0.34 (Cy/EtOAc, 8:2).

1.4.11 Synthesis of *tert*-butyl (1*Z*,5*Z*)-naphtho[2,3-*d*]azocine-3(4*H*)-carboxylate (5k)

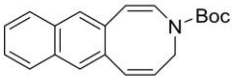

According to **GP1**, azetine **3** (47 mg, 0.31 mmol, 1.2 eq.) was added to a mixture of phthalazine **1k** (45 mg, 0.25 mmol, 1.0 eq.) and **BDLA** catalyst (2.6 mg, 13 µmol, 5.0 mol%) in diglyme at 110 °C. Purification via flash chromatography [12 g silica gel, cyclohexane/EtOAc (100:0 to 97.5:2.5)] followed by a second flash chromatography [8 g silica gel, cyclohexane/EtOAc (100:0 to 97:3)] yielded azocine **5k** as a colorless oil (54 mg, 0.18 mmol, 71%) that solidified slowly upon storage at room temperature.

^{1}H NMR (400 MHz, CD_2Cl_2): δ = 7.78 – 7.68 (m, 2H), 7.60 (s, 1H), 7.53 (s, 1H), 7.46 – 7.35 (m, 2H), 7.10 (d, *J* = 10.3 Hz, 1H), 6.92 (b, 1H), 6.14 – 6.02 (m, 1H), 5.57 (s, br, 1H), 4.34 (d, *J* = 8.5 Hz, 2H), 1.51 (s, 9H) ppm.

^{13}C{^{1}H} NMR (101 MHz, CD_2Cl_2): δ = 136.4 (br), 135.0, 133.9, 133.7, 132.3, 130.1 (br), 128.5, 127.7, 127.5, 127.1, 126.6, 126.5, 126.2, 106.5 (br), 81.9 (br), 41.1 (br), 28.3 (3C) ppm.

Due to peak broadening caused by conformational changes, one signal can't be detected (compare Figure S9 and Figure S10).

HRMS (ESI): *m/z* calculated for $C_{20}H_{21}NO_2$+Na: 330.1464 $[M+Na]^+$, found: 330.1457.

R_f: 0.32 (Cy/EtOAc, 95:5).

Melting Point: 157-158 °C.

1.4.12 Synthesis of *tert*-butyl (1*Z*,5*Z*)-9-methylbenzo[*d*]azocine-3(4*H*)-carboxylate and *tert*-butyl (1*Z*,5*Z*)-8-methylbenzo[*d*]azocine-3(4*H*)-carboxylate (5l)

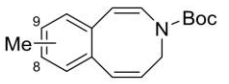

According to **GP1**, azetine **3** (48 mg, 0.31 mmol, 1.2 eq.) was added to a mixture of phthalazine **1l** (36 mg, 0.25 mmol, 1.00 eq.) and **BDLA** catalyst (2.6 mg, 13 µmol, 5.0 mol%) in diglyme at 125 °C. Purification via automated flash chromatography [12 g silica gel, cyclohexane/EtOAc (98:2 to 97:3), dry loading on celite with CH_2Cl_2] yielded a mixture of azocines **5l** as a colorless oil (15 mg, 0.055 mmol, 22%, regioisomeric ratio: 53:47).

^{1}H NMR (400 MHz, CD_3CN): δ = 7.07 (dd, *J* = 8.0, 1.2 Hz, 1H), 7.05 – 6.97 (m, 2H), 6.98 – 6.74 (m, 7H), 6.22 – 5.95 (m, 2H), 5.34 (s, br, 2H), 4.30 and 4.29 (two overlapping d, *J* = 8.4 Hz, 4H), 2.28 and 2.27 (two overlapping s, 6H), 1.48 and 1.47 (two overlapping s, 18H) ppm.

^{13}C NMR{^{1}H} (101 MHz, CD_3CN): δ = 139.0, 137.7 (br), 137.2, 136.4, 135.1, 133.7, 132.8, 132.4, 132.3, 130.7, 130.2, 129.9, 128.6 (br), 128.2, 127.3, 126.9, 107.8 (br), 82.2 (br), 42.8 (br), 41.6 (br), 28.3, 21.0, 20.8 ppm.

NMR spectra could not be assigned unambiguously. Due to peak broadening caused by conformational changes, some ^{13}C signals can't be detected (compare Figure S9 and Figure S10).

HRMS (ESI): *m/z* calculated for $C_{17}H_{21}NO_2$+Na: 294.1464 $[M+Na]^+$, found: 294.1464.

R_f: 0.41 (Cy/EtOAc, 9:1).

1.4.13 Synthesis of *tert*-butyl (1*Z*,5*Z*)-9-methoxybenzo[*d*]azocine-3(4*H*)-carboxylate and *tert*-butyl (1*Z*,5*Z*)-8-methoxybenzo[*d*]azocine-3(4*H*)-carboxylate (5m)

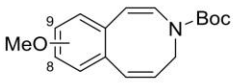

According to **GP1**, azetine **3** (48 mg, 0.31 mmol, 1.2 eq.) was added to a mixture of phthalazine **1m** (40 mg, 0.25 mmol, 1.00 eq.) and **BDLA** catalyst (2.6 mg, 13 µmol, 5.0 mol%) in diglyme at 140 °C. Purification via automated flash chromatography [12 g silica gel, cyclohexane/EtOAc (98:2 to 94:6), dry loading on celite with CH_2Cl_2] yielded a mixture of azocines **5m** as a colorless oil (12 mg, 0.042 mmol, 17%, regioisomeric ratio: 53:47).

^{1}H NMR (400 MHz, CD_3CN): δ = 7.05 (d, *J* = 8.6 Hz, 1H), 6.97 (d, *J* = 8.4 Hz, 1H), 6.92 – 6.73 (m, 6H), 6.69 (d, *J* = 2.7 Hz, 1H), 6.61 (d, *J* = 2.8 Hz, 1H), 6.21 – 5.96 (m, 2H), 5.33 (s, br, 2H), 4.31 and 4.30 (two overlapping d, *J* = 8.3 Hz, 4H), 3.76 (s, 3H), 3.75 (s, 3H), 1.48 and 1.47 (two overlapping s, 18H) ppm.

^{13}C{^{1}H} NMR (101 MHz, CD_3CN): δ = 160.7, 159.4, 138.0, 137.5 (br), 136.6, 133.6, 131.5, 128.9, 127.8, 127.6, 126.3, 117.0, 115.1, 115.0 (br), 113.3, 107.5 (br), 82.2 (br), 55.9, 55.9, 28.3 ppm.

NMR spectra could not be assigned unambiguously. Due to peak broadening caused by conformational changes, some ^{13}C signals can't be detected (compare Figure S9 and Figure S10).

HRMS (ESI): *m/z* calculated for $C_{17}H_{21}NO_3$+Na: 310.1414 $[M+Na]^+$, found: 310.1415.

R_f: 0.51 (Cy/EtOAc, 8:2).

1.4.14 Synthesis of di-*tert*-butyl (2a*R*,3*s*,8*s*,8a*S*,9*S*,10*R*)-4,7-difluoro-2a,3,8,8a-tetrahydro-8,3-[2,3]epazetonaphtho[2,3-*b*]azete-1,11(2*H*)-dicarboxylate (6) and regio-/stereoisomers

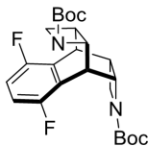

6 (and regio-/stereoisomers)

In a nitrogen filled glove box, phthalazine **1b** (17 mg, 0.10 mmol, 1.0 eq.) and **BDLA** catalyst (1 mg, 5 µmol, 5 mol%) were suspended in anhydrous and degassed 1,4-dioxane (1 mL) in a 4 mL-screw cap vial. Azetine **3** (48 mg, 0.31 mmol, 3.0 eq.) was added, the vial was sealed and taken out of the glove box. The mixture was stirred at 80 °C overnight. Afterwards, the solvent was removed *in vacuo* and the residue was purified via automated flash chromatography [12 g silica gel, cyclohexane/EtOAc (94:6 to 27:73), dry loading on celite with CH_2Cl_2]. A mixture of double Diels-Alder adducts containing the *meso* compound **6** was obtained as a highly viscous, pale yellow oil (43 mg, 0.096 mmol, 93%).

^{1}H NMR (400 MHz, CD_3CN, mixture of regio- and stereoisomers): δ = 7.28 – 6.82 (m, 2H), 4.63 – 3.51 (m, 6H), 2.85 – 2.75 (m, 2H), 2.75 – 2.49 (m, 2H), 1.63 – 0.98 (m, 18H) ppm.

^{13}C{^{1}H} NMR (101 MHz, CD_3CN, mixture of regio- and stereoisomers): δ = 159.3 – 158.4 (m), 156.7 – 156.2 (m), 155.4, 155.1 – 154.5 (m), 127.6, 127.5, 127.4, 127.3, 127.1 – 126.5 (m), 126.4 – 125.8 (m), 115.9 – 114.0 (m), 79.8, 79.6, 62.0, 61.5, 60.5, 60.4, 59.9, 53.4, 52.9, 51.6, 51.0, 35.6, 35.3, 34.2, 33.8, 32.6, 30.7, 30.4, 28.4, 28.2, 27.9 ppm.

^{19}F{^{1}H} NMR (377 MHz, CD_3CN, mixture of regio- and stereoisomers): δ = -128.32 (d, *J* = 21.1 Hz), -128.82 (d, *J* = 21.4 Hz), -128.93 (d, *J* = 21.1 Hz), -129.85 to -130.01 (m), -130.16 to -130.37 (m), -130.67 (d, *J* = 21.1 Hz), -131.02 (d, *J* = 21.1 Hz), -131.37 (d, *J* = 21.4 Hz) ppm.

NMR spectra could not be assigned unambiguously.

HRMS (ESI): *m/z* calculated for $C_{24}H_{30}F_2N_2O_4$+Na: 471.2066 $[M+Na]^+$, found: 471.2069.

R_f: 0.40 (Cy/EtOAc, 1:1).

The obtained mixture of isomers was further purified via preparative HPLC and the structure of the *meso* compound **6** was further verified via X-ray crystallography. (See sections 1.5 and 3).

1.4.15 Synthesis of di-*tert*-butyl 2,2'-oxy(2*S*,2'*S*,5*Z*,5'*Z*)-bis(1,4-dihydrobenzo[*d*]azocine-3(2*H*)-carboxylate) (7)

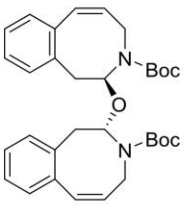

The hemiaminal ether **7** was formed quantitatively as a mixture of stereoisomers from an NMR sample of azocine **5a** in unstabilized $CDCl_3$ by keeping the solution at rt for several days. Evaporation of the solvent yielded a white solid. All attempts to obtain single crystals suitable for X-ray diffraction measurements from the racemic mixture were unsuccessful. Separation of the enantiomers via preparative chiral HPLC (see section 1.5) yielded **7** as a white crystalline solid. The enantioenriched product showed higher crystallinity compared to the racemic mixture, allowing the structure of hemiaminal ether **7** to be further confirmed via single crystal X-ray crystallography (See section 3).

^{1}H NMR (400 MHz, CD_2Cl_2): δ = 7.25 – 7.08 (m, 8H), 6.45 – 6.36 (m, 2H), 5.76 – 5.62 (m, 2H), 5.45 – 5.25 (m, 2H, overlying with residual solvent signal), 4.42 – 4.18 (m, 2H), 4.12 – 3.95 (m, 2H), 3.19 – 3.02 (m, 2H), 2.91 – 2.78 (m, 2H), 1.23 – 0.84 (m, 18H) ppm.

^{13}C{^{1}H} NMR (101 MHz, CD_2Cl_2): δ = 154.3, 154.0, 137.4, 136.8, 134.8, 134.6, 134.5, 131.0, 130.9, 130.8, 130.7, 130.5, 130.4, 130.2, 130.2, 130.0, 129.9, 129.9, 127.5, 127.4, 127.4, 127.3, 127.2, 127.1, 127.0, 126.8, 126.7, 82.8, 81.8, 80.9, 80.0, 79.9, 79.6, 42.0, 41.6, 41.3, 41.0, 39.9, 39.4, 39.1, 28.5, 28.3, 27.9, 27.6 ppm.

NMR spectra could not be assigned unambiguously.

HRMS (ESI): *m/z* calculated for $C_{32}H_{40}N_2O_5$+Na: 555.2829 $[M+Na]^+$, found: 555.2833.

R_f: 0.36 (Cy/EtOAc, 8:2).

Melting Point: 185-186 °C (partial decomposition).

The structure of the hemiaminal ether **7** was further verified via X-ray crystallography. (See section 3).

1.5 Structure elucidation and purification of side products

1.5.1 Double Diels-Alder adducts

To further elucidate the structure of the side products formed in the IEDDA/thermal ring expansion sequence, the mixture of double Diels-Alder adducts (**6** and isomers) obtained from the reaction of phthalazine **1b** with an excess of azetine **3** (see section 1.4.14) was analyzed via HPLC (Figure S1) and the two peaks were separated via preparative HPLC (Eurospher II C18 column 250 x 8 mm, 70% MeCN, 30% H_2O, 4 mL/min).

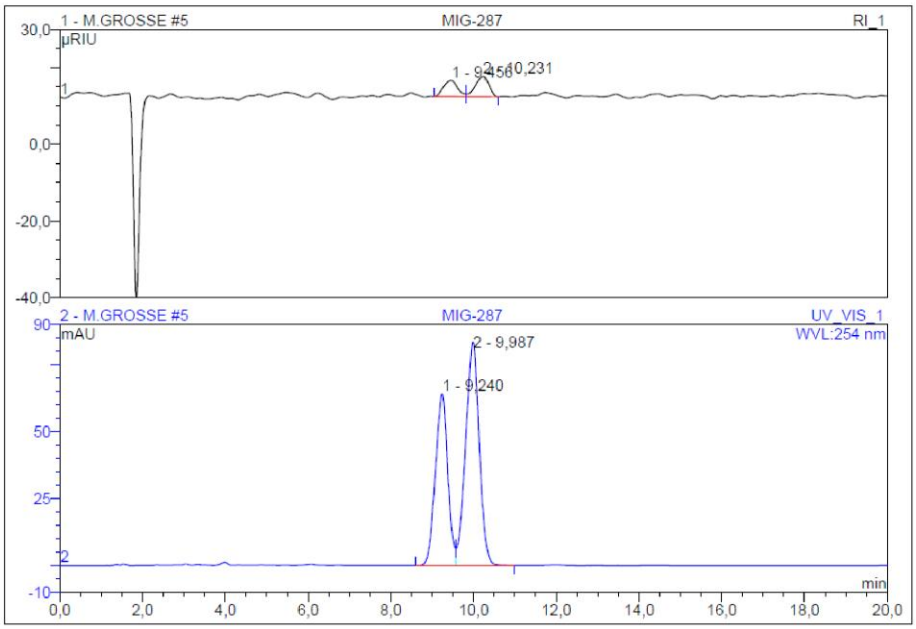

No.	Ret.Time min	Peak Name	Height µRIU	Area µRIU*min	Rel.Area %	Amount n.a.	Type
1	9,46	n.a.	4,184	1,671	45,53	n.a.	BM
2	10,23	n.a.	5,287	1,999	54,47	n.a.	MB
Total:			9,471	3,669	100,00	0,000	

No.	Ret.Time min	Peak Name	Height mAU	Area mAU*min	Rel.Area %	Amount n.a.	Type
1	9,24	n.a.	63,888	22,173	41,04	n.a.	BM
2	9,99	n.a.	83,120	31,851	58,96	n.a.	MB
Total:			147,007	54,024	100,00	0,000	

Figure S1. HPLC chromatogram (Eurospher II C18 column 250 x 4 mm, 70% MeCN, 30% H_2O, 1 mL/min) of the double Diels-Alder adducts (**6** and isomers).

The comparison of the NMR spectra of peaks 1 and 2 with the original product mixture are shown in Figure S2 and Figure S3. As can be seen from the ^{19}F NMR spectra (Figure S3), a mixture of products was obtained for both separated peaks. The compound mixture of peak 1 was obtained as a white, crystalline solid while the compound mixture of peak 2 was obtained as a white, waxy solid. We hypothesized that peak 1 corresponds to the isomers shown in Figure S4-A, as their nitrogen atoms are located on the same side of the molecule, resulting in a higher dipole moment and, consequently, increased polarity. Peak 2 was assigned to the isomers shown in Figure S4-B, as their nitrogen atoms are located on opposite sides of the molecule, resulting in a lower dipole moment and decreased polarity. This is supported by the ^{19}F NMR spectroscopic analysis: the spectrum that corresponds to peak 2 (Figure S3-C) shows two singlets (overlapping with two doublets), which can be assigned to the Diels-Alder adducts **S10** and **S11**, as both contain two equivalent fluorine atoms. In contrast, all other Diels-Alder adducts contain two non-equivalent fluorine atoms resulting in two doublets per isomer.

Single crystals suitable for X-ray diffraction measurements were obtained by vapor diffusion of *n*-pentane into a solution of the compound mixture of peak 1 in dichloromethane. The results of the X-ray diffraction measurements are shown in section 3.

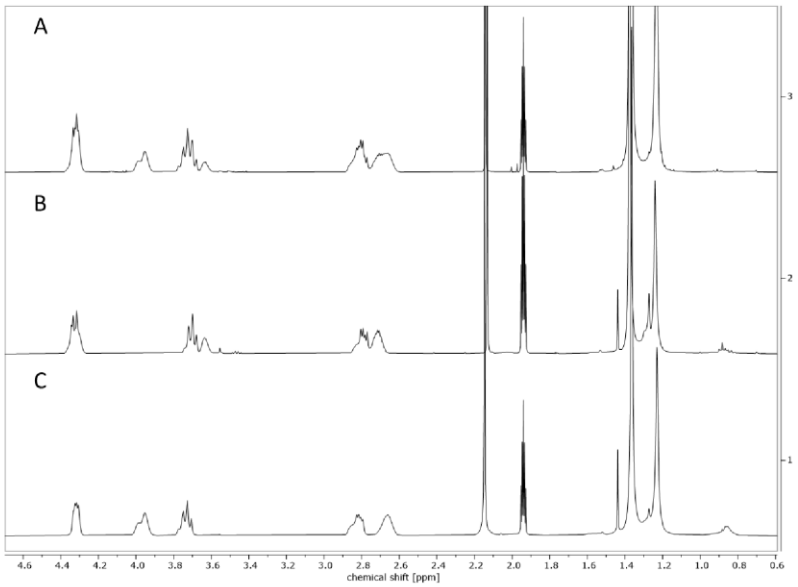

Figure S2. Excerpts of the ^{1}H NMR spectra (400 MHz, CD_3CN) of the double Diels-Alder adducts (**6** and isomers) before (A) and after (peak 1: B; peak 2: C) separation via preparative HPLC.

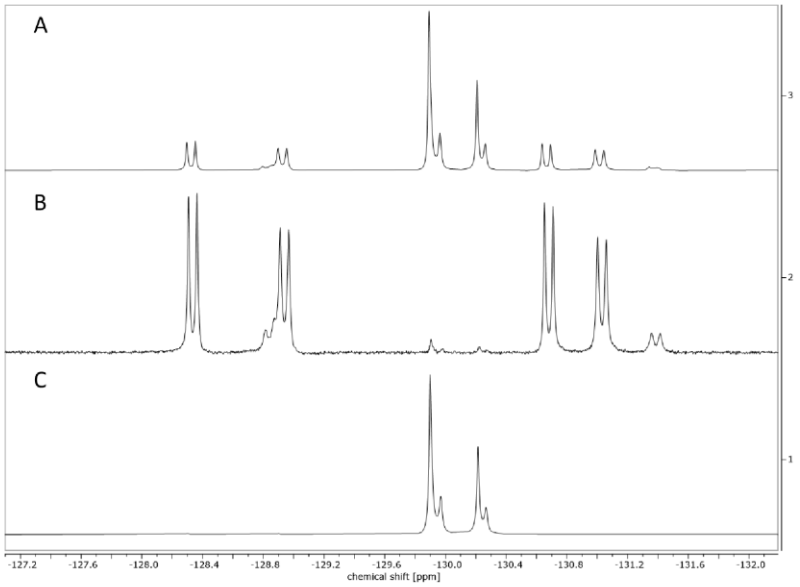

Figure S3. Excerpts of the $^{19}F\{^{1}H\}$ NMR spectra (377 MHz, CD_3CN) of the double Diels-Alder adducts (**6** and isomers) before (A) and after (peak 1: B; peak 2: C) separation via preparative HPLC.

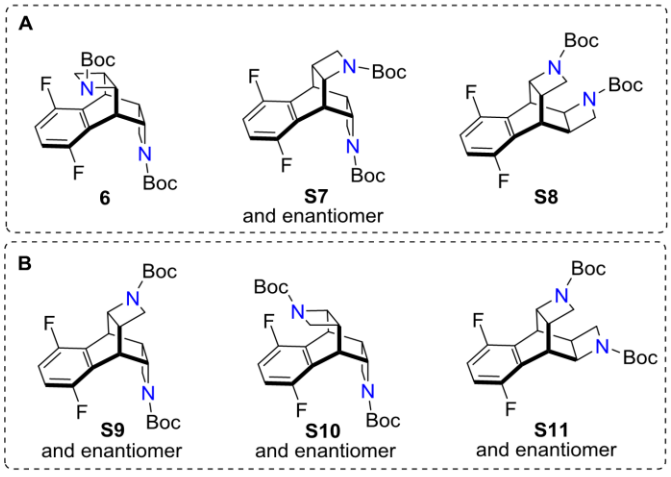

Figure S4. Structures of all possible isomers formed in the Diels-Alder reaction between *o*-QDM **4** and azetine **3**, grouped according to relative positions of the nitrogen atoms (A: nitrogen atoms on same side; B: nitrogen atoms on opposite sides).

1.5.2 Hemiaminal ether 7

To further elucidate the structure of the hemiaminal ether **7** formed from azocine **5a** in unstabilized $CDCl_3$ (see section 1.4.15), the obtained white solid was analyzed via chiral HPLC (Figure S5) and the two main peaks were separated via preparative chiral HPLC (CHIRAL ART Cellulose-SC column 250 x 10 mm, 85% *n*-hexane, 15% EtOAc, 4 mL/min). Two white, crystalline products were obtained.

Single crystals suitable for X-ray diffraction measurements were obtained by dissolving the product of peak 1 in EtOAc under heating and slowly evaporating the solvent. The results of the X-ray diffraction measurements are shown in section 3.

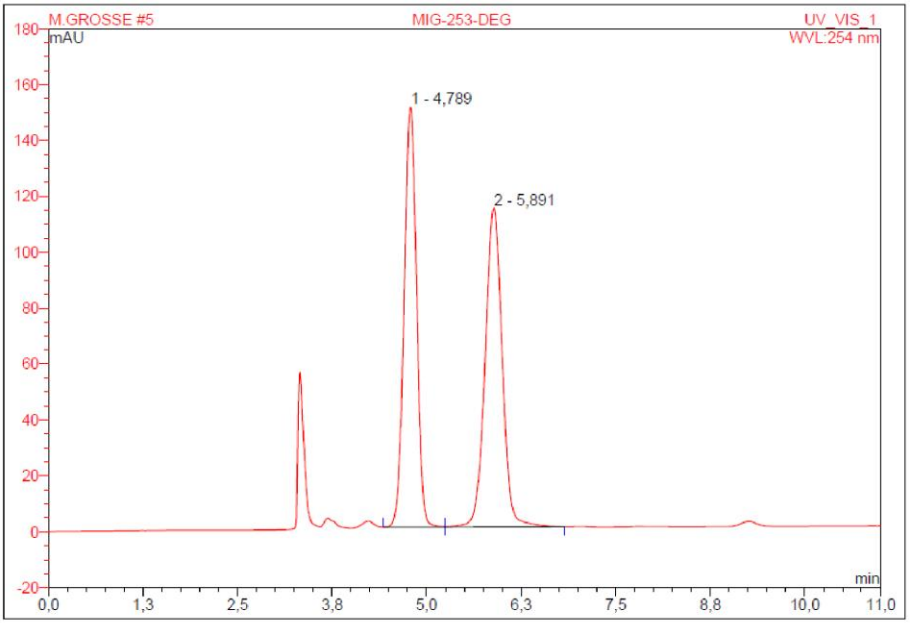

No.	Ret.Time min	Peak Name	Height mAU	Area mAU*min	Rel.Area %	Amount n.a.	Type
1	4,79	n.a.	150,181	28,673	48,97	n.a.	BM
2	5,89	n.a.	113,997	29,878	51,03	n.a.	MB
Total:			264,179	58,551	100,00	0,000	

Figure S5. Chiral HPLC chromatogram (CHIRALPAK IC column 250 x 4.6 mm, 85% *n*-hexane, 15% EtOAc, 1 mL/min) of the hemiaminal ether **7**.

3 XRD Analysis

3.1 General crystallographic experimental details

Suitable single crystals for X-ray structure determination were selected and transferred in protective perfluoropolyether oil on a microscope slide. The selected and mounted crystals were transferred to the cold gas steam on the diffractometer. The diffraction data were obtained at 100 K on a Bruker D8 three circle diffractometer, equipped with a PHOTON 100 CMOS detector and a IμS microfocus sources with Quazar mirror optics (Mo-Kα radiation, λ = 0.71073 Å).

The data obtained were integrated with SAINT and a semi-empirical absorption correction from equivalents with SADABS-2016/2 was applied.[10] The structures were solved by direct methods using SHELXT-2018/2.[11] Structure refinement was done using SHELXT-2018/3.[12] All non-hydrogen atoms were refined anisotropically and C-H hydrogen atoms were positioned at geometrically calculated positions and refined using a riding model. The isotropic displacement parameters of all hydrogen atoms were fixed to 1.2x or 1.5x (CH_3 hydrogens) the U_{eq} value of the atoms they are linked to.

3.2 Crystallographic details of the double Diels-Alder adduct 6

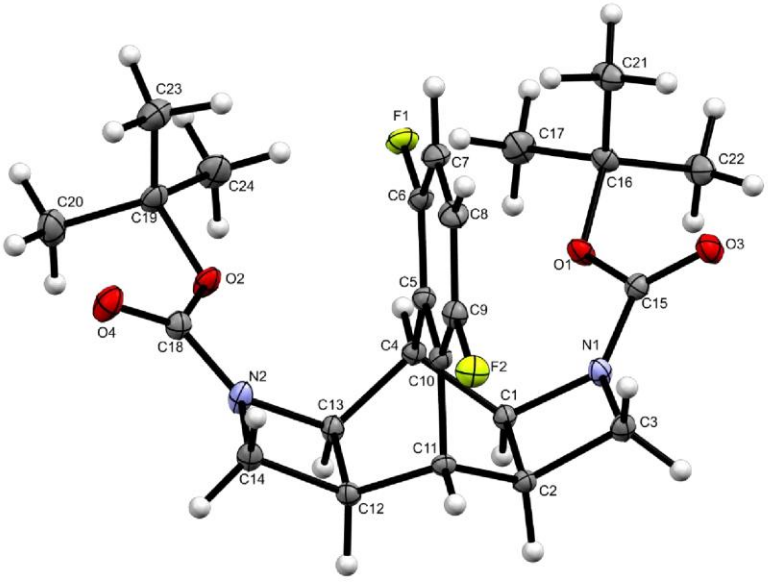

Figure S32. Thermal ellipsoid plot of **6** with the anisotropic displacement parameters drawn at the 50% probability level.

3.3 Crystallographic details of the hemiaminal ether 7

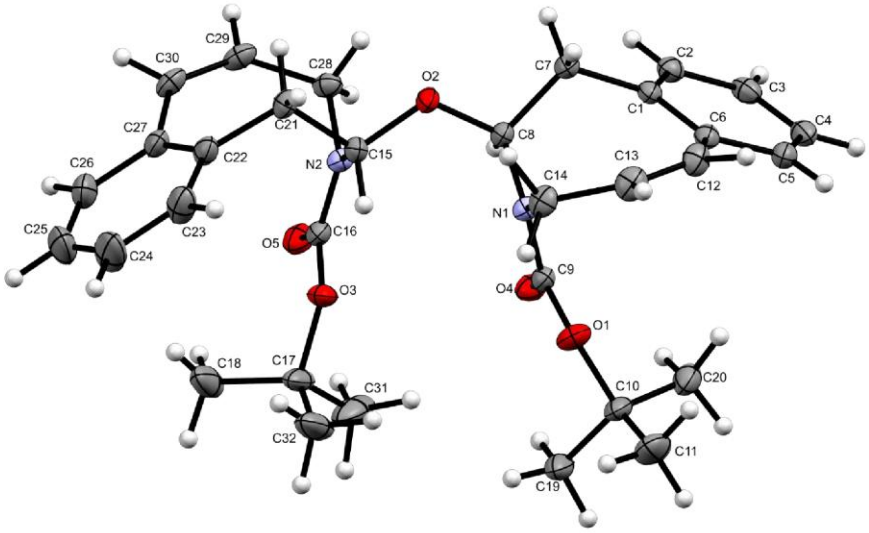

Figure S33. Thermal ellipsoid plot of **7** with the anisotropic displacement parameters drawn at the 50% probability level.

A solvent accessible void at 0.000 -0.021 0.000 with a volume of 166 Å^3 and an equivalent of 40 electrons was identified by SQUEEZE[13] as implemented in PLATON.[14–17] The disordered solvent was modelled by SQUEEZE and the model was included as a .fab file into the refinement. The Flack parameter was determined to be 0.3(2), indicating that the absolute structure is likely correct, although with some degree of uncertainty.

4 References

(1) Kessler, S. N.; Neuburger, M.; Wegner, H. A. Bidentate Lewis Acids for the Activation of 1,2-Diazines – A New Mode of Catalysis. *Eur. J. Org. Chem.* **2011**, *2011* (17), 3238–3245. DOI: 10.1002/ejoc.201100335.

(2) Kessler, S. N.; Wegner, H. A. One-pot synthesis of phthalazines and pyridazino-aromatics: a novel strategy for substituted naphthalenes. *Org. Lett.* **2012**, *14* (13), 3268–3271. DOI: 10.1021/ol301167q.

(3) Kessler, S. N.; Neuburger, M.; Wegner, H. A. Domino inverse electron-demand Diels-Alder/cyclopropanation reaction of diazines catalyzed by a bidentate Lewis acid. *J. Am. Chem. Soc.* **2012**, *134* (43), 17885–17888. DOI: 10.1021/ja308858y.

(4) Große, M.; Wegner, H. A. Bidentate Lewis Acid-Catalyzed Inverse Electron-Demand Diels–Alder Reaction of Phthalazines and Cyclooctynes. *Synlett* **2024**, *35* (09), 1019–1022. DOI: 10.1055/a-2204-9522.

(5) Synthesis of 6,7-Dichloro-5,8-phthalazinedione and Its Derivatives. *Bull. Korean Chem. Soc.* **2002**, *23* (10), 1425–1446. DOI: 10.5012/bkcs.2002.23.10.1425.

(6) Berthold, H.; Schotten, T.; Hoffmann, F.; Thiem, J. A Highly Versatile Octasubstituted Phthalocyanine Scaffold for ex post Chemical Diversification. *Synthesis* **2010**, *2010* (05), 741–748. DOI: 10.1055/s-0029-1218602.

(7) Lutz, J. P.; Davydovich, O.; Hannigan, M. D.; Moore, J. S.; Zimmerman, P. M.; McNeil, A. J. Functionalized and Degradable Polyphthalaldehyde Derivatives. *J. Am. Chem. Soc.* **2019**, *141* (37), 14544–14548. DOI: 10.1021/jacs.9b07508.

(8) Hodgson, D. M.; Pearson, C. I.; Kazmi, M. Generation and electrophile trapping of N-Boc-2-lithio-2-azetine: synthesis of 2-substituted 2-azetines. *Org. Lett.* **2014**, *16* (3), 856–859. DOI: 10.1021/ol403626k.

(9) Su, C.; Dallaston, M. A.; Watson, R. D.; Fahrenhorst-Jones, T.; Cameron, J. P.; Pierens, G. K.; Bernhardt, P. V.; Savage, G. P.; Williams, C. M. The (±)-5-Aza1.0triblattane Skeleton via Azetine Cycloaddition. *Org. Lett.* **2024**, *26* (14), 2827–2831. DOI: 10.1021/acs.orglett.3c03655.

(10) Krause, L.; Herbst-Irmer, R.; Sheldrick, G. M.; Stalke, D. Comparison of silver and molybdenum microfocus X-ray sources for single-crystal structure determination. *J. Appl. Crystallogr.* **2015**, *48* (Pt 1), 3–10. DOI: 10.1107/S1600576714022985.

(11) Sheldrick, G. M. SHELXT - integrated space-group and crystal-structure determination. *Acta Crystallogr. A* **2015**, *71* (Pt 1), 3–8. DOI: 10.1107/S2053273314026370.

(12) Sheldrick, G. M. Crystal structure refinement with SHELXL. *Acta Crystallogr. C* **2015**, *71* (Pt 1), 3–8. DOI: 10.1107/S2053229614024218.

(13) Spek, A. L. PLATON SQUEEZE: a tool for the calculation of the disordered solvent contribution to the calculated structure factors. *Acta Crystallogr. C* **2015**, *71* (Pt 1), 9–18. DOI: 10.1107/S2053229614024929.

(14) Spek, A. L. Single-crystal structure validation with the program PLATON. *J. Appl. Crystallogr.* **2003**, *36* (1), 7–13. DOI: 10.1107/S0021889802022112.

(15) Spek, A. L. Structure validation in chemical crystallography. *Acta Crystallogr. D* **2009**, *65* (Pt 2), 148–155. DOI: 10.1107/S090744490804362X.

(16) Spek, A. L. What makes a crystal structure report valid? *Inorg. Chim. Acta* **2018**, *470*, 232–237. DOI: 10.1016/j.ica.2017.04.036.

(17) Spek, A. L. checkCIF validation ALERTS: what they mean and how to respond. *Acta Crystallogr. E* **2020**, *76* (Pt 1), 1–11. DOI: 10.1107/S2056989019016244.

8.3 Reprint of Parts of the Supporting Information: Modular Assembly of Conformationally Dynamic Dinaphthocycloocta-1,5-dienes

Supporting Information

Modular Assembly of Conformationally Dynamic Dinaphthocycloocta-1,5-dienes

Michel Große[†,‡], Christopher M. Leonhardt[†,‡] and Hermann A. Wegner[†,‡,*]

[†]Institute of Organic Chemistry, Justus Liebig University Giessen, Heinrich-Buff-Ring 17, 35392 Giessen, Germany

[‡]Center for Materials Research (LaMa), Justus Liebig University Giessen, Heinrich-Buff-Ring 16, 35392 Giessen, Germany

*hermann.a.wegner@org.chemie.uni-giessen.de

Table of Contents

1 Experimental procedures and characterization data

1.1 General experimental

Chemicals were purchased from Sigma-Aldrich, Acros Organics, Alfa Aesar, chemPUR, abcr GmbH, TCI Europe or BLDpharm. Deuterated solvents were purchased from Deutero GmbH or Sigma-Aldrich. Technical grade solvents used during work-up and purification were distilled prior to use. The Bidentate Lewis acid **BDLA** was synthesized according to the literature,[1] stored and handled in a nitrogen-filled MBRAUN UNIlab glove box. Phthalazines **1b-1i** (Figure **S1**) were synthesized according to literature.[2–4]

Sensitive reactions were performed in dry glassware under nitrogen atmosphere using Schlenk techniques or in a nitrogen-filled MBRAUN UNIlab glove box. Oil baths or sand baths were used for all reactions requiring heating.

NMR spectra were measured on a Bruker Avance II 400 MHz, Avance III 400 MHz HD or Bruker Avance III HD 600 MHz spectrometer at 25 °C if not stated otherwise. Chemical shifts (δ) are reported in parts per million (ppm) relative to residual solvent signals. Coupling constants (*J*) are reported in Hertz (Hz). Multiplicities are abbreviated as s (singlet), d (doublet), t (triplet), q (quartet) and m (multiplet).

Flash chromatography was carried out with Silica 60 (0.04 – 0.063 mm) from Marcherey-Nagel GmbH & Co. KG. Automated flash chromatography was performed on an Advion Interchim puriFlash XS 520 Plus system using PF-30SIHP or PF-15SIHP columns. Thin layer chromatography was performed on Polygram®SIL G/UV254 from Macherey Nagel GmbH & Co. KG. Spots were visualized under UV-light and with basic $KMnO_4$ stain.

High-resolution mass spectra were recorded on a Bruker Impact II spectrometer featuring a quadrupole time-of-flight (Q-TOF) mass analyzer. Samples were dissolved in methanol.

Melting points were measured on a M5000 melting point meter from A. KRÜSS Optronic GmbH, Germany.

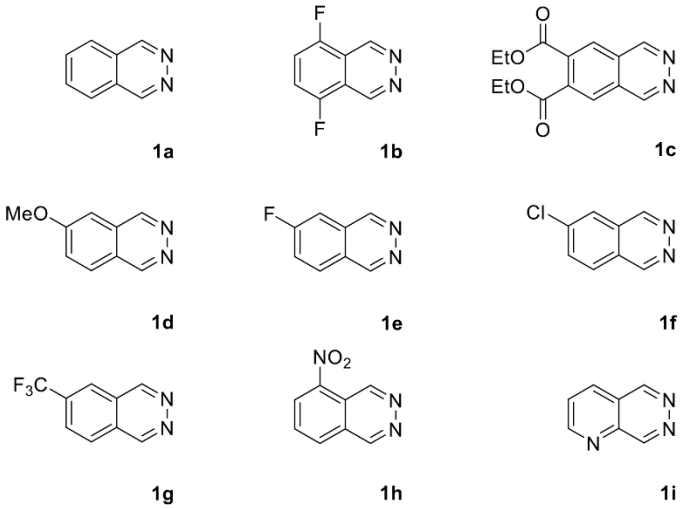

Figure S1. Overview of phthalazines and pyridazino-aromatics.

1.2 Synthesis of (1*E*,5*E*)-dibromocycloocta-1,5-diene (5)

The synthesis of (1*E*,5*E*)-dibromocycloocta-1,5-diene (**5**) was adapted from literature with slight modifications:[5]

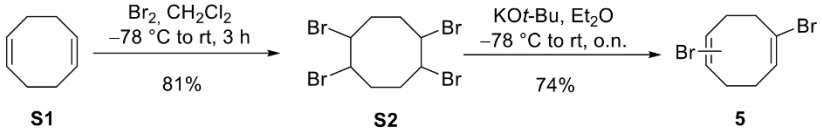

Scheme S1. Synthesis scheme of (1*E*,5*E*)-dibromocycloocta-1,5-diene (**5**).

Synthesis of 1,2,5,6-tetrabromocyclooctane (S2**)**

A solution of bromine (6.45 mL, 125 mmol, 2.25 eq.) in anhydrous CH_2Cl_2 (100 mL) was slowly added to a solution of 1,5-cyclooctadiene (**S1**) (6.9 mL, 56 mmol, 1.0 eq.) in anhydrous CH_2Cl_2 (200 mL) at −78 °C under nitrogen atmosphere over 1.5 h. The resulting yellow suspension was allowed to warm to rt and stirred for another 3 h. Afterwards, a saturated aqueous solution of $Na_2S_2O_3$ (250 mL) was added. After stirring for 10 min, the layers were separated and the aqueous layer was extracted with CH_2Cl_2 (3 x 200 mL). The combined organic extracts were dried ($MgSO_4$), filtered and concentrated *in vacuo*. Cold hexane (50 mL) was added to the residual oil and the mixture was placed in the fridge overnight. Afterwards, the solvent was decanted and the remaining solid was washed with cold hexane (25 mL). The crude tetrabromide **S2** was obtained as a white solid (19.5 g, 45.6 mmol, 81%) which was used in the next step without further purification.

^{1}H NMR (200 MHz, $CDCl_3$): δ = 5.12 – 4.17 (m, 4H), 3.02 – 1.90 (m, 8H) ppm.

Analytical data corresponds to literature.[5]

Synthesis of (1*E*,5*E*)-dibromocycloocta-1,5-diene (5)

Diethyl ether (300 mL) was added to a stirred mixture of powdered tetrabromocyclooctane **S2** (10.0 g, 23.4 mmol, 1.00 eq.) and KO*t*-Bu (8.04 g, 70.2 mmol, 3.00 eq.) at −78 °C under nitrogen atmosphere over 30 min. The suspension was allowed to warm to rt and stirred overnight. Afterwards, a saturated aqueous NH_4Cl solution (120 mL) and water (100 mL) were added to the mixture and it was stirred for 10 min. The aqueous layer was separated and extracted with ethyl acetate (1 x 200 mL, 2 x 100 mL). The combined organic layers were washed with brine, dried ($MgSO_4$) and filtered. Silica gel (20 g) was added to the filtrate and it was concentrated *in vacuo*. Purification via column chromatography (180 g silica gel, cyclohexane) yielded the vinylbromide **5** as a pale yellow oil (mixture of isomers) (4.50 g, 16.9 mmol, 72%) which solidified upon storage at −20 °C.

Mixture of isomers:

^{1}H NMR (200 MHz, $CDCl_3$): δ = 6.17 – 5.94 (m, 2H), 3.00 – 2.76 (m, 4H), 2.51 – 2.25 (m, 4H).

Analytical data corresponds to literature.[5]

1.3 General procedure for the synthesis of cyclooctanaphthalenes 4a-d (GP1)

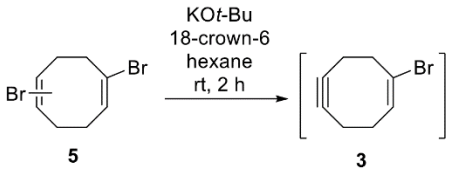

Scheme S2. Synthesis of alkyne **3** from dibromocycloocta-1,5-diene **5**.

A solution of vinyl bromide **5** (665 mg, 2.50 mmol, 1.00 eq.) in anhydrous hexane (35 mL) was added dropwise to a suspension of KO*t*-Bu (1.13 g, 9.83 mmol, 3.93 eq.) and 18-crown-6 (0.16 mg, 0.62 mmol, 0.25 eq.) in anhydrous hexane (115 mL) at rt under nitrogen atmosphere. The resulting dark brown mixture was stirred for further 2 h at rt. Afterwards, a saturated aqueous solution of NH_4Cl (25 mL) and water (25 mL) was added. The aqueous phase was separated and extracted with pentane (3 x 25 mL). The combined organic layers were washed with brine, dried (Na_2SO_4), filtered and concentrated *in vacuo* (bath temp. < 40 °C) to obtain approx. 1 mL of a brown oil containing the crude alkyne **3**. The oil was transferred to a Schlenk tube, diluted with anhydrous 1,4-dioxane (15 mL) and degassed by three freeze-pump-thaw cycles. This solution was used in the following step without further purification.

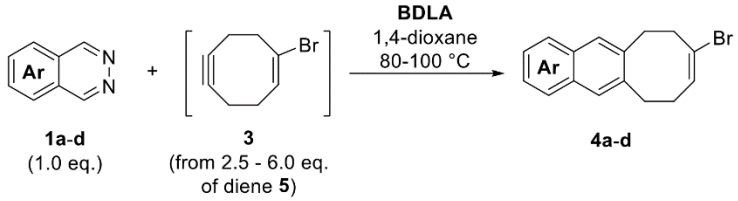

Scheme S3. Synthesis cyclooctanaphthalenes **4a-d** via IEDDA reaction.

In a nitrogen filled glove box, phthalazine **1a-d** (1.00 mmol, 1.00 eq.) and **BDLA** catalyst (5.1 mg, 25 µmol, 2.5 mol%) were suspended in anhydrous 1,4-dioxane (15 mL). A stir bar was added, the flask was sealed and taken out of the glove box. A degassed solution of the crude alkyne **3** (obtained from 2.5 – 6.0 eq. of diene **5**) in anhydrous 1,4-dioxane (15 mL) was added to the phthalazine-**BDLA** suspension and stirred at the indicated temperature for the indicated time. Afterwards, the solvent was removed *in vacuo* and the residue was purified via column chromatography (conditions noted below). Additional purification steps are noted below.

Synthesis of (*E*)-8-bromo-6,7,10,11-tetrahydrocycloocta[*b*]-naphthalene (4a**)**

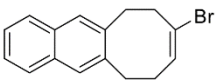

According to **GP1**, vinyl bromide **5** (1.06 g, 4.00 mmol, 4.00 eq.) in anhydrous hexane (50 mL) was treated with KO*t*-Bu (1.80 g, 15.7 mmol, 15.7 eq.) and 18-crown-6 (262 mg, 0.990 mmol, 0.990 eq.) in anhydrous hexane (120 mL). The crude alkyne **3** was dissolved in anhydrous 1,4-dioxane (15 mL), degassed and added to a suspension of phthalazine (**1a**) (131 mg, 1.00 mmol, 1.00 eq.) and **BDLA** catalyst (5.1 mg, 25 µmol, 2.5 mol%) in anhydrous 1,4-dioxane (10 mL). The mixture was stirred at 100 °C for 48 h. The crude product was purified via column chromatography [40 g silica gel, cyclohexane/toluene (95:5), dry loading (CH_2Cl_2)] to obtain a brown oil. Pentane (0.5 mL) was added and the mixture was placed in the fridge overnight. Afterwards, the solvent was removed with a cannula and the remaining solid was washed with cold pentane (0.5 mL) to obtain the substituted naphthalene **4a** as a pale yellow solid (206 mg, 717 µmol, 72%).

^{1}H NMR (400 MHz, $CDCl_3$): δ = 7.81 – 7.70 (m, 2H), 7.60 (s, 1H), 7.53 (s, 1H), 7.45 – 7.37 (m, 2H), 5.81 (t, *J* = 7.1 Hz, 1H), 3.24 (t, *J* = 7.1 Hz, 2H), 3.15 (t, *J* = 7.1 Hz, 2H), 3.09 (t, *J* = 7.1 Hz, 2H), 2.52 (q, *J* = 7.1 Hz, 2H).

^{13}C{^{1}H} NMR (101 MHz, $CDCl_3$): δ = 138.6, 137.6, 132.8, 132.6, 130.5, 128.7, 128.1, 127.3, 127.1, 125.5, 125.4, 124.2, 39.4, 33.6, 33.4, 30.3 ppm.

HRMS (ESI): *m/z* calculated for $C_{16}H_{15}Br+Na^+$: 309.0249 $[M+Na]^+$, found: 309.0250.

Melting point: 63 – 64 °C.

Synthesis of (*E*)-8-bromo-1,4-difluoro-6,7,10,11-tetrahydro-cycloocta[*b*]naphthalene (4b**)**

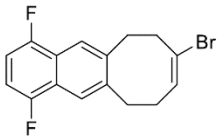

According to **GP1**, vinyl bromide **5** (665 mg, 2.50 mmol, 2.50 eq.) in anhydrous hexane (35 mL) was treated with KO*t*-Bu (1.13 g, 9.83 mmol, 9.83 eq.) and 18-crown-6 (164 mg, 0.620 mmol, 0.620 eq.) in anhydrous hexane (115 mL). The crude alkyne **3** was dissolved in anhydrous 1,4-dioxane (15 mL), degassed and added to a suspension of phthalazine **1b** (166 mg, 1.00 mmol, 1.00 eq.) and **BDLA** catalyst (5.1 mg, 25 µmol, 2.5 mol%) in anhydrous 1,4-dioxane (15 mL). The mixture was stirred at 80 °C for 24 h. The crude product was purified via column chromatography [30 g silica gel, cyclohexane/toluene (95:5), dry loading (CH_2Cl_2)] to obtain a yellow solid that was washed with a small amount of pentane (1 mL) to give the desired substituted naphthalene **4b** as a pale yellow solid (233 mg, 721 µmol, 72%).

^{1}H NMR (400 MHz, $CDCl_3$): δ = 7.82 (s, 1H), 7.75 (s, 1H), 7.00 – 6.92 (m, 2H), 5.81 (t, *J* = 7.1 Hz, 1H), 3.27 (t, *J* = 7.1 Hz, 2H), 3.18 (t, *J* = 7.1 Hz, 2H), 3.11 (t, *J* = 7.1 Hz, 2H), 2.54 (q, *J* = 7.1 Hz, 2H) ppm.

^{13}C{^{1}H} NMR (101 MHz, $CDCl_3$): δ = 155.8 – 155.6 and 153.4 – 153.2 (m, 2C), 140.3, 139.3, 130.3, 124.0, 123.8 (dd, *J* = 15.2, 6.0 Hz), 123.6 (dd, *J* = 14.1, 6.0 Hz), 121.6 – 121.4 (m), 121.1 – 120.9 (m), 108.2 (dd, *J* = 22.2, 8.0 Hz), 108.1 (dd, *J* = 23.2, 9.0 Hz), 39.2, 33.7, 33.5, 30.0 ppm.

^{19}F{^{1}H} NMR (377 MHz, $CDCl_3$): δ = -128.52 (dd, *J* = 148.5, 21.8 Hz) ppm.

HRMS (ESI): *m/z* calculated for $C_{16}H_{13}BrF_2$+Na^+: 345.0061 $[M+Na]^+$, found: 345.0057.

Melting point: 99 – 100 °C.

Synthesis of diethyl (*E*)-8-bromo-6,7,10,11-tetrahydrocyclo-octa[*b*]naphthalene-2,3-dicarboxylate (4c**)**

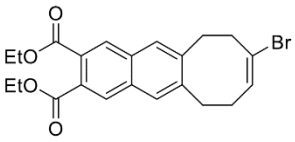

According to **GP1**, vinyl bromide **5** (1.02 g, 3.82 mmol, 2.55 eq.) in anhydrous hexane (40 mL) was treated with KO*t*-Bu (1.69 g, 14.7 mmol, 9.83 eq.) and 18-crown-6 (246 mg, 0.930 mmol, 0.620 eq.) in anhydrous hexane (90 mL). The crude alkyne **3** was dissolved in anhydrous 1,4-dioxane (6 mL), degassed and added to a suspension of phthalazine **1c** (411 mg, 1.50 mmol, 1.00 eq.) and **BDLA** catalyst (7.7 mg, 38 µmol, 2.5 mol%) in anhydrous 1,4-dioxane (9 mL). The mixture was stirred at 80 °C for 24 h. The crude product was purified via column chromatography [40 g silica gel, cyclohexane/EtOAc (98:2 to 62:38), dry loading (CH_2Cl_2)] to obtain a yellow solid. Pentane (0.5 mL) was added and the mixture was placed in the fridge overnight. Afterwards, the solvent was removed with a cannula and the remaining solid was washed with cold pentane (2 x 0.5 mL) to obtain the substituted naphthalene **4c** as a pale yellow solid (507 mg, 1.18 mmol, 78%).

^{1}H NMR (400 MHz, $CDCl_3$): δ = 8.17 (s, 1H), 8.13 (s, 1H), 7.67 (s, 1H), 7.59 (s, 1H), 5.78 (t, *J* = 7.0 Hz, 1H), 4.40 (two overlapping q, *J* = 7.1 Hz, 4H), 3.24 (t, *J* = 7.1 Hz, 2H), 3.16 (t, *J* = 7.2 Hz, 2H), 3.09 (t, *J* = 7.1 Hz, 2H), 2.52 (q, *J* = 7.0 Hz, 2H), 1.40 and 1.39 (two overlapping t, *J* = 7.1 Hz, 6H) ppm.

^{13}C{^{1}H} NMR (101 MHz, $CDCl_3$): δ = 168.1, 168.0, 141.7, 140.7, 132.7, 132.5, 130.3, 129.5, 129.4, 129.3, 128.9, 128.5, 128.4, 123.9, 61.7 (2C), 39.0, 33.6, 33.3, 29.9, 14.3 (2C) ppm.

HRMS (ESI): *m/z* calculated for $C_{22}H_{23}BrO_4$+Na^+: 453.0672 $[M+Na]^+$, found: 453.0672.

Melting point: 74 – 76 °C.

Synthesis of (*E*)-8-bromo-2-methoxy-6,7,10,11-tetrahydro-cycloocta[*b*]naphthalene and (*E*)-9-bromo-2-methoxy-6,7,10,11-tetrahydrocycloocta[*b*]naphthalene (4d**)**

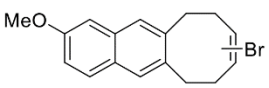

According to **GP1**, vinyl bromide **5** (1.60 g, 6.00 mmol, 6.00 eq.) in anhydrous hexane (70 mL) was treated with KO*t*-Bu (2.70 g, 23.6 mmol, 23.6 eq.) and 18-crown-6 (393 mg, 1.49 mmol, 1.49 eq.) in anhydrous hexane (150 mL). The crude alkyne **3** was dissolved in anhydrous 1,4-dioxane (15 mL), degassed and added to a suspension of phthalazine **1d** (160 mg, 1.00 mmol, 1.00 eq.) and **BDLA** catalyst (5.1 mg, 25 µmol, 2.5 mol%) in anhydrous 1,4-dioxane (10 mL). The mixture was stirred at 100 °C for 72 h. The crude product was purified via column chromatography [35 g silica gel, cyclohexane/toluene (8:2), dry loading (CH_2Cl_2)] to obtain an orange oil. Pentane (0.5 mL) was added and the mixture was placed in the fridge overnight. Afterwards, the solvent was removed with a cannula and the remaining solid was washed with cold pentane (0.5 mL) to obtain the substituted naphthalene **4d** (mixture of 8-bromo and 9-bromo isomer) as a pale yellow solid (215 mg, 676 µmol, 68%).
Mixture of regioisomers:

^{1}H NMR (400 MHz, $CDCl_3$): δ = 7.69 – 7.60 (m, 2H), 7.54 – 7.48 (m, 2H), 7.47 – 7.41 (m, 2H), 7.11 – 7.02 (m, 4H), 5.81 (t, *J* = 7.0 Hz, 2H), 3.93 – 3.87 (m, 6H), 3.25 – 3.15 (m, 4H), 3.16 – 3.03 (m, 8H), 2.56 – 2.45 (m, 4H) ppm.

^{13}C{^{1}H} NMR (101 MHz, $CDCl_3$): δ = 157.5, 157.4, 139.1, 138.1, 136.1, 135.1, 133.8, 133.6, 130.6, 130.4, 128.8, 128.6, 128.5, 128.3, 128.1, 128.0, 127.7, 127.1, 124.3, 124.1, 118.3, 118.2, 105.3, 105.1, 55.4 (2C), 39.5, 39.4, 33.7, 33.4 (2C), 33.2, 30.3, 30.3 ppm.

HRMS (ESI): *m/z* calculated for $C_{17}H_{17}BrO+Na^+$: 339.0355 $[M+Na]^+$, found: 339.0355.

Melting point: 80 – 81 °C.

1.4 General procedure for the synthesis of alkynes 6 (GP2)

A solution of vinyl bromide **4** (1.00 eq.) in a mixture of anhydrous hexane (10 mL) and anhydrous benzene (10 mL) was added dropwise to a suspension of KO*t*-Bu (2.5 eq.) and 18-crown-6 (0.25 eq.) in anhydrous hexane (45 mL) at 0 °C under nitrogen atmosphere. Afterwards, the mixture was stirred for 2 h at 0 °C and 1 h at rt. The resulting suspension was filtered and the filter cake was rinsed with EtOAc. The combined filtrates were washed with water and brine, dried ($MgSO_4$), filtered and concentrated *in vacuo*. The crude product was purified via filtration over silica gel (3 – 4 g) with CH_2Cl_2 to afford the desired alkyne **6**. If additional purification was required, it is noted below.

Synthesis of 8,9-didehydro-6,7,10,11-tetrahydrocycloocta[*b*]-naphthalene (6a**)**

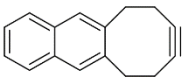

According to **GP2**, treatment of vinyl bromide **4a** (180 mg, 0.630 mmol, 1.00 eq.) with KO*t*-Bu (179 mg, 1.57 mmol, 2.50 eq.) and 18-crown-6 (41 mg, 0.16 mmol, 0.25 eq.) afforded the alkyne **6a** as a white solid (116 mg, 0.56 mmol, 89%).

^{1}H NMR (400 MHz, CD_2Cl_2): δ = 7.82 – 7.73 (m, 2H), 7.66 (s, 2H), 7.49 – 7.37 (m, 2H), 3.45 (td, *J* = 12.3, 3.6 Hz, 2H), 3.07 (dt, *J* = 12.5, 2.9 Hz, 2H), 2.60 – 2.49 (m, 2H), 2.40 – 2.26 (m, 2H) ppm.

^{13}C{^{1}H} NMR (101 MHz, CD_2Cl_2): δ = 140.5 (2C), 132.8 (2C), 129.7 (2C), 127.3 (2C), 125.9 (2C), 99.2 (2C), 38.0 (2C), 24.1 (2C) ppm.

HRMS (APCI): *m/z* calculated for $C_{16}H_{14}+H^+$: 207.1168 $[M+H]^+$, found: 207.1175.

Melting point: slow degradation starting at 100 °C to give a yellow solid and finally a yellow oil above 110 °C.

Synthesis of 1,4-difluoro-8,9-didehydro-6,7,10,11-tetrahydro-cycloocta[*b*]naphthalene (6b**)**

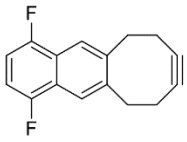

According to **GP2**, treatment of vinyl bromide **4b** (220 mg, 0.680 mmol, 1.00 eq.) with KO*t*-Bu (195 mg, 1.70 mmol, 2.50 eq.) and 18-crown-6 (45 mg, 0.17 mmol, 0.25 eq.) afforded the crude alkyne **6b** as a pale yellow solid (145 mg) that was further purified via column chromatography [10 g silica gel, cyclohexane/toluene (9:1), crude dissolved in eluent with a few drops of CH_2Cl_2] to yield a white solid (103 mg, 0.42 mmol, 62%).

^{1}H NMR (400 MHz, CD_2Cl_2): δ = 7.89 (s, 2H), 7.01 (dd, *J* = 7.5, 6.5 Hz, 2H), 3.50 (td, *J* = 12.3, 3.7 Hz, 2H), 3.11 (dt, *J* = 12.4, 2.9 Hz, 2H), 2.63 – 2.51 (m, 2H), 2.41 – 2.28 (m, 2H) ppm.

^{13}C{^{1}H} NMR (101 MHz, CD_2Cl_2): δ = 154.8 (dd, *J* = 248.9, 5.2 Hz, 2C), 142.5 (2C), 123.7 (dd, *J* = 13.2, 10.5 Hz, 2C), 122.4 (t, *J* = 3.0 Hz, 2C), 108.6 (dd, *J* = 18.2, 13.4 Hz, 2C), 99.1 (2C), 38.2 (2C), 24.0 (2C).

^{19}F{^{1}H} NMR (377 MHz, CD_2Cl_2): -129.26 ppm.

HRMS (APCI): *m/z* calculated for $C_{16}H_{12}F_2$+H^+: 243.0980 $[M+H]^+$, found: 243.0982.

Melting point: slow degradation starting at 100 °C to give a yellow solid and finally a yellow oil above 130 °C.

Synthesis of 2-methoxy-8,9-didehydro-6,7,10,11-tetrahydro-cycloocta[*b*]naphthalene (6d**)**

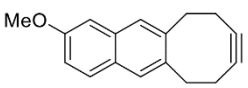

According to **GP2**, treatment of vinyl bromide **4d** (197 mg, 0.620 mmol, 1.00 eq.) with KO*t*-Bu (177 mg, 1.55 mmol, 2.50 eq.) and 18-crown-6 (41 mg, 0.16 mmol, 0.25 eq.) afforded the alkyne **6d** as a white solid (131 mg, 0.55 mmol, 89%).

^{1}H NMR (400 MHz, CD_2Cl_2): δ = 7.70 – 7.63 (m, 1H), 7.57 (s, 1H), 7.56 (s, 1H), 7.12 – 7.03 (m, 2H), 3.90 (s, 3H), 3.49 – 3.36 (m, 2H), 3.08 – 2.98 (m, 2H), 2.59 – 2.46 (m, 2H), 2.39 – 2.23 (m, 2H) ppm.

^{13}C{^{1}H} NMR (101 MHz, CD_2Cl_2): δ = 158.0, 141.0, 138.0, 133.9, 129.5, 128.9, 128.7, 128.3, 118.7, 105.3, 99.4, 99.2, 55.6, 38.0, 37.8, 24.1, 24.1 ppm.

HRMS (ESI): *m/z* calculated for $C_{17}H_{16}O+Na^+$: 259.1093 $[M+Na]^+$, found: 259.1095.

Melting point: slow degradation starting at 140 °C to give a yellow solid and finally a yellow oil above 160 °C.

1.5 General procedure for the synthesis of arene-fused CODs (2) (GP3)

In a nitrogen filled glove box, (substituted) phthalazine **1** (1.0 eq.), alkyne **6** (1.0 eq.) and **BDLA** catalyst (5 mol%) were suspended in anhydrous 1,4-dioxane (2.0 mL) in a 4 mL-screw cap vial with a stir bar. The vial was sealed and taken out of the glove box. The mixture was stirred at the given temperature for the given time. Afterwards, the reaction mixture was concentrated *in vacuo*. Purification conditions are noted below.

Synthesis of 1,4-difluoro-6,7,14,15-tetrahydrocycloocta[1,2-*b*:5,6-*b'*]dinaphthalene (2ab**)**

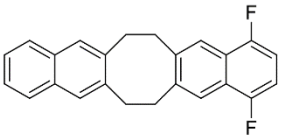

According to **GP3**, phthalazine **1b** (20 mg, 0.12 mmol, 1.0 eq.), alkyne **6a** (26.0 mg, 0.126 mmol, 1.05 eq.) and **BDLA** catalyst (1.2 mg, 6.0 µmol, 5.0 mol%) in 1,4-dioxane (2.0 mL) were stirred at 80 °C for 24 h. The mixture was concentrated *in vacuo* and the remaining solid was recrystallized from toluene. Dinaphthalene **2ab** was obtained as a white solid (26 mg, 76 µmol, 63%).

^{1}H NMR (400 MHz, CD_2Cl_2/CS_2): 7.67 (s, 2H), 7.65 – 7.58 (m, 2H), 7.45 (s, 2H), 7.33 – 7.26 (m, 2H), 6.86 (t, *J* = 6.9 Hz, 2H), 3.41 (s, 8H) ppm.

^{13}C{^{1}H} NMR (101 MHz, CD_2Cl_2/CS_2): δ = 154.7 (dd, *J* = 249.1, 5.1 Hz, 2C), 141.3 (2C), 138.7 (2C), 132.9 (2C), 128.5 (2C), 127.4 (2C), 125.7 (2C), 123.7 (dd, *J* = 13.1, 10.4 Hz, 2C), 121.1 (t, *J* = 3.0 Hz, 2C), 108.3 (dd, *J* = 18.2, 13.2 Hz, 2C), 35.9 (2C), 35.5 (2C).

^{19}F{^{1}H} NMR (377 MHz, CD_2Cl_2/CS_2): δ = -127.61 ppm.

HRMS (ESI): *m/z* calculated for $C_{24}H_{18}F_2$+Na^+: 367.1269 $[M+Na]^+$, found: 367.1261.

Melting point: 233 – 234 °C.

Synthesis of 1,4,9,12-tetrafluoro-6,7,14,15-tetrahydrocyclo-octa[1,2-*b*:5,6-*b'*]dinaphthalene (2bb)

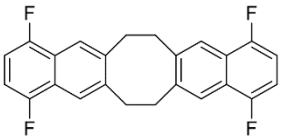

According to **GP3**, phthalazine **1b** (17 mg, 0.10 mmol, 1.1 eq.), alkyne **6b** (23 mg, 0.093 mmol, 1.0 eq.) and **BDLA** catalyst (1.0 mg, 4.7 µmol, 5.0 mol%) in 1,4-dioxane (2.0 mL) were stirred at 80 °C for 2 d. The mixture was concentrated *in vacuo* and filter over a silica plug with toluene. Dinaphthalene **2bb** was obtained as a white solid (26 mg, 0.068 mmol, 73%). Single crystals suitable for X-ray diffraction measurement (see 5.2) were obtained by recrystallization from toluene and slow cooling to rt over 24 h.

^{1}H NMR (200 MHz, $CDCl_3/CS_2$): δ = 7.66 (s, 4H), 6.84 (dd, *J* = 7.3, 6.4 Hz, 4H), 3.40 (s, 8H) ppm.

$^{13}C\{^{1}H\}$ NMR (101 MHz, $CDCl_3/CS_2$): δ = 154.2 (dd, *J* = 249.7, 5.2 Hz, 4C), 140.1 (br, 4C), 123.3 (dd, *J* = 13.2, 10.4 Hz, 4C), 120.9 (t, *J* = 2.9 Hz, 4C), 108.0 (dd, *J* = 18.1, 13.2 Hz, 4C), 35.2 (4C) ppm.

$^{19}F\{^{1}H\}$ NMR (377 MHz, $CDCl_3/CS_2$): -127.2 ppm.

HRMS (APCI): *m/z* calculated for $C_{24}H_{16}F_4+H^+$: 381.1261 $[M+H]^+$, found: 381.1264.

Melting point: 273 – 275 °C (color change to dark brown).

Synthesis of diethyl 10-methoxy-6,7,14,15-tetrahydro-cycloocta[1,2-*b*:5,6-*b'*]dinaphthalene-2,3-dicarboxylate (2bc**)**

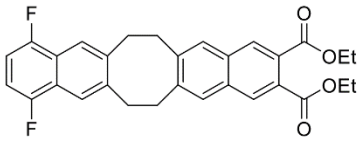

According to **GP3**, phthalazine **1c** (31.8 mg, 116 µmol, 1.00 eq.), alkyne **6b** (28.1 mg, 116 µmol, 1.00 eq.) and **BDLA** catalyst (1.2 mg, 5.8 µmol, 5.0 mol%) in 1,4-dioxane (2.0 mL) were stirred at 80 °C for 24 h. The mixture was concentrated *in vacuo* and purified via flash chromatography [12 g silica gel, cyclohexane/EtOAc (96:4 to 65:35, dry loading (CH_2Cl_2)]. Dinaphthalene **2bc** was obtained as a pale yellow solid (44 mg, 90 µmol, 78%).

^{1}H NMR (400 MHz, CD_2Cl_2): δ = 8.00 (s, 2H), 7.65 (s, 2H), 7.54 (s, 2H), 6.86 (t, *J* = 7.0 Hz, 2H), 4.31 (q, *J* = 7.1 Hz, 4H), 3.40 (s, 8H), 1.33 (t, *J* = 7.1 Hz, 6H) ppm.

^{13}C{^{1}H} NMR (101 MHz, CD_2Cl_2): δ = 168.0 (2C), 154.7 (dd, *J* = 248.2, 5.1 Hz, 2C), 132.6 (2C), 129.4 (2C), 129.0 (2C), 128.7 (2C), 123.6 (dd, *J* = 13.4, 10.5 Hz, 2C), 120.9 (t, *J* = 3.1 Hz, 2C), 108.3 (dd, *J* = 18.3, 13.3 Hz, 2C), 61.8 (2C), 35.1 (br, 4C), 14.3 (2C) ppm.

Due to peak broadening caused by conformational changes, four ^{13}C signals can't be detected (compare section 2.1).

^{19}F{^{1}H} NMR (377 MHz, CD_2Cl_2): δ = -129.16 ppm.

HRMS (ESI): *m/z* calculated for $C_{30}H_{26}F_2O_4$+Na^+: 511.1690 $[M+Na]^+$, found: 511.1690.

Melting point: 186 – 187 °C.

Synthesis of 1,4,10-trifluoro-6,7,14,15-tetrahydrocycloocta[1,2-*b*:5,6-*b'*]dinaphthalene (2be**)**

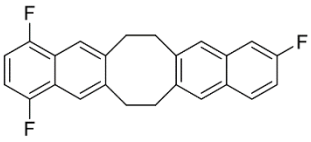

According to **GP3**, phthalazine **1e** (16 mg, 0.11 mmol, 1.0 eq.), alkyne **6b** (27 mg, 0.11 mol, 1.0 eq.) and **BDLA** catalyst (1.1 mg, 5.5 µmol, 5.0 mol%) in 1,4-dioxane (2.0 mL) were stirred at 80 °C for 24 h. The mixture was concentrated *in vacuo*. The remaining yellow solid was dissolved in hot toluene, filtered over silica (4 g) and concentrated *in vacuo*. The remaining pale yellow solid was further purified via automated flash chromatography [12 g silica gel, cyclohexane/toluene (100:0 to 80:20, dry loading (toluene)]. Dinaphthalene **2be** was obtained as a white solid (25 mg, 69 µmol, 63%).

^{1}H NMR (400 MHz, $CDCl_3/CS_2$): δ = 7.64 (s, br, 2H), 7.58 (dd, *J* = 8.7, 5.8 Hz, 1H), 7.42 (s, 1H), 7.37 (s, 1H), 7.19 (d, *J* = 9.4 Hz, 1H), 7.05 (td, *J* = 8.7, 2.6 Hz, 1H), 6.83 (t, *J* = 6.9 Hz, 2H), 3.36 (s, 8H) ppm.

^{13}C{^{1}H} NMR (101 MHz, $CDCl_3/CS_2$): δ = 160.2 (d, *J* = 245.6 Hz), 154.22 (d, *J* = 250.1 Hz), 154.16 (d, *J* = 250.1 Hz), 133.1 (d, *J* = 8.9 Hz), 129.3, 129.3 (d, *J* = 8.9 Hz), 128.0, 127.4 (d, *J* = 5.3 Hz), 123.6 – 123.1 (m, 2C), 120.9 – 120.7 (m, 2C), 115.5 (d, *J* = 25.3 Hz), 110.0 (d, *J* = 20.3 Hz), 108.3 – 107.6 (m, 2C), 36.3 – 34.3 (m, 4C) ppm.

Due to peak broadening caused by conformational changes, four ^{13}C signals can't be detected (compare section 2.1).

^{19}F{^{1}H} NMR (377 MHz, $CDCl_3/CS_2$): δ = -114.27, -127.20 (d, *J* = 21.6 Hz), -127.29 (d, *J* = 21.5 Hz) ppm.

HRMS (ESI): *m/z* calculated for $C_{24}H_{17}F_3+Na^+$: 385.1174 $[M+Na]^+$, found: 385.1175.

Melting point: 225 – 226 °C.

Synthesis of 10-chloro-1,4-difluoro-6,7,14,15-tetrahydrocyclo-octa[1,2-*b*:5,6-*b'*]dinaphthalene (2bf**)**

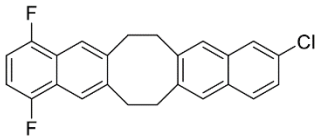

According to **GP3**, phthalazine **1f** (21 mg, 0.13 mmol, 1.1 eq.), alkyne **6b** (28 mg, 0.12 mmol, 1.0 eq.) and **BDLA** catalyst (1.2 mg, 5.8 µmol, 5.0 mol%) in 1,4-dioxane (2.0 mL) were stirred at 80 °C for 2 d. The mixture was concentrated *in vacuo* and remaining yellow solid was purified via flash chromatography [1 g silica gel, cyclohexane/toluene (9:1)]. Dinaphthalene **2bf** was obtained as a white, crystalline solid (33 mg, 0.086 mmol, 75%).

^{1}H NMR (400 MHz, $CDCl_3/CS_2$): 7.64 (s, 2H), 7.58 – 7.48 (m, 2H), 7.41 (s, 1H), 7.35 (s, 1H), 7.22 (dd, *J* = 8.8, 2.1 Hz, 1H), 6.84 (t, *J* = 6.9 Hz, 2H), 3.36 (s, 8H) ppm.

^{13}C{^{1}H} NMR (101 MHz, $CDCl_3/CS_2$): δ = 155.9 – 155.2 and 153.6 – 152.7 (m, 2C), 133.0, 131.1, 130.6, 128.5, 128.0, 127.2, 126.1, 125.7, 123.5 – 123.1 (m, 2C), 121.1 – 120.6 (m, 2C), 107.9 (dd, *J* = 21.2, 10.0 Hz, 2C), 35.4 and 35.1 (4C) ppm.

Due to peak broadening caused by conformational changes, four ^{13}C signals can't be detected (compare section 2.1).

^{19}F{^{1}H} NMR (377 MHz, $CDCl_3/CS_2$): -127.18 (d, *J* = 21.7 Hz), -127.28 (d, *J* = 21.7 Hz) ppm.

HRMS (APCI): *m/z* calculated for $C_{24}H_{17}ClF_2+H^+$: 379.1060 $[M+H]^+$, found: 379.1062.

Melting point: 216 – 217 °C.

Synthesis of 1,4-difluoro-10-(trifluoromethyl)-6,7,14,15-tetrahydrocycloocta[1,2-*b*:5,6-*b'*]dinaphthalene (2bg**)**

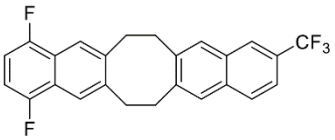

According to **GP3**, phthalazine **1g** (22 mg, 0.11 mmol, 1.0 eq.), alkyne **6b** (27 mg, 0.11 mol, 1.0 eq.) and **BDLA** catalyst (1.1 mg, 5.5 µmol, 5.0 mol%) in 1,4-dioxane (2.0 mL) were stirred at 80 °C for 24 h. The mixture was concentrated *in vacuo* and the remaining solid was recrystallized from toluene. Dinaphthalene **2bg** was obtained as a white solid (26 mg, 63 µmol, 57%).

^{1}H NMR (400 MHz, $CDCl_3/CS_2$): δ = 7.90 (s, 1H), 7.71 (d, *J* = 8.5 Hz, 1H), 7.65 (s, 2H), 7.53 and 7.50 (two overlapping s, 2H), 7.45 (d, *J* = 8.5 Hz, 1H), 6.84 (t, *J* = 6.9 Hz, 2H), 3.40 (s, 8H) ppm.

^{13}C{^{1}H} NMR (101 MHz, $CDCl_3/CS_2$): δ = 155.8 – 155.0 and 153.3 – 152.6 (m, 2C), 133.5, 131.1, 128.9, 128.03, 127.98, 127.1 (q, *J* = 32.1 Hz), 124.7 (q, *J* = 4.5 Hz), 124.3 (q, *J* = 272.4 Hz), 123.6 – 123.1 (m, 2C), 121.0 – 120.6 (m, 3C), 108.3 – 107.7 (m, 2C), 35.5 – 34.7 (m, 4C) ppm.

Due to peak broadening caused by conformational changes, four ^{13}C signals can't be detected (compare section 2.1).

^{19}F{^{1}H} NMR (377 MHz, $CDCl_3/CS_2$): δ = -62.0, -127.2 (d, *J* = 21.6 Hz), -127.4c (d, *J* = 21.6 Hz) ppm.

HRMS (APCI): *m/z* calculated for $C_{25}H_{17}F_5$+Na^+: 435.1142 [M+Na]$^+$, found: 435.1134.

Melting point: 223 – 224 °C.

Synthesis of 1,4-difluoro-9-nitro-6,7,14,15-tetrahydrocyclo-octa[1,2-*b*:5,6-*b'*]dinaphthalene (2bh**)**

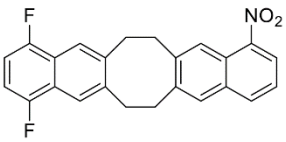

According to **GP3**, phthalazine **1h** (7.0 mg, 0.040 mmol, 1.0 eq.), alkyne **6b** (10 mg, 0.040 mmol, 1.0 eq.) and **BDLA** catalyst (0.5 mg, 2.5 µmol, 6.0 mol%) in 1,4-dioxane (2.0 mL) were stirred at 80 °C for 24 h. The mixture was concentrated *in vacuo* and the remaining solid was purified via automated flash chromatography [4 g silica gel, cyclohexane/toluene (100:0 to 50:50, dry loading (CH_2Cl_2)]. Dinaphthalene **2bh** was obtained as a pale yellow solid (12 mg, 31 µmol, 77%).

^{1}H NMR (200 MHz, $CDCl_3/CS_2$): δ = 8.26 (s, 1H), 8.08 (d, *J* = 7.8 Hz, 1H), 7.90 (d, *J* = 7.8 Hz, 1H), 7.66 (s, 2H), 7.54 (s, 1H), 7.37 (t, *J* = 7.8 Hz, 1H), 6.88 – 6.80 (m, 3H), 3.57 – 3.31 (m, 8H) ppm.

^{13}C{^{1}H} NMR (101 MHz, $CDCl_3/CS_2$): δ = 155.7 – 155.4 and 153.0 – 152.7 (m, 2C), 145.7, 133.7, 133.5, 128.8, 124.2, 123.6 – 123.2 (m, 5C), 121.2 – 121.0 (m), 120.8 – 120.6 (m), 108.3 – 107.8 (m, 2C), 35.7 – 34.7 (m, 4C) ppm.

Due to peak broadening caused by conformational changes, four ^{13}C signals can't be detected (compare section 2.1).

^{19}F{^{1}H} NMR (377 MHz, $CDCl_3/CS_2$): δ = -126.73 (d, *J* = 21.7 Hz), -127.38 (d, *J* = 21.7 Hz) ppm.

HRMS (APCI): *m/z* calculated for $C_{24}H_{17}F_2NO_2$+H^+: 390.1303 $[M+H]^+$, found: 390.1300.

Melting point: 254 – 256 °C (color change to dark brown).

Synthesis of 9,12-difluoro-6,7,14,15-tetrahydronaphtho-[2',3':5,6]cycloocta[1,2-*g*]quinoline (2bi**)**

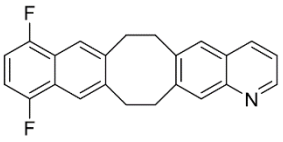

According to **GP3**, phthalazine **1i** (16.7 mg, 128 µmol, 1.10 eq.), alkyne **6b** (28.0 mg, 116 µmol, 1.00 eq.) and **BDLA** catalyst (1.2 mg, 5.8 µmol, 6.0 mol%) in 1,4-dioxane (2.0 mL) were stirred at 80 °C for 24 h. The mixture was concentrated *in vacuo* and purified via column chromatography [5 g silica gel, toluene/EtOAc (9:1)]. Quinoline **2bi** was obtained as a white solid (33 mg, 96 µmol, 82%).

^{1}H NMR (200 MHz, CD_2Cl_2): δ = 8.68 (dd, *J* = 4.0, 2.0 Hz, 1H), 7.94 (d, *J* = 8.0 Hz, 1H), 7.73 – 7.63 (m, 3H), 7.43 (s, 1H), 7.21 (dd, *J* = 8.0, 4.0 Hz, 1H), 6.86 (dd, *J* = 8.0, 6.0 Hz, 2H), 3.55 – 3.29 (m, 8H).

^{13}C{^{1}H} NMR (101 MHz, CD_2Cl_2): δ = 156.1 – 155.7 and 153.8 – 153.3 (m, 2C), 150.1, 147.9, 143.0, 141.2 (2C), 139.9, 135.2, 129.7, 128.0, 127.3, 123.9 – 123.3 (m, 2C), 121.3 – 120.6 (m, 3C), 108.2 (dd, *J* = 22.8, 8.8 Hz, 2C), 35.3 (2C), 35.1, 34.9 ppm.

^{19}F{^{1}H} NMR (377 MHz, CD_2Cl_2): δ = -128.97 (d, *J* = 22.6 Hz), -129.30 (d, *J* = 22.6 Hz) ppm.

HRMS (ESI): *m/z* calculated for $C_{23}H_{17}F_2N+Na^+$: 368.1221 $[M+Na]^+$, found: 368.1223.

Melting point: 216 – 217 °C (color change to dark brown).

Synthesis of diethyl 10-methoxy-6,7,14,15-tetrahydro-cycloocta[1,2-*b*:5,6-*b'*]dinaphthalene-2,3-dicarboxylate (2dc**)**

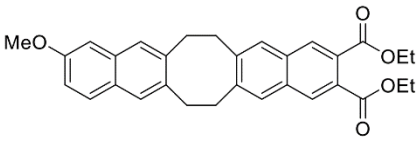

According to **GP3**, phthalazine **1c** (27.4 mg, 100 µmol, 1.00 eq.), alkyne **6d** (23.6 mg, 100 µmol, 1.00 eq.) and **BDLA** catalyst (1.0 mg, 5.0 µmol, 6.0 mol%) in 1,4-dioxane (2.0 mL) were stirred at 80 °C for 24 h. The mixture was concentrated *in vacuo* and purified via flash chromatography [12 g silica gel, cyclohexane/EtOAc (97:3 to 54:46, dry loading (CH_2Cl_2)]. Dinaphthalene **2dc** was obtained as a white solid (41 mg, 86 µmol, 86%).

^{1}H NMR (400 MHz, CD_2Cl_2): δ = 8.01 (s, 2H), 7.79 – 7.45 (m, 3H), 7.35 (d, *J* = 4.6 Hz, 2H), 6.98 – 6.91 (m, 2H), 4.32 (q, *J* = 7.1 Hz, 4H), 3.81 (s, 3H), 3.34 (s, br, 8H), 1.34 (t, *J* = 7.1 Hz, 6H) ppm.

^{13}C{^{1}H} NMR (101 MHz, CD_2Cl_2): δ = 167.8, 167.8, 157.4, 142.7 (br), 133.5, 132.3, 129.1, 129.1, 128.6, 128.5, 128.4, 128.3, 128.3, 127.9, 127.7, 126.9, 117.9, 105.1, 61.5 (2C), 55.3, 35.2 (br), 35.2 (br), 34.9 (br), 34.6 (br), 14.1(2C) ppm.

Due to peak broadening caused by conformational changes, four ^{13}C signals can't be detected (compare section 2.1).

HRMS (ESI): *m/z* calculated for $C_{31}H_{30}O_5$+Na^+: 505.1985 $[M+Na]^+$, found: 505.1983.

Melting point: 143 – 146 °C.

2 Variable temperature (VT) NMR studies

2.1 VT ^{13}C NMR spectra of quinoline 2bi

For all synthesized dinaphthalenes **2**, several ^{13}C signals could not be observed or were detected as very broad peaks with low intensity. To show that this is due to conformational changes, ^{13}C NMR spectra of quinoline **2bi** were measured at different temperatures (Figure S2). With increasing the temperature up to 60 °C, three sharp signals emerged, which were assigned to the sp^2-hybridized carbon atoms of the cyclooctadiene core (Figure S3 and Figure S4).

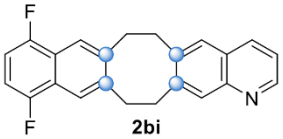

2bi

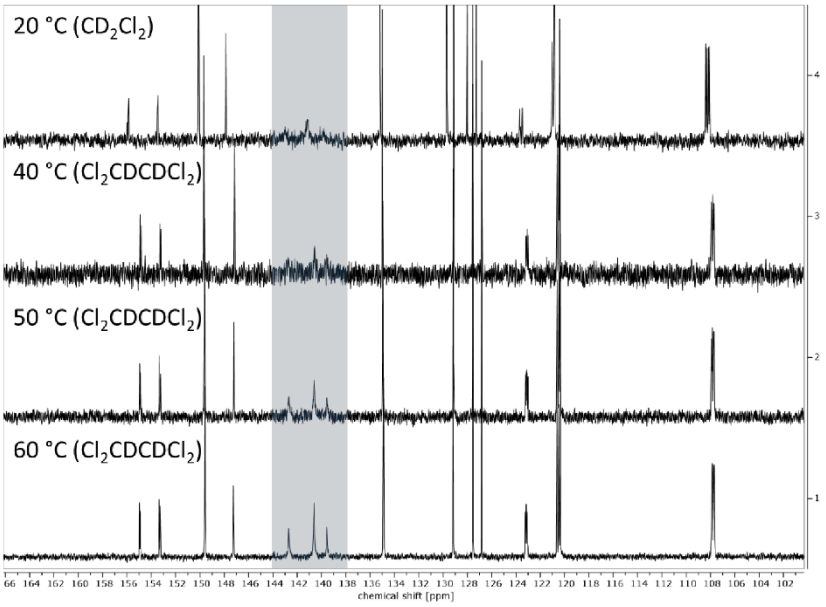

Figure S2. Excerpts of the ^{13}C{^{1}H} NMR spectra (151 MHz) of quinoline **2bi** at different temperatures.

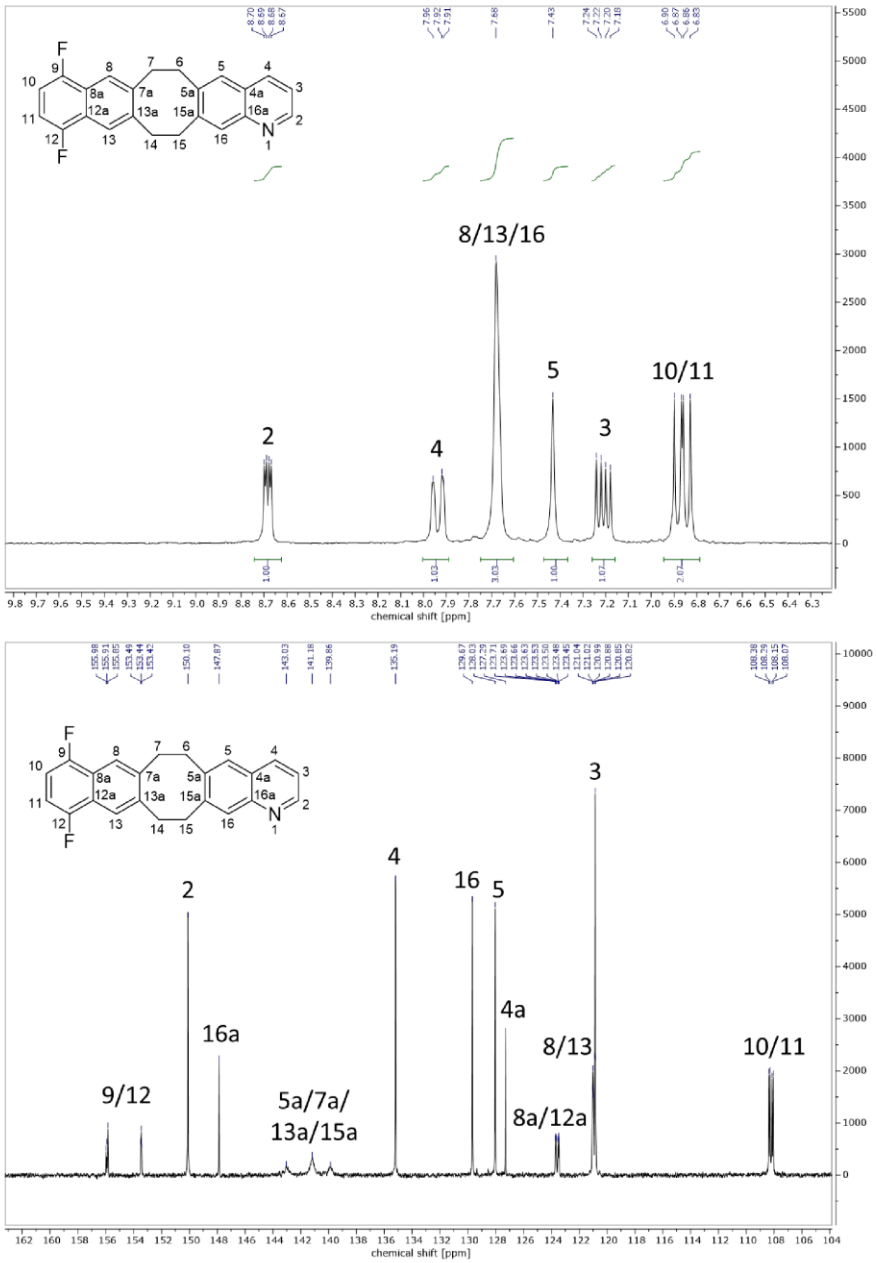

Figure S3. Assignment of the aromatic ^{1}H (400 MHz) (top) and $^{13}C\{^{1}H\}$ (101 MHz) (bottom) NMR signals (CD_2Cl_2) of quinoline **2bi**.

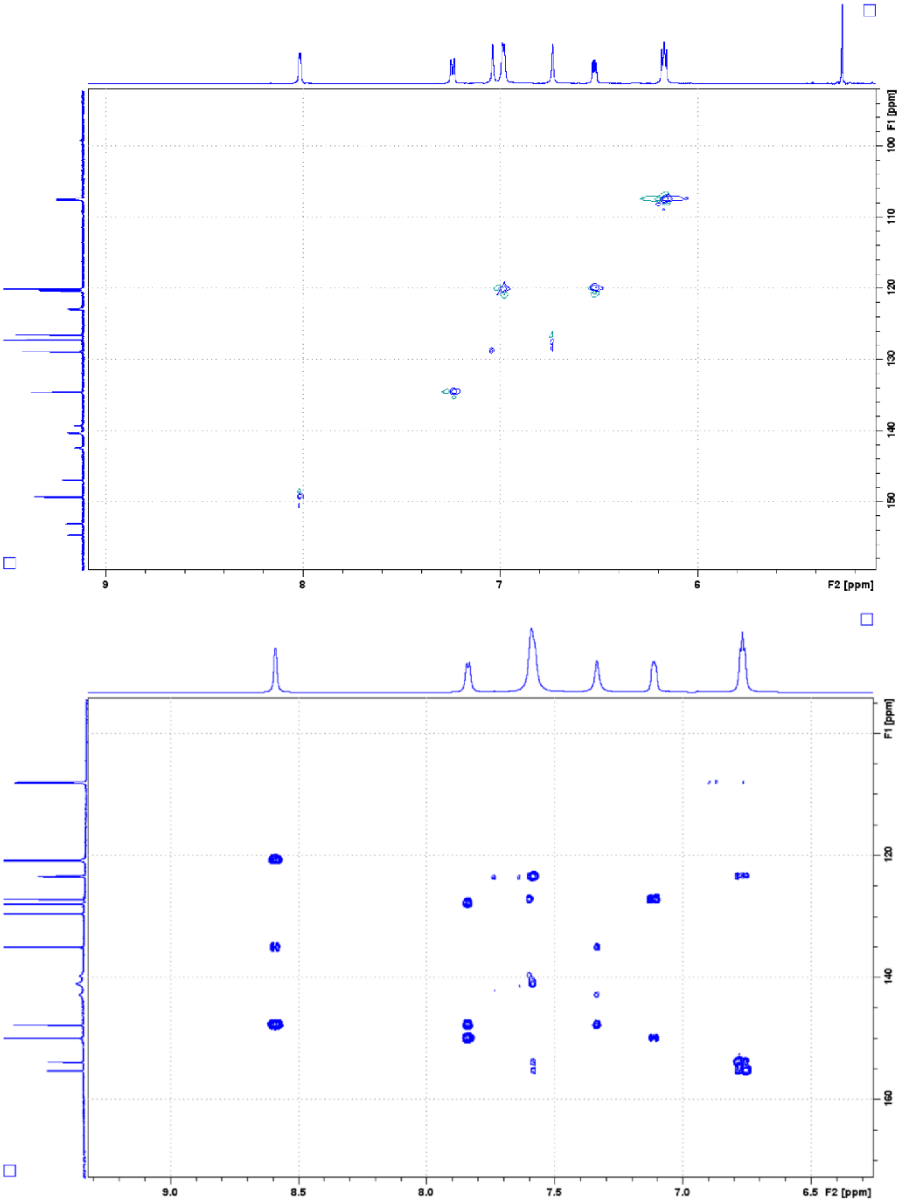

Figure S4. Excerpts of the ^{1}H-^{13}C HSQC (top) and ^{1}H-^{13}C HMBC (bottom) NMR spectra (CD_2Cl_2) of quinoline **2bi**.

2.2 VT ^{1}H NMR studies of the twist-boat/chair conversion

2.2.1 VT ^{1}H NMR spectra

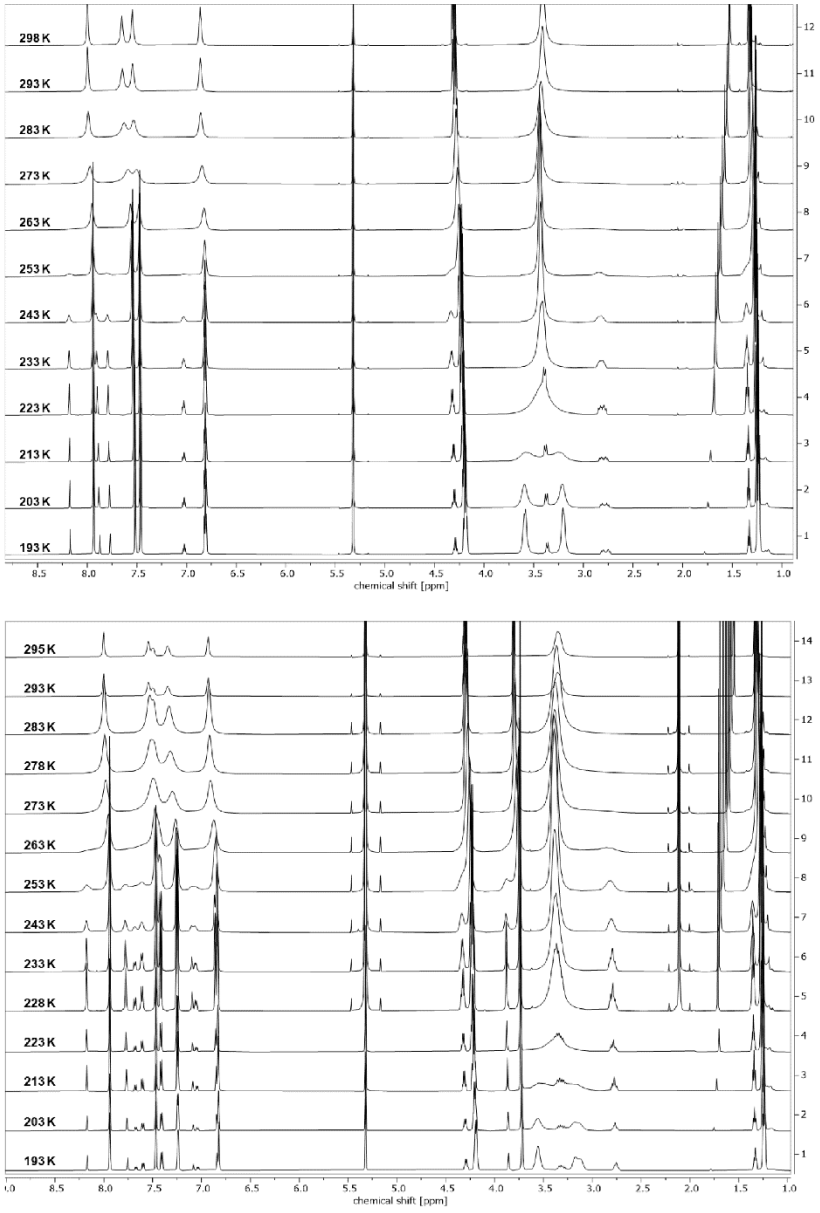

Figure S5. VT ^{1}H NMR spectra (600 MHz, CD_2Cl_2) of dinaphthalenes **2bc** (top) and **2dc** (bottom).

Dinaphthalene ***2bc***:

For the VT NMR analysis of dinaphthalene **2bc**, ^{1}H NMR signals at 223 K were assigned to the twist-boat (tb) and the chair (c) conformation by analyzing the 2D EXSY/NOESY spectrum (Figure S6).

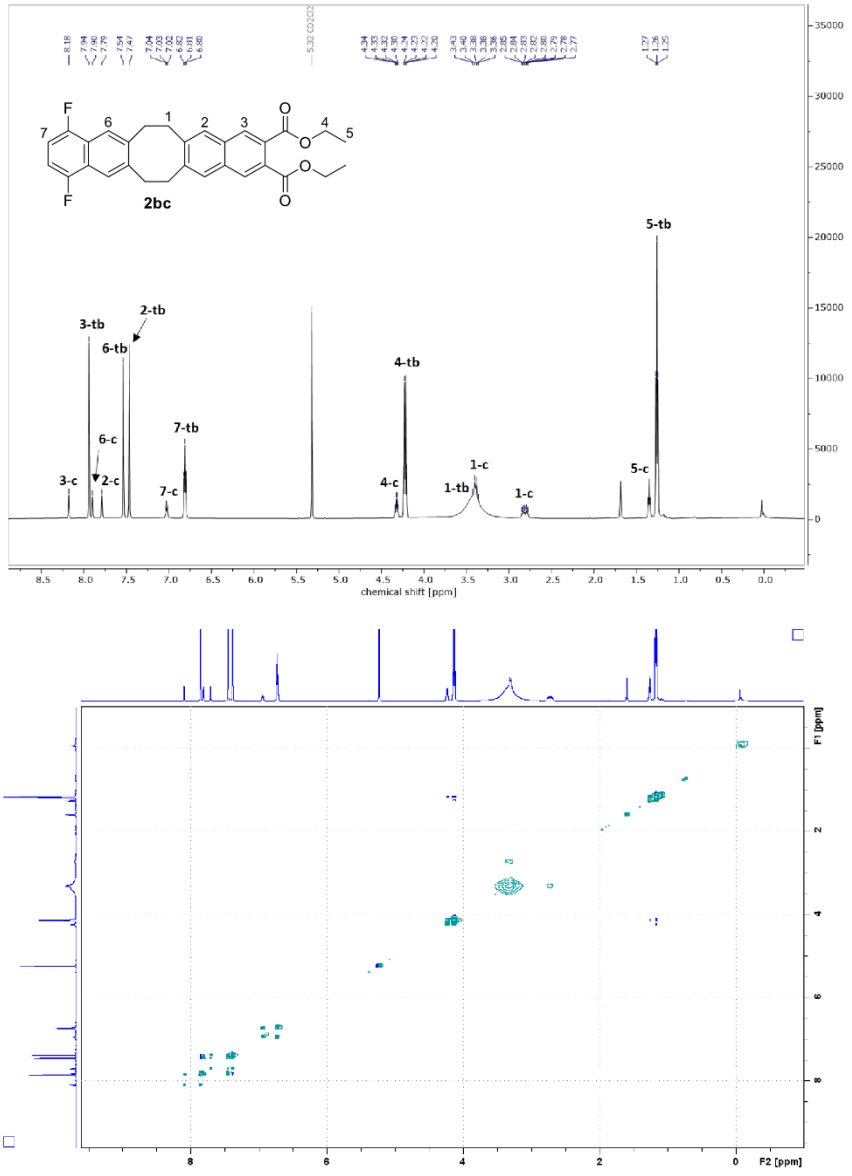

Figure S6. ^{1}H NMR spectrum with peak assignment (top) and ^{1}H-^{1}H EXSY/NOESY NMR spectrum (bottom) of dinaphthalene **2bc** at 223 K (600 MHz, CD_2Cl_2).

Dinaphthalene ***2dc***:

For the VT NMR analysis of dinaphthalene **2dc**, ^{1}H NMR signals at 228 K were assigned to the twist-boat (tb) and the chair (c) conformation by analyzing the 2D EXSY/NOESY spectrum (Figure S7).

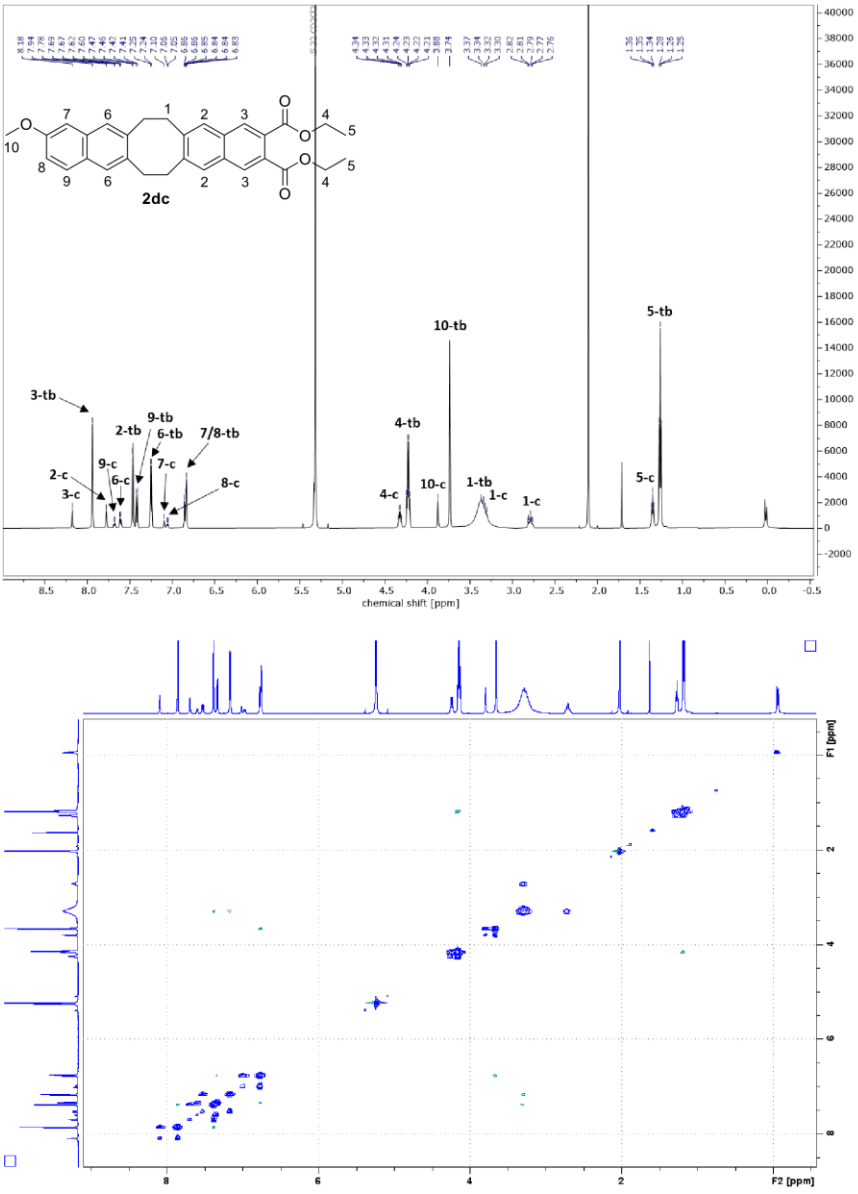

Figure S7. ^{1}H NMR spectrum with peak assignment (top) and ^{1}H-^{1}H EXSY/NOESY NMR spectrum (bottom) of dinaphthalene **2dc** at 228 K (600 MHz, CD_2Cl_2).

2.2.2 Thermodynamic study

The thermodynamic parameters of the twist-boat/chair equilibrium were studied by analyzing the ratio of twist-boat to chair conformation at different temperatures via integration of well separated signals in the ^{1}H NMR spectra. NMR spectra were measured on a Bruker Avance III HD 600 MHz spectrometer using CD_2Cl_2 as solvent and a sample concentration of 4 mg/mL. Changing the sample concentration to 8 mg/mL had virtually no effect on the equilibrium. Peak areas were obtained using the line fitting tool in MestReNova (version 14.2.1-27684). As significant peak broadening was observed around the coalescence temperature, the analysis was restricted to spectra acquired at and below 233 K. The ratios of twist-boat to chair conformer were used to calculate the equilibrium constants K_{eq} at different temperatures. A plot of $\ln K_{eq}$ vs. 1/T yielded a linear correlation that was fitted using OriginPro® 2020 (64-bit). ΔH^0 and ΔS^0 were determined from the slope and the y-intercept, respectively, of the linear fit using the following equation:

$$\ln K_{eq} = -\frac{\Delta H^0}{R} \cdot \frac{1}{T} + \frac{\Delta S^0}{R}$$

The Gibbs free energy difference ΔG^0 at 298 K of the two conformers was calculated from the following equation:

$$\Delta G^0 = \Delta H^0 - T \cdot \Delta S^0$$

Dinaphthalene ***2bc***:

The signals 2-c (δ_c = 7.79 ppm) and 2-tb (δ_{tb} = 7.47 ppm) were integrated at different temperatures to determine the populations of chair and twist-boat conformers, respectively, from which the equilibrium constants K_{eq} were calculated. The results are shown Table S1.

Table S1. Equilibrium constants K_{eq} of the tb/c equilibrium of dinaphthalene **2bc** at different temperatures determined from tb and c populations.

T [K]	Population of c	Population of tb	K_{eq}
193	0.1382	0.8618	0.160
203	0.1472	0.8528	0.173
213	0.1580	0.8420	0.188
223	0.1758	0.8242	0.213
228	0.1760	0.8240	0.214
233	0.1808	0.8192	0.221

The linear fit of $\ln K_{eq}$ vs. 1/T is shown in Figure S8 and was used to calculate the differences in enthalpy (ΔH^0) and entropy (ΔS^0) of tb and c conformer (Table S2).

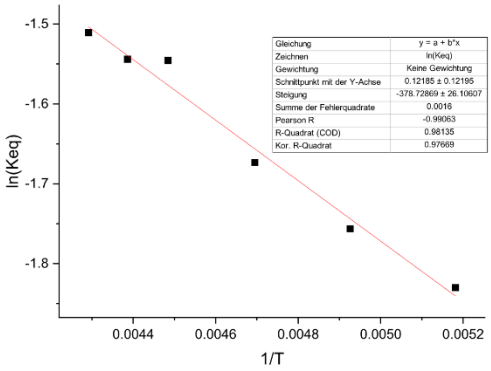

Figure S8. Linear fit of $\ln K_{eq}$ vs. 1/T of dinaphthalene **2dc**.

Table S2. Enthalpy (ΔH^0), entropy (ΔS^0) and Gibbs free energy (ΔG^0) difference of tb and c conformation of dinaphthalene **2bc** calculated from the linear fit of $\ln K_{eq}$ vs. 1/T.

y-intercept	slope [K]	ΔH^0 [kJ/mol]	ΔS^0 [J/K·mol]	ΔG^0 [kJ/mol] at 298 K
0.12±0.12	-378.7±26.1	3.1	1.0	2.8

Dinaphthalene ***2dc***:

The signals 10-c (δ_c = 3.88 ppm) and 10-tb (δ_{tb} = 3.74 ppm) were integrated at different temperatures to determine the populations of chair and twist-boat conformers, respectively, from which the equilibrium constants K_{eq} were calculated. The results are shown in Table S3.

Table S3. Equilibrium constants K_{eq} of the tb/c equilibrium of dinaphthalene **2dc** at different temperatures determined from tb and c populations.

T [K]	Population of c	Population of tb	K_{eq}
193	0.1738	0.8262	0.210
203	0.1846	0.8154	0.226
213	0.1904	0.8096	0.235
223	0.2003	0.7997	0.251
233	0.2068	0.7932	0.261

The linear fit of $\ln K_{eq}$ vs. 1/T is shown in Figure S9 and was used to calculate the differences in enthalpy (ΔH^0) and entropy (ΔS^0) of tb and c conformer (Table S4).

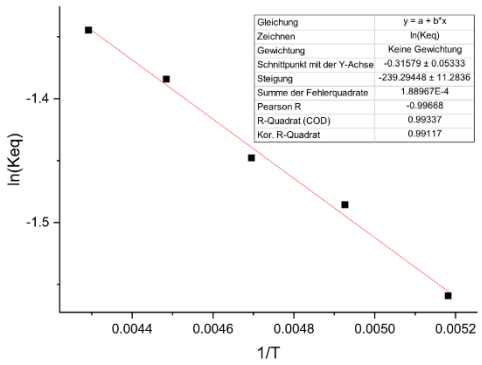

Figure S9. Linear fit of $\ln K_{eq}$ vs. 1/T of dinaphthalene **2dc**.

Table S4. Enthalpy (ΔH^0), entropy (ΔS^0) and Gibbs free energy (ΔG^0) difference of tb and c conformation of dinaphthalene **2dc** calculated from the linear fit of $\ln K_{eq}$ vs. 1/T.

y-intercept	slope [K]	ΔH^0 [kJ/mol]	ΔS^0 [J/K·mol]	ΔG^0 [kJ/mol] at 298 K
-0.32±0.07	-239.3±11.3	2.0	-2.6	2.8

2.2.3 Kinetic study

The kinetics of the twist-boat/chair conversion were studied below the coalescence temperature using the dynamic NMR (DNMR) lineshape analysis tool integrated in Brukers TopSpin (version 4.1.4). NMR spectra were measured on a Bruker Avance III HD 600 MHz spectrometer using CD_2Cl_2 as solvent and a sample concentration of 4 mg/mL. The temperatures of the measurements are given below in Table S5 and Table S7.

The chemical shifts of exchanging nuclei were identified and a region of the spectrum that showed well separated signals was used for the DNMR analysis. The selected region was simulated using an unequally populated two-site model. The rate constant k at each temperature was obtained by iterative refinement of the simulated spectrum until the best overlap (>90%) with the experimental data was obtained. A plot of ln(k/T) vs. 1/T yielded a linear correlation that was fitted using OriginPro® 2020 (64-bit). The activation parameters $\Delta H^{\ddagger}$ and $\Delta S^{\ddagger}$ were determined from the slope and the y-intercept, respectively, of the linear fit using the Eyring–Polanyi equation:

$$\ln\frac{k}{T} = -\frac{\Delta H^{\ddagger}}{R}\cdot\frac{1}{T} + \ln\frac{k_B}{h} + \frac{\Delta S^{\ddagger}}{R}$$

The Gibbs free energy of activation $\Delta G^{\ddagger}$ at 298 K was calculated from the following equation:

$$\Delta G^{\ddagger} = \Delta H^{\ddagger} - T\cdot\Delta S^{\ddagger}$$

Dinaphthalene ***2bc***:

The signals 2-c (δ_c = 7.79 ppm) and 2-tb (δ_{tb} = 7.47 ppm) were used for the determination of k via DNMR lineshape analysis. The results are shown in Table S5.

Table S5. Rate constants k for the twist-boat/chair conversion of dinaphthalene **2bc** determined via DNMR lineshape analysis at different temperatures.

T [K]	k [s^{-1}]
223	8.2
228	11.8
233	21.6
238	35.2
243	50.0
248	74.2

The linear fit of ln(k/T) vs. 1/T is shown in Figure S10 and was used to calculate the activation parameters (Table S6).

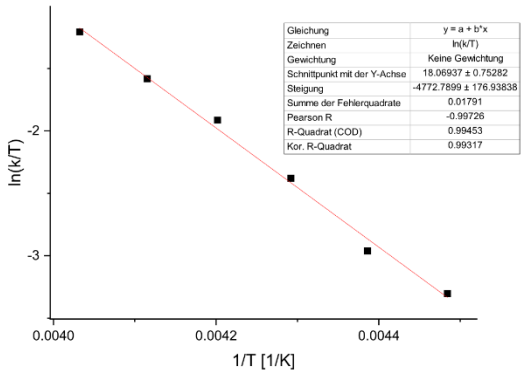

Figure S10. Linear fit of ln(k/T) vs. 1/T of dinaphthalene **2bc**.

Table S6. Activation parameters of the twist-boat/chair conversion of dinaphthalene **2bc** calculated from the linear fit of ln(k/T) vs. 1/T.

y-intercept	slope [K]	$\Delta H^{\ddagger}$ [kJ/mol]	$\Delta S^{\ddagger}$ [J/K·mol]	$\Delta G^{\ddagger}$ [kJ/mol] at 298 K
18.07±0.75	-4772±177	39.7	-47.3	53.8

*Dinaphthalene **2dc***:

The signals 10-c (δ_c = 3.88 ppm) and 10-tb (δ_{tb} = 3.74 ppm) belonging to the protons of the methoxy group were used for the determination of k via DNMR lineshape analysis. The results are shown in Table S7.

Table S7. Rate constants k for the twist-boat/chair conversion of dinaphthalene **2dc** determined via DNMR lineshape analysis at different temperatures.

T [K]	k [s^{-1}]
228	15.2
233	19.7
238	34.4
243	46.3
248	67.4
253	88.7
258	126.9

The linear fit of ln(k/T) vs. 1/T is shown in Figure S11 and was used to calculate the activation parameters (Table S8).

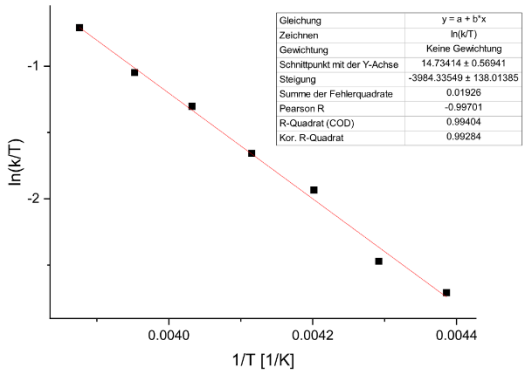

Figure S11. Linear fit of ln(k/T) vs. 1/T of dinaphthalene **2dc**.

Table S8. Activation parameters of the twist-boat/chair conversion of dinaphthalene **2dc** calculated from the linear fit of ln(k/T) vs. 1/T.

y-intercept	slope [K]	$\Delta H^{\ddagger}$ [kJ/mol]	$\Delta S^{\ddagger}$ [J/K·mol]	$\Delta G^{\ddagger}$ [kJ/mol] at 298 K
14.73±0.57	-3984±138	33.1	-75.0	55.5

2.2.4 Determination of the twist-boat to chair ratio above the coalescence temperature

At temperatures above the coalescence temperature T_c, the ratio of twist-boat to chair conformers was determined from the chemical shift of the coalesced signal of H-3 (δ_{obs}) relative to the chemical shifts of the corresponding signals assigned to the twist-boat (δ_{tb}) and chair (δ_c) conformation below T_c.[6] The following equations were used to calculate the population of twist-boat and chair, respectively:

$$Population\ of\ tb = \frac{\delta_c - \delta_{obs}}{\delta_c - \delta_{tb}}$$

$$Population\ of\ c = \frac{\delta_{obs} - \delta_{tb}}{\delta_c - \delta_{tb}}$$

The observed chemical shifts at 298 K and the corresponding chair and twist-boat populations of dinaphthalenes **2bc** and **2dc** are shown in Table S9.

Table S9. Populations of chair and twist-boat conformer at 298 K calculated from the observed chemical shifts of H-3.

Compound	δ_{obs} [ppm]	δ_c [ppm]	δ_{tb} [ppm]	Population of c	Population of tb
2bc	7.998	8.180	7.940	0.242	0.758
2dc	8.003	8.177	7.940	0.266	0.734

3 Theoretical calculations

3.1 Computational methods

Initial Geometry optimizations were carried out using extended tight binding (XTB),[7–11] followed by conformer screenings with the conformer rotamer ensemble sampling tool (CREST).[12–15] The resulting conformers of the twist-boat, chair and boat family were optimized by the means of Density Functional Theory (DFT) calculations. All calculations were carried out using the ORCA software package.[16] Geometry optimizations and frequency calculations were carried out on a PBE0/def2-TZVP/D4/CPCM(CH2Cl2) level of theory.[17–21] On all atoms, the def2/J auxiliary basis set was used for the RIJCOSX approximation.[22–32]

For a more accurate implicit solvation, single point energy calculations were carried out on a PBE0/def2-TZVPP/D4/SMD(CH2Cl2) level of theory to obtain both electrostatic and cavity-dispersion interactions.[33] Finally, single point energies were refined using the domain based local pair natural orbital (DLPNO)-CCSD(T) method.[34–38] Thermodynamic corrections as well as solvent interactions were taken from aforementioned DFT calculations.

Visualization of non-covalent interactions (NCIs) were carried out using the NCIPLOT software package and the visual molecular dynamics (VMD) program. Visualization was carried out using the VMD template supplied in the NCIPLOT software package.[39,40]

3.2 Calculated energies

Table S10. Calculated energies of dinaphthalene **2bc**.

	G_{abs}^{DFT}/Hartree	G_{rel}^{DFT}/kcal/mol	G_{abs}^{corr}/Hartree	G_{rel}^{corr}/kcal/mol
twist-boat	-1657.900	0.000	-1656.878	0.000
chair	-1657.899	1.100	-1656.874	2.554
twist	-1657.893	4.445	-1656.868	5.927

Table S11. Calculated energies of dinaphthalene **2dc**.

	G_{abs}^{DFT}/Hartree	G_{rel}^{DFT}/kcal/mol	G_{abs}^{corr}/Hartree	G_{rel}^{corr}/kcal/mol
twist-boat	-1573.920	0.000	-1572.970	0.000
chair	-1573.918	1.090	-1572.967	2.302
twist	-1573.912	4.769	-1572.961	5.998

3.4 Non-covalent interaction plots

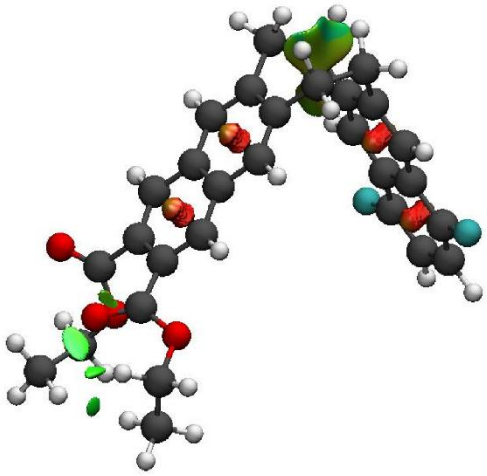

Figure S12. NCI plot of the twist-boat conformer of dinaphthalene **2bc**.

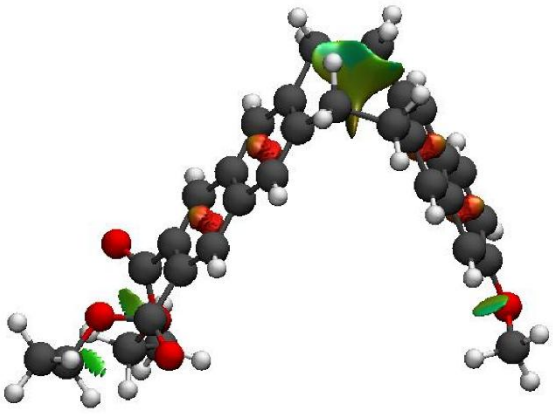

Figure S13. NCI plot of the twist-boat conformer of dinaphthalene **2dc**.

5 XRD analysis

5.1 General crystallographic experimental details

Suitable single crystals for X-ray structure determination were selected and transferred in protective perfluoropolyether oil on a microscope slide. The selected and mounted crystals were transferred to the cold gas steam on the diffractometer. The diffraction data were obtained at 100 K on a Bruker D8 three circle diffractometer, equipped with a PHOTON 100 CMOS detector and a IμS microfocus sources with Quazar mirror optics (Mo-Kα radiation, λ = 0.71073 Å).

The data obtained were integrated with SAINT and a semi-empirical absorption correction from equivalents with SADABS-2016/2 was applied.[41] The structures were solved by direct methods using SHELXT-2018/2.[42] Structure refinement was done using SHELXT-2018/3.[43] All non-hydrogen atoms were refined anisotropically and C-H hydrogen atoms were positioned at geometrically calculated positions and refined using a riding model. The isotropic displacement parameters of all hydrogen atoms were fixed to 1.2x or 1.5x (CH_3 hydrogens) the U_{eq} value of the atoms they are linked to.

5.2 Crystallographic details of 2bb

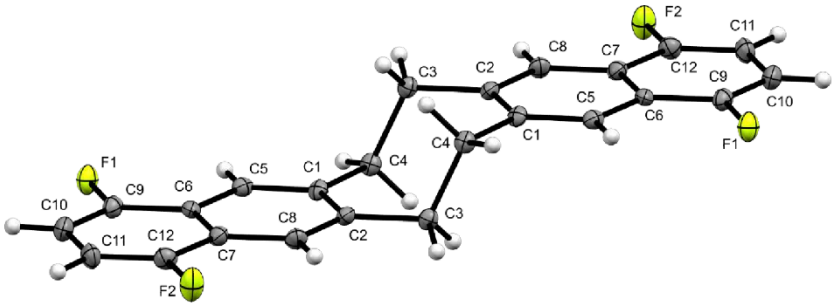

Figure S41. Thermal ellipsoid plot of **2bb** with the anisotropic displacement parameters drawn at the 50% probability level.

6 References

1 S. N. Kessler, M. Neuburger and H. A. Wegner, *Eur. J. Org. Chem.*, 2011, **2011**, 3238–3245.

2 S. N. Kessler and H. A. Wegner, *Org. Lett.*, 2012, **14**, 3268–3271.

3 J.-S. Kim, K.-J. Shin, D.-C. Kim, Y.-K. Kang, D.-J. Kim, K.-H. Yoo and S.-W. Park, *Bull. Korean Chem. Soc.*, 2002, **23**, 1425–1446.

4 M. Große, C. M. Leonhardt, P. A. R. Campbell and H. A. Wegner, *Org. Lett.*, 2025, **27**, 4893–4897.

5 B. R. Varga, M. Kállay, K. Hegyi, S. Béni and P. Kele, *Chem. Eur. J.*, 2012, **18**, 822–828.

6 W. Fu, T. M. Alam, J. Li, J. Bustamante, T. Lien, R. W. Adams, S. J. Teat, B. J. Stokes, W. Yang, Y. Liu and J. Q. Lu, *J. Am. Chem. Soc.*, 2020, **142**, 16651–16660.

7 C. Bannwarth, E. Caldeweyher, S. Ehlert, A. Hansen, P. Pracht, J. Seibert, S. Spicher and S. Grimme, *WIREs Comput. Mol. Sci.*, 2021, **11**, e1493.

8 S. Grimme, C. Bannwarth and P. Shushkov, *J. Chem. Theory Comput.*, 2017, **13**, 1989–2009.

9 C. Bannwarth, S. Ehlert and S. Grimme, *J. Chem. Theory Comput.*, 2019, **15**, 1652–1671.

10 P. Pracht, E. Caldeweyher, S. Ehlert and S. Grimme, *ChemRxiv*, 2019. DOI: 10.26434/chemrxiv.8326202.v1.

11 S. Ehlert, M. Stahn, S. Spicher and S. Grimme, *J. Chem. Theory Comput.*, 2021, **17**, 4250–4261.

12 P. Pracht, F. Bohle and S. Grimme, *Phys. Chem. Chem. Phys.*, 2020, **22**, 7169–7192.

13 P. Pracht, S. Grimme, C. Bannwarth, F. Bohle, S. Ehlert, G. Feldmann, J. Gorges, M. Müller, T. Neudecker, C. Plett, S. Spicher, P. Steinbach, P. A. Wesołowski and F. Zeller, *J. Chem. Phys.*, 2024, **160**, 114110.

14 P. Pracht and C. Bannwarth, *J. Chem. Theory Comput.*, 2022, **18**, 6370–6385.

15 S. Grimme, *J. Chem. Theory Comput.*, 2019, **15**, 2847–2862.

16 F. Neese, *WIREs Comput. Mol. Sci.*, 2022, **12**, e1606.

17 C. Adamo and V. Barone, *J. Chem. Phys.*, 1999, **110**, 6158–6170.

18 F. Weigend, *Phys. Chem. Chem. Phys.*, 2006, **8**, 1057–1065.

19 F. Weigend and R. Ahlrichs, *Phys. Chem. Chem. Phys.*, 2005, **7**, 3297–3305.

20 V. Barone and M. Cossi, *J. Phys. Chem. A*, 1998, **102**, 1995–2001.

21 C. Riplinger and F. Neese, *J. Chem. Phys.*, 2013, **138**, 34106.

22 L. Wittmann, I. Gordiy, M. Friede, B. Helmich-Paris, S. Grimme, A. Hansen and M. Bursch, *Phys. Chem. Chem. Phys.*, 2024, **26**, 21379–21394.

23 E. Caldeweyher, J.-M. Mewes, S. Ehlert and S. Grimme, *Phys. Chem. Chem. Phys.*, 2020, **22**, 8499–8512.

24 E. Caldeweyher, S. Ehlert, A. Hansen, H. Neugebauer, S. Spicher, C. Bannwarth and S. Grimme, *J. Chem. Phys.*, 2019, **150**, 154122.
25 E. Caldeweyher, C. Bannwarth and S. Grimme, *J. Chem. Phys.*, 2017, **147**, 34112.
26 F. Neese, *J. Comp. Chem.*, 2023, **44**, 381–396.
27 B. Helmich-Paris, B. de Souza, F. Neese and R. Izsák, *J. Chem. Phys.*, 2021, **155**, 104109.
28 M. Garcia-Ratés and F. Neese, *J. Comput. Chem.*, 2020, **41**, 922–939.
29 M. Garcia-Ratés and F. Neese, *J. Comput. Chem.*, 2019, **40**, 1816–1828.
30 D. Bykov, T. Petrenko, R. Izsák, S. Kossmann, U. Becker, E. Valeev and F. Neese, *Molec. Phys.*, 2015, **113**, 1961–1977.
31 F. Neese, F. Wennmohs, A. Hansen and U. Becker, *Chem. Phys.*, 2009, **356**, 98–109.
32 F. Neese, *J. Comp. Chem.*, 2003, **24**, 1740–1747.
33 A. V. Marenich, C. J. Cramer and D. G. Truhlar, *J. Phys. Chem. B*, 2009, **113**, 6378–6396.
34 F. Neese, A. Hansen and D. G. Liakos, *J. Chem. Phys.*, 2009, **131**, 64103.
35 F. Neese, F. Wennmohs and A. Hansen, *J. Chem. Phys.*, 2009, **130**, 114108.
36 C. Riplinger, B. Sandhoefer, A. Hansen and F. Neese, *J. Chem. Phys.*, 2013, **139**, 134101.
37 C. Riplinger, P. Pinski, U. Becker, E. F. Valeev and F. Neese, *J. Chem. Phys.*, 2016, **144**, 24109.
38 G. Bistoni, C. Riplinger, Y. Minenkov, L. Cavallo, A. A. Auer and F. Neese, *J. Theo. Comp. Chem.*, 2017, **13**, 3220–3227.
39 W. Humphrey, A. Dalke and K. Schulten, *J. Mol. Graph.*, 1996, **14**, 33-8, 27-8.
40 J. Contreras-García, E. R. Johnson, S. Keinan, R. Chaudret, J.-P. Piquemal, D. N. Beratan and W. Yang, *J. Chem. Theory Comput.*, 2011, **7**, 625–632.
41 L. Krause, R. Herbst-Irmer, G. M. Sheldrick and D. Stalke, *J. Appl. Crystallogr.*, 2015, **48**, 3–10.
42 G. M. Sheldrick, *Acta Crystallogr. A*, 2015, **71**, 3–8.
43 G. M. Sheldrick, *Acta Crystallogr. C*, 2015, **71**, 3–8.